ADAPTIVE EQUALIZERS FOR MULTIPATH COMPENSATION

IN DIGITAL MICROWAVE COMMUNICATIONS

A thesis submitted to the Faculty of Science of the

University of Edinburgh, for the degree of

Doctor of Philosophy

by

Wai-ki WONG (BSc MSc C Eng MIEE)

September 1987

UNIVERSITY OF EDINBURGH

ABSTRACT OF THESIS (Regulation 7.9)

Name of Candidate ..... Wai-ki WONG .....

Address [redacted]

Degree ..... PhD ..... *Date* ..... 28 Sept 1987 .....

Title of Thesis ..... Adaptive Equalizers for Multipath Compensation in Digital Microwave Radio Communications .....

No. of words in the main text of Thesis ..... 30,000 approx. .....

This thesis compares various digital implementations of baseband transversal equalizers for combating multipath fading effects in Line Of Sight (LOS) digital microwave radio communication systems. A general Quadrature Amplitude Modulation (QAM) radio system is used, and both symbol (T) spaced and half symbol (T/2) spaced transversal equalizer designs have been addressed.

Various degradations like: finite step size; number of quantization levels in the analogue to digital converter; demodulation phase error and rounding error in the arithmetic, in particular the early termination effect have all been evaluated and verified by computer simulations. As a result, the required number of taps, input quantization level, and arithmetic accuracy requirements for practical T-spaced equalizer designs are proposed for QPSK to 1024QAM radio systems.

The effect of sampling phase error is investigated. Although the non-overlapped sampling spectrum characteristics of the T/2-spaced equalizer yields lower sampling phase sensitivity, an analysis shows this equalizer to suffer from an ill-conditioning problem which degrades its overall performance and makes it a non-optimum choice for the present application.

Finally, during non-stationary conditions, the local minima phenomenon in the decision directed operation is analysed and the importance of the choice of step size is further discussed. A preliminarily investigation into the use of two equalizers to combat the phase transition problems during multipath fading is also presented.

DECLARATION OF ORIGINALITY

This thesis and the work reported herein was conducted exclusively by myself.

Wai-ki WONG

ACKNOWLEDGEMENTS

The author would like to express his gratitude to Dr P M Grant for all his help and guidance in advising the author's part time study at the University of Edinburgh.

The encouragement and support by Dr C F N Cowan, Mr B Williamson and Dr T Crawford are also greatly appreciated. Finally, the author would like to thank Hewlett Packard Ltd., South Queensferry, for its financial support and allowing the use of HP3000 computer.

CONTENTS

Abbreviations

AM	: Amplitude Modulation
ADC	: Analog to Digital Converter
AT&T	: American Telephone and Telegraph
BER	: Bit Error Ratio
BPF	: Bandpass Filter
BPSK	: Binary Phase Shift Keying
CCIF	: International Telephone Consultative Committee
CCIR	: International Radio Consultative Committee
CCIT	: International Telegraph Consultative Committee
CCITT	: International Telegraph and Telephone Consultative Committee
CEPT	: Conference of European Post and Telecommunication Administration
DPSK	: Differential Phase Shift Keying
DSB-SC	: Double Sideband Suppressed Carrier
FM	: Frequency Modulation
FCC	: Federal Communications Commission
FDM	: Frequency Domain Multiplexing
FEC	: Forward Error Correcting Code
FSK	: Frequency Shift Keying
IF	: Intermediate Frequency
ISI	: Intersymbol Interference
ITT	: International Telephone and Telegraph
ITU	: International Telecommunication Union
I Channel	: In Phase Channel
LMS	: Least Mean Square
LOS	: Line of Sight
LPF	: Low Pass Filter
LSB	: Least Significant Bit in tap weight
MSE	: Mean Square Error
MSK	: Minimum Shift Keying
MMSE	: Minimum Mean Square Error
NTT	: Nippon Telegraph and Telephone
OOK	: On Off Keying
OK-QPSK	: Offset Keyed Quaternary Phase Shift Keying
PM	: Phase Modulation
PAM	: Pulse Amplitude Modulation
PCM	: Pulse Code Modulation
PDF	: Probability Density Function
PSK	: Phase Shift Keying
QAM	: Quadrature Amplitude Modulation
QPRS	: Quadrature Partial Response Signalling
QPSK	: Quaternary Phase Shift Keying
Q Channel	: Quadrature Channel
RF	: Radio Frequency
RBQPSK	: Reduced Bandwidth Quaternary Phase Shift Keying
SSB	: Single Sideband
TDM	: Time Domain Multiplexing
TWT	: Travelling Wave Tube
XPD	: Cross Polarization Discrimination
XPI	: Cross Polarization Isolation

Mathematical Notation

$\bar{A}$	: A after the quantization effect of ADC
$\breve{A}$	: A after the quantization effect of ADC and finite arithmetic
$\hat{A}$	: A value in the decision directed operation
$\underline{A}$	: Matrix A
img $\underline{A}$	: imaginary part of matrix $\underline{A}$
real $\underline{A}$	: real part of matrix $\underline{A}$
$\underline{A}^*$	: conjugate of matrix $\underline{A}$
$\underline{A}^t$	: transpose of matrix $\underline{A}$
$\underline{A}^h$	: conjugate and transpose of matrix $\underline{A}$
$\|a\|$	: absolute value of a
Int{a}	: integer format of a
Max(A,B)	: take the maximum value between A and B
E<.>	: statistical expectation operator

Mathematical Glossary

$E\langle|e_{final}|^2\rangle$: the final MSE including the degradation due to step size

$E\langle|e_{early}|^2\rangle$: the MSE due to the early termination effect of step size

$E\langle A_k A_k^*\rangle$: $2\,[\,(2L)^2 - 1\,]\,/\,3$, the average power of an ideal channel

Δ_q : noise power due to quantization error in ADC

Δ_c : noise power due to arithmetic rounding error

$\Delta_{u'}$: difference of MMSE for u=u' and u=u'/50

φ : rotation angle between I and Q channel, refer to Fig 4.2

θ : demodulation phase

$\emptyset$: sample phase

β : correction factor for the degradation due to finite step size for the T-spaced equalizer

$\mathcal{E}_{min}$: ideal minimum mean square error for a given channel and number of taps in equalizer

$(\mathcal{E}_{min})_s$: $\mathcal{E}_{min}$ corresponds to BER of 10^{-3}

C/N : Carrier to Noise ratio

$(C/N)_s$: Carrier to Noise ratio corresponds to BER of 10^{-3}

$\underline{C}$: tap weight matrix

$\underline{C}_{opt}$: optimum tap weight matrix

$\underline{D}$: cross-correlation matrix, $D_i = E\langle A_m (\sum_{k=-\infty}^{\infty} A_k P^{\theta\emptyset}{}_{m-i-k})^*\rangle$

$\underline{D}'$: $\underline{D}/E\langle A_k A_k^*\rangle$, normalized auto-correlation matrix

$\underline{R}$: $\underline{U} + \underline{V}$, auto-correlation matrix

$\underline{R}'$: $\underline{R}/E\langle A_k A_k^*\rangle$, normalized auto-correlation matrix

$\underline{U}$: covariance matrix of the signal comprising the received samples,

$$U_{ij} = E\langle (\sum_{k=-\infty}^{\infty} A_k P^{\theta\emptyset}{}_{m-j-k})(\sum_{k=-\infty}^{\infty} A_k P^{\theta\emptyset}{}_{m-i-k})^*\rangle$$

$\underline{V}$: covariance matrix for the noise in the received samples $V_{ij} = E\langle V_j V_i^*\rangle$

A_m : desired response at time mT

b : fade depth in the 3-ray model

B : $P_{av}/E\langle A_k A_k^* \rangle$, normalize average power

c/r : $n/E\langle A_k A_k^* \rangle$, normalized noise power, where c is the radio parameter and r is carrier to noise ratio

C_n : tap weight element n

C_n' : optimum tap weight element n

C(jw) : frequency response of the equalizer

d : correction factor for $\sum_{i=-N}^{N} Q_i Q_i^* \sum_{j=-N}^{N} Q_j Q_j^*$ estimate

d' : correction factor for the degradation due to finite step size for the T/2-spaced equalizer

e : instantaneous error between equalizer output and desired response

e_I : instantaneous error between equalizer output and the desired response of I channel

e_{min} : instanteous error for the optimum tap weight values

$E_f(jw)$: overall folded frequency response of H(jw)C(jw) from 0 to 1/T

ERR : difference between the desired response and the result from the decision directed operation

f_o : fade notch position referred to band-center in Hz

g : equalizer gain

g' : equalizer gain with MMSE

H(jw) : frequency response of the overall channel including transmitter, receiver and transmission channel

$H_f(jw)$: overall folded frequency response of H(jw) from 0 to 1/T

l_c : arithmetic range for tap weight

2L : total number of levels in I or Q channel

M : total number of states in QAM system

M(jw) : frequency response of multipath fading channel

n : Gaussian Noise power

n_1 : number of bits in ADC

n_2 : number of bits in finite precision arithmetic

n_3 : step size in terms of number of LSB of tap weight

n_3' : minimum n_3 value to avoid early termination effect

N_q : extra mean square error due to quantization in ADC

N_c : extra mean square error due to rounding error in arithmetic

$N(jw)$: frequency response from $(1+a)/(2T)$ to $(3-a)/(2T)$

$P^{\theta\emptyset}$: pulse response of $H(jw)$ with sample phase $\emptyset$, demodulation phase θ.

P_{total} : total input power in the equalizer on 1 ohm resistor, i.e. $(2N+1)P_{av}$ for the T-spaced equalizer

P_{av} : average power on 1 ohm resistor

$Q(t)$: baseband received signal at time t

Q_k : baseband received signal at time kT

S : summation of the square of the tap weight element

$S(jw)$: frequency response from 0 to $(1+a)/(2T)$ and $(3-a)/(2T)$ to $2/T$

T : symbol period

T_d : delay time in the 3-ray model

u : step size

u' : step size corresponds to maximum convergence rate during initial start up condition

u_{max} : maximum step size

W_o : fade notch position referred to band-center in rad/s

x : quantization error in ADC

y : rounding error in arithmetic

Z^+ : positive integer

CHAPTER 1 INTRODUCTION

The growth of LOS digital radio has been rapid since the early 1970's. Compared with optical fiber, it is much cheaper to install digital radio systems -- particularly over rugged terrains. Compared with satellite, digital radio provides much better bandwidth efficiency, i.e. it offers higher bit rate per frequency bandwidth, as well as providing a much smaller propagation delay. It is anticipated that these features will result in LOS digital radio continuing to grow in application at least over the next two or three decades.

The main trend in LOS digital radio technology development is to increase the bandwidth efficiency, and this can be accomplished by two separate techniques.

(1) Frequency Re-use

The most common re-use technique is dual-polarization where the horizontal and vertical polarizations are deployed to achieve simultaneous transmission with dual channels and hence doubling the bandwidth efficiency. Co-channel or overlapping interleaved arrangements [35] are both possible transmission methods. The current antenna technique can provide a Cross Polarization Discrimination (XPD) of ~40dB under normal conditions, which is adequate for existing radio systems like 16 QAM. However, as the number of modulation levels increases beyond 16, improved antenna design and the

incorporation of a cross polarization canceller [67,72,86] are likely to be required.

Another possible technique which is under development is to use co-frequency transmission and reception on the same link. This also relies on the high performance antenna design and the use of interference cancelling techniques.

(2) High Order Modulation

As the number of modulation levels increases, higher Carrier to Noise (C/N) ratio is required for a given Bit Error Ratio (BER). This can be implemented by increasing the system gain or simply the transmitting power. However, high level QAM systems, like 64QAM, have multi-amplitudes and hence are sensitive to the non-linearity effect of power amplifiers. Post-distortion or particularly pre-distortion are the most common techniques [44] used to overcome this problem, where a pre-defined distortion is added to compensate for the non-linearity of the power amplifier. Furthermore, the developments in GaAs FET amplifiers are expected to give further improvements, particularly for under 6GHz operation.

As for modulation levels above 64, the imperfection due to the equipment starts to increase the residual error rate. This can be overcome by employing coding technique such as Forward Error Correcting (FEC) [65,66].

Under normal conditions, these imperfections can be controlled well within 10dB of C/N when compared with ideal

case. It was discovered in the 1970's that the major technical problem in high level modulation development was on the propagation path distortion and that frequency selective multipath fading effects would be responsible for significant outages.

Various countermeasure techniques such as combining of two diversity signals, IF amplitude and time domain equalizers have been developed since the 1970's. As the number of modulation levels increases, the complex signal processing capabilities of the time domain equalizer is expected to play an increasingly important role in radio development because only limited improvements can be achieved from IF amplitude equalizers and diversity techniques.

Although both baseband and IF equalizer implementations are possible, the baseband structure is normally preferred because of its lower frequency operation. It is anticipated that this type of equalizer will be required equipment in all the future radio systems. They will not only compensate for the multipath distortion, but also for some of the imperfections of the equipment such as filter limiting, carrier phase offset, cross polarization distortion .. etc.

The use of digital baseband transversal equalizers for combating multipath fading is the primary subject area of this thesis. In chapter 2, after a brief review of microwave radio and international standards, various modulation techniques are discussed and compared. Following a discussion

on the propagation degradation, multipath fading models are described and their characteristics compared.

Chapter 3 deals with current diversity systems and IF amplitude equalizers which appear to be the 1st generation equalizer technology for multipath compensation. The importance of the more sophisticated transversal equalizer is also outlined here and its benefits are discussed.

In chapter 4, the basic theory of the symbol spaced adaptive equalizer and the Least Mean Square Algorithm (LMS) are described for a generalized QAM system. The effects of finite step size, limited number of quantization levels, finite precision arithmetic, demodulation phase and sampling phase error are all addressed.

Chapter 5 extends this to the half symbol spaced equalizer which provides superior filtering and equalizer properties. The only evident problem in this structure, susceptibility to ill-conditioning behaviour, is explained in detail.

Chapter 6 extends these structures to decision directed operation, investigating and analysing the existence of the local minima. It is shown that these minima correspond to the low values of equalizer gain. The importance of setting an appropriate step size value during non-stationary conditions is also discussed.

Finally in chapter 7, overall conclusions, future trends and further application for the transversal equalizers in microwave digital radio are reported.

CHAPTER 2 PRINCIPLES OF DIGITAL MICROWAVE COMMUNICATION SYSTEMS

2.1 Background History

Digital transmission by means of electric telegraph was probably the earliest method of transmitting information electronically. The earliest known transmission was in 1753, when an electrostatic generator was used as the transmitter, which was connected to an acoustic receiver via 26 wires; one for each letter of the alphabet. This system was modified by S.T. Sommering in 1809 and provided successful transmission over a 2000ft path.

In 1837, Wheaton and Cooke developed the needle telegraph; their system was adopted by the Great Western Railway company in England in 1840. On May 1844, the first public link using Morse Code telegraph apparatus was demonstrated between Washington DC and Baltimore MD. Since then, the electric telegraph has become available to the general public. In 1876, Alexander Graham Bell invented the telephone, and opened the area of analogue transmission.

During the period when telephone and telegraph cable systems were growing in the late 19th century, the development of wireless communication was also initiated. In 1896, Guglielmo Marconi successfully transmitted a Morse Code message over a distance of 2 miles by using a spark gap transmitter and a

receiver based on the Lodge coherer. By 1901, he had transmitted signals between Poldu, England and St. Johns, Newfoundland.

The early systems normally used carrier frequencies below 300MHz. The invention of the triode vacuum tube by Lee de Forest in 1907 marked the birth of microwave technology. One of the first microwave links was set up by Clavier in March 1931, across the English channel between Dover and Calais. The system (called the Micro-Ray radio) used an amplitude modulated 1.7GHz carrier. It was soon found that Amplitude Modulation (AM) did not provide the quality required for telephone traffic, so developments on Frequency Modulation (FM) were started. One of the first commercial FM links was set up by Telefunken in 1939. Since then, most commercial analogue microwave links have used frequency modulated carriers.

With the 2nd World War came the development of Radar and associated microwave devices. The invention of the Travelling Wave Tube (TWT) at that time by Rudolph Kompfner gave another breakthrough in microwave technology. It was first applied to a microwave radio by International Telephone and Telegraph Corporation (ITT) in 1952, and has been extensively used since then.

During the 1930's, Frequency Division Multiplexing (FDM) was widely used in microwave radio. In FDM, the allocated frequency band is divided into small segments with one

assigned to each voice band. However, noise and distortion accumulate over a long multi-hop system. Initial studies into sampling and Time Division Multiplexing (TDM) were also made at that time. In TDM, time is divided into a number of time slots one for each transmitted channel. It was found that TDM was best suited to the transmission of digital signals.

In 1937, Reeves from the Paris laboratories of ITT invented Pulse Code Modulation (PCM). The French patent was filed in 1938, and was followed by British and American patents in 1939 and 1942 respectively. In PCM, the analogue signal is first sampled, then quantized, and encoded, to generate a digital signal representing the quantized analogue signal. Unlike FDM, the overall performance of PCM is virtually independent of distance if regenerative repeaters are used. However this requires precise timing between transmitter, repeaters and receiver. Although it occupies more bandwidth, the required extra bandwidth was cheap and easily obtainable at that time.

Little further work was done until 1948, when studies at Bell Laboratories demonstrated that PCM was well understood. However, the international acceptance of FDM systems and the hardware complexity of PCM hindered its development into a marketable product. Furthermore, advancements in analogue systems also delayed the shift in emphasis to digital. With the advent of the transistor and semi-conductors in the 1950's, realistic development of PCM became possible. By the late 1950's, the American Telephone and Telegraph Corporation

(AT&T) began to develop the T1 carrier system (1.544Mb/s) which has a capacity of 24 voice channels. The first commercial application was in Ohio, in 1962.

The success of the T1 carrier system created a milestone for digital transmission. Since then, PCM has been widely accepted and adopted all over the world; the Japanese 24-channel PCM system went into service in 1965. One of the first PCM Quaternary Phase Shift Keying (QPSK) radio system was also developed there [1]. In Europe, most countries used a 24-channel format initially and changed in the 1970's to a 30-channel format (2.048Mb/s) to accommodate more signalling facilities.

The growth of PCM and data communications led to the rapid development of digital communication. The motivation for "going digital" has grown steadily and a lot of effort has gone into LOS digital microwave radio since the 1960's. The early systems used Pulse Amplitude Modulation (PAM) and multi-Phase Modulation (PM). Due to advances in technology and studies on propagation paths, the modulation scheme switched from QPSK in the early 1970's to 16QAM in the late 1970's, with a doubling of bandwidth efficiency. Recent developments in semi-conductors and applications of signal processing to adaptive equalizers have even enabled the use of the 64QAM scheme, with a further 50% increase in bandwidth efficiency compared with 16QAM. This provides efficiencies comparable to that of FM radio. A 256QAM scheme is also under development at Nippon Telegraph and Telephone (NTT) [2]. The

introduction of such high level modulation schemes will give further advances in digital microwave radio.

Although the capacities* of existing digital microwave radio are still far below that of Single Side Band (SSB) AM systems, the capability of handling various types of data, virtual independence of path length and greater economy per kilobit of transmitted data make digital transmission more attractive than the corresponding analogue system in most conditions.

2.2 Digital Microwave System Configurations

2.2.1 Transmitter & Receiver

A typical simplified block diagram of a multi-channel radio transmitter is shown in Fig 2.1. The input traffic streams enter a scrambler circuit to eliminate the transmission of discrete spectral line components. The scrambled data is then encoded to a proper format for application to the digital modulator. Normally differential encoding is used to get round the need for a coherent reference signal at the receiver. Furthermore, Gray coding may also be incorporated to reduce the Bit Error Ratio (BER). Fig 2.2 [3] shows the constellation diagram of a 64QAM system. The first two bits are differential encoded to denote a quadrant signal. The remaining four bits are represented as a decimal number

*number of voice circuit per RF channel (one polarity)

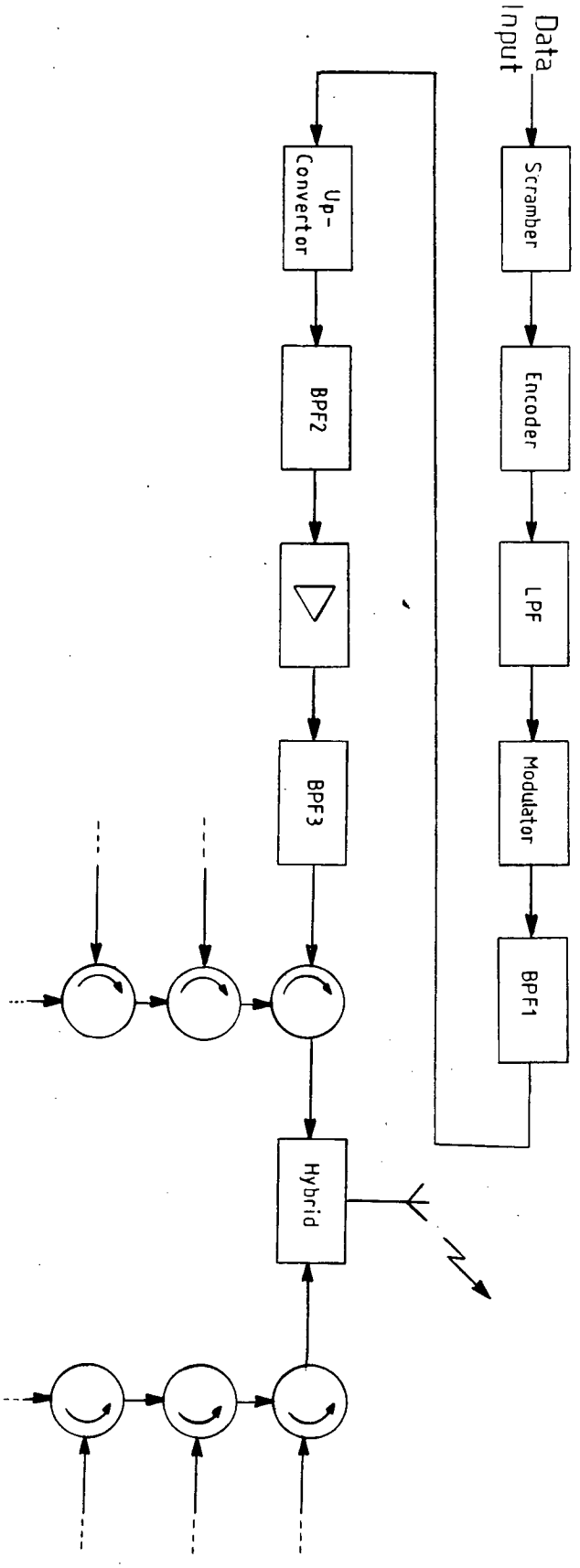

Fig 2.1 Block Diagram of a multi-channel transmitter

corresponding to the Gray code, such that adjacent states differed in only one bit position.

The baseband low pass filter (LPF), Intermediate Frequency (IF) bandpass filter (BPF1) and Radio Frequency (RF) bandpass filters (BPF2 & BPF3) are all used to control the transmit spectrum; any combination of them may be used in a practical radio system. The encoded data passes through a modulator and varies the amplitude (AM), frequency (FM), phase (PM) or a combination of these parameters, on a high frequency sine wave carrier. For practical reasons, it is advisable to use the same intermediate frequency already recommended for

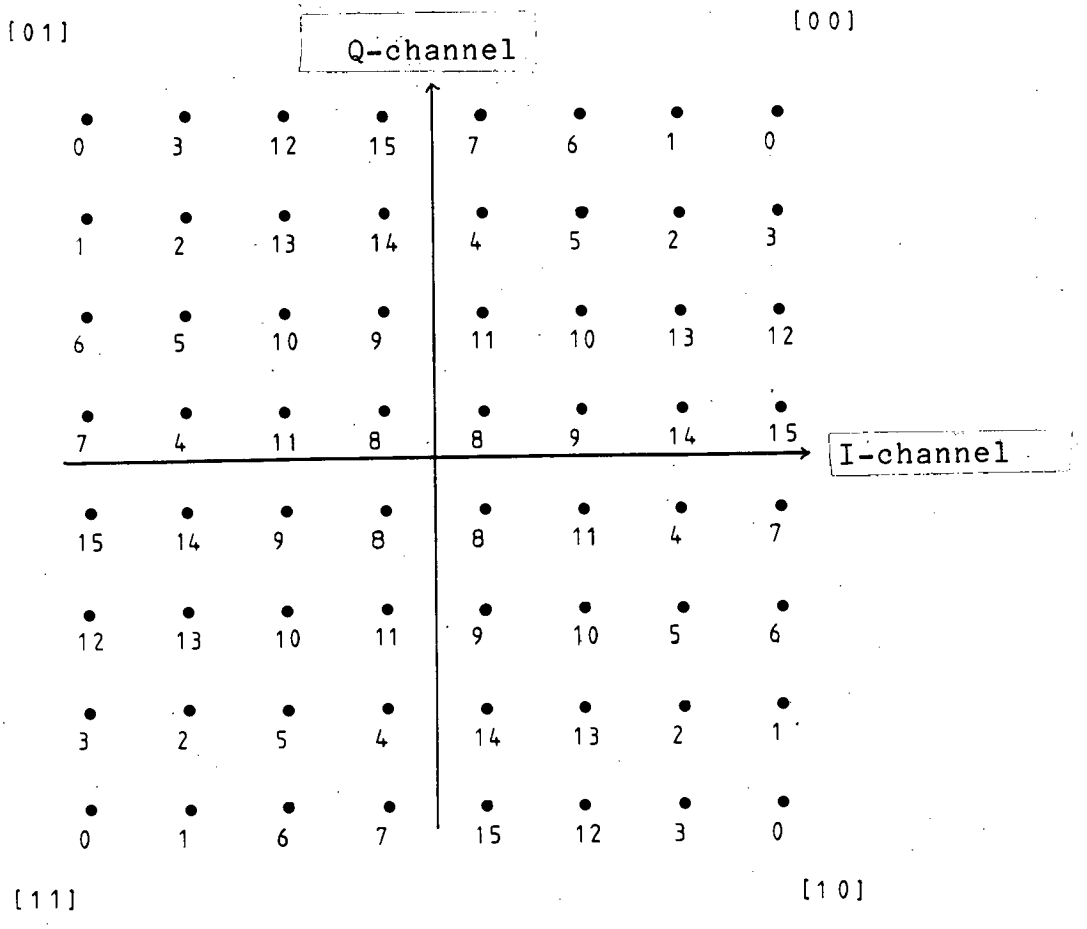

Figure 2.2 Constellation Diagram of a 64QAM

analogue systems -- 70MHz or 140MHz [4]. Modulation schemes will be discussed in detail in section 2.4.

The modulated signal is then up-converted to RF and amplified. The RF signal is connected to other channels via RF circulators to cross polarization filters which provide combined polarization diversity signals to the transmit antenna. This dual polarization scheme can be used for independent transmission at the same frequency or adjacent channels can be overlapped on a given route. The channel capacity is thus doubled without increasing bandwidth.

The radio waves are concentrated into highly directional beams by the antenna. For sufficient transmission quality, the path between the transmit and receive antennae must have adequate clearance to obstacles which cause obstructive fading. Hence such antennae are normally mounted on towers.

At the receiver side, the reverse process is employed in order to retrieve the original data.

2.2.2 Repeater

For long distance transmission, repeaters are normally required. The distance between repeaters is typically from ten to a few tens of kilometers (km) for under 10GHz, depending on the radio system design, terrain factor..etc.

In some countries, e.g. the U.S.A., the spacing between repeaters is limited by regulations. Table 2.1 [5] lists the

minimum transmission path length for different frequency bands. Most digital microwave radio systems use regenerative repeaters; the received signal goes through the complete demodulation-regeneration-modulation process. Noise and distortion are largely removed by this process, and so are not accumulated.

Frequency Band (GHz)	Distance (km)
2.110 - 2.130	5
2.160 - 2.180	5
3.700 - 4.200	17
5.925 - 6.425	17
10.700 - 11.700	5

Table 2.1 Minimum Repeater Spacing in U.S.A.

2.3 International Standards for Telecommunications

With the need for telecommunication services to cross national boundaries, the requirement for co-ordination of systems became significant. It is widely recognized that the International Telecommunication Union (ITU), has profoundly influenced the development and evolution of telecommunications. Even though it does not have regulatory

power, its recommendations are highly respected and implemented by most nations. A brief history of the ITU is as follows [6,7,8]:

1865 International Telegraph Union established by 20 European states

1923 - 1925 International Telephone Consultative Committee (CCIF) and International Telegraph Consultative Committee (CCIT) established.

1927 International Radio Consultative Committee (CCIR) established.

1932 International telegraph and radiotelegraph conference combined to form ITU. The new term "Telecommunication" was first defined as "Any telegraphic and telephonic communication of signs, signals, writing, facsimile and sounds of any kind, by wire, wireless or other systems or processes of electric signalling or visual signalling (semaphores)."

1956 CCIF and CCIT combined to form International Telegraph and Telephone Consultative Committee (CCITT).

The ITU has four permanent organs, the General Secretariat, the International Frequency Registration Board (IFRB), CCIR, and the CCITT. Among them, CCIR is responsible for technical matters and operating questions relating to radio communications, and CCITT covers the standardization of techniques and operations in telecommunications. Currently there are 11 and

15 study groups in CCIR and CCITT respectively, and two joint study groups from CCIR and CCITT. Study groups 5 and 9 of CCIR are in the area of "Propagation in Non-ionized Media" and "Fixed Service using Radio-Relay Systems" respectively, and study group XVIII of CCITT is in "Digital Networks". The results of the study groups are mainly presented in the form of reports and recommendations, and are published in a series of volumes which are re-issued and brought up to date after each Plenary Assembly. The XVth and VIIIth Plenary Assemblies of CCIR and CCITT were held in 1982 and 1984 respectively. The English version of the CCIR documents consist of green covered volumes and are always referred to as "The Green Books". The colour of the CCITT documents' covers changes after each Plenary Assembly, and it is quite common to refer to each issue by its colour.

In Europe, the Conference of European Posts and Telecommunications Administrations (CEPT) was formed in the late 1950's. It has two committees -- the Post Committee and the Telecommunications Committee. Its Working Groups work closely with CCITT, and provide collaboration in Europe.

The frequency allocations recommended by CCIR for digital microwave systems are shown in Table 2.2 [9-14]. Due to the rapid growth of digital systems, more frequency allocations are to be established. This was agreed after the Interim meeting of study group 9 of CCIR in 1984 [4]. Recommendation 594 [15] and Report 930 [16] concerning the performance

Frequency Range (GHz)	Channel Spacing (MHz)	no of Channels (go and return)	Capacities	CCIR Rec number
1.70 - 1.90 1.90 - 2.10 2.10 - 2.30 2.50 - 2.70	14	6	low/medium	283-4
3.80 - 4.20	29	6	2 X 34Mb/s 2 X 45Mb/s	382-3
6.43 - 7.11	40	8	140 Mb/s	384-3
10.70-11.70	40	22	low/medium	387-3
12.75-13.25	28	8	2X34Mb/s *	497-2
	14	addit-ional	2X8.4Mb/s	
17.70-19.70	220	2X4 **	2X140Mb/s	595
		7		
	110	2X8 **	140 Mb/s	
		15		
	27.5	2X35 **	34 Mb/s	

* if dual polarization is used

** dual polarization is used in the co-channel arrangement

Table 2.2 Frequency Allocations Recommended by CCIR

objective of digital radio systems were also revised after this meeting. The new drafted recommendation 594, for a 2500km hypothetical reference digital path (HRDP) of 64kb/s channel, is as following:

(1) BER should not exceed 10^{-6} during more than 0.4% of any month with integration time one minute.

(2) BER should not exceed 10^{-3} during more than 0.054% of any month with integration time one second.

(3) total error seconds should not exceed 0.32% of any month.

Some countries have their own regulations and frequency allocations, such as the Federal Communications Commission (FCC) in U.S.A. The FCC regulations are probably the most stringent at the present time. Table 2.3 lists the allowable bandwidths* and minimum capacities for voice transmission below 15GHz [5]. Dual polarization is allowed to achieve the required minimum capacities. AT&T in U.S.A also provides technical guidelines, see for examples in Bell 43501 [17], 43502 [18] where the requirements and objectives of 6 and 11GHz digital microwave radios respectively are specified.

Not only the frequency allocations and regulations, but also the digital hierarchies are different in some countries. There are now at least four hierarchies; dominated by North America, Japan and Europe, as shown in Table 2.4 [19]. This

*The definition of FCC bandwidth can be found in [5]

Frequency Range (GHz)	Bandwidth (MHz)	Minimum Number of voice channels
2.110 - 2.130	3.5	96
2.160 - 2.180	3.5	96
3.700 - 4.200	20	1152
5.925 - 6.425	30	1152
10.700 - 11.700	40	1152

Table 2.3 FCC Regulations on Frequency Allocations

	information rate Mb/s(no of voice channels)		
Hierarchy level	North America	Japan	Europe
1	1.544 (24)	1.544 (24)	2.048 (30)
2	6.312 (96)	6.312 (96)	8.448 (120)
3	44.736 (672)	32.064 (480)	34.368 (480)
4	274.176 (4032)	97.728(1440)	139.268(1920)
	432 *	397.2 (5760)	565 *
	1300 *	800 *	1200 *

* Nominal value only, precise rates to be agreed and released

Table 2.4 Principle Digital Hierarchies

divergence is a significant impediment to efficient communication on a global basis.

2.4 General Modulation Techniques

2.4.1 Amplitude Modulation (AM)

AM is the most familiar modulation process. For a binary signal, the general form of Double Sideband carrier (DSB) AM is

$$A(t) = G [1 + m(t)] \cos(wt)$$

where m(t) is the modulating signal and may be 0 or 1; w and G are respectively the frequency and amplitude of the carrier. Since the carrier contains no information, efficiency can be increased by using the Double Sideband Suppressed Carrier (DSB-SC) technique, which has the form

$$A(t) = G\, m(t) \cos(wt)$$

For digital modulation, the carrier is switched on and off to implement On-Off-Keying (OOK).

Another form of AM is known as PAM. Here the binary input signal is coded several bits at a time and converted into a multi-level PAM signal. This technique was used in an early radio system [20].

Although the hardware realizations for the above modulation methods are simple compared with others, they are seldom applied to new digital radio systems, for the following reasons:

(1) poor utilization of the transmitted power, i.e. they require high C/N for a given BER
(2) sensitivity to non-linearity of power amplifiers
(3) sensitivity to multipath fading

2.4.2 Frequency Modulation (FM)

Unlike AM, FM keeps the amplitude constant but changes the frequency of the carrier. For digital transmission, the simplest FM waveform is two level Frequency Shift Keying (FSK). Two separate frequencies will be switched in the modulator according to the input signal states (0 or 1).

There are many versions of FSK, e.g. Minimum Shift Keying (MSK) [21]. Unfortunately, their wide main lobes give them poor efficiency when compared with the corresponding Phase Shift Keying (PSK) technique in application to LOS digital radio.

However, FSK and its variations still have application in many area of communications. For example, two level FSK is commonly employed in voiceband modems for transmission over voice grade telephone lines at rates of 1800 b/s and below, where bandwidth is not a serious problem. See for example,

the V.23 recommendations of CCITT [22]. However, at rates of 2400 b/s to 4800 b/s, phase modulation is standard because it offers efficient spectral utilization with acceptable insensitivity to noise and phase jitter.

2.4.3 Phase Modulation (PM)

PM is one of the most popular techniques in digital microwave radio systems. the generalised form for Phase Shift Keying (PSK) is

$$A(t) = G \cos(wt+\theta)$$

where the instantaneous phase, θ, may have any of the discrete set of values $2\pi k/M$, $0 \leq k < M$, where M is the number of states in the modulator. The simplest modulation scheme is binary PSK (BPSK) where M=2. LOS microwave radio systems usually use Quaternary PSK (QPSK) where M=4 and octal PSK (8PSK) where M=8.

PSK can be detected coherently or Differentially (DPSK). Coherent detection requires a synchronised phase reference signal. This signal can be obtained from a separate pilot tone [23], or more normally extracted from the incoming signal by some non-linear method, e.g. a Costas Loop [24]. In this case, differential encoding is often employed to eliminate the difficulties of distinguishing constant phase offset, e.g. 0^{o} and 180^{o} in BPSK. In differential encoding, the present phase is chosen with respect to the previous

phase. The constant offset problem can thus be eliminated. This results in a slight degradation in C/N, since a current bit decision error will induce another error on the subsequent bit.

In DPSK, the phase reference is provided by the previous bit, so no absolute phase reference is required. This introduces noise on both ports of the demodulator. For a given BER, DPSK will require a higher C/N than normal PSK. Differential encoding is also used in DPSK. The difference between DPSK and differentially encoded PSK is in the phase detector. No attempt is made to extract a coherent phase reference in DPSK.

With normal QPSK, an abrupt phase transition of 180^{o} may occur when the In-phase channel (I) and Quadrature channel (Q) are added together. The carrier envelope may then go to zero after bandpass filtering. This is overcome in Offset Keyed QPSK (OK-QPSK), or so-called staggered QPSK, where the symbols in the Q channel are shifted by T/2 with respect to the I-channel; T being the symbol duration. Hence when I and Q are added together, the possibility of 180^{o} phase change is avoided, but phase changes will occur every T/2 instead of T. Another significant improvement of OK-QPSK is its lower value of signal to phase reference noise ratio [25]. This offset scheme can be applied to other two dimensional modulation systems e.g. M-QAM.

However it has been shown that offset keying increases the degradation caused by a given amplitude slope in a distorted

channel [26]. Using a first order complex polynomial model of the fading channel, the inferiority of the offset scheme has been reported by Greenstein et al [27].

2.4.4 Hybrid Modulation Schemes

The most common hybrid scheme is the combination of AM and PM. This class includes Quadrature Amplitude Modulation (QAM) and Quadrature Partial Response Signalling (QPRS). Although combinations of AM and FM [28] or PM and FM [29] are also reported, their bandwidth efficiencies are poor in LOS application.

2.4.4.1 Quadrature Amplitude Modulation (QAM)

QAM is obtained by adding two 90^{o} out of phase AM signals together. It has the form

$$A(t) = G\,[\, a(t)\cos(wt) - b(t)\sin(wt)\,]$$

where a(t), b(t) are the symbols in the I and Q channels respectively, are normally chosen within the set $\{\pm 1, \pm 3, .., \pm(2N-1)\}$, $N \in Z^{+}$. For practical reasons, the total number of states is $M = 2^{p}$ where p is the largest integer satisfying the equation

$$2^{p} \leq (2N)^{2}$$

For N equals 1, this reduces to the same format as QPSK. M-QAM system can also be implemented by superimposing four M/4-QAM, one in each quadrant. See for example in [30], where 16QAM is constructed from four QPSK. This modulation scheme is commonly employed in the design of new radios because of its high bandwidth efficiency and acceptable hardware complexity.

2.4.4.2 Quadrature Partial Response Signalling (QPRS)

QPRS involves summing two duobinary signals which are generated with relative phase displacements of 90^{o}. Since the system is linear, the same result can be obtained by passing a QAM signal through a partial response filter, which has the form

$M(jw) = Y \cos(wT/2)$ for $w \leq \pi/T$

$= 0$ for other w

where Y is a constant and T is the symbol duration

See for example in [31], where 49QPRS is generated by passing a 16QAM signal through a partial response filter.

Unlike other modulation schemes, it has finite memory rather than zero memory. This implies that there is a correlation between the present bit and the previously transmitted bit, and results in spectral re-shaping [32].

2.4.5 Reduced Bandwidth Quaternary Phase Shift Keying (RBQPSK)

In RBQPSK, the bandwidth efficiency is increased by reducing the overall channel bandwidth (3dB) to about half of the Nyquist bandwidth. This inevitably causes a great amount of Inter-Symbol Interference (ISI) to such an extent that normal channel operation is not possible. This kind of ISI is deterministic and can be eliminated to some degree by an equalization method; decision feedback is found to be the most appropriate [33,34]. This type of modulation can be classified as a finite memory scheme since a decision on the present symbol will depend on the previous received symbols.

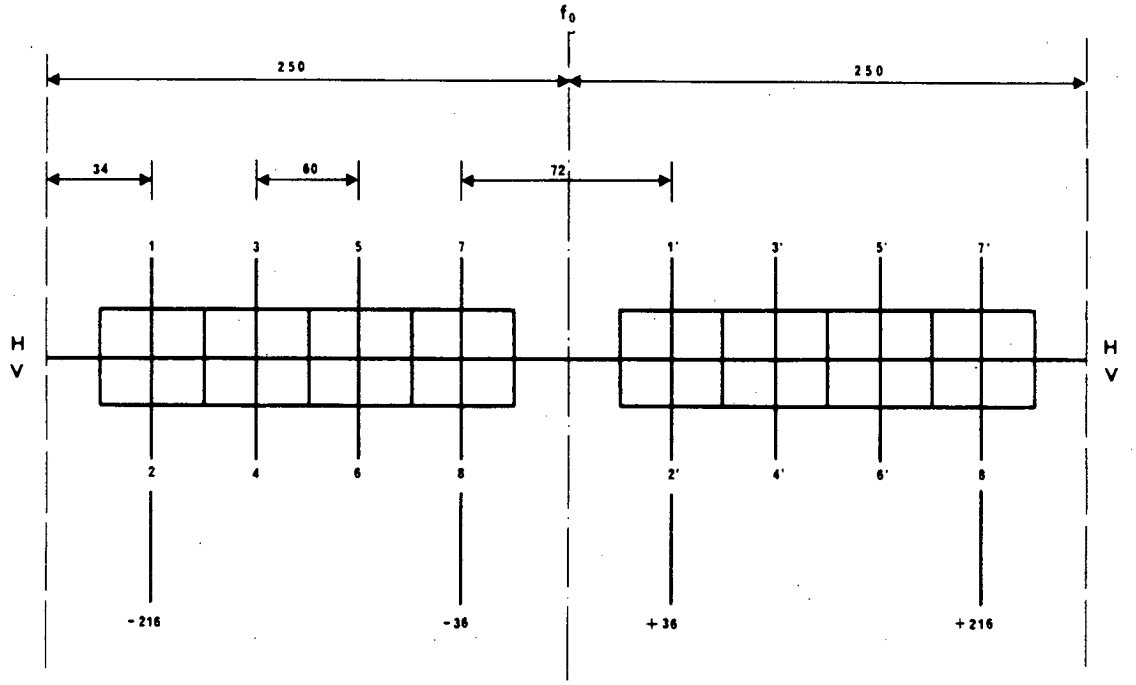

(All frequencies are in MHz)

f_0: centre frequency (MHz) = 6175 MHz
H: horizontal polarization of emission
V: vertical polarization of emission

Fig 2.3 Frequency Allocation of RBQPSK in 6GHz

The proposed plan for radio frequency channel allocation is shown in Fig 2.3 [35], for a 140Mb/s system. The channel spacing is 60MHz, about one half of that used in standard QPSK and 0.8 of the Nyquist bandwidth. This results in a doubling of the bandwidth efficiency. The 3dB bandwidth of the RF filter and baseband filter at the demodulator is approximately 60MHz and 15MHz respectively [34]. Although the channel spacing is comparable to that recommended for analogue systems -- 59.3MHz if co-polar channel planning is used [36], it is not recommended that this planning scheme be used in conjunction with an analogue system on the same route. This is because of its wide spread RF spectrum.

2.5 The Comparison of Representative Modulation Methods

Although many modulation techniques exist in digital microwave transmission, only a few are well suited to LOS radio systems. These include M-PSK, M-QPRS, M-QAM and RBQPSK. Reference [37] provides a survey of Japanese & North American digital microwave radio systems with their modulation methods and channel capacities in the late 1970's.

The chief reasons for the widespread use of these techniques are: relative simplicity of modulator/demodulator design, bandwidth efficiency and performance in an additive white Gaussian noise environment. In Fig 2.4, the relationship between BER and C/N for the above modulation techniques are

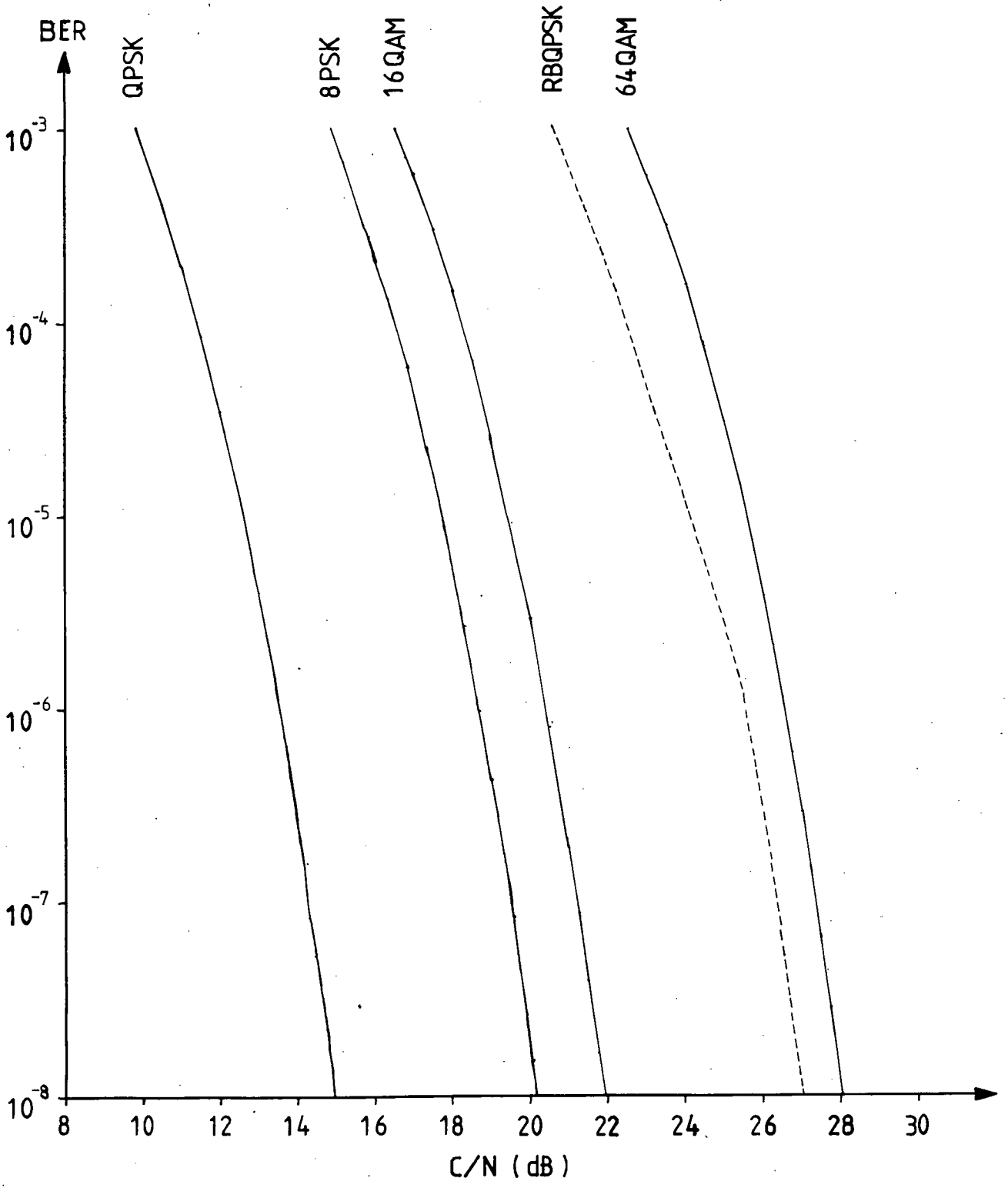

Fig 2.4 BER vs C/N for different Modulation Schemes

illustrated. All the curves, with the exception of RBQPSK [34], are plotted with ideal brick wall Nyquist filters with double sided Gaussian noise. However, the actual BER will be higher at the descrambler output because of the error multiplication. A completed Gray coding scheme is assumed. If non-Gray coding is used, the required C/N may need to be increased by ~0.5dB and ~1.4dB for QPSK and 64QAM respectively at BER=10^{-3}.

These figures will be degraded by typically 2-6dB for a practical system because of the limitations imposed by the real world, e.g. imperfect filter design, sampling phase error..etc. For the RBQPSK curve, overall filtering including equalization has been considered. The measured result is very close to the theoretical value [34]. For a practical QAM radio system with 16 states or above, a non-complete Gray coding is normally used with differential encoding. An extra ~1dB degradation in C/N is likely to be required.

Only coherent PSK has been plotted since DPSK requires ~3dB higher C/N typically for $M \geq 4$ [38]. The choice between coherent or differential detection depends on the importance of the necessary additional transmitted power. However the non-ideal extraction and generation of the carrier frequency will slightly degrade the performance of coherent PSK. The detection efficiency of DPSK may approach that of coherent PSK under noisy phase estimation conditions. Further studies into the performance of coherent and differential PSK in practical systems can be found in [38]. Again, if

differential encoding is used, the C/N ratio will be degraded by ~0.5dB at BER = 10^{-3}, for a QPSK system.

The bandwidth efficiency of 9QPRS lies between that of QPSK and 8PSK. It requires only ~3dB more C/N than QPSK, but 2.2b/s/Hz can be obtained practically [39]. The most important advantage of 9QPRS is its hardware simplicity as compared to QPSK [40]. Furthermore, it can detect errors without requiring redundant bits. For a given C/N, M-QPRS normally can give comparable performance to the corresponding QAM systems.

In the mid 1970's, QPSK and 8PSK dominated the market. The demand for high capacity, bandwidth efficient schemes in the late 1970's led to the development of high level modulation methods. Among them, five modulation schemes are likely practical candidates. The first is RBQPSK and the next four all use 16-state constellations, as shown in Fig 2.5 a,b,c,d. They are 16QAM, 16PSK, the V.29 recommendation of CCITT [41], and the constellation proposed by Foschini et al [42]. Among the four 16 state schemes, 16QAM is preferred in LOS digital microwave applications, because:

(1) The states in 16QAM are evenly packed in two dimensions. This means 16PSK and the V.29 recommendation will be more sensitive to noise and ISI under the same peak power condition. 16PSK requires ~3dB higher C/N typically.

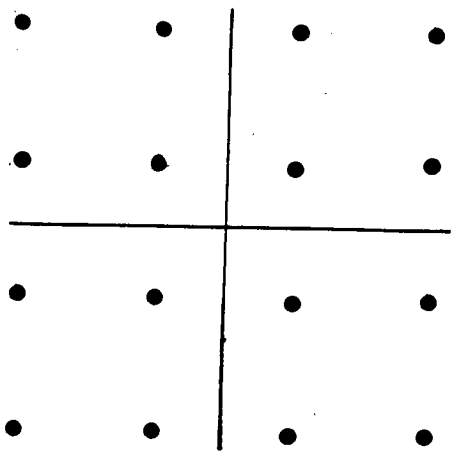

(a) 16QAM

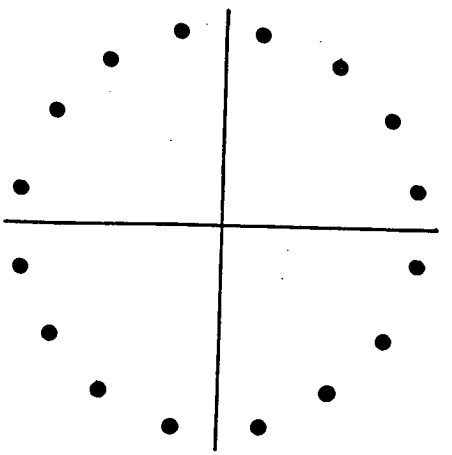

(b) 16PSK

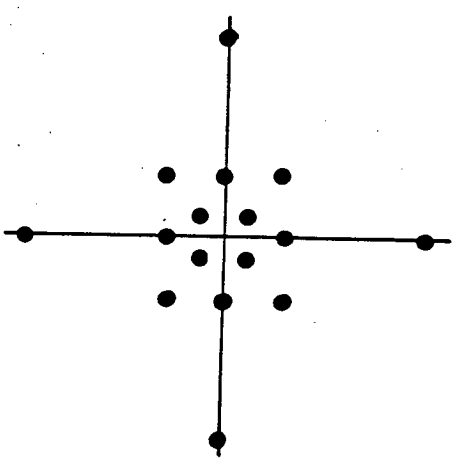

(c) V.29

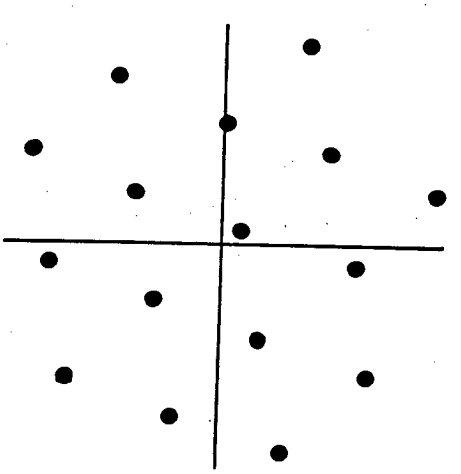

(d) Optimun

Figure 2.5 Four 16 Constellation Schemes

(2) Modulation and Demodulation are simple. Although the constellation in Fig 2.5d can provide the best possible resistance to Gaussian noise, the improvement is only ~0.5dB compared to that of 16QAM and the hardware will be more complex to implement.

However, in a voiceband modem when phase jitter is the important degradation factor, V.29 is recommended.

This led to the development of 16QAM and RBQPSK. In the U.K., RBQPSK was adopted because of: (1) the previous experience gained in the design and operation of existing QPSK, (2) basically the same equipment as a conventional QPSK is required, except for the narrow channel filters and equalizer. As a result, RBQPSK appeared to be the simplest and cheapest, and could provide an economical solution in the 1980's. However, further development of this modulation scheme will be limited. For example, further reducing the bandwidth to increase the efficiencies not only increases the ISI, but also causes severe pattern dependent demodulated symbol level variations.

Although the number of voice channels per RF channel of RBQPSK is comparable to that of 16QAM, its transmit spectrum spreads very widely. When the FCC bandwidth [5] is used as a measurement standard, its bandwidth efficiency is less than that of 16QAM. Therefore RBQPSK does not appear to be an appropriate solution for the U.S.A. and countries where digital and analogue links may co-exist on the same route.

Furthermore, the performance of RBQPSK was initially uncertain; this led to the development of 16QAM in most countries in the late 1970's.

The success of 16QAM in the early 1980's and the increased demand for digital transmission led to the development of 49QPRS and 64QAM. This made the transmission of 3XDS3 streams (3X44.7Mb/s) in a 30MHz bandwidth* become practicable. An even higher order modulation scheme -- 256QAM is also under development at NTT [2] in Japan. The success of this will greatly depend on the equalizer design and the non-linear compensation technique needed for the power amplifier. This perhaps places a limit on QAM(256) and QPRS(225) scheme in this decade. Further increases to 1024QAM or 961QPRS in 30MHz bandwidth* sound impractical at present.

2.6 Microwave Line-Of-Sight Propagation

Under normal atmospheric conditions, with the refractive index of air close to 1, the free space attenuation between two isotropic antennae is given by [45]:

$$20 \log \left(\frac{4\pi d}{\lambda} \right) = (92.5 + 20 \log d + 20 \log f) \text{ dB}$$

where d : distance (km)

λ : wavelength (km)

f : frequency (GHz)

*FCC bandwidth [5]

This type of attenuation can be simply overcome by using directional antennae and high transmission power. However, it is the anomalous behaviour of the atmosphere that gives the major problems in LOS transmission. The radio waves do not in fact travel in exactly straight lines. This is because the refractive index n of the lower atmosphere is a function of atmospheric pressure P (mb), water vapour pressure e (mb) and absolute temperature T_t (^oK), related as [46] follows:

$$(n-1)\ 10^6 = \frac{77.6}{T_t}\ \left(P + 4810\ \frac{e}{T_t} \right)$$

Normally the refractive index has a negative vertical gradient and is not a function of horizontal distance in most conditions. This means the radio wave may be refracted and undergo bending in the vertical plane. However this propagation path can be considered as being rectilinear above a hypothetical earth of effective radius "ka", where "a" is the nominal value of the earth radius and "k" is a correction factor. This "k" value varies according to atmospheric conditions and the length of the path. For a 50km long path in a continental temperate climate, "k" will be greater than 0.8 for more than 99.9% of the time [43].

Variations in atmospheric conditions may produce a positive gradient of refractive index. The radio waves will then bend in such a way that the earth becomes an obstructive object and introduces diffraction fading. This is equivalent to a low value of "k" for a rectilinear radio wave. This type of fading can be alleviated by installing antennae at sufficient

height so that 60% of the first Fresnel Zone radius is cleared even with a minimum value of "k" [43].

2.6.1 Multipath Fading

Due to the imhomogeneous refractive index and non-ideal characteristics of the antennae, the frequency response of the radio path can be expressed as

$$M(jw) = a + \sum_{i=1}^{\infty} a\, b_i \exp(-wT_{d_i})$$

$$= a \left[1 + \sum_{i=1}^{\infty} b_i \exp(-wT_{d_i}) \right] \quad \ldots\ldots\ldots\ldots\ldots\ldots (2.1)$$

where "a" is the amplitude of the main ray (the strongest ray), "$a\, b_i$" and "T_{d_i}" are the amplitude and phase of the interference rays respectively and $b_i \geq 0$.

Under normal conditions, the main ray is dominant, the effects of interference rays are negligible, i.e. $b/a \ll 1$. An anomalous propagation may occur when there is a rapid variation or discontinuities in the refractive index, or when reflections from the ground become significant. The main ray may diverge from the receive antenna and the magnitude of the interference rays may increase. This results in so-called multipath fading.

Investigations on multipath properties for LOS microwave links started in the 1950's at AT&T, using the swept

frequency [47] and the short pulse response [48] method for a path of 22.6 mile over-water. The results showed that more than three significant interference rays with delay time up to ~11ns might occur. Since then, experimental studies have been undertaken in other countries.

In 1971, Ruthroff from AT&T [49] estimated that the maximum path delay time caused by a layer of air having anomalous refractive index, equals 3.7 (L/20)^3 ns, with L being the path length in miles. This seems to be corroborated by some measured results. Early studies emphasised on path length differences or path delay times, and their impact on FDM-FM systems. It was soon found that multipath would mainly degrade the received signal level in FDM-FM systems, and could be overcome by simply increasing the transmitted power. The term "Fade Margin" is applied to the maximum allowable fade depth for a given criterion, and is often used as a performance factor in FDM-FM systems.

With the growth of digital LOS microwave radio systems in the 1970's, it was soon found that this concept could no longer be universally applied. Multipath fading will not only decrease the received signal power but also causes inband amplitude and delay distortions. This introduces ISI and cross talk in quadrature channels, and is responsible for most of the outage in digital systems during multipath fading. See for examples in [50], where the experimental outage distribution (BER$\geq 10^{-3}$) of a 45Mb/s, 8PSK, 4GHz radio was plotted, as shown in Fig 2.6. Only ~1/6 of the total outage

is caused by fades deeper than the "Fade Margin". The system outage is not sensitive to the transmitted power [87]. This was also confirmed by experiments carried out in the U.K. [51]. Various authors introduced new concepts like "Effective Fade Margin" [52], "Composite Fade Margin" [64] or "Net Fade Margin", to compare with the traditional "Fade Margin" or the so-called "Flat Fade Margin". The probability density function of fading characteristics also depends on path length, terrain factor..etc., and can be found in [53].

In dual polarization schemes, multipath fading also introduces cross talk between orthogonal channels. Cross Polarization Discrimination (XPD) and Cross Polarization Isolation (XPI) are often used as a measure of this cross talk. XPD is defined as the ratio of the co-polarized to the cross-polarized received signal with only one polarization channel being transmitted. XPI is defined as the ratio of the co-polarized signal to the cross-polarized signal in that channel with both the orthogonal polarization channels transmitted at the same power. Propagation experiments normally used XPD for ease of measurement.

Normally the decrease of XPD in clear weather conditions is due to multipath fading [54]. This could be a problem for a dual polarization schemes. Fortunately, the two orthogonal channels rarely fade simultaneously for the majority of time. Detailed distributions of XPD can be found in [53,55].

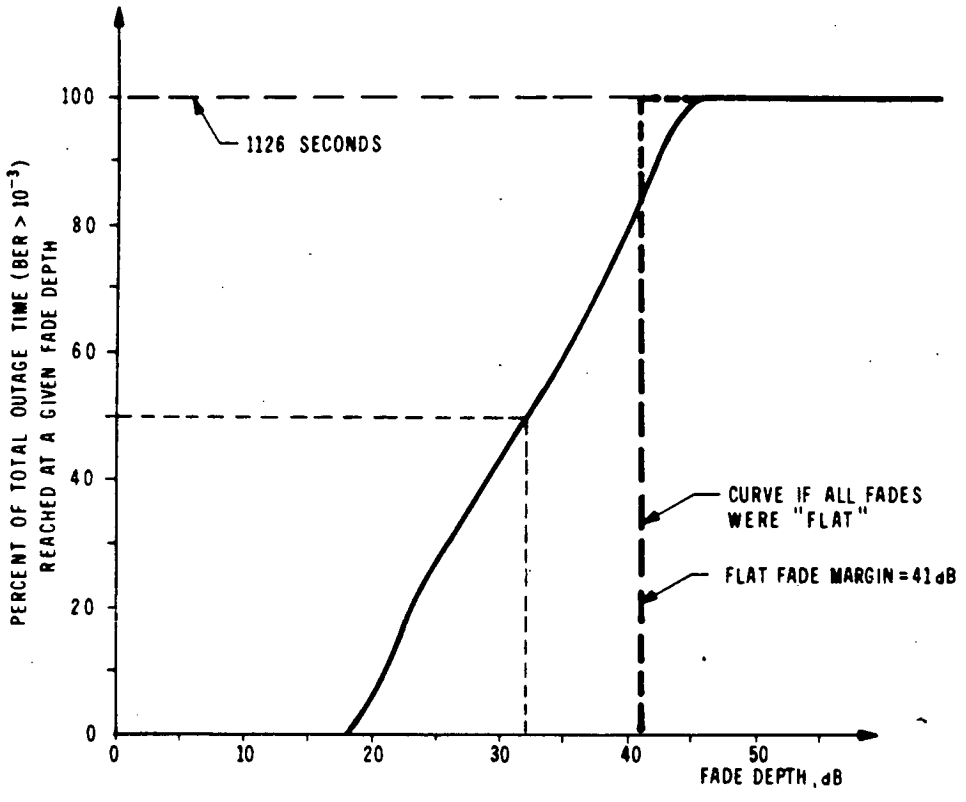

Fig 2.6 Outage distribution of a 45Mb/s 8PSK radio

2.6.2 Fading Models

Radio system performance in the presence of multipath fading conditions can be predicted if the statistics of the fade frequency response is known. This can be done by direct measurement of the IF spectrum of a radio link under multi-path fading. In most fading conditions, a notch can be found in the IF spectrum. The exact evaluation sounds impossible because the refractive index of the air is uncontrollable. However some simplified versions do give good approximations in most conditions. These are the 2-ray, 3-ray and polynomial models.

2.6.2.1 2-Ray Model

The 2-ray model is perhaps the earliest model and was widely adopted in the 1970's. It consists of a main ray and one interference ray. From equation 2.1, with a=1* , this becomes

$$M(jw) = 1 + b \exp(-jwT_d) \quad \ldots\ldots\ldots\ldots\ldots\ldots\ldots\ldots\ldots\ldots\ldots\ldots (2.2)$$

In most multipath fading conditions, this simple 2-ray model will give a reasonable prediction. The main advantages of this model are:

(1) simple for theoretical evaluation
(2) gives reasonably good predictions
(3) is easy to implement in laboratory simulations
(4) provides a physical meaning

However, the over simplification of this model does cause some constraints. For example, the delay time, T_d, of the interference ray depends on the notch position. The shape of the fade notch is described by fade depth, b, only, which is insufficient in most conditions.

In order to evaluate the performance of the radio systems under multipath fading, the idea of signature is often used. A signature is normally referred to the contours of BER with notch depths against notch positions. For BER at 10^{-4}, the speech is not noticeably affected, but at 10^{-3} or worse, the

*the value of "a" is not significant in most multipath fading conditions

circuit cannot be regarded as serviceable.* Therefore BER=10^{-4} and especially 10^{-3} are often used as contours for signature plotted, and 10^{-3} will be used throughout this thesis unless otherwise specified. Furthermore, all the signature calculations are based on assuming the Probability Density Function (PDF) of ISI is a Gaussian distribution** and Gray coding is used.

Curve A in Fig 2.7 represents the signature of a 90.4Mb/s 16QAM radio with overall 0.3 raised cosine filtering, 22.6MHz bandwidth and 70MHz IF frequency. Normally an "M" shape will be obtained. This is because the cross talk between quadra-

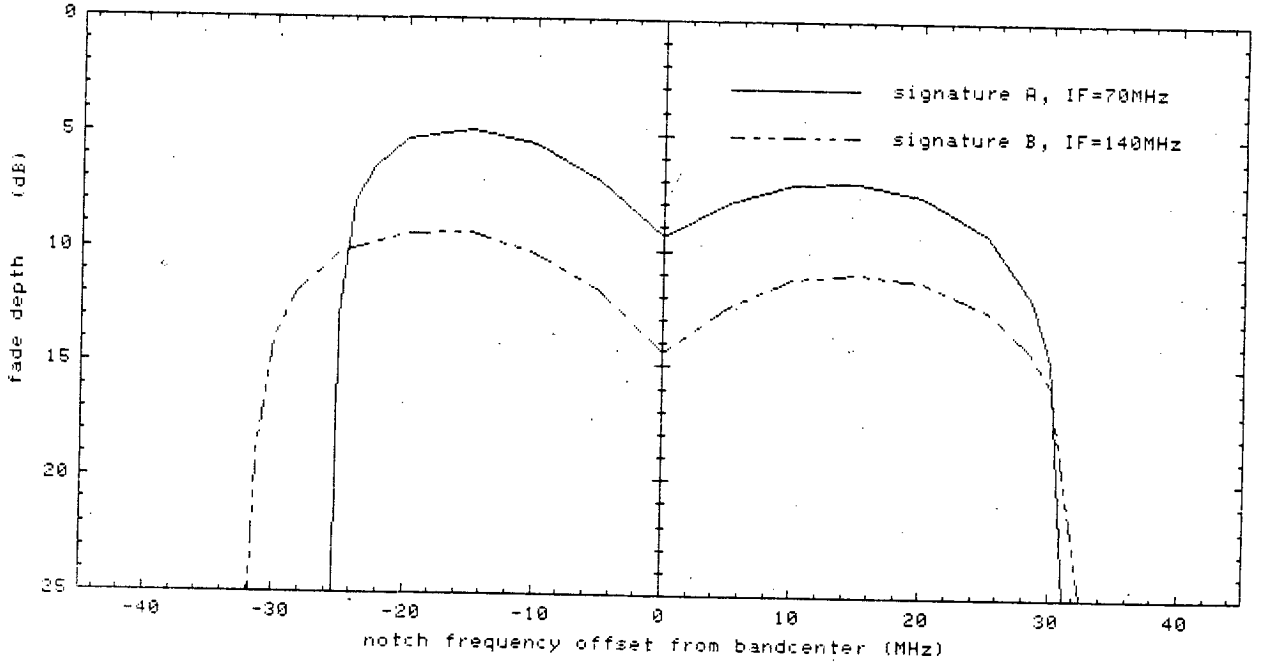

Fig 2.7 Signatures of a 16QAM Radio (2-ray model)

*BER=10^{-4} can also be used as an early warning signal for BER=10^{-3} during fading conditions.
**Refer to section 7.3 for the validation of this assumption.

ture channels is less when the notch is near the center frequency -- IF, and will be higher as it moves to the band edge. Normally the cross talk or ISI will be high for a long delay time (assuming the delay time is much less than a symbol duration) if the notch is within the Nyquist bandwidth, and vice versa. As a result, the signature will rise more quickly and drop more sharply for negative notch offsets than positive notch offsets, as shown in Fig 2.7, and will be asymmetric about its center frequency (IF).

Similarly, the signature will also change for a different center frequency. This arises from the delay time of the interference ray being different even for the same offset notch frequency. This causes a change of distortion pattern and results in a different signature. Normally for a higher center frequency, the signature will be lower but wider, as in curves A,B in Fig 2.7, where curve B has the same parameters as curve A except that the center frequency is 140MHz.

The above analysis casts severe doubt on using this 2-ray model for high reliability evaluation of multipath fading.

2.6.2.2 3-ray Model

The inconsistencies of the 2-ray model led to the development of other models, and a normal 3-ray model seems to be the next candidate. This model consists of a main ray and two interference rays, the equation 2.1 can be reduced to:

$$M(jw) = a\,[\,1 + b_1 \exp(-jwT_{d_1}) + b_2 \exp(-jwT_{d_2})\,] \quad \ldots\ldots (2.3)$$

This undoubtedly will be more accurate. However, the degeneracies for the value of a, b_1, b_2, T_{d_1}, T_{d_2} in practical measurement conditions hindered its further development. In 1978, Rummler from AT&T [56,57] proposed his simplified 3-ray model based on statistical data derived from a 26.4 mile hop near Atlanta, Georgia, U.S.A. In this model, two rays having approximately the same path length are assumed. Let us represent the amplitude and phase of this vector sum by "a" and "$w_0T_d-\pi$" respectively, where "w_0" is the radian frequency of the notch frequency and "T_d" is the delay difference between the third ray and the first two rays. With the amplitude of the third ray equals "ab", the channel frequency response is found to be

$$M(jw) = a\,[1-b\,\exp\pm(j(w-w_0)T_d)] \qquad b<1 \ast \quad \ldots\ldots\ldots\ldots (2.4)$$

The plus and minus signs in the exponent* correspond to non-minimum and minimum phase states respectively. When the magnitude of the third ray is greater than the first two rays, a non-minimum phase occurs.

In this 3-ray model, the shape of the notch can be described by b and T_d, and is completely independent of the notch frequency. The signature no longer depends on the center frequency and will have a symmetric "M" shape. This however,

*The non-minimum phase can also be described by setting b>1 and a -ve sign in the exponent. This may be more appropriate for a minimum to non-minimum phase transition analysis, or vice versa.

does require an ideal radio with no cross talk between the quadrature channels under non fading conditions and no correlations between I and Q data. The detailed proof can be found in Appendix 1.

Rummler further suggested a statistical fixed delay time of 6.3ns for the 30MHz, 6GHz radio with 26.4 mile path. However, it is questionable whether this fixed delay can be applied to other radio paths and frequencies, since it is not a physical delay time. Consider the case of the same radio route at 6GHz using a 16QAM system with different bandwidths, i.e. 11.3, 22.6, 33.9MHz. The signatures are plotted in Fig 2.8 with a fixed delay time of 6.3ns, minimum phase conditions, and normalized bandwidth, i.e. (notch offset frequency)/(Nyquist Bandwidth). They are all different, the 11.3MHz system having the best signature, and the 33.9MHz system the worst, when the notch frequency is within the Nyquist Bandwidth. No further analytic experiments have been done to prove the applicability of this 6.3ns delay time to other bandwidths.

Another approach which is widely used is to assume that the distortion will be same for all bandwidths. This means the signature will be the same for the normalized frequency plot. In such cases, the fixed delay is modified to $T_d=6.3X30/BW$ ns, where BW is the bandwidth* of the radio in MHz.

*Strictly speaking this means FCC bandwidth, however 3dB bandwidth can be used without losing too much generality.

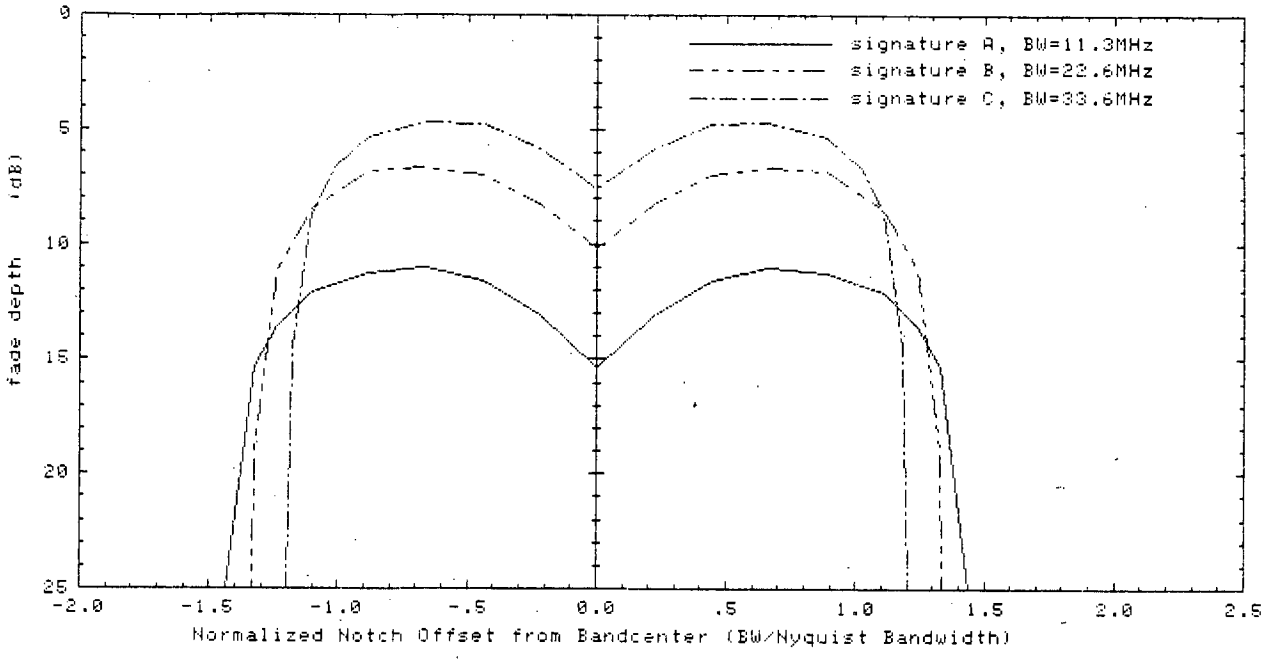

Fig 2.8 Signatures of a 16QAM Radio (3-ray model)

However, neither of these fixed delay times will be a good approach for a reliable multipath fading evaluation. Undoubtedly the actual delay time will depend on path length, terrain factor..etc., even if it is only a statistical parameter instead of a physical delay time. The best approach is to measure it on an actual radio link.

Although the 3-ray model is not a physical model, it has been widely adopted in the 1980's because of its simplicity and accuracy. Most radio manufacturers use it to give estimations of their radio equipment performance under multipath fading conditions. Various researchers may prefer to call it a 2-ray model because equation 2.4 can be regarded as having

one interference ray with delay time T_d and phase "$w_0T_d-\pi$", as shown:

$$M(jw) = a\ [\ 1 + b\ \exp(-jwT_d)\ \exp(j(w_0T_d-\pi))\ ]$$
$$= a\ [\ 1 - b\ \exp(-j(w-w_0)T_d)\ ]$$

where only the minimum phase condition has been considered, and the non-minimum phase case will be similar. However, the term "3-ray" model will be used to describe equation 2.4 throughout this thesis.

2.6.2.3 Polynomial Model

Based on the same set of fading data as used by Rummler, Greenstein from AT&T proposed his Polynomial Model [59] in 1978, which takes the form:

$$M(jw) = A_0 + \sum_{n=1}^{\infty} C_n\,{}^n(jw) \quad \ldots\ldots\ldots\ldots\ldots\ldots\ldots\ldots \quad (2.5)$$

where $C_n = A_n + jB_n$ and A_0, A_n, B_n are all real numbers, A_0 is the gain at the center frequency (w=0), and all the frequencies are referenced to the center frequency.

From the power calculation, it was shown that a first order approximation is sufficient to describe a fading channel [59]. However, this model did not draw too much attention from the public, because:

(1) When compared with Rummler's 3-ray model, it is completely non-physical, and is purely a statistical model. The coefficients are difficult to comprehend

whereas parameters in the 3-ray model -- b, w_0 and T_d are well understood.

(2) If a higher order polynomial series is required to describe a multipath fading chanel, it will be sensitive to noise.

(3) It is difficult to implement in the laboratory as a fading simulator to check the radio performance.

(4) It seems more tedious when compared with Rummler's fixed delay 3-ray model to extract the coefficients for outage analysis.

2.6.3 The Effects of Hydrometeors

2.6.3.1 Attenuation

Due to the frequency congestion below 10GHz, one development trend has been towards using higher carrier frequencies. However, as well as multipath fading, attenuation by hydrometeors (rain, cloud, snow, fog) becomes significant at higher frequencies and is responsible for most of the outages at frequencies above 18GHz. Of these effects, rain attenuation is dominant. Fig 2.9 shows a typical curve of attenuation coefficient A, against frequency for different rainfall rates [60]. Spherical drops are assumed, and A can be approximated by the well known formula $A = p R^q$, where R is the rain rate in mm/hr and p, q are functions of frequency and polarization. For predicting rain attenuation on LOS radio

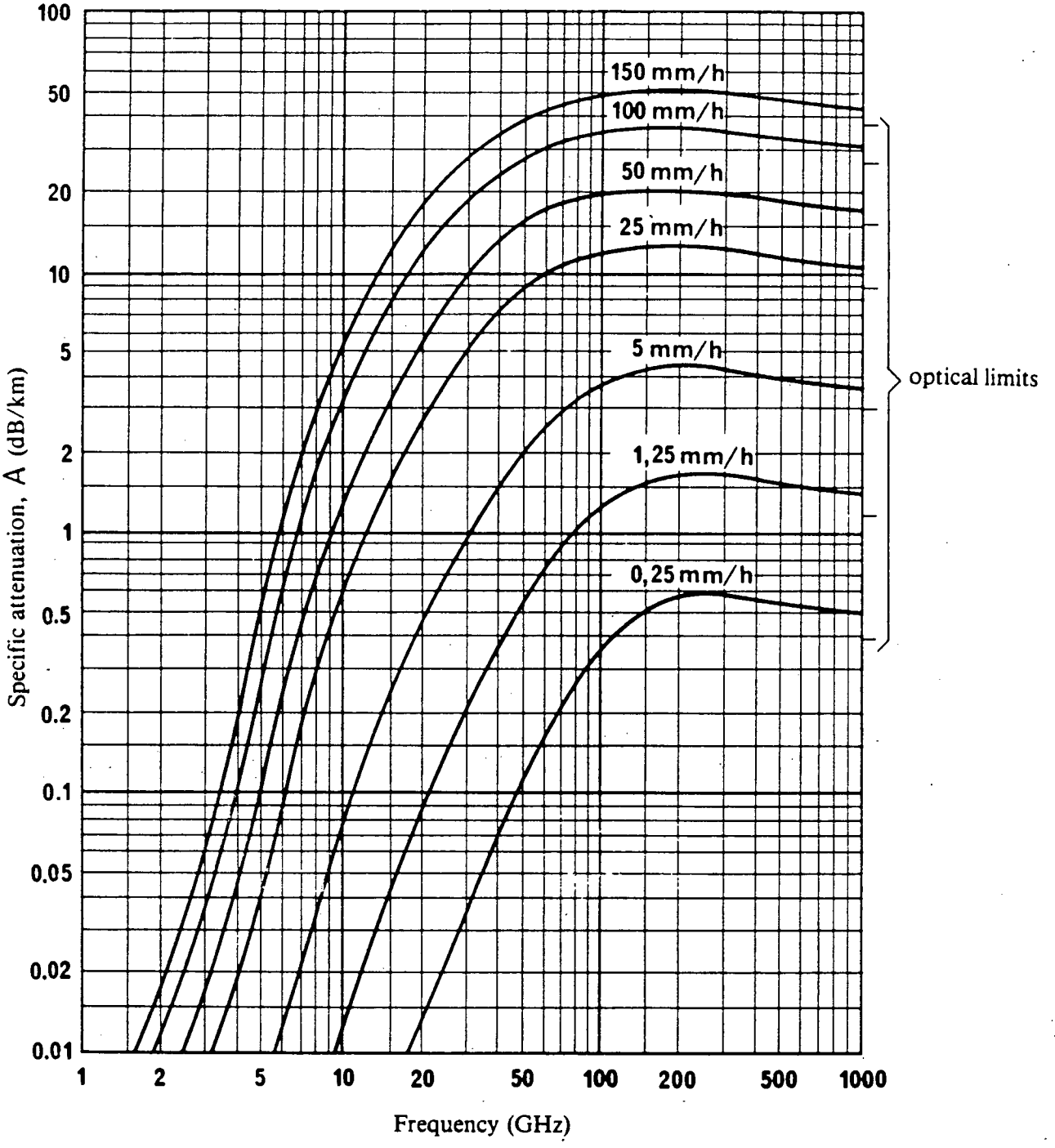

Fig 2.9 Attenuation Coefficient against Frequency

links, an empirical formula A L K may be used, where L is the path length in km and K is the appropriate reduction coefficient. Different K values have been proposed:

(1) CCIR [53], $K = \frac{90}{90 + 4L}$ ..... (2.6)

(2) Lin [61], $K = \frac{1}{1 + [\, L\,(R - 6.2)/2636\,]}$ (R>10mm/hr) ..... (2.7)

(3) Garcia-Lopez & Peiro [62],

$$K = \frac{1}{a + [\, L\,(b\,R + c\,L + d)/e\,]} \quad \text{.. (2.8)}$$

where a, b, c, d, e depend on the integration time of the rain rate measurement and geographical area

The K value from CCIR seems to be the simplest but may not provide accurate results. Lin's model is based on the long term (over 20year) distribution of 5 minute rain rates. Garcia-Lopez & Peiro's model is just an extension of Lin's using 1 minute rain rate distribution and with a correction factor for geographical area. It may be more accurate, but the poorly defined values for a, b, c, d, e make it the least generally applicable.

On the other hand, rain drops donot only fall at an angle with respect to the vertical but also are not perfectly spherical. Because of their asymmetric oblate spheroidal shape, they cause more attentuation of horizontal polarization than vertical. The difference may be as great as 4dB.

The attenuation coefficient due to fog and cloud is normally

less than 0.5dB/km below 30GHz, which is much less significant than that of rain. Although wet snow may cause higher attenuation than rain, it does not dominate the attenuation statistics in most countries; dry snow is similar to fog and cloud in its effects. However, the accumulation of snow on the reflecting surfaces of an antenna may cause a major degradation. The snow adheres to the antenna even when the snow has stopped falling in the path. The attenuation will depend on the antenna design and may be 5~20dB [63].

Since attenuation increases linearly with distance, the repeater spacing will be less than when using lower frequencies, e.g. 6GHz. This leads to the requirement for more repeaters, more radio equipment and higher maintenance costs for a given path length. There are, however, some advantages in using high frequencies. Small, high gain antennae can be used and hence smaller supporting structures and repeater sites are possible. There is also no frequency congestion problem and the requirement for bandwidth efficiency is less stringent than for low frequency channels. This implies that simpler modulation techniques can be used. Furthermore, a closer repeater spacing also reduces the outage due to multipath fading.

2.6.3.2 Cross-Polarization

Hydrometeors not only cause attenuation, but also introduce cross talk between two orthogonally polarized signals. This phenomenon is likely to put a constraint on the frequency

reuse technique particularly when the number of modulation levels increases. Again, rain is the dominant problem. In order to predict cross-polarization statistics from rain fall statistics, the following model may be applied [55]:

$$XPD = U - V \log(CPA) \quad \ldots\ldots\ldots\ldots\ldots\ldots\ldots\ldots\ldots\ldots \quad (2.9)$$

where CPA is the Co-Path-Attenuation, V depends primarily on frequency and U is a function of : frequency, rain drop size, raindrop orientation distribution, rain drop temperature..etc. Normally the relationship between XPD and CPA is an exponential curve. XPD decreasing as ~-20log(frequency) between 4-35GHz is quite typical.

Although dry snow produces less path attenuation than rain, it causes more depolarization. In contrast, wet snow normally produces more path attenuation but less depolarization than rain. The accumulation of snow on an antenna may also contribute to the depolarization effect. Obviously it is better to adopt a design that minimizes the chance of snow accumulation, e.g. having smooth surfaces and the use of a radome.

2.7 Summary

The requirement for the high bandwidth efficiency has pushed the development of LOS digital microwave radio from constant amplitude modulation in 1970's to the multi-amplitude modulation in 1980's.

The use of high level QAM starts to be popular since the late 1970's. It is anticipated that QAM will be dominant or even to be a standard in the LOS digital microwave communication in this few years.

Recent investigations show that most of the outage is due to the multipath fading and the improvement by simply increasing the flat fade margin is very limited. This is because the multipath will generate severe ISI and corrupt the normal data pattern. A lot of investigations have been conducted over the last twenty years about multipath phenomena, and Rummler's 3-ray model has become well accepted by researchers and radio manufacturers because of its simplicity and accuracy.

Apart from multipath fading, the attentuation due to hydrometeors starts to be significant for over 10GHz operation. This effect is not as severe as multipath fading, and it can be mostly overcome by simply increasing the flat fade margin of the radio system. However, in the dual polarization operation, the cross polarization effect of hydrometeors starts to be significant as the number of modulation levels increases above 16QAM.

CHAPTER 3 CURRENT TECHNIQUES FOR MULTIPATH COMPENSATION

Apart from rain fading above 11GHz, it is well known that multipath fading is a major contributor to degradation in radio system performance. The radio is not serviceable under severe multipath fading especially when high level modulation is used. To ensure high reliability and the objectives set by CCIR or individual countries* , a number of techniques are often employed. These include: frequency diversity, space diversity, frequency domain equalization, time domain equalization and combinations of these techniques.

3.1 Frequency Diversity

In frequency diversity, a few channels are reserved for protection. This technique has commonly been adopted in analogue radio. The data stream is switched to the protection channel from an unserviceable channel. The improvement relies on the frequency selective behavior of multipath fading. This has been confirmed by measured data in the U.S.A. [68].

Although the performance factor in analogue systems was evaluated empirically by Vigants and Pursley [69] from AT&T in 1979, little work has been done on digital systems. Generally, performance will be improved with increasing

*See the descriptions in section 2.3

frequency separation between the protection and unserviceable channels; and with the ratio of the number of protection channels to the number of working channels.

However, there are some practical factors which will degrade its overall performance:

(1) A burst of error may occur during switching.

(2) The requirement of feedback from the receiver site will slow down the response.

(3) It make less efficient use of the frequency spectrum.

Currently, one protection channel for several working channels, up to 11, is quite typical. This spare channel can also serve for routine equipment maintenance and testing as well as protection diversity. In some countries, e.g. the U.S.A., the number of protection channels is limited by regulations. Table 3.1 lists the requirements in 4, 6, 11GHz frequency band [5].

Frequency Band	No of protection Channels	Comment
3.700 - 4.200	1	at least 3 working channels
5.925 - 6.425	1	at least 3 working channels
10.700 - 11.700	N.A.	max. ratio of 1/3 of protection channels to working channels

Table 3.1 The number of protection channels in different frequency bands

3.2 Space Diversity

Space diversity provides an alternative or additional form of multipath compensation. Although both transmitting diversity and receiving diversity are possible, receiving diversity is the normally employed technique in LOS microwave radio and is termed space diversity. This definition is also used in this thesis.

In receiving diversity, normally two receiving antennae are used. The received signals can be processed in any desired way according to some suitable criterion. In transmitting diversity, a single antenna is used at the receiver site and two or more vertically separated transmitting antennae are used in the transmitter site. The requirement for the feedback control from the receiving site is neither practical nor feasible, this has hindered its application in diversity systems. Since the diversity antenna is normally vertically separated from the main antenna, various radio manufacturers may use the term height diversity.*

The outage improvement obtained from space diversity depends on the multipath activity, the method of processing the diversity signal, antenna separation, etc., and is typically a factor of 2 to 5. Due to the fact that the correlation of multipath distortion in the two receiving antennae decreases with their height separation, the improvement due to space

*Although the use of horizontal space diversity is also reported [83], its usage is far less common. However it may be applied when the vertical diversity is difficult to achieve or expensive.

diversity normally increases with this separation. However, too wide a separation will cause other problems, e.g. a high mounting tower is required which causes mechanical problems, and the received signal level at the diversity antenna will be decreased because of the highly directional transmitting antenna. A separation of ~10 meters is typical for existing diversity systems.

Switching and combining are the two major techniques used to process the diversity signal. Theoretically they can be implemented at RF, IF or baseband. However, not all of these are adopted in current radio designs.

3.2.1 Switching Techniques

By monitoring the two received signals and choosing the one with better performance, switching can be controlled. IF and even more so RF switching appear to be more economical than baseband switching. Switching can be activated by detecting signal levels. Since no attempt is made to equalize the phase or delay of the received signals, a burst of errors may occur during this hard switching. This will degrade the performance of the radio system directly, so these techniques are not normally adopted in current radio system designs.

Baseband switching requires a complete demodulation process on each receiver and is the most expensive method. However, hitless switching is possible because the baseband frequency is much lower. Switching is normally activated by detecting

the BER of the two signals. Hysteresis is used to reduce switching activity near the threshold point. The baseband switching technique is normally employed when hot-standby receiver equipment is available.

3.2.2 Combining Techniques

3.2.2.1 RF Combining

A typical combining technique is to align the phase of the received signal from the diversity antenna to that from the main antenna. An endless phase shift network is normally inserted in the diversity path to implement the phase adjustment. In order to take full advantage of this technique, the absolute time delay of the signals at the combiner input should be properly equalized.

In the UK, an RF combiner was proposed by Robinson et al. [70] in 1981, based on an idea from Lewis [71] in 1962. The schematic diagram of their endless phase shift network is shown in Fig 3.1a [70]. By controlling the currents in the PIN diodes with an 8 bit D/A converter, it is possible to obtain the required phase shift. The control algorithm is implemented by adding a 400Hz oscillation at the endless phase shifter about the required mean value. Thus the resultant combined signal has a 400Hz AM component, as shown in Fig 3.1b [70]. Minimum AM value will be obtained if the two signals are correctly aligned in phase.

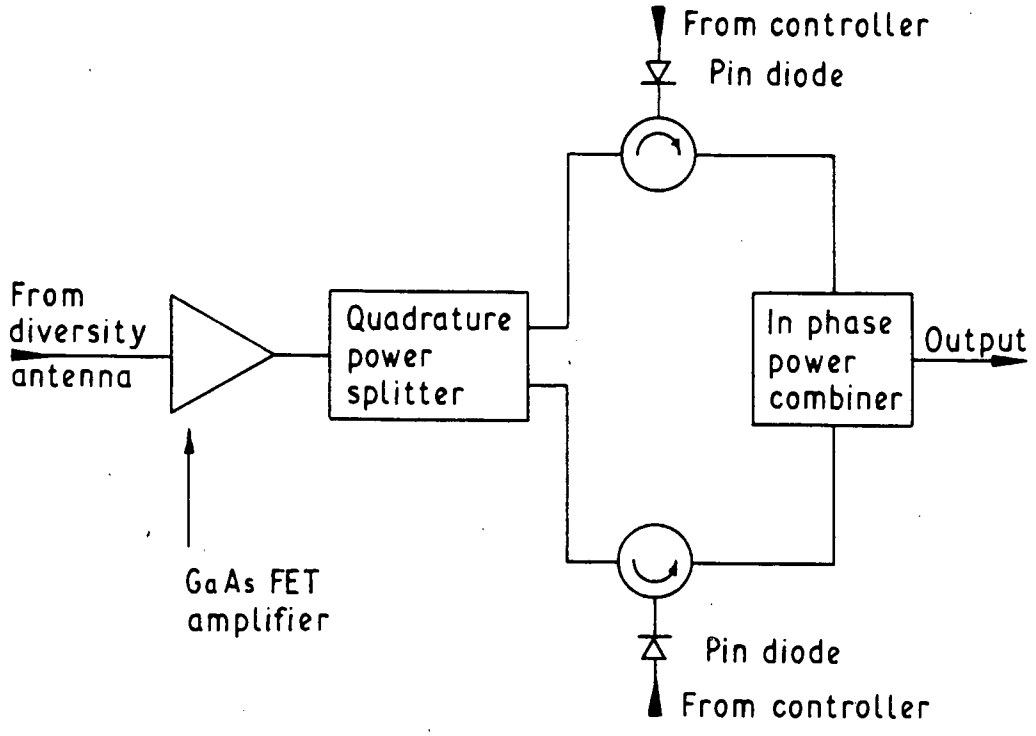

Fig 3.1a Schmatic of the Endless Phase Shift Network

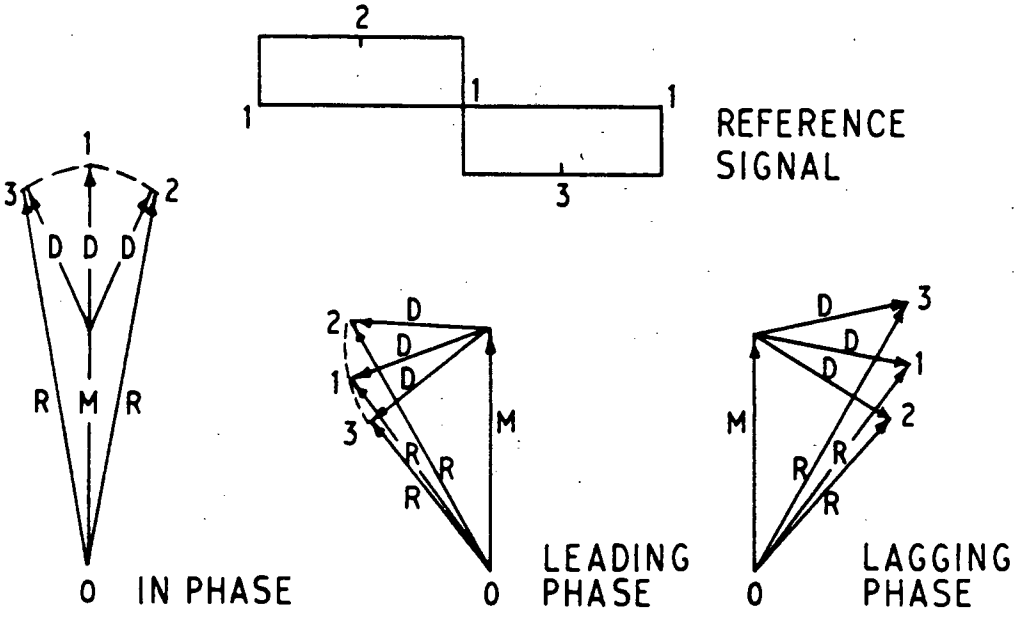

Fig 3.1b Vector Diagram of the Combined Signal

The performance of this technique depends on its tracking capability under dynamic conditions. At 6GHz operation, a 0.1ns delay difference* between the two received signals implies a 216° phase change. Even under normal atmosperic conditions, subnanosecond delay difference between the paths are very likely to occur.

At 400Hz modulation rate, Robinson et al. [70] claim that the tracking rate of their combiner is about 1000°/s. In other words, it corresponds to a delay time changing rate of 0.46ns/s at 6GHz. The adequacy of this figure is questionable even under shallow selective fading. On the other hand, if the modulation rate is increased, the combiner will become sensitive to noise. This results in severe limitation in the performance of this RF combining technique.

3.2.2.2 IF Combining

The lack of adequate tracking capability in an RF combiner can be eliminated by employing the IF combining technique. A 1000°/s tracking rate implies rate of change of delay of 40ns/s, if 70MHz IF is used. This is adequate in most conditions. Since the combining process is done at IF, duplication of both the RF and IF sections is required, so the cost will be higher than when using an RF combining technique. Principal methods in IF combining include in-phase combining [52] and interfering ray cancelling [73].

---

*Under normal atmospheric conditions, the long delay is equalized by a fixed delay network

In-phase IF combining techniques have been widely adopted in North America since the late 1970's. The basic principle is similar to the in-phase RF combining technique. An endless phase shifter is inserted in the diversity signal path at the IF stage to maintain the two IF signals in phase at the combiner. This method also aims to maximize the power at the combiner output. Thus the term "maximum power combiner" is frequently used.

However, in-band dispersion is not minimized during multipath fading when the in-phase method is used. This spurred the development of another method in Japan. In 1980's, Komaki et al. [73,84] from NTT proposed an interfering ray cancelling method for their 200Mb/s 16QAM radio.

Again, an endless phase shifter is inserted in one of the received signal paths in the IF stage, and the two signals are combined at IF. Here, the level of the two IF signals and the amplitude slope at the combiner output are monitored. The amplitude slope is obtained by monitoring two frequencies, one above the center frequency (IF frequency) and the other below. The control reaches equilibrium when the amplitude slope becomes zero. Thus the term "amplitude slope combiner" may be preferable. The term "minimum dispersion combiner" is also used by some researchers to distinguish it from the in-phase combiner.

If both antennae suffer from the same depth of fading, the improvement is much greater than that obtained from the in-phase method, as shown in Fig 3.2 [73], where the combiner

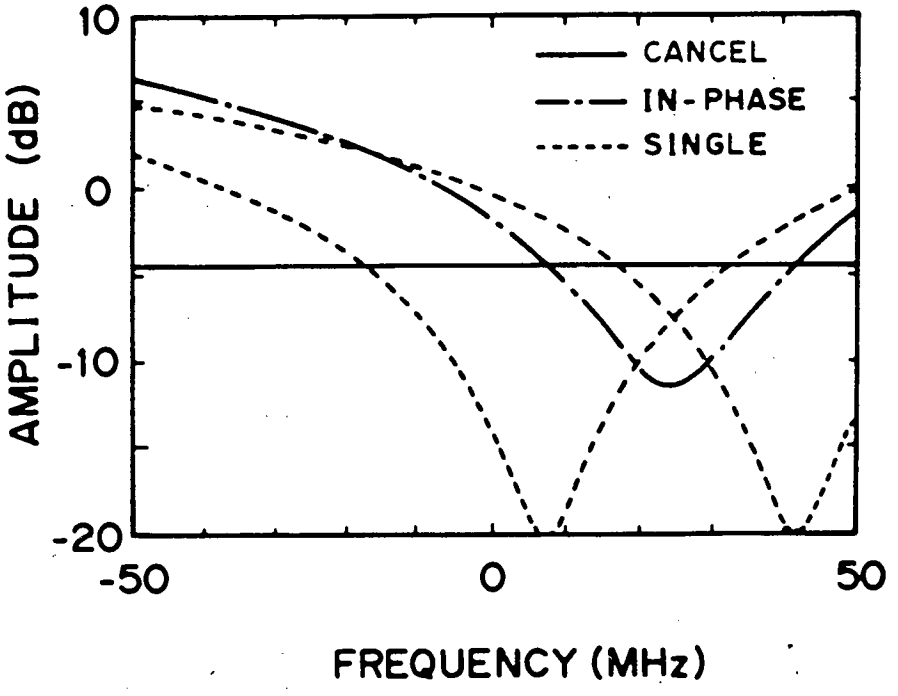

Fig 3.2 Response of Interfering Ray Cancelling Methods

output exhibits a completely flat spectrum. On the other hand, its hardware implementation is more complex and care must be taken to prevent the combiner cancelling all the main signals instead of the interfering signals.

However, when only one antenna experiences the selective fading, as happens the majority of times, the performance of these two methods are similar and depends on the fading activity, e.g. the position of the notch. This is because amplitude dispersion is not a completely valid criterion for comparison* of the methods. The outage due to 10dB amplitude dispersion at band-center and at band-edges are different.

*Nevertheless, it is a convenient and simple method for a rough estimation.

The overall system improvement will be heavily dependent on the type of equalizer incorporated with the combiner. This will be discussed in detail in section 3.3.

3.2.2.3 Baseband Combining

In addition to RF and IF combining, baseband combining is also possible [74]. The two received signals go through the whole demodulation process to baseband before they are directly combined together. No control signal is required between them. This technique is the simplest but is not the most effective. The performance is worse than that of an IF combiner during frequency selective fading. With RF or IF combining, the combiner output spectrum is altered according to some criterion. Inter-Symbol Interference (ISI) and cross talk is normally reduced after the combiner. However in baseband combining, no attempt is made to change the ISI pattern or reduce the cross talk between the quadratic channels.

Although the performance of a baseband combiner may be better than that of an IF combiner under normal atmospheric conditions, this improvement is not critical to most radio links. Thus simple baseband combining does not seem to be a suitable candidate for implementation space diversity. If it is affordable, baseband switching is far superior.

3.3 Frequency Domain Equalizers

The limited improvement from frequency and space diversity techniques has led to the development of adaptive equalizers. The frequency domain equalizers were the earliest solution. Prior to the 1980's, the phenomenon of multipath was not well understood. Various researchers over optimistically predicted that amplitude slope was the main degradation factor caused by multipath fading [75], and ignored the importance of group delay distortion. The fading models proposed by Rummler and Greenstein from AT&T [56,59] also used solely amplitude characteristics for fading channels. This led to the development of a series of amplitude equalizers -- simple linear slope, multi-bump* and movable notch, to compensate for amplitude distortion. Therefore these classes of equalizers are referred to as "amplitude equalizers".

Virtually all these kinds of equalizer were implemented at IF and appeared as the first generation of adaptive equalizers in LOS digital radio. The equalization is implemented by flattening the overall spectrum. Even now, this type of equalizer still attracts the attention of radio manufacturers because of its simplicity, effectiveness under minimum phase multipath condition and the possibility of its being used in combination with time domain equalizers.

*The multi-bump equalizer was developed in the early 1980's, the possibility of handling both minimum and non-minimum phase is discussed in [76].

3.3.1 Simple Linear Slope Equalizer

This type of equalizer simply corrects the overall amplitude slope in the IF stage. Typically two frequencies are monitored by bandpass filtering, with one at the high end and the other at the low end of the signal band. The equalization is done by adjusting the amplitude slope such that the two frequencies have the same level. Normally amplitude slope of 1/3 to 2/3 dB/MHz can be compensated adequately. The term "amplitude tilt" equalizer is also used frequently.

This type of equalizer is the simplest and provides a first order correction factor. The outage is typically improved by a factor of 2 to 5 [52,77,78]. Surprisingly, when used in conjunction with in-phase combining space diversity, the overall improvement exceeds the product of the separate diversity and adaptive equalizer improvement factors of 5 to 20 [52,77,78] are typical. This is because normally only one received signal experiences severe frequency selective fading. When an in-phase combiner is used, one side of the spectrum will be added in phase while the other side will be added out of phase. Consequently, the combiner is able to replace in band notches with a coarse linear slope. This is the best condition that can be corrected by a simple linear slope equalizer.

On the other hand, this type of equalizer is not suitable for use in combination with interfering ray cancelling space diversity. This is because the zero amplitude slope algorithm

has already been implemented in the combiner. I predict that the overall improvement will be less than the product of the separate diversity and adaptive equalizer improvements in most of the fading conditions.

3.3.2 Multi-Bump Equalizer

Multi-bump equalizers were an enhancement of frequency domain equalizers developed in the early 1980's. The major improvement involves correcting band notches without requiring space diversity. While a simple amplitude slope equalizer will only work effectively with space diversity.

Each bump circuit provides a gain to compensate for the notch due to selective fading. A few bumps are cascaded and set at different frequencies. Three and five bump systems were developed in GTE Lenkurt Inc [79] and Farinon [76] respectively.

Based on the 2-ray and 3-ray models, if the notch frequency is the same as one of the bump frequencies, the response of the equalizer will be good as long as the fade depth is less than the maximum gain of the bump circuit. The improvement will be degraded if the notch frequency is half way between the two bump frequencies, as shown in [76].

Nevertheless the improvement gained from this type of equalizer is limited, because:

(1) The maximum gain of the bump circuit is constrained to ~25dB because of the limitations of existing analogue techniques.

(2) The number of bumps is limited, otherwise very high Q circuitry is required which is expensive.

(3) If the shape of the multipath distortion differs from that of the 2-ray or 3-ray models, the performance of the equalizer will be degraded.

3.3.3 Movable Notch Equalizer

During the development of the linear slope equalizer in North America, Komaki et al. from NTT proposed their movable notch equalizer [58]. Three frequencies are monitored -- low end, center and high end of the IF spectrum. A variable resonator is used to implement the equalization. The tuning frequency can be controlled by detecting the difference betweeen the high end and low end spectrum. The Q factor can be adjusted by detecting the difference between the center frequency spectrum and the average of the high end and low end spectra.

The improvement depends on the accuracy of the resonator setting and the shape of multipath distortion. The performance will be good when used in conjunction with interfering ray cancelling space diversity instead of in-phase combiner space diversity. This is because the equalizer is inherently good at correcting in-band notches. This type of equalizer appears to be the most cost effective frequency domain

equalization solution without employing the space diversity. However, care should be taken with its stability during multipath fading.

3.4 Time Domain Equalizers

The significance of group delay distortion was realized in the late 1970's. The performance of amplitude equalizers was found to be highly degraded during non-minimum phase fade conditions because of the increased group delay distortion [58]. The remedy is to employ a different technique such that both amplitude and group delay distortions can be equalized properly. Time domain equalizers appear to be the best candidate and are the present countermeasures being developed for digital radio systems.

The theory and principles of time domain equalizers have been known for some time, and they have been widely adopted in voice band telephony in the last ten years. With the advent of high speed digital technology, the implementation of them at 10's MHz has become practical for digital microwave radio applications.

The main aim of the time domain equalizer is to reduce the ISI and cross talk such that the original data can be restored accurately. It tries to equalize the impulse response of the channel in the time domain. In other words, the frequency response of the overall channel is equalized.

Basically, it can be classified into two categories -- linear and non-linear.

3.4.1 Linear Equalizer

There are a number of alternative structure for linear equalizers in the time domain. However, the transversal filter structure appears to be the simplest effective arrangement; the basic block diagram is shown in Fig 3.3. It consists of a tapped delay line, tap weight multipliers and a summer.

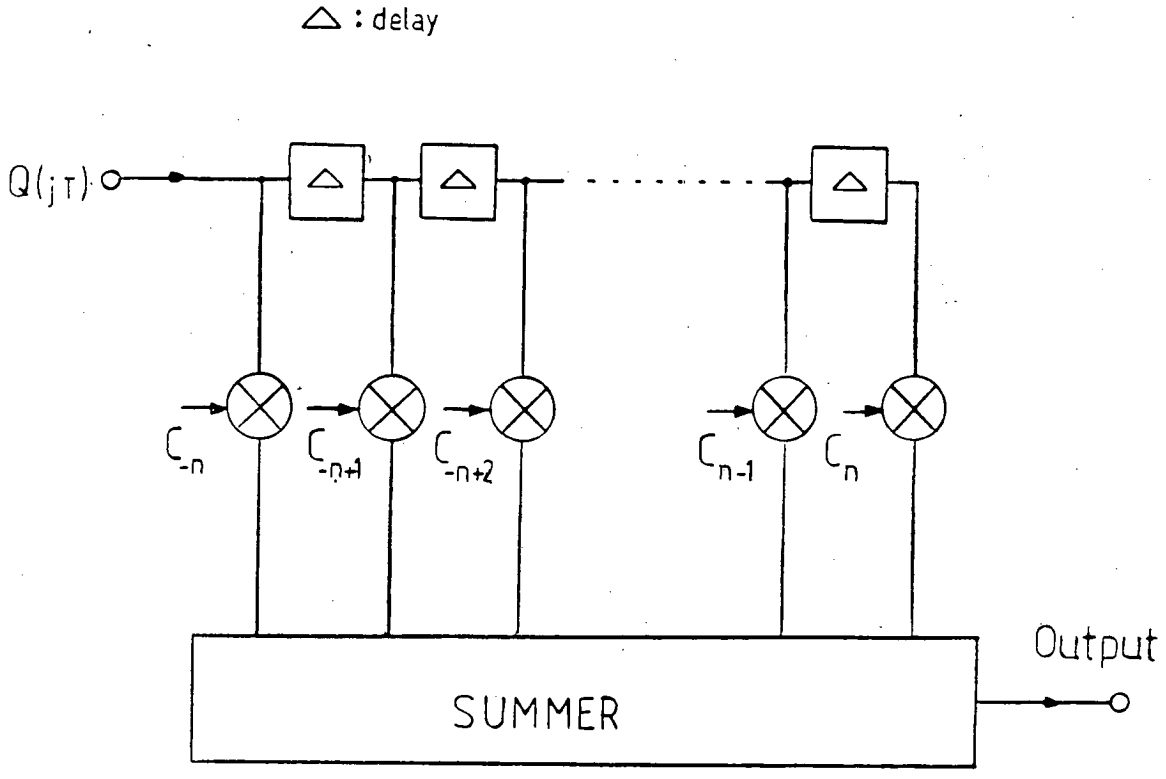

Fig 3.3 Block Diagram of Transversal Equalizer

A number of investigations have been performed to assess the optimum equalizer tap spacing [80]. Symbol spacing (T) or half symbol spacing (T/2) seem to be the most applicable due to the ease of clock extraction. Although a T-spaced equalizer requires about half the number of taps to span a given channel dispersion, it is sensitive to the timing phase or delay in the channel. Its performance will also be degraded when the fading notch is near to the band-edge. On the other hand, the T/2-spaced equalizer suffers from ill conditioning [81]. These effects will be discussed in detail in chapter 4 and 5.

Although both IF and baseband implementations are possible, the baseband approach is normally adopted at the present time because of the low frequencies involved, see for example in [82]. Here a nine tap baseband transversal equalizer is used in a 64QAM system. The equalization is done by adjusting the tap weights to correct the overall response of the channel, using an estimation algorithm.

3.4.2 Non-Linear Equalizer

The most common non-linear equalizer is the decision feedback equalizer [85]. In general, it consists of two parts, feed-forward and feedback section as shown in Fig 3.4. Feedforward can be used to combat pre-echoes and feedback for post-echoes. Since the data are quantized after the decision circuitry, multiplication with the feedback tap weights is

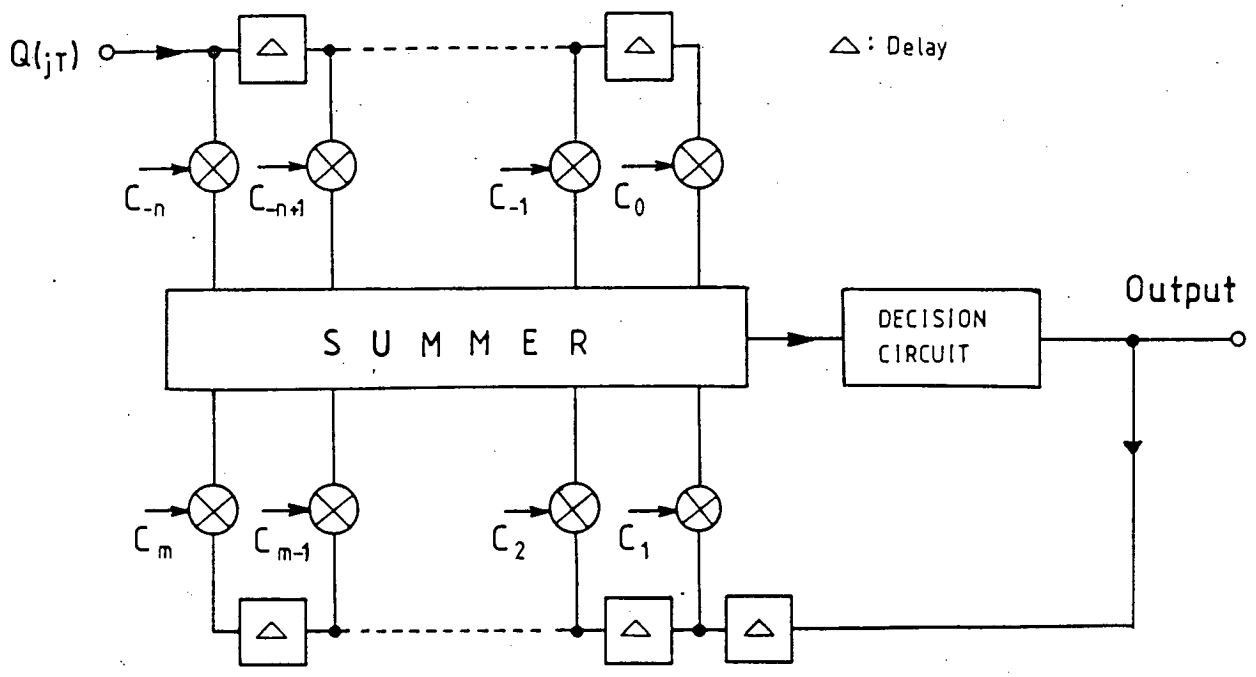

Fig 3.4 Block Diagram of Decision Feedback Equalizer

easily implemented. However, this advantage decreases as the number of modulation levels increase. This technology was widely adopted in voice grade telephony and was first applied to LOS digital radio by Dudek and Robinson [34] in 1980 for their RBQPSK system.

However, this design requires a high carrier to noise ratio to avoid incorrect decisions perturbing the weight convergence. On the transition between minimum and non-minimum phase fades, the equalizer may lose its stability because of changes in the tap weight values. Care must be taken to control the stability of the equalizer under deep fading conditions when the tap weights of feedback or feedforward taps

are close to the main tap value. This puts a severe contraint on its application in LOS digital radio.

3.5 Summary

Frequency diversity and space diversity with baseband switching have been employed in analogue radio for a considerable time. They were quickly adopted in digital radio particularly in the early stage when the multipath phenomena was not well understood.

From theoretical studies and experimental work on multipath fading, various combining techniques for space diversity were conceived and a series of IF amplitude equalizers were developed in the late 1970's and the beginning of 1980's.

The combining technique is inherently hitless and with a suitable IF amplitude equalizer, the overall performance can be better than the product of the individual improvement. However all these techniques aim at amplitude equalization only and the performance is very dependent on the fading parameters.

The discovery of the importance of group delay distortion in the late 1970's spurred the development of time domain (transversal) equalizers. The use of combining technique at IF with transversal equalizers at baseband to improve the overall performance then started to become popular, see for example in [23].

The main attractions of transversal equalizer are:

(1) unconditional stability

(2) the performance is loosely dependent on fading parameters and it can compensate both minimum and non-minimum phase fades

(3) a lot of experience has been gained in voice-band frequency applications can now be transfered to microwave radio systems

It is anticipated that this type of equalizer will become increasingly popular in digital radio application and it appears to form the basis of the next generation of equalizer techniques for combating multipath fading.

CHAPTER 4 T-SPACED TRANSVERSAL EQUALIZER

An equalizer is a device which performs the function of data equalization or reconstruction at the output of a distorting channel. One of the earliest transversal equalizers was investigated by Kallmann [90], using cable as the delay line medium. Many of the later developments were aimed at equalization of telephone channels in data communications. In 1965, Lucky from AT&T demonstrated his automatic equalizer [91], where a training signal was first applied to train the equalizer and then the equalizer's tap weights were fixed during data transmission. Subsequent developments focused on equalizers which could be readjusted continuously. Such an equalizer is known as an adaptive equalizer and is widely used in digital communications.

T-spaced, or the so-called symbol spaced synchronized adaptive transversal equalizer is the most commonly used configuration, where the tap spacing is equal to the symbol spacing. A theoretical study on its performance under stationary multipath fading will be discussed in this chapter.

4.1 Basic Theory

First of all, let us start with the baseband equivalent model of a radio channel. The effect on the upconverter and downconverter operations on a multipath channel is small

because their frequencies are much higher than the baseband frequency and their operation is basically independent of the baseband data. It is difficult to be general about problems in the demodulator carrier recovery circuit; they will be implementation dependent. However its operation will not be affected too much under normal fading conditions unless the inband fade depth is very high, e.g. 50dB. It will be shown in section 4.6 that a small frequency offset can be compensated by the equalizer without too much difficulty. The only problem is in the clock recovery circuitry, it will produce a certain amount of degradation, like timing jitter. In order to simplify the analysis, a constant sampling phase is used to evaluate the effect of timing problems.

Therefore we make the following assumptions:

(1) The overall operation of the upconverter/downconverter will be ideal.

(2) A coherent carrier frequency can be established in the receiver.

(3) The baseband received filter will completely reject all the unwanted high frequencies produced by demodulation.

(4) The clock recovery circuit will work correctly, i.e. the receiver can sample the data properly, with a certain amount of phase error.

(5) The I and Q channels are identical. This assumption is used to simplify the calculations and computations. The

physical difference is small if we consider them separately.

Consider the frequency response, H(jw), of the whole baseband equivalent channel:

$$H(jw) = T(jw)\, M(jw)\, R(jw)$$

where T(jw) and R(jw) are the overall baseband equivalent frequency responses of transmitter and receiver respectively, M(jw) is the overall baseband equivalent frequency response of the multipath channel. In order to get high bandwidth efficiency, T(jw)~R(jw), and the product of T(jw)R(jw) is often set to a raised cosine filter shape.** The raised cosine filter is deployed because it can produce ISI free digital transmission [93]. The frequency response of the raised cosine filter is:

$$T(jw)R(jw) = 1/\mathrm{sinc}(wT/2) \qquad \text{for } 0 \leq w < \pi(1-a)/T$$

$$T(jw)R(jw) = 1/[2\,\mathrm{sinc}(wT/2)]\,\{1 - \sin[(w-\pi/T)T/(2a)]\} \qquad \text{for } \pi(1-a)/T \leq w < \pi(1+a)/T$$

$$T(jw)R(jw) = 0 \qquad \text{for other frequencies}$$

where $0 \leq a \leq 1$ is the fraction of excess Nyquist bandwidth, and $\mathrm{sinc}(x)=\sin(x)/x$ is the correction factor for the transmit data with symbol period T, as the raised cosine function is defined for an infinitely narrow pulse with infinite height.

**Although some radio manufacturers like GEC in the U.K. tend to use combinations of Bessel, Butterworth and Chebychev filters together with a phase equalizer, their overall responses are quite close to a raised cosine filter type.

The use of a = 0.3 and 0.5 were quite common for the North American and the Japanese radio manufacturers respectively. Recent developments tend to use 15% or less excess bandwidth, i.e. a $\leq$ .15, for some narrowband transmission systems. However, the narrower the bandwidth, the more degradation will result from sampling phase error, especially in a high level modulation scheme. This is shown in Fig 4.1, where the "eye" diagrams for a 16QAM radio are plotted with a=.1 and a=.5. Normally most of the raised cosine filtering is per-

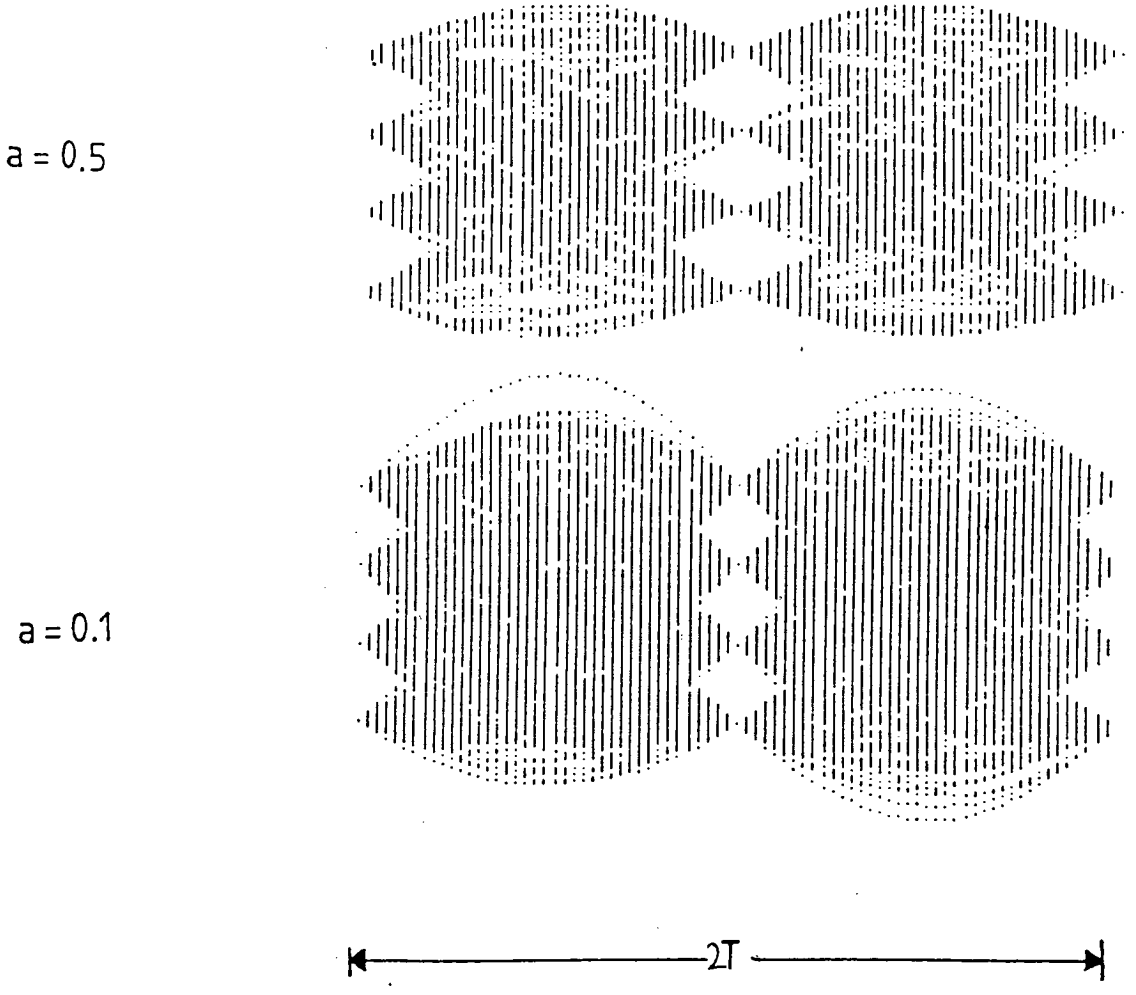

Fig 4.1 "Eye" Diagram for 16QAM Radio Transmissions

formed at baseband because of the relatively easy design compared with that in IF or RF stages. This type of filter will be used for all the calculations and simulations in the thesis.

Let A(t) be the complex transmit data as defined in section 2.4.4.1. The receiver output, Q(t), which is sampled at symbol rate 1/T, is as follows:

$$Q_j = \sum_{k=-\infty}^{\infty} A_k \; P^{\theta\emptyset}{}_{j-k} + V_j \qquad \ldots\ldots\ldots\ldots\ldots\ldots\ldots\ldots \quad (4.1)$$

where $Q_j = Q(jT)$; $A_k = A(kT)$;

$V_j = V(jT)$ is the added White Gaussian Noise component with zero mean distribution;

$P^{\theta\emptyset}{}_{j-k} = P^{\theta\emptyset}{}_{((j-k)T)}$ is the complex pulse response of H(jw) evaluated at (j-k)T with sample phase $\emptyset$, demodulation phase θ,** and it is normalized such that the summation of the mainlobe plus all the ISI terms equals 1.

According to the sampling theorem, the frequency response of a T-spaced equalizer is periodic and the period is equal to 1/T. With different tap weight settings, it is possible to control its frequency response. Generally, two criteria are used -- Zero Forcing and Least Mean Square (LMS) error, for calculating the correct tap weights.

**sample phase =0 is defined as the maximum "eye" opening phase for an ideal channel and demodulation process; demodulation phase =0 is defined by zero cross talk between I & Q channels at sampling instant, i.e. time slot zero, for an ideal channel.

4.1.1 Zero Forcing Algorithm

The zero forcing algorithm forces the overall pulse response of the equalizer and the combined channel to be zero at all time slots except the main one, satisfying the Nyquist zero ISI criterion. It is simply an inverse filter and neglects the noise performance. In 1965, Lucky [91] also showed that the zero forcing equalizer is not guaranteed to converge if the peak distortion before equalization is greater than 1. Thus this algorithm is not recommended for highly distorted or noisy channels.

However, due to its implementation simplicity, it was one of the early popular algorithms for equalization and for multi-path compensation over the last few years [3,94,95].

4.1.2 Least Mean Square (LMS) Algorithm

Instead of performing inverse filtering, the LMS algorithm minimizes the Mean Square Error (MSE) at the equalizer output. Here both the ISI terms and noise are minimized. This leads to a more robust structure. One of the earliest proposals was by Widrow and Hoff in 1960 [96]. This algorithm has been widely adopted in data communications since the late 1960's when the limited performance of the zero forcing algorithm became evident.

With the equalizer structure shown in Fig. 3.3, the error at the equalizer output at time mT will be:

$$e_m = \sum_{n=-N}^{N} C_n \, Q_{m-n} - A_m$$

Assuming the noise and data are uncorrelated, the MSE becomes:

$$E\langle |e_m|^2 \rangle = \underline{C}^h (\underline{U} + \underline{V}) \, \underline{C} - \underline{D}^h \underline{C} - \underline{C}^h \underline{D} + E\langle A_m A_m^* \rangle \quad \ldots\ldots\ldots\ldots\ldots\ldots\ldots\ldots \quad (4.2)$$

where _ represents the matrix format, * and h are the conjugate and the combination of conjugate & transpose of the matrix respectively. $E\langle . \rangle$ is the statistical expectation operator.

$\underline{C}$ is the (2N+1)x1 tap weight matrix ..... (4.3a)

$\underline{U}$ is the (2N+1)x(2N+1) covariance matrix of the received signal samples, $U_{ij} = E\langle (\sum_{k=-\infty}^{\infty} A_k P^{\theta\emptyset}{}_{m-j-k}) \, (\sum_{k=-\infty}^{\infty} A_k P^{\theta\emptyset}{}_{m-i-k})^* \rangle$

..... (4.3b)

$\underline{V}$ is the (2N+1)x(2N+1) covariance matrix of the noise present in the received samples, $V_{ij} = E\langle V_j V_i^* \rangle$ ..... (4.3c)

$\underline{D}$ is the cross-correlation matrix, $D_i = E\langle A_m (\sum_{k=-\infty}^{\infty} A_k P^{\theta\emptyset}{}_{m-i-k})^* \rangle$

..... (4.3d)

Applying the LMS criterion to the tap weight, i.e.

$$\frac{\partial E\langle |e_m|^2 \rangle}{\partial C_n} = 0;$$

Solving the above linear equations gives the following matrix equation for the optimum tap weight $\underline{C}_{opt}$:

$$(\underline{U} + \underline{V}) \, \underline{C}_{opt} = \underline{D} \quad \ldots\ldots\ldots\ldots\ldots\ldots\ldots\ldots\ldots\ldots\ldots\ldots \quad (4.4)$$

Assuming the transmit data A_m is random (i.e. $E\langle A_i A_j^* \rangle = \delta_{ij} E\langle A_i A_j^* \rangle$, where δ_{ij} is the Kronecker delta, defined by $\delta_{ij}=0$ if $i \neq j$ and $\delta_{ij}=1$ if $i=j$), Gaussian noise is bandlimited to the Nyquist bandwidth and $E\langle V_j V_i^* \rangle = n\, \delta_{ij}$, where n is the Gaussian noise power level. The following result can be obtained:

$$U_{ij} = E\langle A_k A_k^* \rangle \; E\langle P^{\theta\emptyset}{}_{l-j} P^{\theta\emptyset}{}_{l-i}{}^* \rangle$$

$$D_i = E\langle A_k A_k^* \rangle \; P^{\theta\emptyset}{}_{-i}{}^*$$

$$V_{ii} = n$$

$$= c\, E\langle A_k A_k^* \rangle / r$$

where c is a constant depending on the overall channel (excluding the equalizer) and r is the carrier to noise ratio.

$$E\langle A_k A_k^* \rangle = \frac{2\,[\,1^2 + 3^2 + .. + (2L-1)^2\,]}{L} = \frac{2\,[\,(2L)^2 - 1\,]}{3} \quad \ldots\ldots\ldots\ldots\ldots\ldots\ldots\ldots\ldots\ldots \quad (4.5)$$

where 2L is the total number of levels in the I or Q channel.

Re-arranging equation (4.4),

$$\underline{C}_{opt} = \underline{R}^{-1}\, \underline{D} \quad \ldots\ldots\ldots\ldots\ldots\ldots\ldots\ldots\ldots\ldots\ldots\ldots\ldots\ldots \quad (4.6a)$$

$$\text{where } \underline{R} = \underline{U} + \underline{V} \quad \ldots\ldots\ldots\ldots\ldots\ldots\ldots\ldots\ldots\ldots\ldots\ldots \quad (4.6b)$$

$$\text{or } E\langle A_k A_k^* \rangle \; [\; \underline{R}'\, \underline{C}_{opt} \;] = E\langle A_k A_k^* \rangle \; \underline{D}'$$

$$\text{where } R_{ij}' = E\langle P^{\theta\emptyset}{}_{l-j} P^{\theta\emptyset}{}_{l-i}{}^* \rangle + c/r\, \delta_{ij}$$

$$D_i' = P^{\theta\emptyset}{}_{-i}{}^*$$

i.e. $\underline{C}_{opt} = \underline{R}'^{-1}\,\underline{D}'$ ..... (4.6c)

The existence of the inverse of $\underline{R}$ or $\underline{R}'$ is already proved in [98]. The matrix $\underline{R}'$ or $\underline{D}'$ are channel parameters only and do not depend on the number of transmit levels. Thus **for a given carrier to noise ratio, the optimum tap weights are independent of the number of levels in the QAM system.**

The Minimum Mean Square Error (MMSE) achieved is:

$$\mathcal{E}_{min} = E\langle A_k A_k^* \rangle \left[1 - \underline{D}'^{h}\,\underline{C}_{opt} \right] \quad \ldots\ldots\ldots\ldots\ldots \quad (4.7)$$

or $$\mathcal{E}_{min} = E\langle A_k A_k^* \rangle \left[1 - \underline{D}'^{h}\,\underline{R}'^{-1}\,\underline{D}'\right] \quad \ldots\ldots\ldots\ldots\ldots \quad (4.8)$$

Equation (4.8) means that **for a given carrier to noise ratio, the MMSE is directly proportional to $E\langle A_k A_k^* \rangle$.****

There is an interesting result from equation (4.7). Let us separate $\underline{D}'$ and $\underline{C}_{opt}$ into real and imaginary parts. The overall imaginary part of the right hand side will be:

$$E\langle A_k A_k^* \rangle \left[(\text{real } \underline{D}'^{t})(\text{img } \underline{C}_{opt}) - (\text{img } \underline{D}'^{t})(\text{real } \underline{C}_{opt})\right] \quad \ldots\ldots\ldots\ldots\ldots\ldots \quad (4.9)$$

where t is the transpose of the matrix

Since $\mathcal{E}_{min}$ is real, the terms in (4.9) must be zero. However, (real $\underline{D}'$) and (-img $\underline{D}'$) are the real and imaginary parts of the pulse response of the channel. The two terms inside the bracket [ ] are just the convolution process of the combined pulse responses (imaginary part) of the overall

---

**In this thesis, the thresholds of the QAM radio systems are normalized for easy comparison of the equalizer responses.

channel and the equalizer. This implies **there is no cross talk between I and Q channels at this point, independent of the number of taps and number of levels in the QAM systems.****

A constellation display demonstrates the effect of cross talk, as shown in Fig 4.2. The magnitude of the cross talk can be calculated by the simple trigonometric equation:

$$@ = \tan^{-1}\left[\frac{(\text{real } \underline{D}^t)(\text{img } \underline{C}_{opt}) - (\text{img } \underline{D}^t)(\text{real } \underline{C}_{opt})}{(\text{real } \underline{D}^t)(\text{real } \underline{C}_{opt}) + (\text{img } \underline{D}^t)(\text{img } \underline{C}_{opt})}\right] \quad \ldots\ldots\ldots\ldots\ldots\ldots\ldots\ldots \quad (4.10)$$

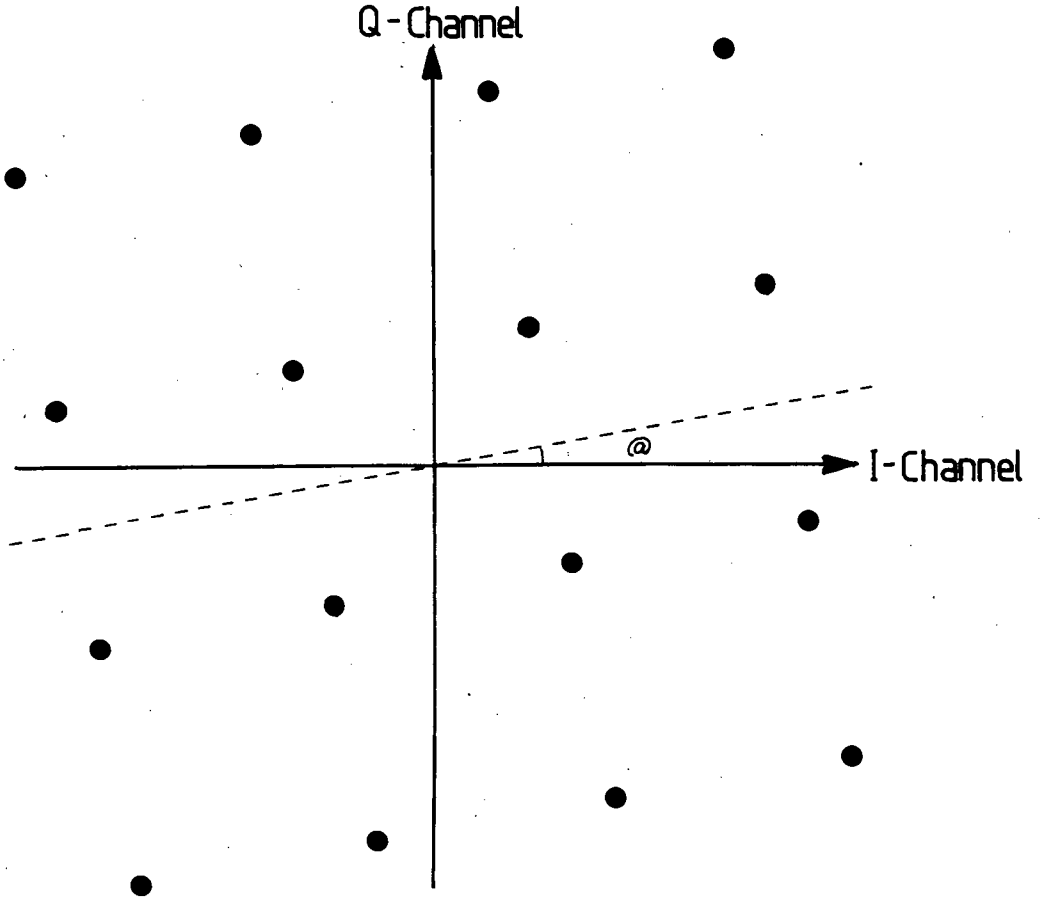

Fig 4.2 Constellation display for a 16QAM Signals

**the number of taps is greater than or equal to 1

The numerator and denominator are respectively the imaginary and real parts of the overall pulse responses of the combined channel and equalizer at time slot zero.

4.2 Least Mean Square (LMS) Algorithm with Gradient Estimate

From the above discussion, the optimum tap weights can be solved by inverting the matrix $\underline{R}$ or $\underline{R}'$. However, this gives two major problems:

(1) It is impractical to solve the inverse of a matrix

(2) The channel characteristics may not be constant. It will affect the accuracies for matrix element estimation.

Widrow and Hoff [97,100] suggest a gradient estimation method. Here the tap weights are estimated as the opposite direction of the gradient of MSE with respect to that tap weight, and is normally replaced by a $-u\ e_j\ \underline{Q}_j^*$ estimator where u is the step size of positive value. As shown in equation (4.11), the tap weight $\underline{C}$ at iteration j+1 is:

$$\underline{C}_{j+1} = \underline{C}_j - u\ e_j\ \underline{Q}_j^* \quad \ldots\ldots\ldots\ldots\ldots\ldots\ldots\ldots \quad (4.11)$$

This gives the fairly simple iteration method to solve for the optimum tap weights. By re-arranging equations (4.2) and (4.6a), the MSE at iteration 1 becomes:

$$E\langle |e_1|^2 \rangle = \xi_{min} + E\Big\langle \sum_{i=-N}^{N} (C_i - C_i')^* Q_i^* \sum_{j=-N}^{N} Q_j (C_j - C_j') \Big\rangle \quad \ldots\ldots\ldots\ldots\ldots\ldots\ldots\ldots \quad (4.12)$$

where C_i' is the optimum tap weight.

Once the equalizer converges to its final MSE, the tap weight will still have a finite variance about $\underline{C}_{opt}$ if finite step size u is used. This will cause the so called Gradient noise. Gitlin and Weinstein [98] from AT&T investigated the upper bound of this excess error in 1979. However there are two basic limitations:

(1) If the channel is highly distorted, the upper bound limit which is dependent on the maximum and average eigenvalues of matrix $\underline{R}'$ may not be a good estimate.

(2) For a given distorting channel, the eigenvalues of matrix $\underline{R}$ or $\underline{R}'$ are not obvious.

At the same time, Mazo [99] from AT&T solved this excess error problem by simply considering one dimensional binary transmission without Gaussian noise. In this thesis, a solution is provided for a general QAM system with additive Gaussian noise. The basic methodology will be similar, but no co-ordination transformation for the eigenvalues will be used.

Substituting equation (4.11) into (4.12), as shown in Appendix 3, the MSE at iteration l+1 will be:

$$E\langle|e_{l+1}|^2\rangle = E\langle|e_l|^2[1-u(\sum_{i=-N}^{N} Q_iQ_i^*)]^2\rangle + E\langle u(\sum_{i=-N}^{N} Q_iQ_i^*)(e_{min}e_l^*+e_le_{min}^*)\rangle \quad \ldots\ (4.13)$$

where e_{min} is the instantaneous error for the optimum tap weights.

4.2.1 Convergence Properties

Let us consider the convergence properties first. The second term in equation (4.13), $E\langle u(.)(.)\rangle$, is less effective when compared with the first term, $E\langle |.|[.]\rangle$, because $|e_1|$ is normally much higher than $|e_{min}|$ for the start up condition. Furthermore, the second term is always a positive value for a positive step size. Therefore, if the MSE converges, then the maximum step size should satisfy the following:

$$[\ 1 - u_{max}\ (\sum_{i=-N}^{N} Q_i Q_i^*)\ ]^2 < 1$$

$$\text{or}\quad u_{max} < \frac{2}{\sum_{i=-N}^{N} Q_i Q_i^*} \qquad \ldots\ldots\ldots\ldots\ldots\ldots\ldots\ldots\ldots\ldots \quad (4.14)$$

For a random data sequence,

$$E\langle \sum_{i=-N}^{N} Q_i Q_i^* \rangle = (2N+1) P_{av} \qquad \ldots\ldots\ldots\ldots\ldots\ldots\ldots\ldots \quad (4.15a)$$

$$P_{av} = E\langle Q_i Q_i^* \rangle = E\langle A_k A_k^* \rangle\ E\langle P^{\theta\phi}{}_i P^{\theta\phi}{}_i^* + c/r \rangle \quad .. \quad (4.15b)$$

$$\text{or}\quad P_{av} = B\ E\langle A_k A_k^* \rangle \qquad \ldots\ldots\ldots\ldots\ldots\ldots\ldots\ldots\ldots\ldots \quad (4.15c)$$

where P_{av} is the average sampling power at demodulation phase θ and sampling phase ϕ, on a one ohm resistance, and B is purely the channel parameter. Fig 4.3 shows the B value of equation (4.15c) against fade position with different fade depths for a 22.6MHz M-QAM radio with 30% excess bandwidth (i.e. a=.3). A 3-ray model with a delay time of 8ns was used. No Gaussian noise is added because of its insignificant effect in most conditions. The sampling phase

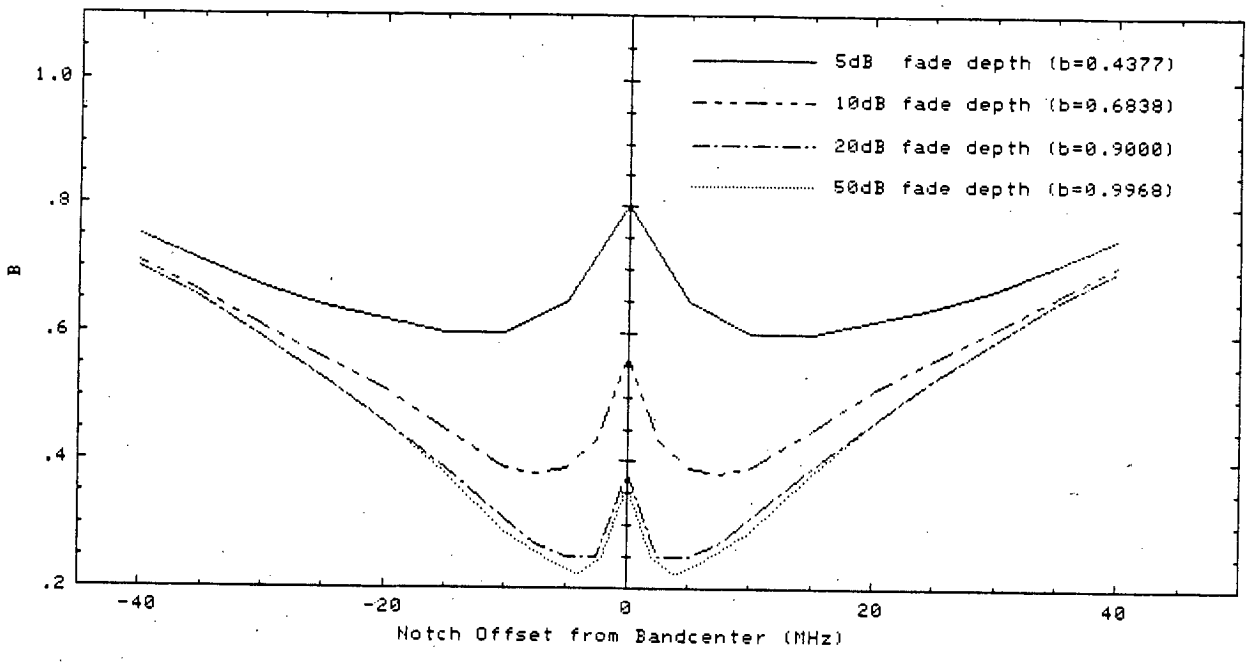

Fig 4.3 The "B" value of the Channel

and demodulation phase are chosen for the maximum B value. Other calculation procedures and definitions can be found in Appendix 4. All the curves show a "W" shape as the ISI increases when the fade notch is at band-edges. For fade depth greater than 20dB, the curve is basically unchanged because the "eye" is completely closed already.

From equations (4.14) and (4.15a):

$$u_{max} < \frac{2}{(2N+1)P_{av}} \qquad (4.16)$$

This result is similar to that obtained by Mazo. During the start up condition, $|e_1|$ is much greater than $|e_{min}|$. As

shown in Appendix 5, the convergence rate will be maximum for step size u' if:

$$u' \sim \frac{1}{\sum_{i=-N}^{N} Q_i Q_i^*} = \frac{1}{(2N+1)P_{av}} \quad \ldots\ldots\ldots\ldots\ldots\ldots \quad (4.17a)$$

$$\text{or} \quad u' \sim 1/2\, u_{max} \quad \ldots\ldots\ldots\ldots\ldots\ldots\ldots\ldots \quad (4.17b)$$

The result is similar to that proposed by Gitlin [98]. However, average power is used instead of eigenvalue bound. Thus maximum convergence can be obtained by using half of the maximum step size for the start up conditions. Equations (4.16) and (4.17a) also imply that for a given P_{av}, the convergence properties are independent of the number of levels in the QAM system.

Consider the following channel for a 22.6MHz 16QAM radio system with a = 0.3:

3 ray model with delay time = 8 ns;
fade depth = 20 dB;
fade position = 20 MHz;
Gaussian Noise = 0;

A 7 tap equalizer is used. From Fig 4.3, B=0.463, and u' can be obtained from equations (4.5), (4.15c) and (4.17a). Five curves have been plotted, as shown in Fig 4.4, with u=7u'/5, 5u'/4, u', u'/2, u'/5. All the initial tap weights are (0,0) with the exception of the center tap weight equals (1,0). The convergence curves are plotted with an ensemble average of 100 runs. These definitions will be used for all the

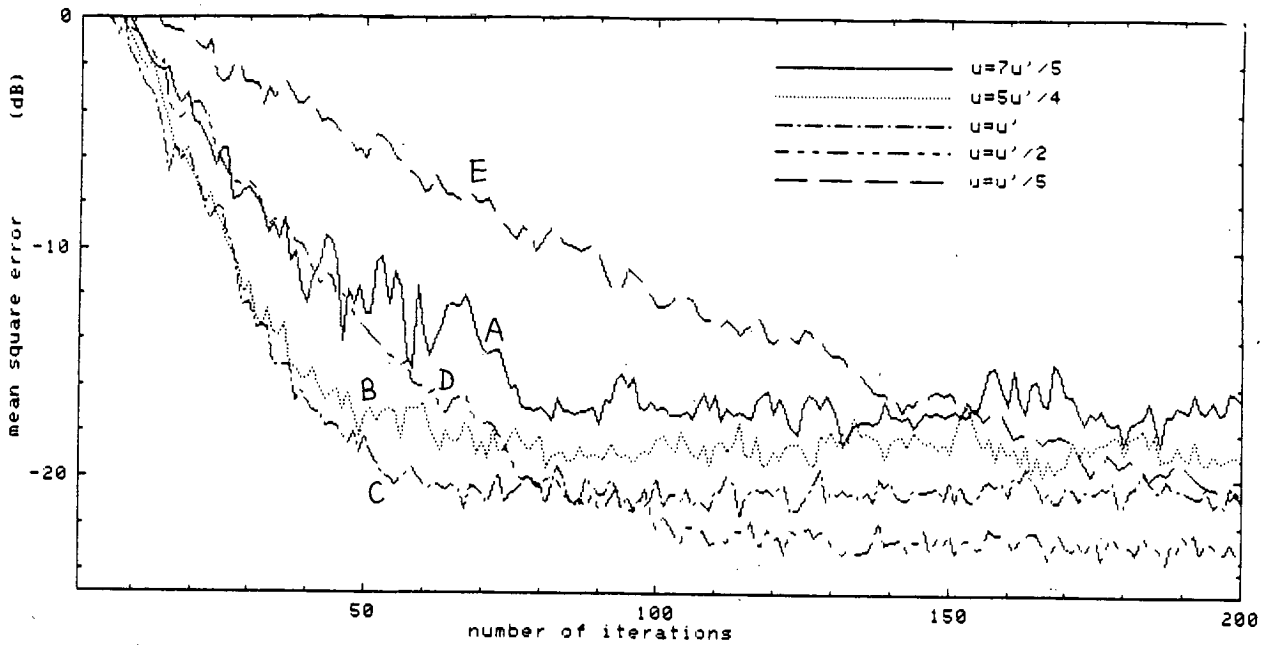

Fig 4.4 Convergence Plots with different Step Size

convergence plots in this thesis. For small step size, u, the MSE convergence rate will increase with u until u~u'. Further increase in u will not only decrease the convergence rate but may also introduce instability.

4.2.2 The Effect of Finite Step Size

When the MSE reaches its final value, the correlation between the input data and e_1 is small. The following can be established:

$$E\langle |e_1|^2 (\sum_{i=-N}^{N} Q_i Q_i^*) \rangle \sim E\langle |e_1|^2 \rangle \, E\langle (\sum_{i=-N}^{N} Q_i Q_i^*) \rangle$$

$$= (2N+1) P_{av} E\langle |e_1|^2 \rangle \quad \ldots\ldots\ldots\ldots \quad (4.18a)$$

Similarly

$$E\langle |e_1|^2 (\sum_{i=-N}^{N} Q_i Q_i^*)^2 \rangle \sim E\langle |e_1|^2 \rangle \, E\langle (\sum_{i=-N}^{N} Q_i Q_i^*)^2 \rangle$$

$$\sim (2N+1)^2 P_{av}^2 E\langle |e_1|^2 \rangle \quad \ldots\ldots\ldots \quad (4.18b)$$

$$E\langle e_{min} e_1^* \sum_{i=-N}^{N} Q_i Q_i^* \rangle \sim (2N+1) P_{av}\, E\langle e_{min} e_1^* \rangle \quad \ldots\ldots\ldots \quad (4.18c)$$

$$E\langle e_1 e_{min}^* \sum_{i=-N}^{N} Q_i Q_i^* \rangle \sim (2N+1) P_{av}\, E\langle e_1 e_{min}^* \rangle \quad \ldots\ldots\ldots \quad (4.18d)$$

$$E\langle |e_{l+1}|^2 \rangle = E\langle |e_l|^2 \rangle = E\langle |e_{final}|^2 \rangle \quad \ldots\ldots\ldots\ldots \quad (4.18e)$$

i.e. from equation (4.13)

$$E\langle |e_{final}|^2 \rangle \sim \frac{E\langle |e_{min} e_{final}^*| \rangle}{1 - u(2N+1)P_{av}/2} \quad \ldots\ldots\ldots\ldots\ldots \quad (4.19)$$

for a small degradation factor,

$$E\langle |e_{min} e_{final}| \rangle \sim \xi_{min} \quad \ldots\ldots\ldots\ldots\ldots\ldots\ldots \quad (4.20a)$$

the following can be achieved:

$$E\langle |e_{final}|^2 \rangle \sim \frac{\xi_{min}}{1 - u(2N+1)P_{av}/2} \quad \ldots\ldots\ldots\ldots\ldots \quad (4.20b)$$

The denominator is the degradation factor. For a very small degradation factor, e.g. u = u'/20, equation (4.20b) can be expressed as:

$$E\langle |e_{final}|^2 \rangle \sim \xi_{min} \left[1 + 1/2\, u(2N+1)P_{av} \right] \quad \ldots\ldots\ldots \quad (4.20c)$$

This turns out to be the result proposed by Widrow and Hoff in 1976 [97].

When the denominator approaches zero, the MSE tends to approach infinity. Equation (4.20b) gives the same maximum step size as in (4.16). In order to reduce the excess error, u should be as small as possible. A standard practice is to use a large u for the start up conditions and reduce it after the MSE converges to predetermined value.

Consider the same fading channel and radio system as in Fig 4.4. Let us compare the MMSE result with the simulation and theoretical value. The simulation result is obtained by averaging the MSE of the last 50 iterations, each iteration is done with 100 ensemble average.** This definition will be used for all the other simulation MMSE unless otherwise specified.

The "Theoretical MMSE A" is obtained by solving equations (4.7), (4.15c) and (4.20b).*** Since the computation of theoretical MMSE and simulated MMSE are done by two different "programs", there exists different computation error between them, particularly the theoretical $\mathcal{E}_{min}$ calculation involves matrix inversion. The column "Theoretical MMSE B" is done by adding or substracting a small offset to theoretical $\mathcal{E}_{min}$ such that it equals simulate MMSE when u=u'/50. This offset is typically less than 0.4dB if $\mathcal{E}_{min}/E\langle A_k A_k^* \rangle$ is higher than -40dB and the number of taps is less than 13. It will always be added or subtracted for the latter $\mathcal{E}_{min}$ calculation.

**The MMSE is reached before the last 50 iterations. This definition will be used for all the simulation MMSE unless otherwise specified. In this example, 400 iterations are used for u=u'/5 and 200 iterations for all the other 4 curves.

***Refer to Appendixes 4, 9 & 10 for all the calculation accuracies, and the Programs to evaluate the theoretical and simulation MMSE

$u' = 0.031$ $\xi_{min} = -24.5$ dB

curve	u	Theoretical MMSE A (dB)	Theoretical MMSE B (dB)	Simulation MMSE (dB)
A	7u'/5	-19.3	-19.2	-16.6
B	5u'/4	-20.2	-20.1	-18.6
C	u'	-21.5	-21.4	-20.7
D	u'/2	-23.3	-23.2	-22.9
E	u'/5	-24.0	-23.9	-23.9

Table 4.1a Comparison between the Theoretical and Simulation MMSE with 7 tap T-spaced equalizer

From Table 4.1a, we find that the theoretical MMSE is reasonably close to the simulation result for $u < u'$. For a larger u value, the theoretical MMSE will deviate considerably from the simulation result. This is because the approximation involves equations (4.20a) and (4.18b),** where the right hand terms are always less than their left hand term. As a result, the degradation factor in equation (4.20b) is always less than the actual condition. The deviation will increase as the step size increases. Furthermore, as the MSE increases, the correlation between the error and the input data Q_j increases for an equalizer with smaller number of taps.

**The error in equation (4.18b) is normally less than 20% if the number of equalizer taps is greater than 5, $\xi_{min}/E\langle A_k A_k \rangle$ less than -20dB.

Actually, equation (4.20a) can also be approximated as follows:

$$E\langle |e_{final} e_{min}| \rangle \sim E\langle \left(\frac{|e_{final}|^2}{e_{min}} \right)^{0.5} |e_{min}| \rangle \quad \ldots\ldots\ldots \quad (4.21a)$$

So it is quite reasonable to assume $E\langle |e_{final} e_{min}| \rangle / \xi_{min}$ is depend on the power of ($E\langle |e_{final}|^2 \rangle / \xi_{min}$), and the following can be obtained:

$$E\langle |e_{final}|^2 \rangle \sim \frac{\xi_{min}}{[\ 1 - u(2N+1)P_{av}/2\ ]^{\beta}} \quad \ldots\ldots\ldots\ldots \quad (4.21b)$$

where β is a function of ξ_{min}, step size, number of taps and channel parameters. The error in equation (4.18b) can also be included with different choice of β. However, from most of the simulation results, the following simplification of β may hold:

$$\beta = 1 + p(u/u') \quad \ldots\ldots\ldots\ldots\ldots\ldots\ldots\ldots \quad (4.21c)$$

where p lies within the range 0.2 to 0.4.**

With p=0.3, Table 4.1b shows the comparison between modified theoretical MMSE and the simulation MMSE. They are very close together.

	E	D	C	B	A
Modified Theoretical MMSE (dB)	-23.9	-23.0	-20.5	-18.5	-17.0
Simulation MMSE (dB)	-23.9	-22.9	-20.7	-18.6	-16.6

Table 4.1b Comparison of the Modified Theoretical MMSE and Simulation MMSE as in Table 4.1a

**With p=0, equations (4.21b) and (4.20b) will be identical.

Gitlin replaced P_{av} in (4.20b) by the product of P_{av} and γ, where γ is the ratio of the maximum eigenvalue to average eigenvalue. For a highly distorted channel, γ may be quite high. If a big step size is used, this bound may not be a good estimate.

	no of taps	fading parameters		step size	simulation MMSE (dB)	$\Delta_{u'}$ (dB)
		b (dB)	$W_o/2$ (MHz)			
A	3	20.0	20	u'	- 6.1	3.9
				u'/50	-10.0	
B	7	20.0	20	u'	-20.7	3.7
				u'/50	-24.4	
C	17	20.0	20	u'	-42.2	3.9
				u'/50	-46.1	
D	17	23.9	10	u'	-20.1	4.0
				u'/50	-24.1	
E	3	2.2	20	u'	-19.7	3.5
				u'/50	-23.2	

$$\Delta_{u'} = (MMSE)_{u'} - (MMSE)_{u'/50}$$

Table 4.1c Comparison of $\Delta_{u'}$ with different Channel Parameters and Number of Taps

Consider the examples in Table 4.1c, with the same radio system as in Table 4.1a. Let $\Delta_{u'}$ be the difference of MMSE with u=u' and u=u'/50. Cases A, B, C are all with the same fading parameters as in Table 4.1a but with 3, 7 and 17 tap equalizers respectively. The MMSE with step size u'/50 is of the same order in cases B, D and E. However 7, 17 and 3 tap

equalizers are used in cases B, D and E respectively, their channel distortion will be significantly different and so are their γ value. Thus a significant difference of Δ_u, will be obtained if Gitlin's bound is used. However, the simulation results show Δ_u, are broadly equivalent in all cases.

4.3 The Effect of Quantization Noise in the Analogue to Digital Converter (ADC)

In a digital implementation of the adaptive algorithm, quantization noise cannot be avoided. The demodulated baseband signal is sampled and converted into digits by the analogue to digital converter (ADC). Let $\bar{}$ be the notation for quantization, and x be the corresponding noise. The received baseband data can be represented as:

$$Q_j = \bar{Q}_j + x_j$$

The matrix element of $\underline{D}$ and $\underline{R}$ in equations (4.3b,c,d) and (4.6b) are:

$$D_i = E\langle A_m \bar{Q}_{m-i}^* \rangle + E\langle A_m x_{m-i}^* \rangle \quad \ldots\ldots\ldots\ldots\ldots\ldots \quad (4.22a)$$

$$R_{ij} = E\langle \bar{Q}_{m-j} \bar{Q}_{m-i}^* \rangle + E\langle x_{m-j} x_{m-i}^* \rangle + E\langle \bar{Q}_{m-j} x_{m-i}^* \rangle + E\langle x_{m-j} \bar{Q}_{m-i}^* \rangle \quad \ldots\ldots\ldots\ldots \quad (4.22b)$$

The exact evaluation of this quantization noise is impractical in general. However we can take the following assumptions to get a rough estimate:

(1) The insignificant correlation of (i) quantization level and quantization noise, (ii) different quantization noises.

(2) The signal is evenly distributed for each quantization level.

(3) The ADC is ideal, i.e. there are no non-linearity, off-set..etc. errors.

So the equations (4.22a,b) can be expressed as:

$$D_i = \bar{D}_i, \quad R_{ij} = \bar{R}_{ij} + \Delta_q \delta_{ij} \quad \text{..... (4.23a)}$$

or similarly

$$D_i' = \bar{D}_i', \quad R_{ij}' = \bar{R}_{ij}' + \Delta_q' \delta_{ij} \quad \text{..... (4.23b)}$$

where Δ_q is $E\langle x_j x_j^* \rangle$, the quantization noise power for each quantization level and Δ_q' is $\Delta_q / E\langle A_k A_k^* \rangle$. As shown in Appendix 6,

$$\Delta_q = \frac{(2L-1)^2}{6\,[2^{2(n_1-1)}]} \quad \text{..... (4.24)}$$

where 2(2L-1) is the peak to peak level in the I or Q channel and n_1 is the number of bits in the ADC (2L is the total number of levels in I or Q channel). Thus for a fixed number of bits in ADC, the quantization noise power will increase as number of level increases.

From equation (4.23a), the modified average power after quantization will be:

$$P_{av} = P_{av} - \Delta_q \quad \text{..... (4.25)}$$

With the same approach as in section 4.1, the optimum MSE will be:

$$\bar{\xi}_{min} = E\langle A_k A_k^* \rangle \left[1 - \underline{D}'^{h} \left(\underline{R}' - \Delta_q' \underline{I} \right)^{-1} \underline{D}' \right] \quad \ldots\ldots\ldots\ldots\ldots\ldots\ldots\ldots \quad (4.26)$$

where $\underline{I}$ is the identity matrix.

If the number of bits in the ADC is high or the channel is not highly distorted, then equation (4.26) may not be valid because it cannot satisfy the assumptions (1) & (2). The exact comparison of the optimum MSE between equation (4.8) and (4.26) is not obvious. An alternative technique is to assume the changes of the optimum tap weight due to quantization noise are small, i.e. $\bar{\underline{C}}_{opt} \sim \underline{C}_{opt}$. Since the quantization noise for each tap weight is uncorrelated with each other, each tap weight symbol will generate its own quantization noise. The overall quantization noise, N_q, at the equalizer output will be:

$$N_q \sim \Delta_q \, \underline{C}_{opt}^{h} \underline{C}_{opt} \quad \ldots\ldots\ldots\ldots\ldots\ldots\ldots\ldots\ldots\ldots\ldots\ldots \quad (4.27)$$

$$\text{i.e.} \quad \bar{\xi}_{min} = \xi_{min} + \Delta_q \, \underline{C}_{opt}^{h} \underline{C}_{opt} \quad \ldots\ldots\ldots\ldots\ldots \quad (4.28)$$

Compared with (4.26), equation (4.28) is more accurate and reliable as it is not dependent on matrix behavior of $\underline{R}'$ and $\underline{D}'$. Furthermore it provides a simple estimation of ξ_{min}.

By substituting equation (4.26) or (4.28) into (4.21b), the degradation due to step size can also be obtained:

$$E\langle|\bar{e}_{final}|^2\rangle \sim \frac{\bar{\xi}_{min}}{[\ 1 - u(2N+1)\bar{P}_{av}/2\ ]^{\beta}} \quad \ldots\ldots\ldots\ldots\ldots \quad (4.29)$$

Consider the same radio system and fading channel as in Fig 4.4. Four curves have been plotted, as shown in Fig 4.5. With the same step size, the MSE convergence properties are basically identical compared with that in Fig 4.4. Since $P_{av} >> \Delta_q$, i.e. $P_{av} \sim \bar{P}_{av}$ in equation (4.25). This implies the convergence properties will basically not be affected, as shown in equations (4.16) and (4.17b).

The final MSE is compared with theoretical calculation using equations (4.21c), (4.28) and (4.29), as shown in Table 4.2. With p=.3 in equation (4.21c), the theoretical MMSE is reasonably close to that from the simulation result.

curve	step size (u)	ADC bits (n_1)	Theoretical MMSE (dB)		Simulation MMSE (dB)
			p=0	p=.3	
A	5u'/4	5	-12.8	-11.2	-11.6
B	u'	5	-14.1	-13.2	-13.5
C	u'/2	6	-20.0	-19.8	-19.7
D	u'/5	6	-20.7	-20.7	-20.6

Table 4.2 Comparison between the Theoretical and Simulation MMSE with Finite ADC Resolution

At voice band frequencies, the quantization noise problem will not be too serious because 10 to 16 bits definition in the ADC are easily obtainable. However in the digital radio

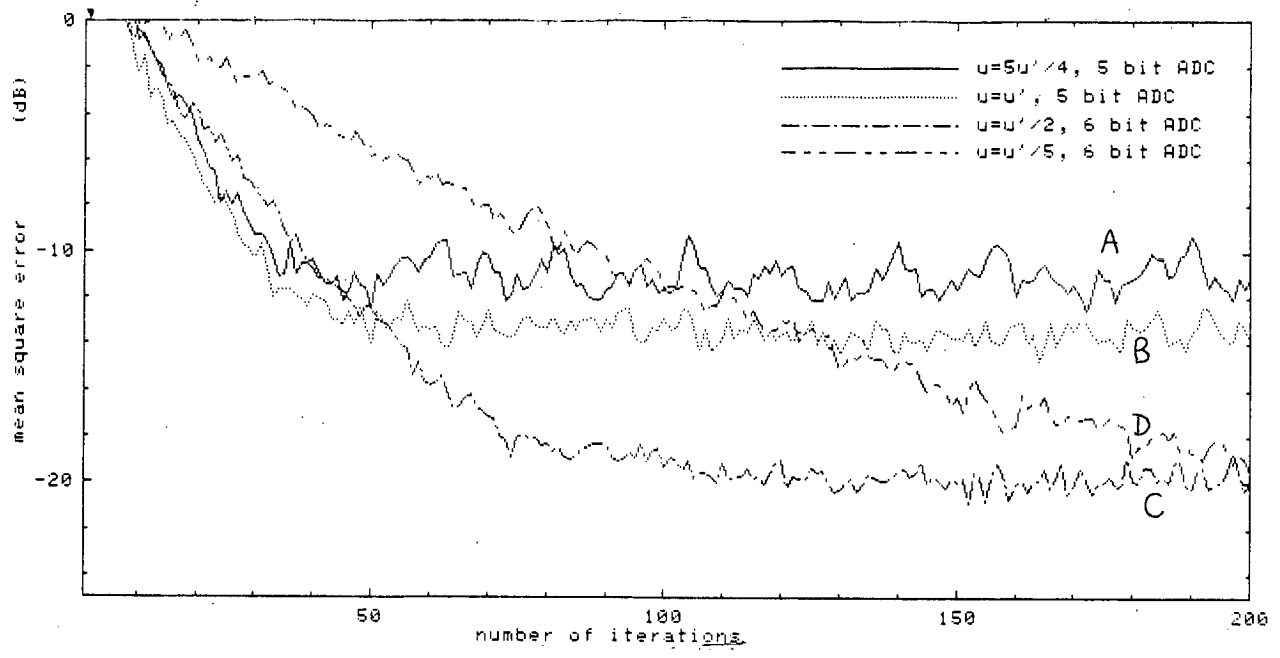

Fig 4.5 Convergence Plots with different Step Size and Precision ADC

application, the typical frequency is normally of the order of 10's MHz, and commerical ADC accuracy at such frequencies is typically 4 to 8 bits. The quantization noise may thus contribute significant degradation under such conditions particularly when high level modulation is used.

4.4 The Effect of Finite Precision Arithmetic

4.4.1 Minimum Mean Square Error

Apart from the quantization noise in the ADC, the round off errors in the arithmetic also contribute to degradations in performance. Let ν be the notation for the round off

condition in arithmetic. From equation (4.12), the following can be obtained:

$$E\langle|e_1|^2\rangle = \xi_{min} + E\langle \sum_{i=-N}^{N} (\check{C}_i - \bar{C}_i')^* \bar{Q}_i^* \sum_{j=-N}^{N} \bar{Q}_j (\check{C}_j - \bar{C}_j')\rangle \quad \ldots\ldots\ldots\ldots\ldots\ldots\ldots \quad (4.30a)$$

or

$$E\langle|e_1|^2\rangle = \check{\xi}_{min} + E\langle \sum_{i=-N}^{N} (\check{C}_i - \check{C}_i')^* \bar{Q}_i^* \sum_{j=-N}^{N} \bar{Q}_j (\check{C}_j - \check{C}_j')\rangle \quad \ldots\ldots\ldots\ldots\ldots\ldots\ldots \quad (4.30b)$$

when the number of bits in arithmetic is large

A rough estimate on MMSE, ξ_{min}, can be obtained if we make the following assumptions:

(a) The optimum tap weight, $\underline{\check{C}}_{opt}$, can be reached and the maximum deviation from $\underline{\check{C}}_{opt}$ is less than half the least significant digit (LSB).

(b) The number of tap weights is large enough such that

$$E\langle \delta C_i^* Q_i^* Q_j \delta C_j\rangle \sim \delta_{ij} \Delta_c R_{ij} \quad \ldots\ldots\ldots\ldots\ldots \quad (4.31)$$

where δC_i is the deviation of tap weight element C_i from $\bar{C}_i'$, Δ_c is the round off noise power. With the same approach as in Appendix 6,

$$\Delta_c = \frac{lc^2}{6\,[2^{2(n_2-1)}]} \quad \ldots\ldots\ldots\ldots\ldots\ldots\ldots \quad (4.32a)$$

or

$$\Delta_c = \frac{(\text{ LSB })^2}{6} \quad \ldots\ldots\ldots\ldots\ldots\ldots\ldots \quad (4.32b)$$

where lc is the maximum range for tap weight value and n_2 is the number of bits employed.

(c) n_2 is large enough such that most of the tap weight elements are non-zero. Otherwise it will correspond to an equalizer with fewer taps.

(d) The desired response, A_m, is exactly one of the quantization levels.**

So the following can be achieved from equations (4.28) and (4.30a,b):

$$\xi_{min} \sim \bar{\xi}_{min} + \Delta_c(2N+1)\bar{P}_{av} \quad \text{..... (4.33a)}$$

$$\sim \xi_{min} + \Delta_q(\underline{C}_{opt})^h\underline{C}_{opt} + \Delta_c(2N+1)\bar{P}_{av} \quad \text{..... (4.33b)}$$

where the quantization noise due to finite arithmetic effects is:

$$N_c \sim \Delta_c(2N+1)\bar{P}_{av} \quad \text{..... (4.34)}$$

4.4.2 Gradient Noise

Denoting $f(ueQ_j^*)$*** to be the quantization representation of gradient estimator ueQ_j^*, and y_j to be its rounding error, then

$$ueQ_j^* = f(ueQ_j^*) + y_j \quad \text{.....(4.35a)}$$

**This implies for a 16QAM radio system, the levels may not be exactly equal to that within the set $\{ \pm 3, \pm 1 \}$.

***Here the subscript of error signal, e_1, has been dropped in order not to be confused with the matrix element subscript.

To evaluate the degradation due to the gradient estimate, we make the following assumptions:

(a) Double precision ($2Xn_2$ bits) is used to evaluate $\sum_{j=-N}^{N} C_j Q_j$ and there is no intermediate overflow.

(b) The correlation between y_j, e and Q_j is negligible.

So the degradation due to the step size can be obtained by using equations (4.33a,b) and with the same approach as in section 4.2.2.

$$E\langle|\check{e}_{final}|^2\rangle \sim \frac{\check{\xi}_{min}}{[\ 1 - 1/2\ u(2N+1)\bar{P}_{av}\ ]^{\beta}} \quad \ldots\ldots\ldots\ldots \quad (4.36a)$$

$$\text{or} \quad \sim \frac{\xi_{min} + \Delta_q\ (\underline{C}_{opt})^h \underline{C}_{opt} + \Delta_c(2N+1)\bar{P}_{av}}{[\ 1 - 1/2\ u(2N+1)\bar{P}_{av}\ ]^{\beta}} \quad \ldots \quad (4.36b)$$

and the convergence properties will be basically unchanged.

u = 0.027 (0.86u')

curve	ADC bits (n_1)	arithmetic bits (n_2)	Theoretical MMSE (dB)		Simulation MMSE (dB)
			p=0	p=.3	
A	5	7	-13.9	-13.3	-12.6
B	5	8	-14.5	-13.9	-13.4
C	6	7	-17.0	-16.4	-15.4
D	6	8	-18.2	-17.6	-17.0

Table 4.3 Comparison between the Theoretical and Simulation MMSE with Finite ADC and Arithmetic Resolution

With the same fading channel, radio system and 7 tap equalizer as in Fig 4.4, four curves with different numbers

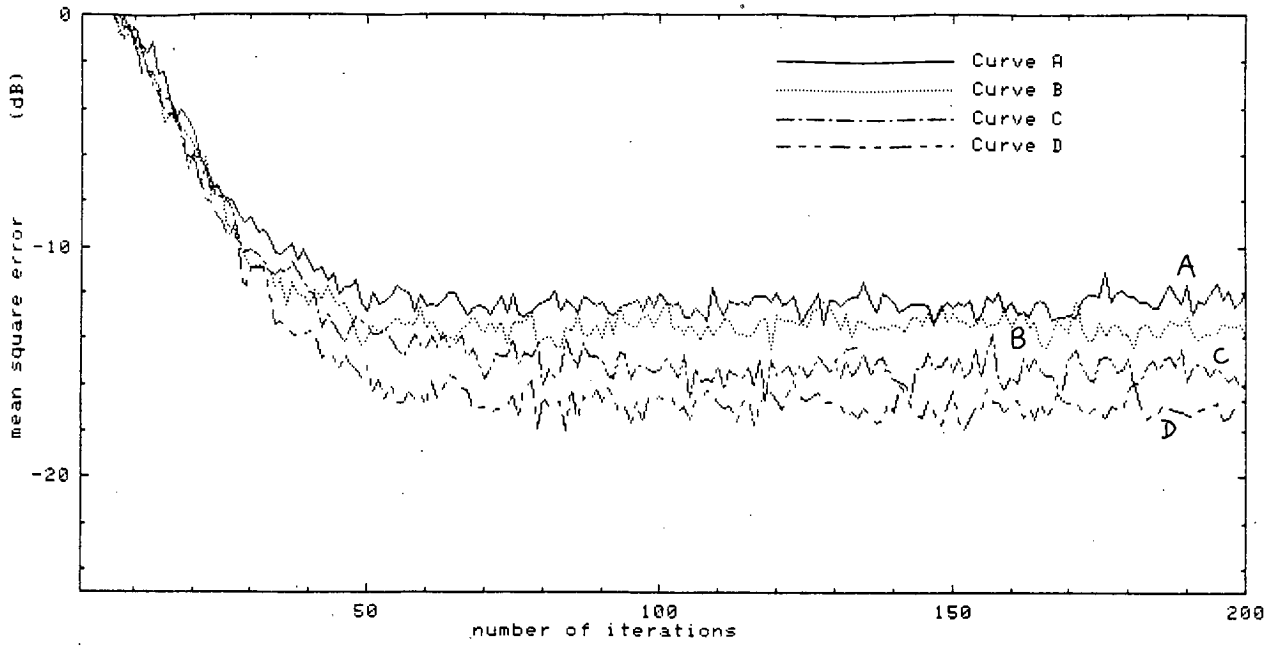

Fig 4.6 Effect of Finite Precision Arithmetic and ADC Accuracy as defined in Table 4.3

of bits in the ADC and arithmetic have been plotted, as shown in Fig 4.6. The step size is fixed to be 0.027, so the MSE convergence rate is basically the same for all curves. With p=0.3 in equation (4.21c), the simulation result is reasonably close to the theoretical estimation using equation (4.36b), as shown in Table 4.3.

4.4.3 Early Termination

As from equations (4.36a,b), the degradation factor can be reduced by simply using a small step size. However as pointed out by Gitlin [98], the tap weight will virtually stop updating if u is too small. This will result in a MSE which is significantly larger than the MMSE as predicted by equations

(4.36a,b). Let us call this an "early termination effect". From equation (4.11), the tap weight will stop the convergence if:

$$|ueQ_i^*| < 1/2 \text{ LSB} \quad \ldots\ldots\ldots\ldots\ldots\ldots\ldots\ldots \quad (4.37a)$$

$$\text{or } u^2|eQ_i^*|^2 < (1/2 \text{ LSB})^2 \quad \ldots\ldots\ldots\ldots\ldots\ldots\ldots \quad (4.37b)$$

Let $E\langle|e_{early}|^2\rangle$ be the final MSE due to the early termination of the tap weight adaptation, and "A $E\langle|e_{early}|^2\rangle$" be the upper bound of square error after convergence to its final value. The approximation of $E\langle|e_{early}|^2\rangle$ can be achieved by using equations (4.37b) and (4.15a):

$$E\langle|e_{early}|^2\rangle \sim \frac{1}{A\ \bar{P}_{av}} \left(\frac{1}{2n_3}\right)^2 \quad \ldots\ldots\ldots\ldots\ldots \quad (4.38a)$$

where n_3 is the number of LSB's for the step size, and the A value depends on channel and equalizer parameters. However we can assume the PDF of the error is close to a Gaussian distribution but with a bounded limit. Then the value of A is typically ~10 and the following result can be obtained:

$$E\langle|e_{early}|^2\rangle \sim \frac{1}{40\ \bar{P}_{av}} \left(\frac{1}{n_3}\right)^2 \quad \ldots\ldots\ldots\ldots\ldots \quad (4.38b)$$

Equation (4.38b) shows that the MMSE due to the early termination will only depend on average power and the n_3 value. Table 4.4 shows the simulation result by using a step size of 1 LSB with an 8 bits ADC, using the same radio channel characteristic as in Fig 4.4.

number of taps	9	9	13	13
arithmetic bits	10	12	10	12
Simulation MMSE (dB)	-22.2	-22.2	-23.2	-22.0
ξ_{min} A (dB)	-29.8		-37.9	
ξ_{min} B (dB)	-29.6		-38.1	
$E\langle\lvert\check{e}_{final}\rvert^2\rangle$ (dB)	-28.2	-28.7	-32.5	-34.0

ξ_{min} A is calculated by equation (4.7)

ξ_{min} B is obtained by adding offset to ξ_{min} A, as described in section 4.2.2

The summation of the tap weight square (S)= 2.6 in all cases

Table 4.4 The effect of early termination on MMSE

The MMSE estimate from equation (4.38b) is -22.7dB. The simulation result is achieved by averaging over the last 1000 iterations of an 100000 iteration** convergence plot with an ensemble average of 20 runs. The $E\langle\lvert\check{e}_{final}\rvert^2\rangle$ is calculated by solving equations (4.36b) and (4.21c) with p=.3. The result given in Table 4.4 demonstrates the loose dependency of $E\langle\lvert e_{early}\rvert^2\rangle$ on N, ξ_{min}, $E\langle\lvert\check{e}_{final}\rvert^2\rangle$ and n_2 when the step size is small.

Apart from the degradation of MMSE, the early termination also affects the convergence properties. When the MSE is about ~3dB above MMSE, the convergence slows down dramatically, as the tap weight is only updated when high MSE occurs, corresponding to a low PDF value. Table 4.5 shows this

**After 100000 iterations, the MMSE will basically remain unchanged.

effect, for the same channel and radio system as in Fig 4.4, with a 9 tap equalizer and 8 bits ADC. The step size is 1 LSB, 12 bits arithmetic is used. The result is obtained from an ensemble average of 20 runs.

iterations	500-520	1000-1020	5000-5020	31000-32000	49000-50000	99000-100000
average MSE (dB)	-6.6	-17.0	-19.4	-21.5	-21.9	-22.2

Table 4.5 The effect of early termination on convergence

Care should be taken in applying equations (4.38a,b), as the estimation of MSE is for the early termination effect only. When it is lower than the estimate of equations (4.36a,b), which assesses finite step size effects, no early termination effect will occur. The final MSE will follow the the estimate from gradient noise, i.e. equations (4.36a,b). The MMSE will not be reduced by simply increasing the step size, u, as predicted in equations (4.38a,b).

Consider the step size such that the MMSE due to early termination is equal to the MMSE due to finite step size. From equation (3.35a), with A=10, the minimum step size in terms of LSBs can be approximated as follow:

$$n_3' \sim \frac{1}{(40\ \bar{P}_{av}\ E\langle |e_{final}|^2 \rangle)^{1/2}} \quad \ldots\ldots\ldots\ldots\ldots\ldots \quad (4.38c)$$

where $n_3' = 0, 1, 2 \ldots$

If n_3 is less than n_3', the early termination effect occurs, with the converse conditions, gradient noise starts to dominate.

4.5 The Effect of Finite Tap Weight Elements

Let us re-arrange equation (4.6c) as $\underline{R}'\underline{C}_{opt}=\underline{D}'$. Under Fourier transformation for an infinite tap weight equalizer, i.e. N=infinity, the following can be established:

$$(|H_f(jw)|^2 + n) C(jw) = H_f(jw)^* \quad \ldots\ldots\ldots\ldots\ldots \quad (4.39a)$$

$$\text{or } C(jw) = \frac{H_f(jw)^*}{|H_f(jw)|^2 + n} \quad \ldots\ldots\ldots\ldots\ldots\ldots\ldots\ldots \quad (4.39b)$$

where $H_f(jw) = \sum_{k=-\infty}^{\infty} H[j(w-2\pi k/T)]$ is the overall folded frequency response of the channel at 0 to 1/T Hz. When the white Gaussian noise, n, approaches zero, equation (4.39b) becomes an inverse filter of $H_f(jw)$ and can compensate for all the linear distortions if $H_f(jw)$ does not completely vanish. However only a finite number of tap weights can be used in practice, this puts a constraint on the equalizer performance. Furthermore, as shown in the previous sections, the degradation due to the gradient noise, finite arithmetic..etc., will be increased with N. All these factors, including the costs should be carefully considered before the implementation of the equalizer is finalized.

4.5.1 Minimum Mean Square Error

Generally speaking $\mathcal{E}_{min}$ will decrease as N increases, and the equalizer will approach the ideal condition. This can be proved by applying equation (4.7) and assuming the tap

weights will not change when N increases.** This can also be explained by using the time or frequency domain method. In the former case, only the ISI which is within the $\pm N$ time slot of the main lobe can be equalized. When N increases, the total unequalized ISI will be reduced. Consider the latter case, the frequency resolution between 0 to 1/T is 1/(2N+1) [101]. The overall equalized frequency response will approach the Nyquist channel as N increases. This will result in reducing $\mathcal{E}_{min}$ as N increases.

The improvement gained from increasing the equalizer order from 2N+1 to 2M+1 (M>N) depends on channel parameters. However, some interesting relationships are obtained as $\mathcal{E}_{min}$ is plotted against N. A log linear curve can be obtained, as shown in Fig 4.7, for the four different channels as shown in Table 4.6.

Curve	Fading Parameters		
	T_d (ns)	$W_o/2\pi$ (MHz)	b (dB)
A	8.0	20	20
B	8.0	15	20
C	8.0	10	20
D	6.3	10	20

Table 4.6 Channel Paramters for Figure 4.7

**However, in the actual condition, the tap weights will be changed as N increases because a finite tap equalizer is equivalent to a infinite tap equalizer with the constraint -- $C_i = 0$ for $i<-N$ and $i>N$.

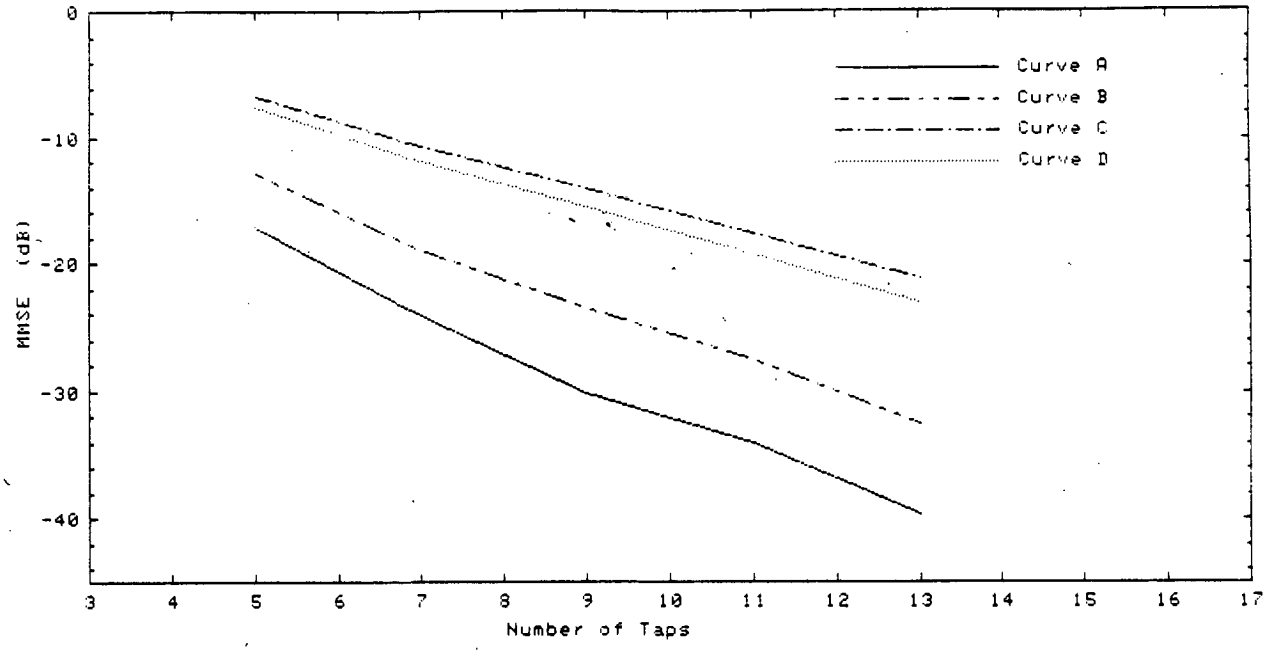

Fig 4.7 $\mathcal{E}_{min}$ against Number of Taps for Channel Parameters given in Table 4.6

Although it is an empirical result and no analytic evaluation has been established, simulation data supports this log linear relationship 2N+1 values in the range 5 to 13 when $\mathcal{E}_{min}$ is higher than -35dB. This may be a useful criterion for prediction of $\mathcal{E}_{min}$ with various numbers of tap weights.

4.5.2 Quantization Error at ADC

The quantization error at the ADC has been evaluated in section 4.3. Generally speaking, the quantization noise is loosely related to the number of taps in the equalizer when 2N+1>5. This is because the center few taps are dominant in equation (4.27). As shown in the following table, the

$(\underline{C}_{opt})^h(\underline{C}_{opt})$ is evaluated for different number of taps. The channel we use is still as in Fig 4.4.

no of taps	3	5	7	13	17
S	2.54	2.67	2.70	2.70	2.70

$$S = (\underline{C}_{opt})^h(\underline{C}_{opt})$$

Table 4.7 The effect of Number of Taps on S

4.5.3 Quantization Error with Finite Precision Arithmetic

As from equation (4.32), the degradation in $\mathcal{E}_{min}$ due to the quantization noise of finite arithmetic, N_c, is proportional to the number of taps -- 2N+1. Nevertheless for a 16QAM radio system with a number of equalizer taps less than 11, an N_c of -15dB or better is easily obtainable if $n_2>7$. Compared with $\mathcal{E}_{min}$, N_c is less sensitive to channel distortion. Under severe multipath fading, $\mathcal{E}_{min}$ will increase dramatically but with only a small change of P_{av}, as shown in the "B" value of Fig 4.3. Consequently a small change of N_c has negligible effect when compared with $\mathcal{E}_{min}$.

Generally speaking, for a good equalizer design, the degradation of the equalizer signature due to N_c is insignificant, even if the value of N is doubled.

4.5.4 Step Size and Convergence Properties of MSE

This will be the major factor which needs to be considered as the number of taps is increased from 2N+1 to 2M+1. In order to maintain the same degradation caused by the step size as in equations (4.36a,b), u should be reduced by (2N+1)/(2M+1). However, recall that in section 4.4.3, care should be taken to avoid the early termination effect as u reduces.** The reduced step size also implies slowing of the MSE convergence rate. To gain the full benefit of increasing the number of taps weights (ξ_{min} reduction), greater resolution in arithmetic is likely to be required.

The MSE convergence properties are also changed when the number of taps changes. Let u_n' and u_m' be the step size for the maximum convergence rate in 2N+1 and 2M+1 tap equalizers respectively (M>N). As from equation (4.17a) $u_n'>u_m'$. The convergence properties in both cases (M and N) will be basically unchanged if the step size u is less than u_m'. However, when u is greater than u_m', the convergence rate for 2M+1 tap equalizer will start to slow down while it is still increasing for the 2N+1 tap equalizer.

Fig 4.8 plots the convergence properties with u=0.019 and 0.027 in both 7 and 11 tap equalizers. The radio system and channel are the same as in Fig 4.4, where u_n' and Convergence

**the early termination effect may not be a serious problem if the signature plot of the radio system is the sole determination factor, because the signature corresponds to high BER. In other words high $E(|\check{e}_{final}|^2)$ where the early termination effect is unlikely to occur for a proper equalizer design.

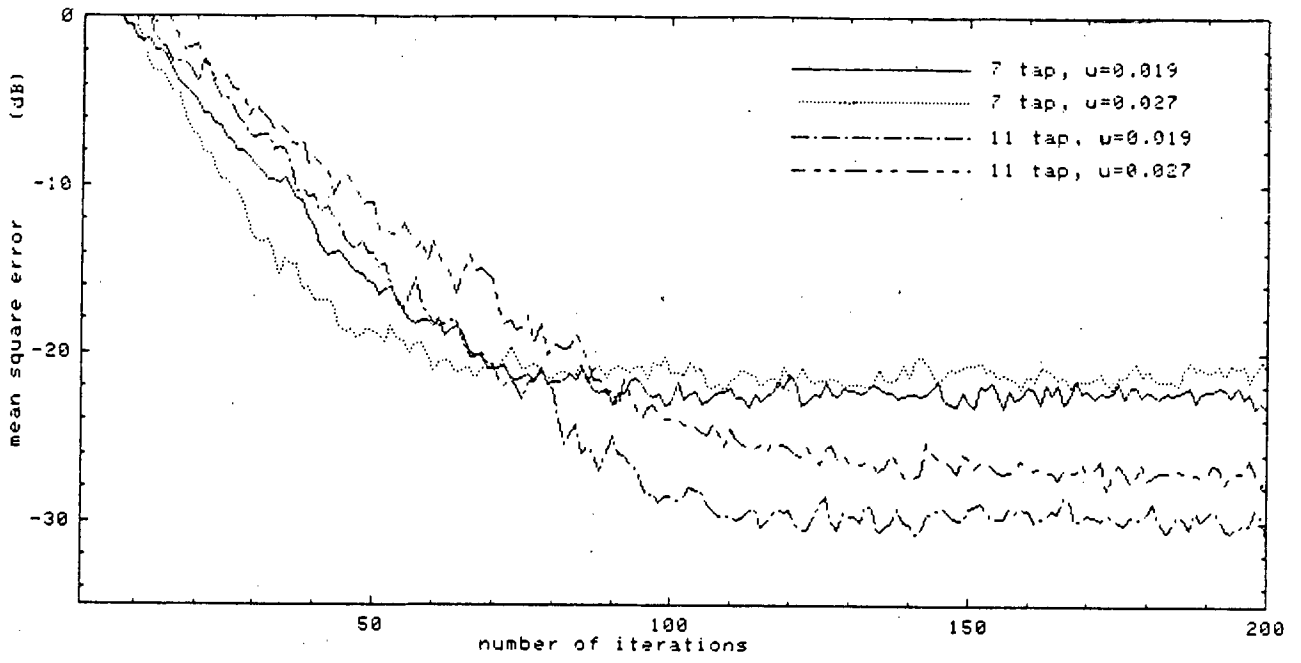

Fig 4.8 Convergence Property with different Number of Taps

Property are equal to 0.031 and 0.020 respectively. The initial convergence rate for both 7 and 11 tap equalizers are basically the same for u=0.019, but it is faster for the 7 tap equalizer when u=0.027. The longer equalizer ultimately offers lower MMSE.

4.6 The Effect of Demodulation Phase

Incorrect demodulation phase will only cause a rotation of the constellation at the equalizer input, as shown in Fig 4.2, with the total ISI around each constellation point remaining unchanged. Comparing the channel pulse response with demodulation phase θ and 0, both with sampling phase $\emptyset$:

$$P^{\theta\phi} = \mathfrak{F}^{-1}[\, H_f(jw)\exp(j\theta)\,] \qquad \mathfrak{F}^{-1}: \text{inverse Fourier transform}$$

$$= \frac{\exp(j\theta)}{N_\theta/N_0}\, P^{0\phi} \quad \ldots\ldots (4.40)$$

where N_θ, N_0 is the normalization constant at demodulation phase θ and 0 respectively, such that the summation of the mainlobe plus all the ISI terms equals 1.

Consider the matrices $\underline{C}_{opt}$, $\underline{R}$ and $\underline{D}$ in equations (4.3b,c,d, and 4.6a,b) and adding the demodulation phase and sampling phase superscript, we get:

$$\underline{R}^{\theta\phi} = \left(\frac{1}{N_\theta/N_0}\right)^2 \underline{R}^{0\phi} \quad \ldots\ldots (4.41a)$$

$$\underline{D}^{\theta\phi} = \left[\frac{\exp(j\theta)}{N_\theta/N_0}\right] \underline{D}^{0\phi} \quad \ldots\ldots (4.41b)$$

$$\text{i.e. } \underline{C}_{opt}^{\theta\phi} = [\exp(i\theta)N_\theta/N_0)]\, \underline{C}_{opt}^{0\phi} \quad \ldots\ldots (4.41c)$$

and from equations (4.6a,c), we can conclude that ξ_{min} will not be changed for various values of demodulation phase θ. However, different demodulation phase values affect the degradation due to quantization error in the ADC and finite arithmetic, from equations (4.27, 4.15b and 4.34):

$$N_q^{\theta\phi} = (\, N_\theta/N_0)^2\, N_q^{0\phi} \quad \ldots\ldots (4.42a)$$

$$P_{av}^{\theta\phi} = \left(\frac{1}{N_\theta/N_0}\right)^2 P_{av}^{0\phi} \quad \ldots\ldots (4.42b)$$

$$N_c^{\theta\phi} = \left(\frac{1}{N_\theta/N_0}\right)^2 N_c^{0\phi} \quad \ldots\ldots (4.42c)$$

assuming fixed range arithmetic, i.e. same LSB value, is used during both conditions.

Fortunately the effect is small because $(N_\theta/N_0)^2$ should be within the range 0.5 to 2. Furthermore, the changes in N_q and N_c tend to cancel each other, as shown in equations (4.42a,c). Again, care should be taken on gradient noise degradation, early termination effect and changes in convergence properties because of the changes in P_{av}.

However in a typical carrier recovery circuit, the rotation angle, @ (refer to Fig 4.2) of the equalizer input signal can be set to zero (or $\pm 90^\circ$) by detecting either the peak levels in the I and Q channels or the received sample data power. When $@=0^\circ$, the received sample data power will be a maximum if the maximum peak level at the I or Q channel is always normalized. Actually the effect of demodulation phase error will be insignificant to the overall equalizer responses and any rotation of constellation at the equalizer input can be compensated without difficulty. As shown in section 4.1.2, @ is always zero at the equalizer output.

4.7 The Effect of Sampling Phase

4.7.1 The Problems of Excess Bandwidth

Compared with demodulation phase, the effect of sampling phase is more serious. The input signal to the equalizer

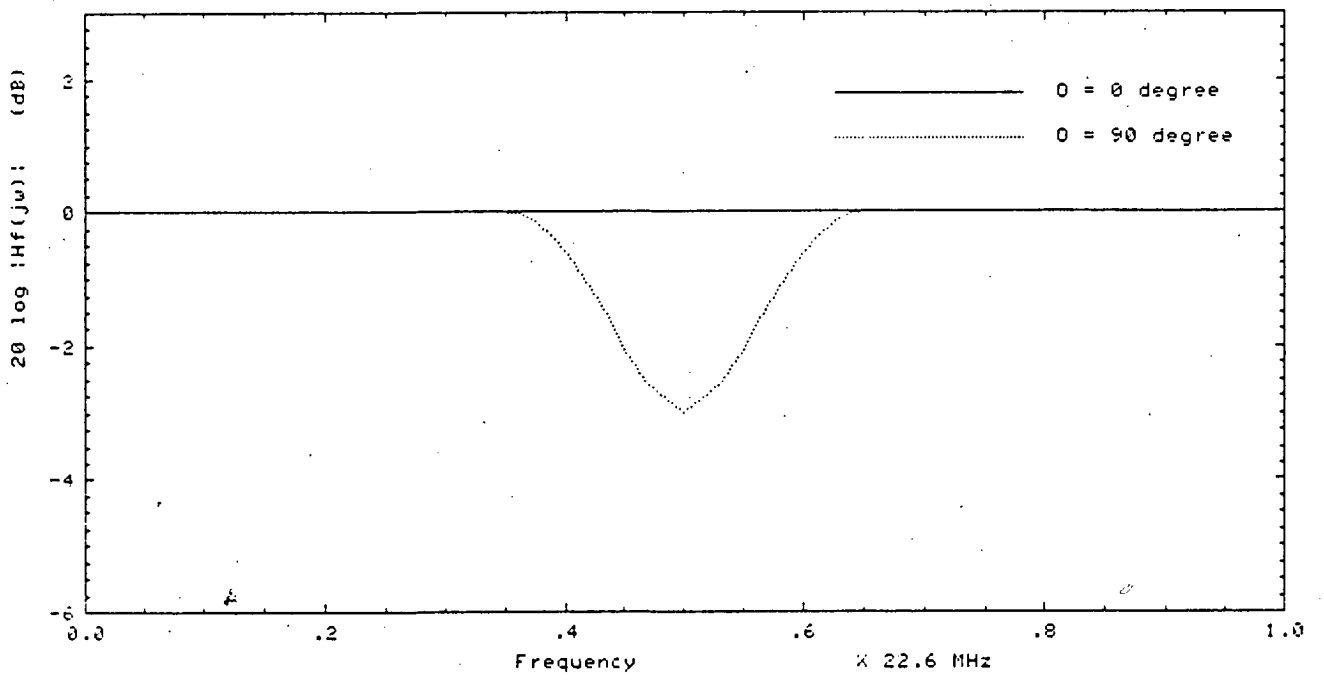

Fig 4.9 Effect of Sampling Phase on $H_f(jw)$

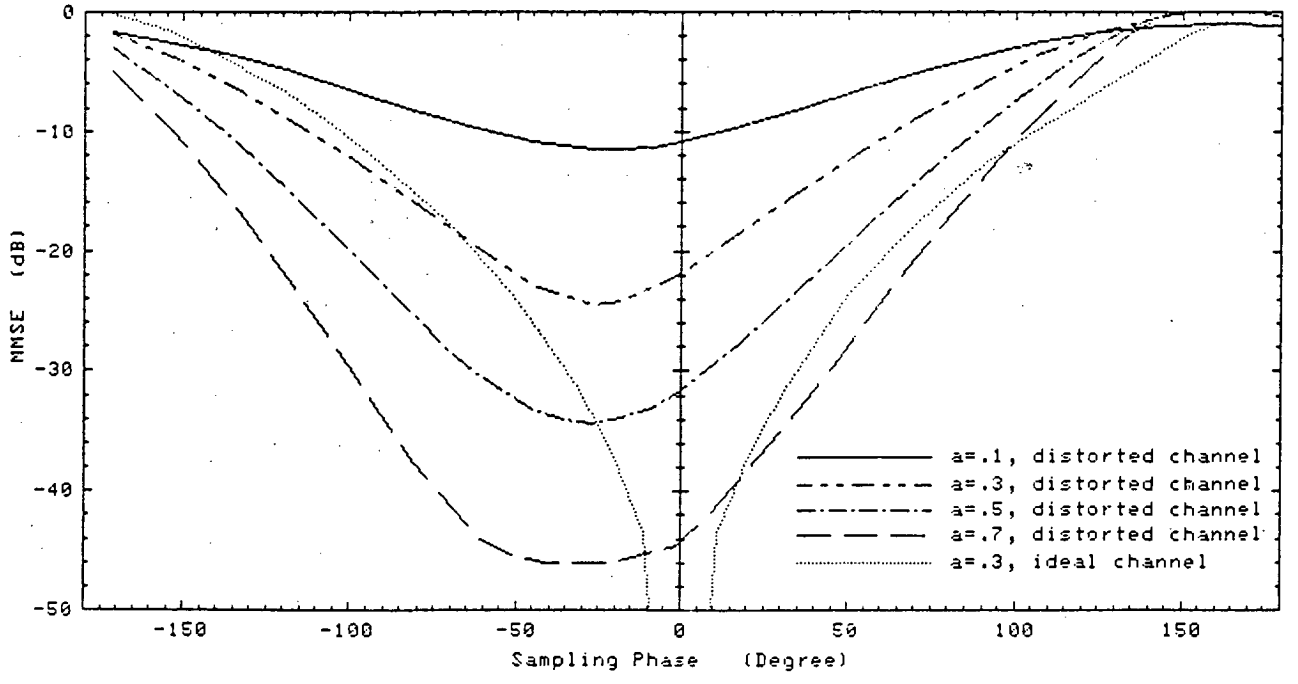

Fig 4.10 $\mathcal{E}_{min}$ Values for different Sampling Phase

comprises samples of the filtered received signal at time $t=nT+\emptyset T/360$, where $\emptyset$ is the sampling phase in degrees. Assume that a raised cosine filter structure is used, the overall folded frequency response from 0 to 1/T is:

$$H_f(jw)=H(jw)\exp(jw\tau)+H[j(w-2\pi/T)]\exp[j(w\tau-2\pi/T)] \quad \ldots\ldots (4.43)$$

where $\tau = \emptyset T/360$

Under ideal conditions, with $\emptyset=0$, $H_f(jw)$ equals a constant for $0 \leq w < 2\pi/T$. If $\emptyset \neq 0$ and $H[j(w\tau-2\pi/T)] \neq 0$, $H_f(jw)$ is no longer a constant value for $0 \leq w < 2\pi/T$. Fig 4.9 shows the $|H_f(jw)|$ for a 0.3 raised cosine filter and 90° sampling phase error.

The effect of sampling phase for an infinite tap equalizer was solved by Mazo [102] who estimated that 2 to 4 dB degradation might be incurred for a 0.1 to 0.15 raised cosine filter. However, for a finite tap equalizer, the degradation may exceed 30dB. Fig 4.10 shows for the same fading condition and radio system as Fig 4.4, on a plot of ξ_{min} against sampling phase. In this figure, 0.1, 0.3, 0.5, 0.7 raised cosine filters are used with an 7 tap equalizer. The response of an ideal channel with 0.3 raised cosine filter and 7 tap equalizer is also plotted as the dotted reference.

From the curves, the worst ξ_{min} values for all the filters are of broadly similar magnitudes and are approximately independent of the excess bandwidth of the raised cosine filter, a, and the channel distortion. This arises from all the plots experiencing a deep null in the folded spectrum as well

as severe group delay distortion by the sampling phase error. On the other hand, the variation of $\mathcal{E}_{min}$ with optimum timing is decreased as the excess bandwidth is increased, as shown in Fig 4.10. In other words, the raised cosine filter with increased excess bandwidth will be more sensitive to the sampling phase, because the overlapped region in $H_f(jw)$ is increased. Nevertheless, the optimum timing not only depends on channel characteristics, but also on the amount of excess bandwidth of the raised cosine filter, as shown in Fig 4.10.

The importance of the sampling phase is demonstrated when the curves with the fading channel and an ideal channel are compared, with a=.3 in both cases. The performance of an equalizer with a fading channel is better than an ideal channel when Ø is between -170^{o} to -80^{o}, as shown in Fig 4.10.

When the signature is used as a performance evaluation factor, the effect of sampling phase is not too serious for 4QAM (or QPSK), because at a BER of 10^{-3}, the channel distortions dominate. However for 16QAM or above, the overall channel distortion and sampling phase degradation should be reduced by a factor of $2/\{E\langle A_k A_k^* \rangle\}$ for the same BER, as shown in equation (4.8). The sampling phase effect thus becomes significant.

Two curves in Fig 4.11a have been plotted to illustrate this effect. Curve A corresponds to QPSK with 26.0dB fade depth, while curve B corresponds to 64QAM with 17.7dB fade depth. Both radios have a bandwidth of 22.6MHz and with a 7 tap

equalizer.** The delay time of the 3-ray model is set at 8ns and the notch is 5MHz above the center frequency. The optimum $\mathcal{E}_{min}$ of the two curves from -261^{o} to 270^{o} have broadly similar magnitudes. However, the difference between the optimum and the worst $\mathcal{E}_{min}$ sampling phase is 6.6dB and 21.4dB for curves A and B respectively. Local minima may also occur for every $n360^{o}$ ($n = \pm 1, \pm 2, \ldots$) apart from the global minimum, as shown in Fig 4.11a.

Another important characteristic is that under severe fading, the global minimum will be a few samples away from the original time slot, as shown in Fig 4.11b. A 64QAM 22.6MHz radio system with 9 tap equalizer is used. The delay time of the 3-ray model is set at 8ns and the 20dB fade notch is at the center frequency. The optimum sampling phase is at -1180^{o}. Although there is over 10dB improvement in MSE when compared with the sampling phase within $\pm$ 200^{o}, under practical environment this global minimum may be difficult to obtain.

4.7.2 Optimum Phase Estimation Algorithm

Several timing estimation methods have been proposed, but most of them are not suitable in our application.

**The use of 22.6MHz QPSK is just for comparison purposes.

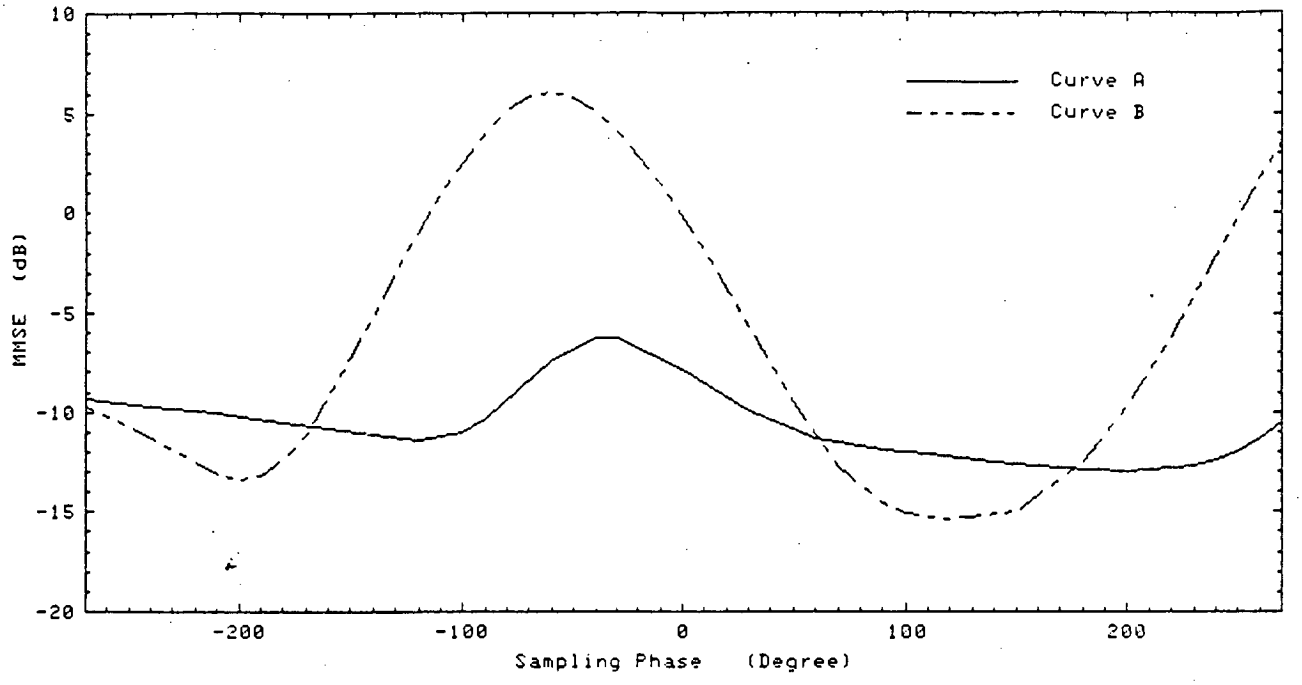

Fig 4.11a Effect of Sampling Phase on $\mathcal{E}_{min}$ for QPSK and 64QAM

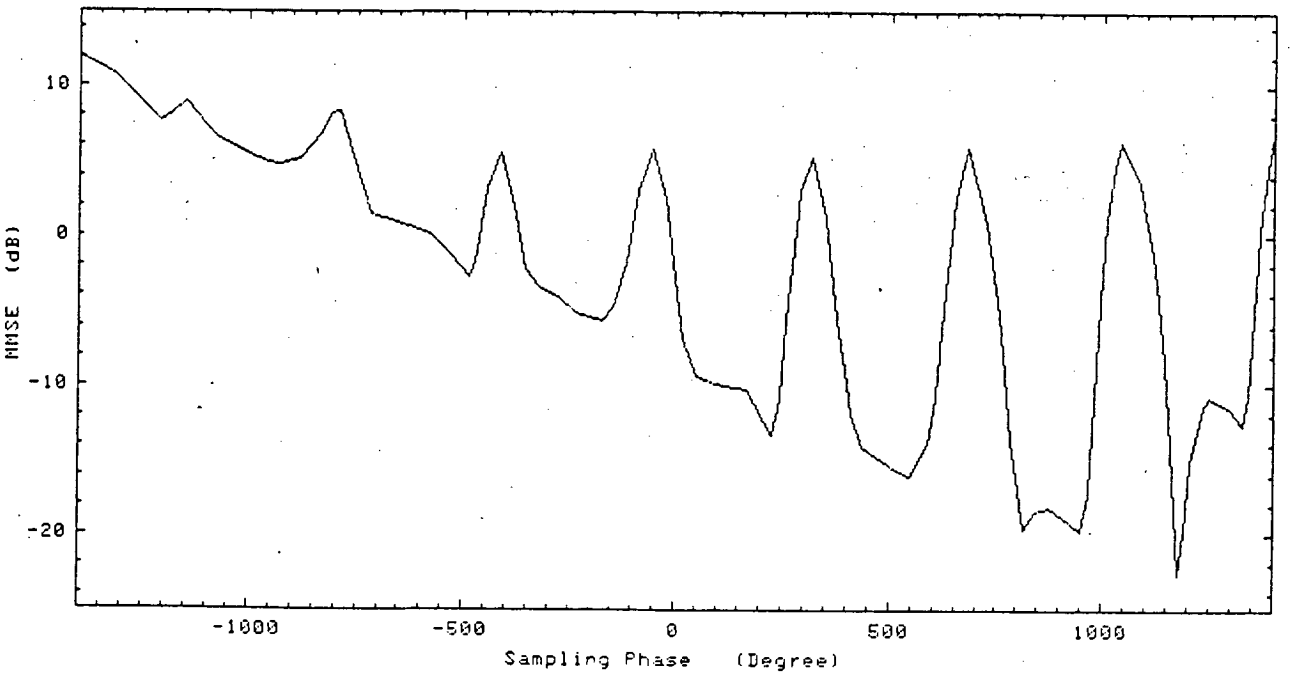

Fig 4.11b Effect of Sampling Phase on $\mathcal{E}_{min}$ under Severe Fading

(A) Zero Crossing

The mean location of the zero crossing is estimated as an optimum timing. This is not an appropriate method in our application since the eye will be completely closed at the equalizer input under deep fading.

(B) Zero Forcing the first post-echo [107]

This is a good and simple estimate if post-echo is the main degradation factor and a 1-dimensional modulation scheme has been used. As for 2-dimensional modulation scheme like QAM, the implementation will become complex. Furthermore, in some multipath conditions pre-echo may dominate and both amplitude and delay distortion will occur.

(C) Zero Forcing the combined first pre- and post-echo [107]

This will be a good estimate for a 1-dimensional baseband transmission when amplitude distortion is dominant. However in multipath fading, both amplitude and group delay distortion may occur. Again, the complexity will increase for 2-dimensional modulation scheme. Thus this method is also not appropriate.

(D) Equalizer Approach [92,88]

With this method, the timing estimate is controlled by the error signals at the sampling instant, just like an equalizer structure. It may reach the optimum timing based on the MMSE

criteria. However it will be too complicated to implement particularly when jointly operated with the receiver equalizer described in this chapter. Furthermore, it may converge to a local minima, as shown in Fig 4.11a,b.

(E) Maximum mainlobe

Although this is not a good estimation technique [89], it will prevent the sampling phase moving to an inferior condition. The exact implementation may not be easy particularly when deep fading occurs.

Here, the author proposes another scheme based on the sampled data power, as mentioned in the beginning of this section. The sampling phase error may introduce a null in the folded frequency response, $H_f(jw)$. Effectively it may reduce overall sampled signal power. If the sampling phase is adjusted such that the overall sampled data power is maximum, then the large null which introduced by the severe phase error will normally be relaxed. Consequently $\mathcal{E}_{min}$ will be reduced.

In Fig 4.12, the sampled data power and $\mathcal{E}_{min}$ are plotted against the sampling phase. The maximum power criteria will be close to the optimum when fade depth is decreased because sampling phase error starts to be dominant. However, care should be taken to make sure the demodulation phase is optimized before the equalizer, i.e. $@=0^{o}$. As shown in Fig 4.12, with $@=45^{o}$, the change of sampled data power with different sample phase values is small. This arises because

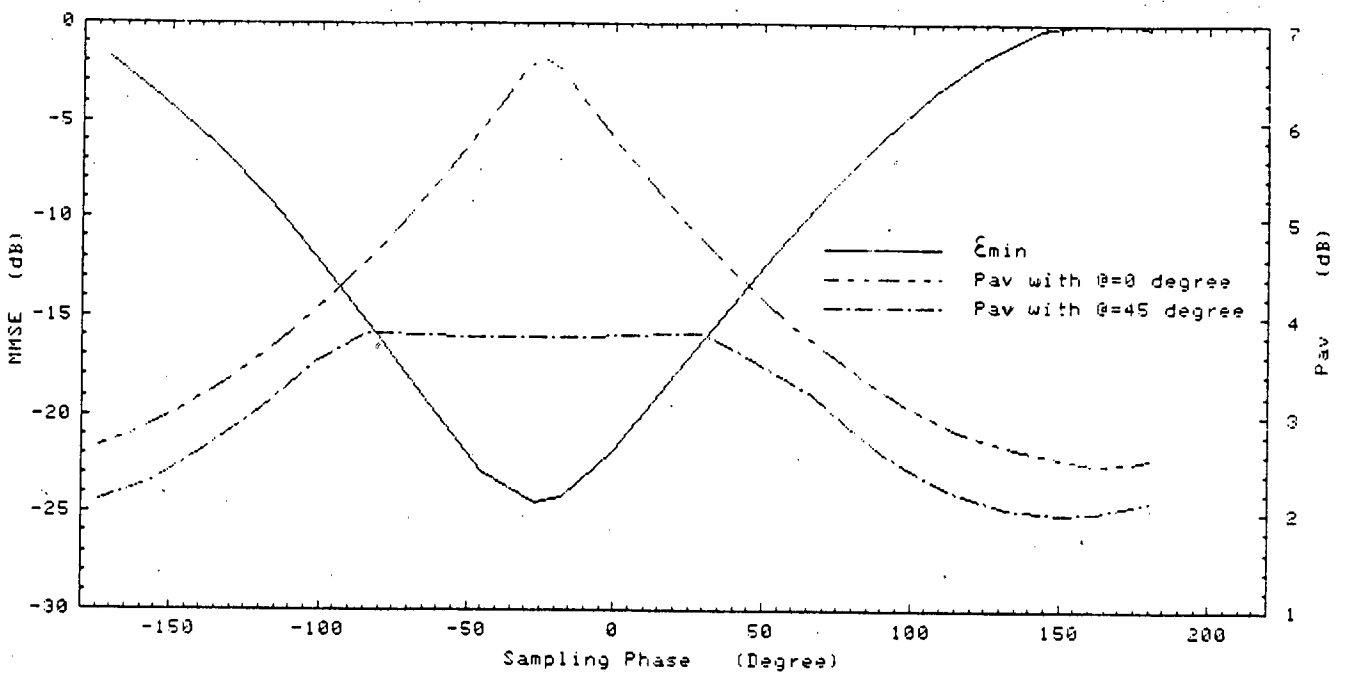

Fig 4.12 Sample Data Power against Sampling Phase

the maximum input level to the equalizer is limited by the receiver gain circuitry. Any rotation ($@\neq 0$) will reduce the input receiver gain which effectively reduces the power measured. On the other hand, it will be acceptable if the receiver gain value has been considered for the power calculation.

Since the received data will have already been sampled in the equalizer section, they can be re-utilized again for the power measurement. The implementation of this extra hardware for the timing control may thus not be too difficult.

A similar approach may be applied to the third or fourth power of the sample data. This may converge faster, but it

will be more sensitive to noise and on the sequence of correlation data. Furthermore, increased arithmetic processing is likely to be required.

4.8 Proposed Complexity

First of all, let us consider the degradation due to quantization noise in the ADC, N_q, and the finite precision arithmetic, N_c. Generally speaking, the tap weight magnitude will increase as channel distortion increases. The following gives an estimated value of the arithmetic range, l_c, and the summation of the tap weight square, S, for BER$\leq 10^{-3}$ and excess bandwidth (a) $\geq$ 30%.

	QPSK	16QAM	64QAM	256QAM	1024QAM
max no of tap	7	9	11	13	13
l_c	4.5	4.0	3.5	3.0	2.5
S	60	50	45	40	30

Table 4.7 Estimated Value of Arithmetic Range and Summation of Tap Weight Square

With $(\mathcal{E}_{min})_s$ ** being the ideal MMSE corresponding to BER of 10^{-3}, the degradation due to N_q and N_c for various QAM system can be evaluated by equations (4.27, 4.34) with the normalized average power (B) of 0.3, and are shown in Fig 4.13 and 4.14a-e respectively.

**$(\mathcal{E}_{min})_s = E\langle A_k A_k \rangle / (C/N)_s$ where $(C/N)_s$ is the C/N at BER of 10^{-3}

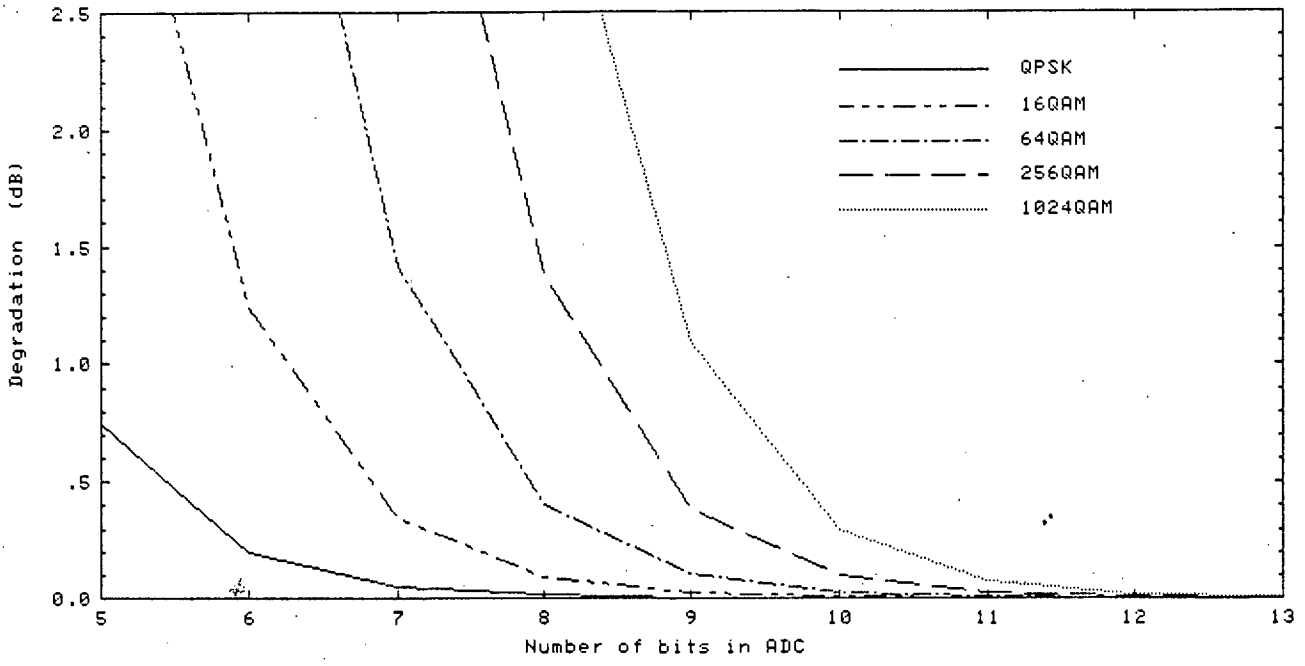

Fig 4.13 Degradation to $(\mathcal{E}_{min})_s$ due to Finite Quantization in ADC

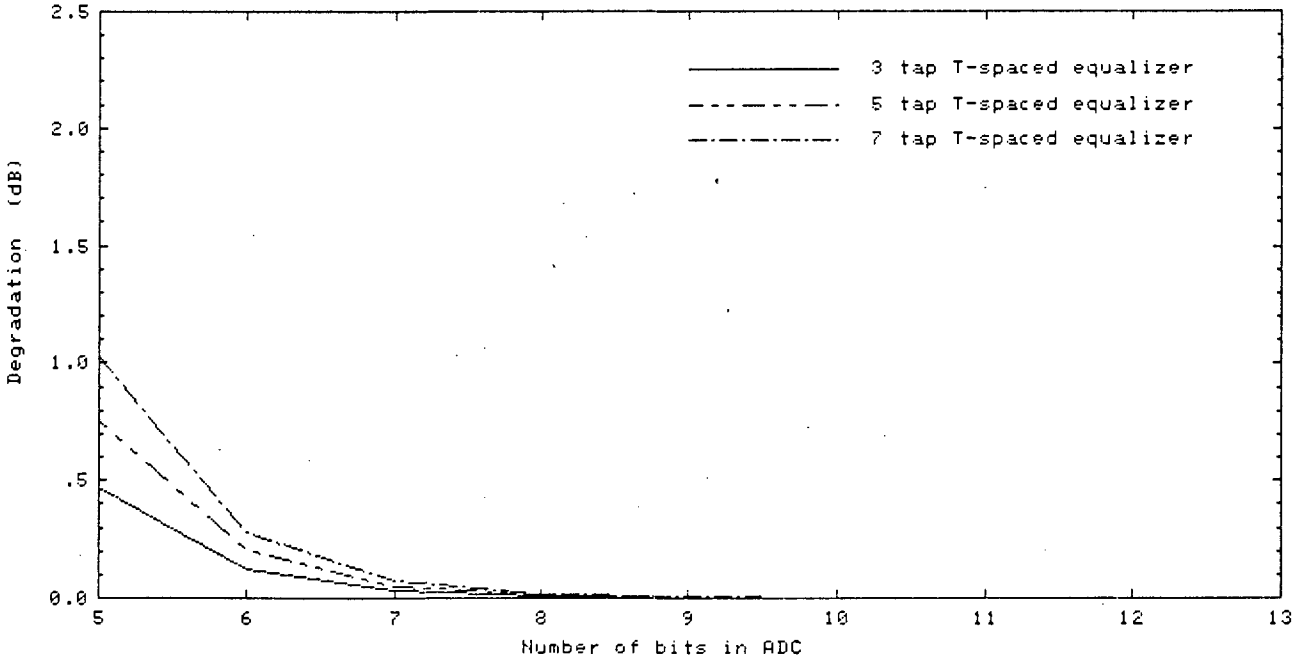

Fig 4.14a Degradation to $(\mathcal{E}_{min})_s$ due to Finite Precision Arithmetic with QPSK

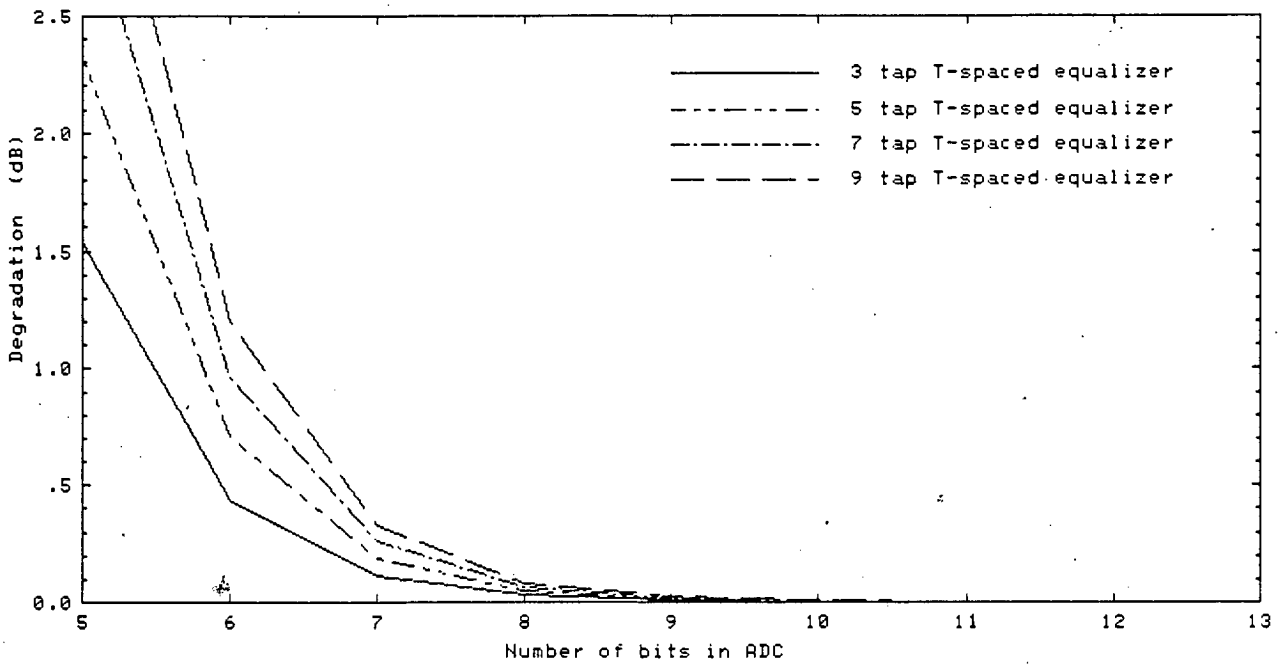

Fig 4.14b Degradation to $(\mathcal{E}_{min})_s$ due to Finite Precision Arithmetic with 16QAM

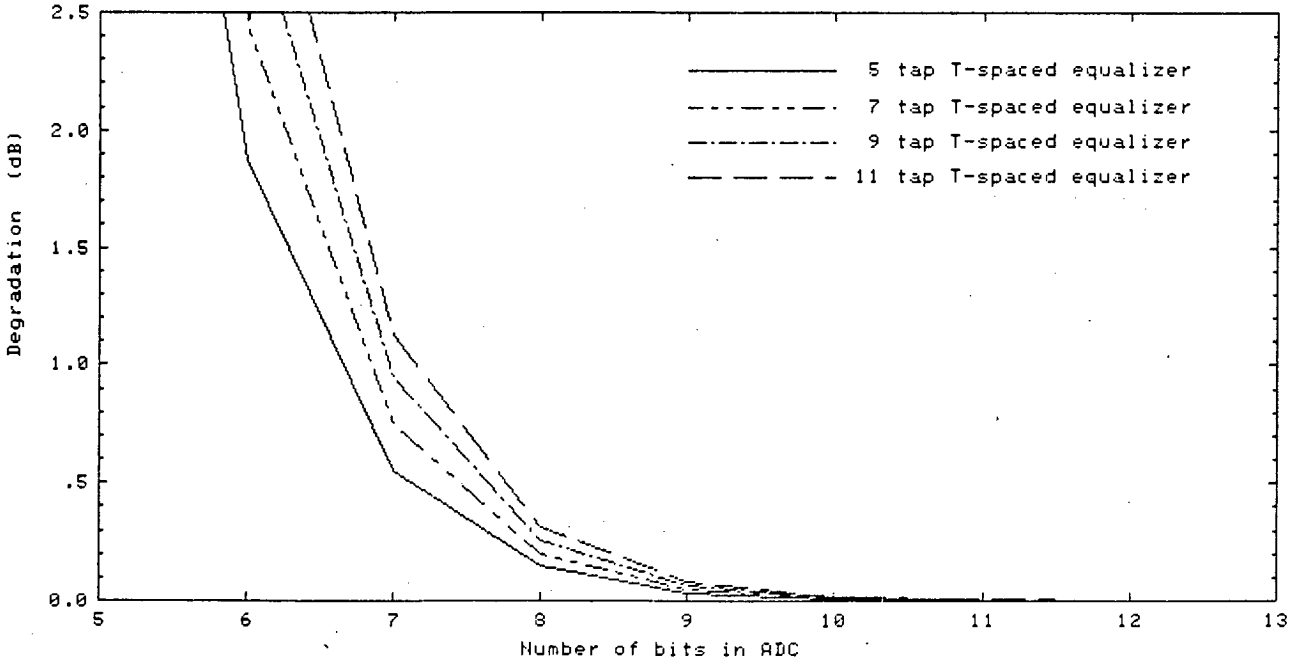

Fig 4.14c Degradation to $(\mathcal{E}_{min})_s$ due to Finite Precision Arithmetic with 64QAM

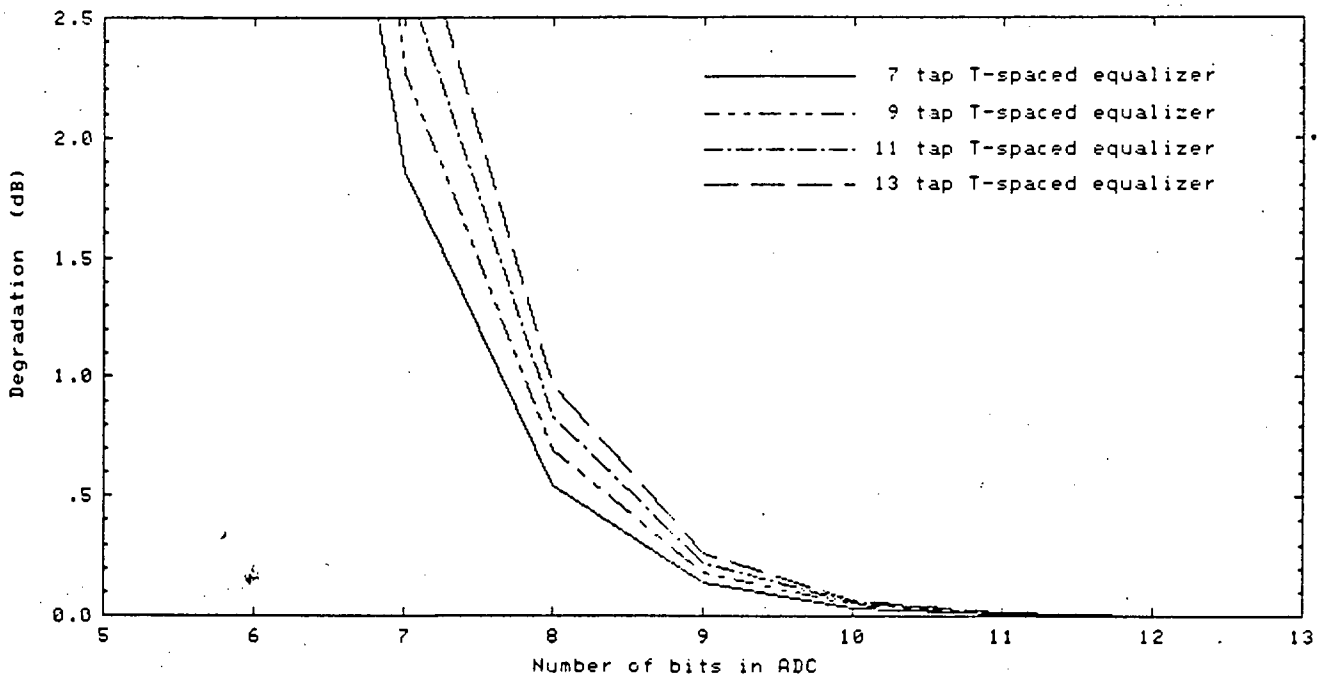

Fig 4.14d Degradation to $(\mathcal{E}_{min})_s$ due to Finite Precision Arithmetic with 256QAM

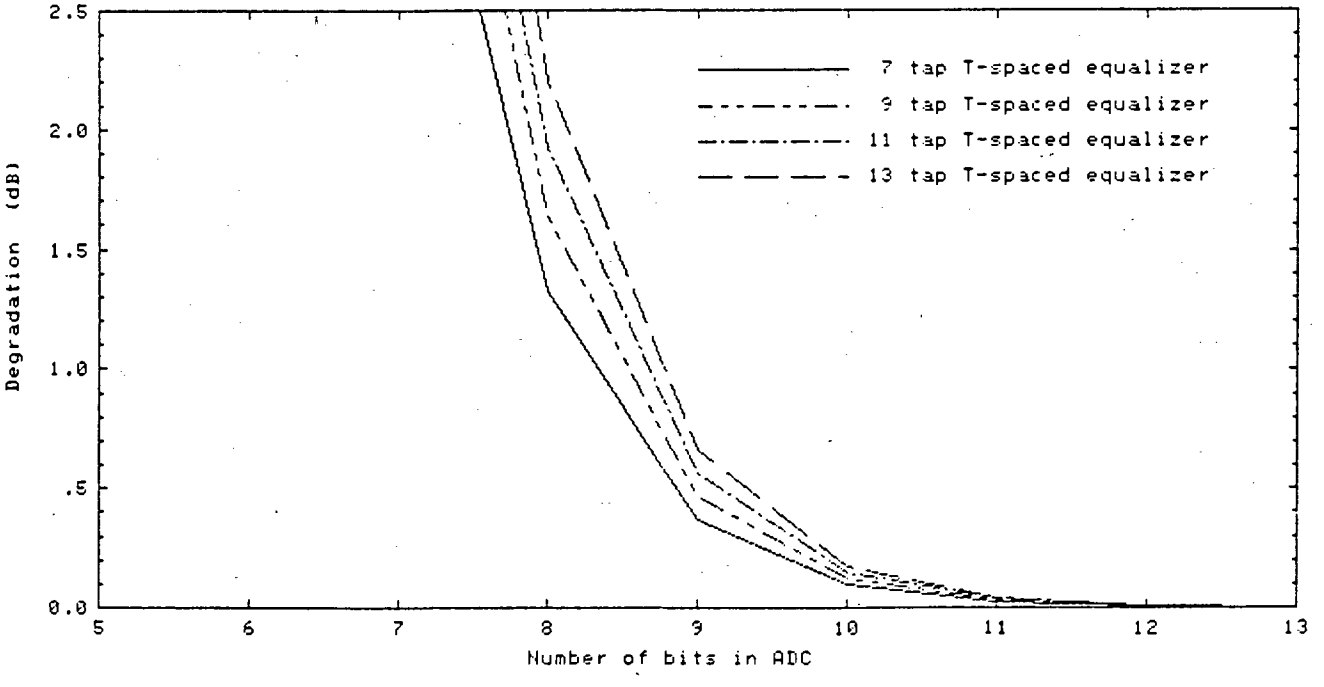

Fig 4.14e Degradation to $(\mathcal{E}_{min})_s$ due to Finite Precision Arithmetic with 1024QAM

As from Fig 4.14a-e, the degradation within 1dB can be obtained easily with reasonably short word length arithmetic. However it is the gradient noise that causes most of the degradation. Table 4.8 shows the minimum number of bits required in the arithmetic if the step size equals 1 LSB of the tap weight element. In order to maintain stability, the maximum step size chosen is less than $3u_{max}/4$ under all conditions.

no of taps	QPSK	16QAM	64QAM	256QAM	1024QAM
5	6	9	11	12	14
7	7	9	11	13	14
9	7	9	11	13	15
11	7	10	12	13	15
13	8	10	12	14	15

Table 4.8 Minimum Number of bits in Arithmetic if Step Size equals 1 LSB

Compared with Fig 4.14a-e, Table 4.8 shows that a few more bits are required to handle the finite step size degradation for modulation levels over 16QAM. A possible technique is to use step size of less than 1 LSB of the tap weight element. However the "early termination effect" may become significant if the step size is too low, as shown in equations (4.38a,b). If the bound of $E<|e_{early}|^2>$ is set to be better than -18dB under normal atmospheric conditions, i.e. no fading, then the following complexity can be evaluated:

	QPSK	16QAM	64QAM	256QAM	1024QAM
max no of taps	7	9	11	13	13
n_1	5	6	7	8	9
n_2	7	8	10	11	11
u	1 LSB	1/2 LSB	1/4 LSB	1/8 LSB	1/16 LSB

Table 4.9 Complexity Requirement for the T-spaced Equalizers Designs

The overall degradation due to N_q, N_c and finite step size is of the order of 1 to 3dB. This will roughly degrade the signature by the same order.

It has already shown in [104] that a 5 tap structure is adequate for QPSK. Now let us consider the number of taps required for 16QAM to 1024QAM. Since most of the fading activites are with notches of less than 20dB, an equalizer with an ideal signature better than 20dB is preferable as 2 to 6 dB degradation is quite typical. Fig 4.15a shows the signature plots of a 3, 5, 7, 9 tap equalizer for a 22.6MHz 16QAM radio with flat fade margin of 40 dB.** A 3-ray model with 8ns delay time is used. Although the signature will be improved with a longer equalizer, the improvement from 7 tap to 9 tap is not very great. Even a 5 tap equalizer can give acceptable performance. So 5-7 tap complexity seems to be an appropriate tap length for 16QAM radio systems.

**As shown in Appendix 8, the signature plot is identical for both minimum and non-minimum phase fades if ideal raised cosine filter is used.

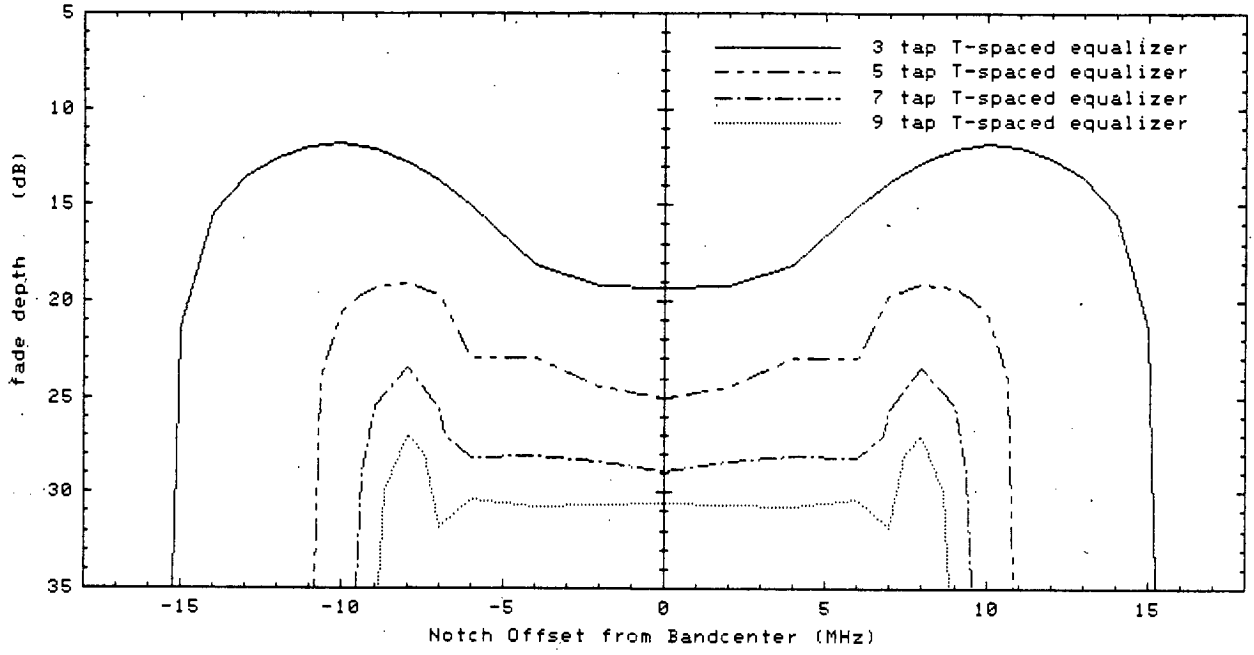

Fig 4.15a Signature Plots for a 16QAM Radio System with different Numbers of Taps

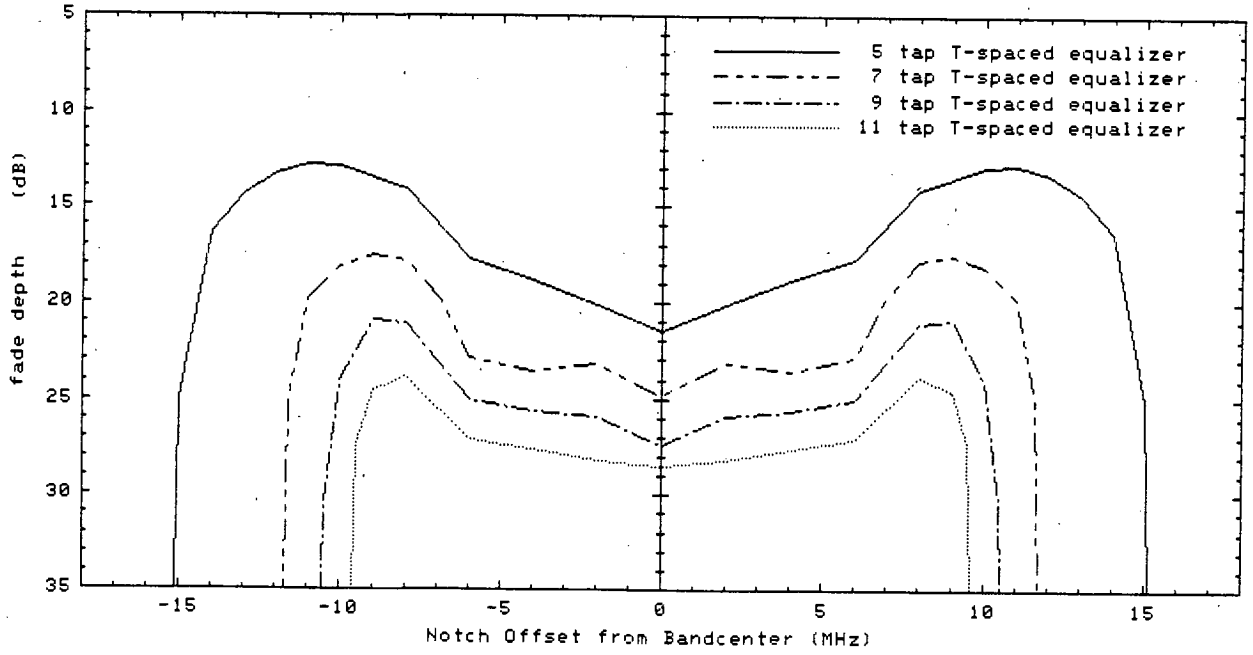

Fig 4.15b Signature Plots for a 64QAM Radio System with different Numbers of Taps

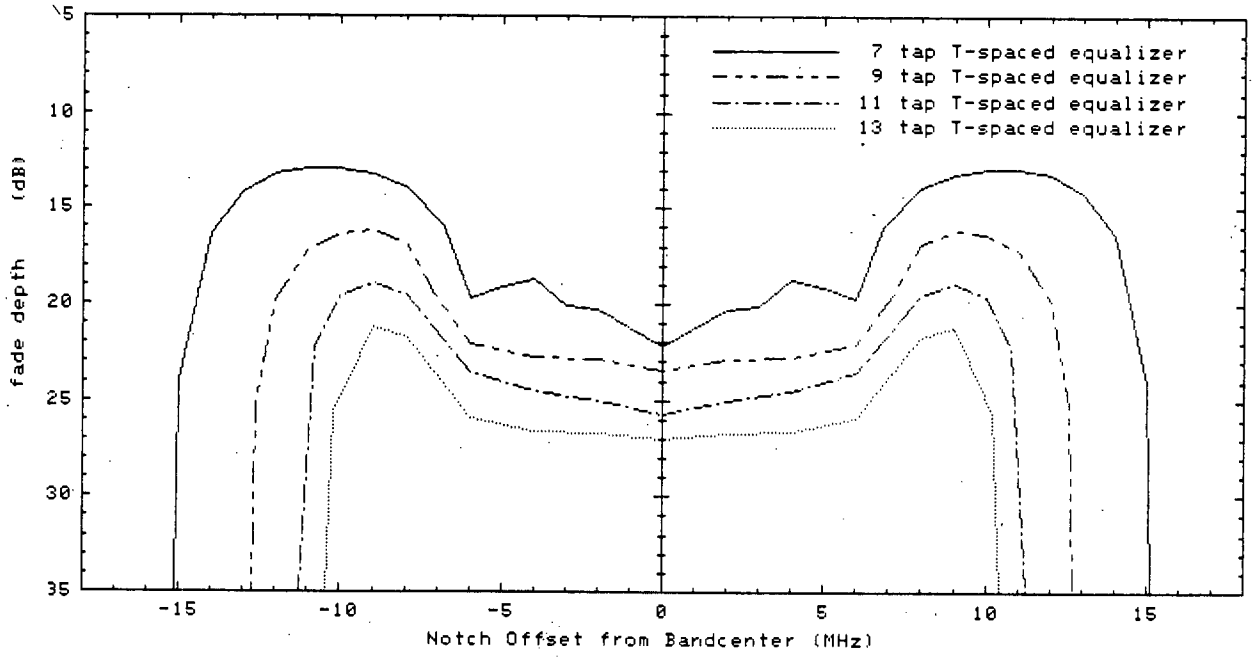

Fig 4.15c Signature Plots for a 256QAM Radio System with different Numbers of Taps

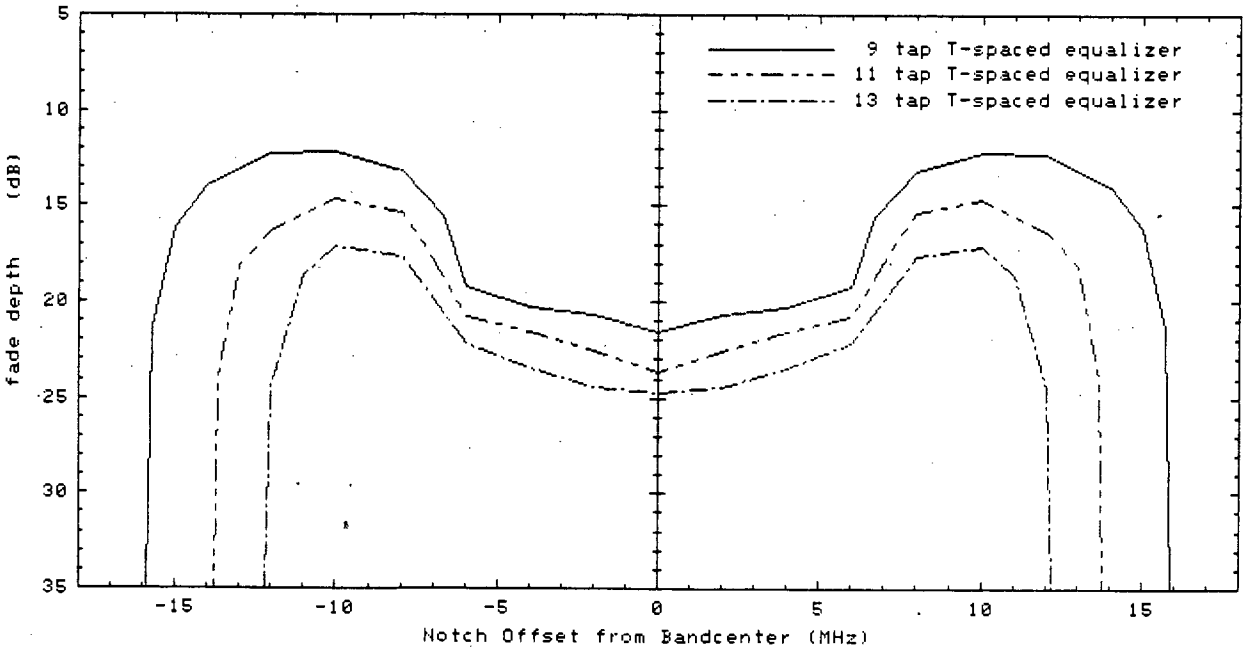

Fig 4.15d Signature Plots for a 1024QAM Radio System with different Numbers of Taps

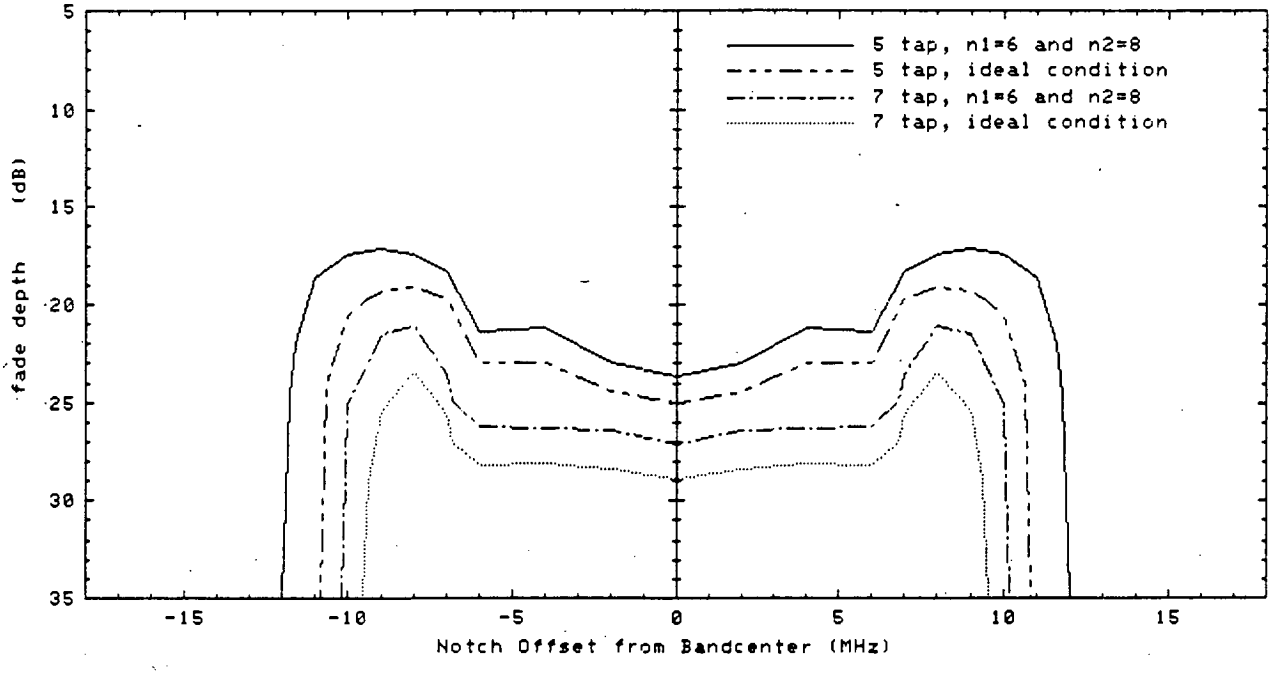

Fig 4.16a Signature Plots for a 16QAM Radio System with ADC and Finite Arithmetic

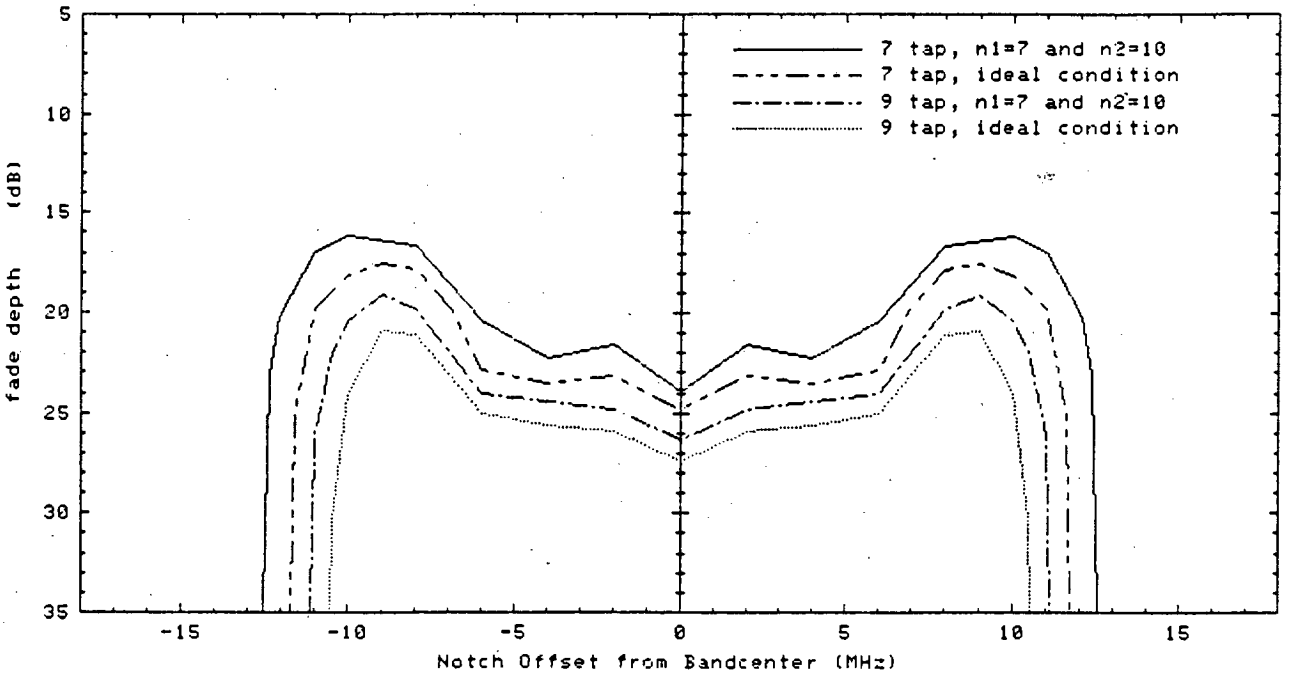

Fig 4.16b Signature Plots for a 64QAM Radio System with ADC and Finite Arithmetic

For 64QAM, a longer equalizer may be required because it is more sensitive to distortion. Fig 4.15b shows the signature plots of a 5, 7, 9, 11 tap equalizers with the same conditions as in Fig 4.15a. It indicates that the best design is around 7-9 tap.

As shown in Fig 4.15c,d, the required number of taps is increase for 256QAM and 1024QAM. However the improvement is small for every 2 taps increases in complexity. The choice for the number of taps will thus very dependent on the cost and the performance objective.

Based on the complexity as described in Table 4.9, Fig 4.16a,b show the signature plots of 16QAM and 64QAM with finite quantization levels and arithmetic where 5 & 7 tap are used for 16QAM and 7 & 9 tap are used for 64QAM. The same order of degradation in signature will also be applied for 256QAM and 1024QAM if the complexity in Table 4.9 is used. If one more bit can be used on both ADC and arithmetic, the signature will be basically identical to that with infinite resolution.

4.9 Various Delay Time and Raised Cosine Filters

With different channel parameters or excess bandwidth in the raised cosine filter, the signature will also be changed. Normally, if the delay time of the 3-ray model is reduced, a better overall signature plot should be obtained. Fig 4.17

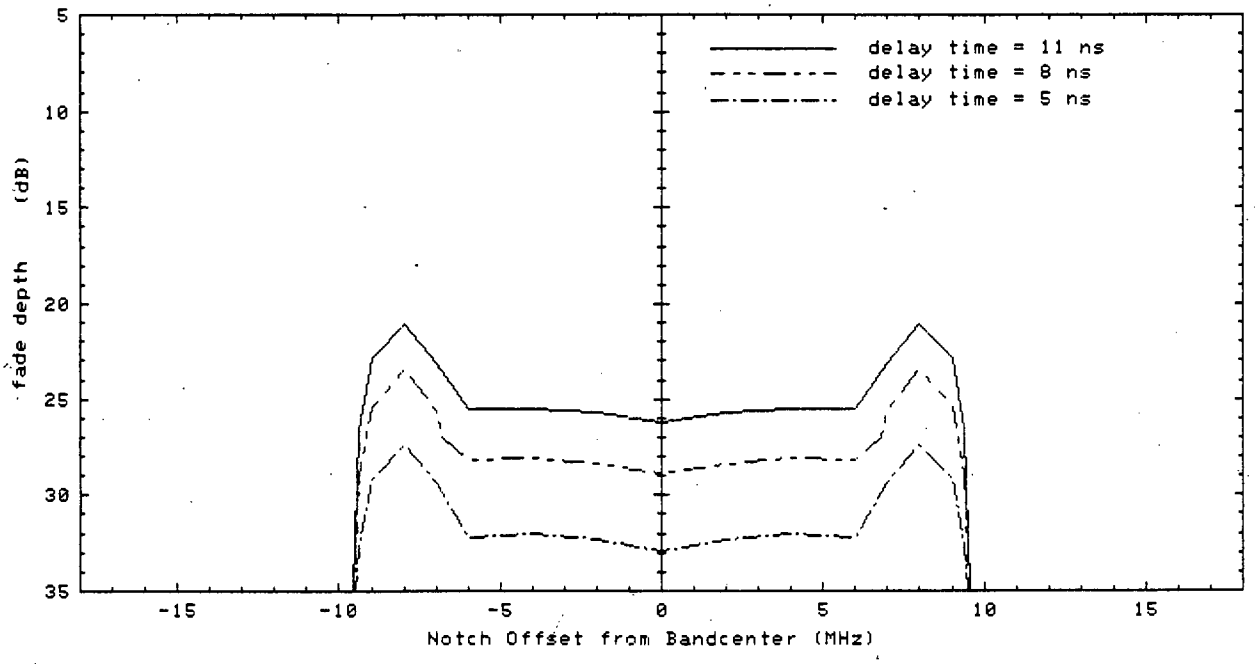

Fig 4.17 Signature Plots for a 16QAM Radio with different Multipath Delay

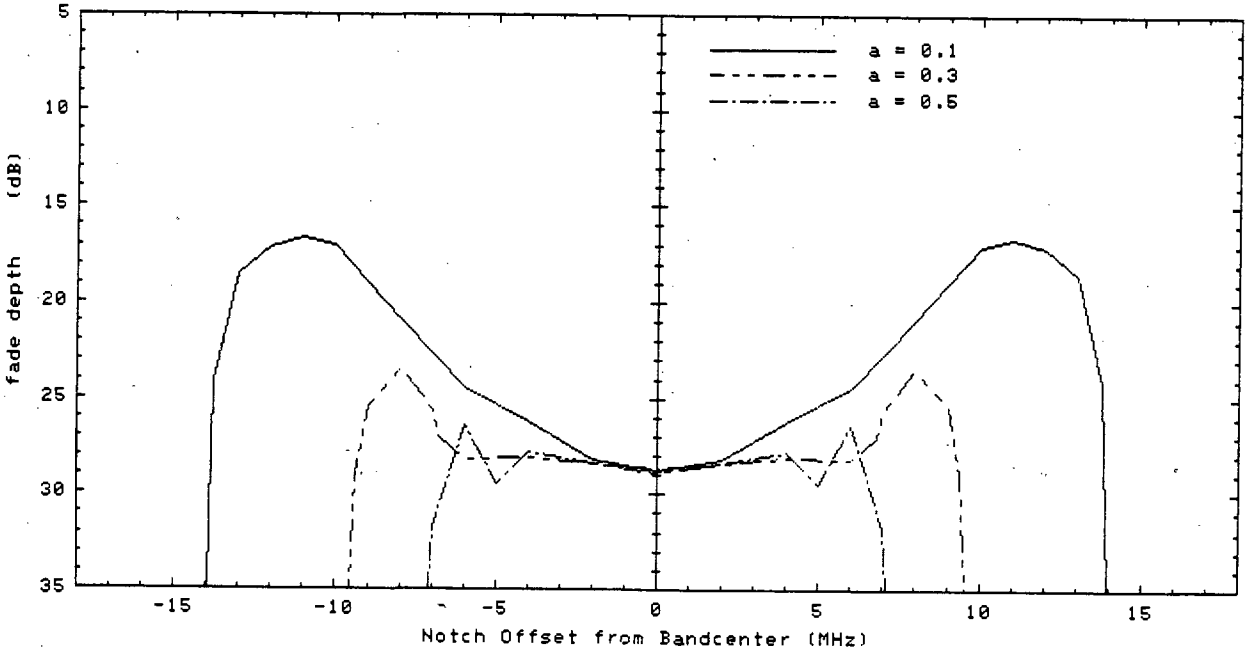

Fig 4.18 Signature Plots for a 16QAM Radio with different Raised Cosine Filter shapes

shows the signature plots with delay time of 5, 8, and 11ns for a 22.6MHz 16QAM radio system with a 7 tap equalizer. The effect of different delay time will basically move the signature up or down but with the width unchanged. The overall signature is progressively improved as delay time is reduced, and is about 1dB/ns for a 7 tap equalizer.

The effect of excess bandwidth is shown in Fig 4.18, where the signatures with a=0.1, 0.3 and 0.5 are plotted. It is predictable that if excess bandwidth increases, a better signature will be obtained. Compared to Fig 4.17, the signature shows little difference when the notch is at band-center, but significant difference as the notch moves away from band-center. This arises from one side of the overlapped spectrum experiencing severe multipath fading. As the excess bandwidth increases, the overall $H_f(jw)$ will be less distorted.

4.10 Summary

The performance of the T-spaced equalizer with LMS algorithm under stationary fading condition is described. Various equations have been evaluated for estimating degradations like quantization in ADC and arithmetic, finite step size and early termination effect. Then the complexity of equalizer has been proposed for QPSK to 1024QAM.

The number of quantization levels in the ADC and arithmetic are all close to optimum in the calculation. Under practical

conditions, one extra bit is normally required in the ADC to provide enough dynamic range for the received data and to compensate for the non-ideal characteristics of the ADC. As for the arithmetic, one more bit is also required to prevent overflow in tap weight and early termination effect, and three to four bits is normally the minimum requirement for the accumulator to prevent intermediate overflow in calculations.

The most severe practical problem in the T-spaced equalizer is its sensitivity to sampling phase. None of the current techniques including the maximum power approach described in this thesis, attempt to find the global minimum of MMSE which may be a few samples away from the original time slot zero. This remains an unsolved problem and is the major degradation factor for the T-spaced equalizer.

The superior performance of 0.5 raised cosine compared with that of 0.3 raised cosine was demonstrated in Fig 4.18. It is questionable therefore whether the 15% reduction in bandwidth is worthwile for 0.3 raised cosine filter.

CHAPTER 5 T/2-SPACED TRANSVERSAL EQUALIZER

As mentioned in section 4.7, one of the most problematical factors in the T-spaced equalizer is its sensitivity to sampling phase. Fractionally spaced transversal equalizers [89,103,105], nevertheless, are inherently less sensitive to sampling phase. If the tap spacing, T', is less than T/(1+a), then there will be no overlapped frequency from 0 to 1/T' as the frequency response is periodic and repeats every 1/T'. The problems caused by the cancellation of the overlapped frequency response and its associated group delay distortion are avoided.

The choice of tap spacing does not only depend on equalizer performance but also on hardware implementation. Compared with the T-spaced equalizer a (L/P)T fractional spaced equalizer (where L and P are relatively prime positive integers and L<P) normally requires P times higher sampling rate and consequently P times more memory and P times higher speed in some logic circuitry, if the gradient estimate algorithm is used.

Among these algorithms, T/2-spaced seems to be the most suitable because of the ease of timing extraction and relatively simple hardware implementation. The speed and memory storage will be less than any other fractional spaced equalizer. Presently this type of equalizer is receiving more attention in the LOS digital microwave radio application.

For a given number of tap weights, the superiority of the fractional spaced equalizer against T-spaced equalizer was reported [103], even though the former only covers half of the time span for equalization. However, this may not always be true for a multipath channel. The performance not only depends on channel distortion, but also on the number of taps and the radio systems design details, e.g. the excess bandwidth of the raised cosine filter.

5.1 Least Mean Square (LMS) Algorithm with Gradient Estimate

The background theory behind the T/2-spaced equalizer is similar to the T-spaced equalizer with the exception that $\underline{R}$ (or $\underline{R}'$) is no longer a Toeplitz matrix. However, Gitlin and Weinstein [106] show that with excess bandwidth of less than 100%, i.e. $a<1$, the matrix $\underline{R}'$ is nonsingular even if the noise is vanishingly small. Thus the equations regarding optimum tap weights and ξ_{min} for the T-spaced equalizer (4.1 to 4.8) are also valid for the T/2 equalizer if $a<1$.**

As with the T-spaced equalizer, the gradient estimate (refer to section 4.2 and equation 4.11) can be used to update the tap weight elements. Although both 1/T or 2/T updating rates are possible, 1/T is normally employed because of the

---

**Assuming the White Gaussian Noise density is evenly distributed from 0 to 1/T'.

difficulty in interpolating signal levels at the mid-symbol interval. This is particularly true when the equalizer operates in the decision directed mode** where no training signal is applied.

5.1.1 Ill-Conditioning Problem in R'

When equation (4.6c) is used to solve for the optimum tap weights, it is found that the result is very sensitive to the accuracy of the computation. This demonstrates the ill-conditioning behaviour in $\underline{R}'$, where small changes in R_{ij} will result in big changes in the $\underline{C}_{opt}$ expression in equation (4.6c)

Let us illustrate this characteristic by the following example:

radio system	:	16QAM with .5 raised cosine filter, 22.6MHz bandwidth
multipath channel	:	3-ray model with 8ns delay time, b=.8, f_0 is 10MHz above center frequency
equalizer	:	T/2 with 13 tap

Two sets of $\underline{C}_{opt}$ and ξ_{min} are shown in Table 5.1 and they are calculated by using equations (4.6c and 4.7). Set A corresponds to normal calculation, and set B corresponds to adding small perturbation terms in the cross-correlation matrix $\underline{D}'$, which is equivalent to adding a small perturbation in the auto-correlation matrix $\underline{R}'$. The magnitude of these

**This is the operating mode that is normally employed in LOS digital microwave transmission. Details will be discussed in the next chapter.

perturbation terms is less than 10^{-4} of the maximum term in $\underline{D}'$. The dramatic difference in $\underline{C}_{opt}$ between the A and B sets clearly illustrates the ill-conditioning problem. When the same perturbation terms are added for the T-spaced equalizer with the same fading channel, number of taps and radio system, the maximum deviation term in $\underline{C}_{opt}$ is less than 0.001 and with the same ξ_{min}.

tap weights	A		B	
	real	img	real	img
C_{-6}	-0.013	0.004	0.047	0.108
C_{-5}	-0.001	0.001	-0.451	-0.246
C_{-4}	0.047	-0.061	1.214	0.199
C_{-3}	0.044	0.104	-1.897	-0.634
C_{-2}	-0.203	0.011	2.922	1.858
C_{-1}	-0.057	-0.061	-4.822	-1.847
C_0	1.901	-1.264	7.331	-1.140
C_1	1.409	1.147	-3.303	1.381
C_2	-0.603	0.665	3.836	2.067
C_3	-0.248	-0.195	-5.134	-1.946
C_4	0.045	-0.203	4.115	-0.132
C_5	0.061	0.077	-1.854	0.953
C_6	0.011	0.001	0.361	-0.405

ξ_{min} for condition A is less than -45 dB
ξ_{min} for condition B is -32.2 dB

Table 5.1 Demonstration of how the Ill-conditioning behaviour in $\underline{R}$ affects the Optimum Weight Values

The reasons behind this ill-conditioning problem can be explained from a frequency domain approach.

(A) 1/T Updating Rate in Gradient Estimate

It is obvious that 1/T updating rate simplifies the adaptive algorithm implementation. However it also has a side effect on the evaluation of $\underline{C}_{opt}$. The equalizer will tend to equalize the overall folded response, i.e. $E_f(jw)$ (or $C(jw)H(jw)+C[j(w-2\pi/T)]H[j(w-2\pi/T)]$), to the Nyquist equivalent channel in the 0 to 1/T region. This implies that even if $C(jw)H(jw)$ is different from the ideal channel, $E_f(jw)$ may still be close to the Nyquist equivalent channel. In other words, based on $C(jw)$ alone, we may not be able to reconstruct $H(jw)$ accurately from a T/2 transversal equalizer.

Let us demonstrate this effect in Fig 5.1a,b. Curves A and B correspond to tap weight set A and B of Table 5.1 respectively with the same channel distortion specified for Table 5.1. Curve C corresponds to an ideal 0.3 raised cosine filter without channel distortion. In Fig 5.1a, $|C(jw)H(jw)|$** is plotted. Curve A is broadly symmetric against 1/T axis, while curve B is obviously not symmetric. However, they all correspond to a low $\mathcal{E}_{min}$ value even though their tap weights are completely different. As shown in Fig 5.1b, $E_f(jw)$** is

---

**The gain of the receiver is also considered in the calculation, such that under ideal condition $|C(jw)H(jw)|$ equals to 0dB at 0Hz and $|E_f(jw)|$ equals to 0dB for the whole frequency range.

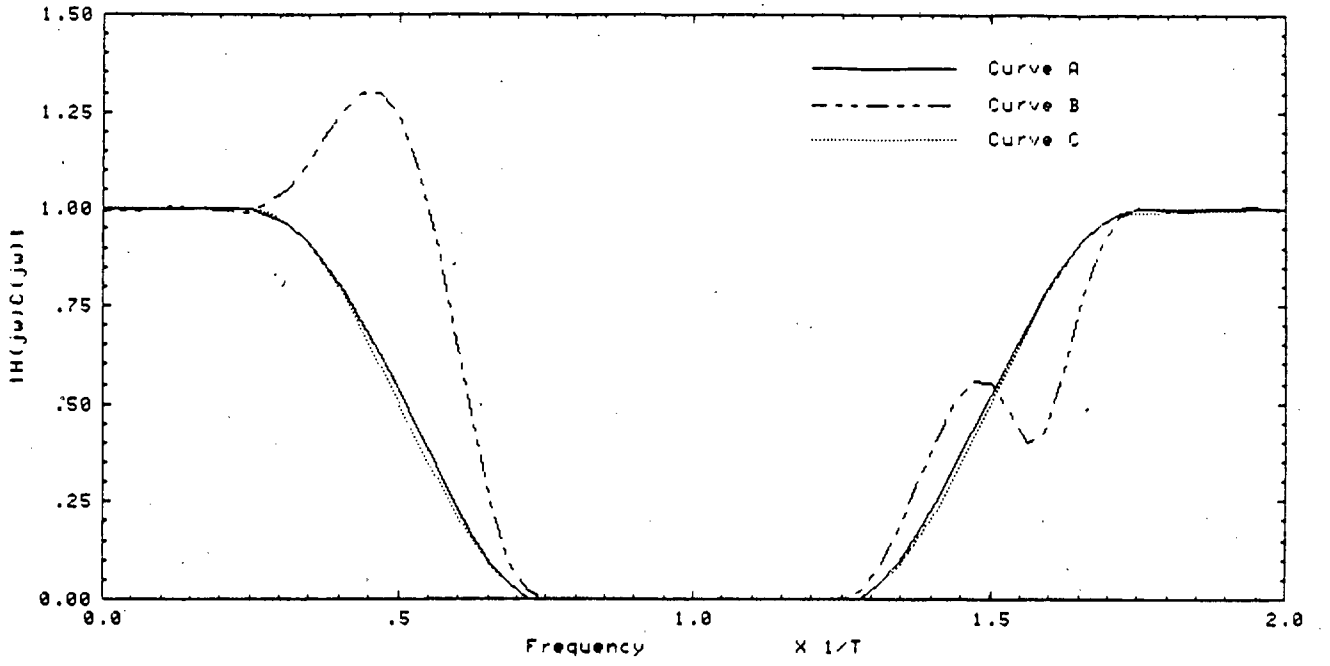

Fig 5.1a |C(jw)H(jw)| Plots with different Tap Weight

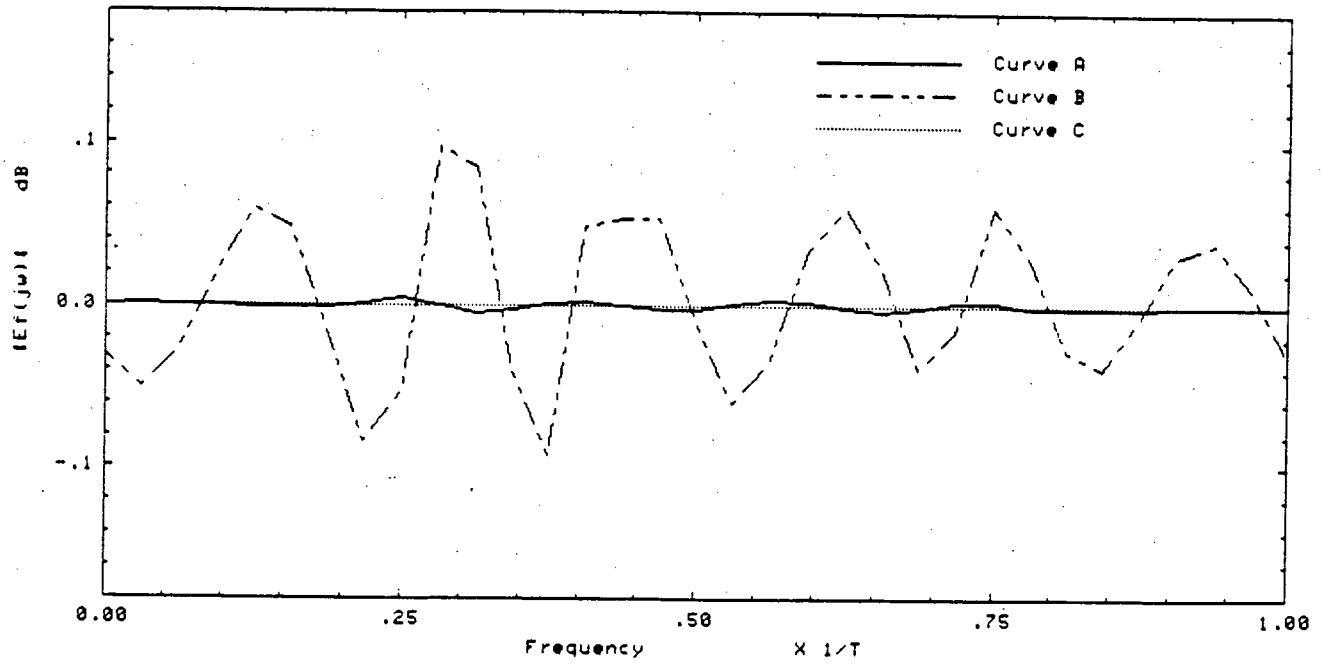

Fig 5.1b $|E_f(jw)|$ Plots with different Tap Weight

plotted, curves A and C are basically identical while curve B is within 0.1dB to an ideal condition.

(B) The Zero Spectral Density Region

With a 2/T sampling rate, the overall frequency response repeats every 2/T. Let us separate this into two regions: S(jw) and N(jw). S(jw) is from 0 to (1+a)/(2T) and (3-a)/(2T) to 2/T, and N(jw) is from (1+a)/(2T) to (3-a)/(2T). If the excess bandwidth is less than 100% and the noise is vanishingly small, the overall response of C(jw)H(jw) will approach zero in N(jw) region.

A small change of C(jw) in the S(jw) region or a large change in the N(jw) region will change the equalizer response slightly, but affect the tap weight dramatically. Curves A

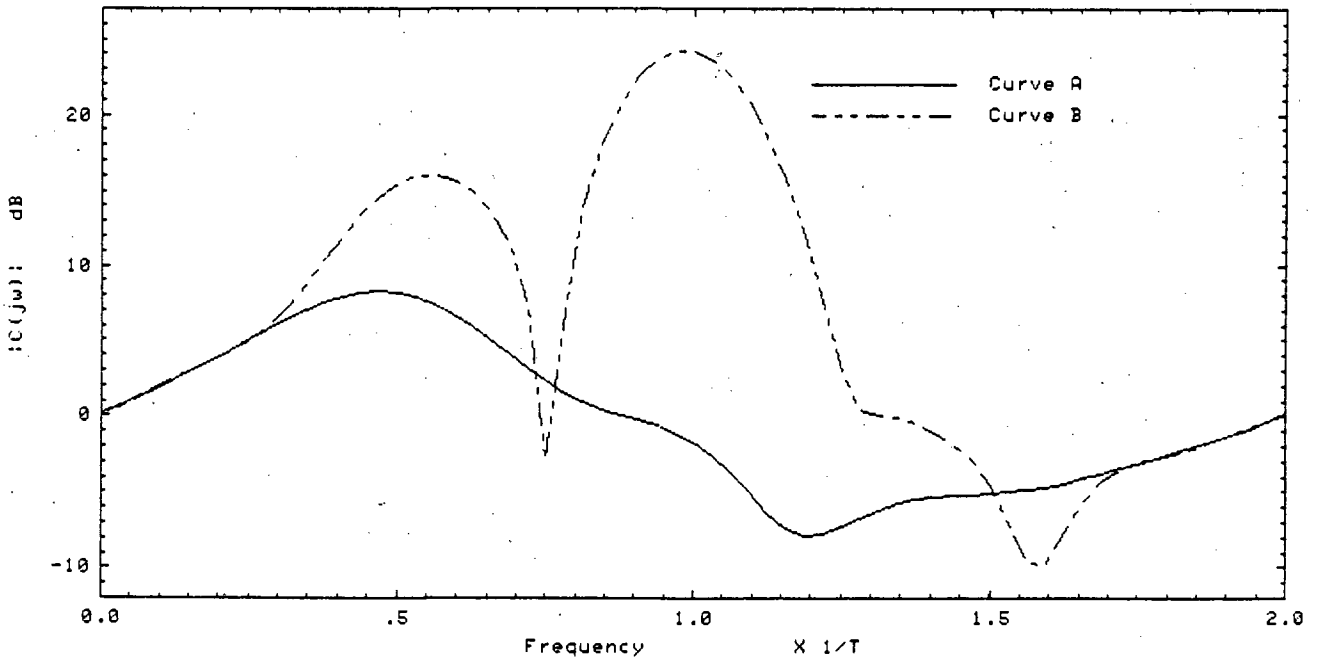

Fig 5.2 |C(jw)| Plots with different Tap Weights

and B in Fig 5.2 show the |C(jw)| with the tap weight sets A and B from Table 5.1 respectively. The curve corresponds to set B tap weights reaches a maximum in N(jw) region, while that with the set A tap weights reaches a minimum in N(jw). Nevertheless $\mathcal{E}_{min}$ is very low in both cases.

If the noise density in N(jw) is not vanishingly small, a high value of C(jw) in this region will result in noise enhancement and affect the equalizer response. However, the LMS algorithm will minimize the mean square error and thus C(jw) will be under control within the N(jw) region. The higher the noise density in N(jw), the better controlled is C(jw) in the N(jw) region. For example, with a C/N ratio of ~40dB before the multipath fading channel, the same conditions as described for set B tap weights in Table 5.1, a completely different set of tap weights and C(jw) can be obtained, as shown in Table 5.2. The spectral responses for |C(jw)H(jw)|, $|E_f(jw)|$ and |C(jw)| are plotted in Fig 5.3 a,b,c respectively. The ideal responses of |C(jw)H(jw)| and $|E_f(jw)|$ are plotted as the dotted reference. Although |C(jw)| is much stable in N(jw) region when compared with curve B in Fig 5.1b, |C(jw)H(jw)| still shows asymmetry against 1/T axis, as shown in Fig 5.3a,c.

The above two reasons perhaps can explain why Gitlin et al.'s T/2 equalizer [106] has many distinct sets of tap weights coresponding to the same MSE.

tap weight	real	img
C_{-6}	-0.036	-0.021
C_{-5}	0.038	-0.094
C_{-4}	0.138	0.299
C_{-3}	-0.137	-0.088
C_{-2}	-0.398	-0.321
C_{-1}	0.598	-0.026
C_0	1.602	-0.271
C_1	0.885	0.060
C_2	0.015	0.784
C_3	-0.262	0.182
C_4	-0.269	-0.299
C_5	0.237	-0.021
C_6	-0.036	0.034

Table 5.2 Tap Weight value with added Gaussian Noise

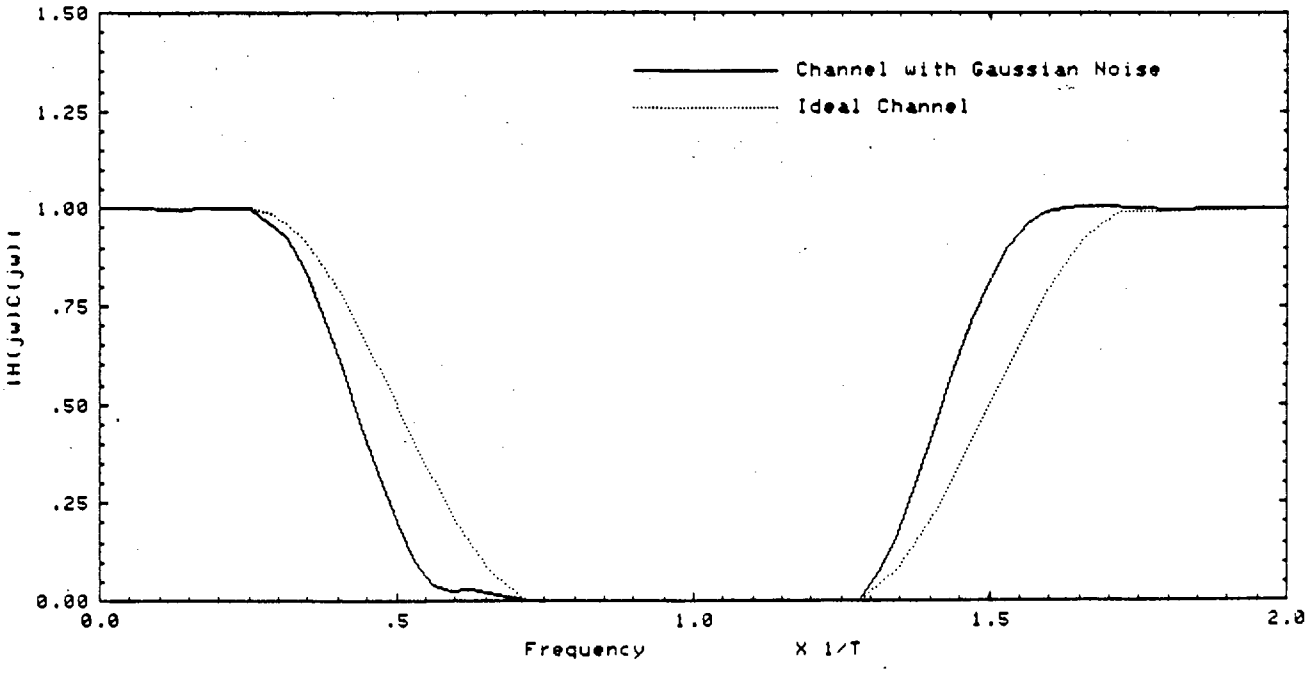

Fig 5.3a |C(jw)H(jw)| with added Gaussian Noise

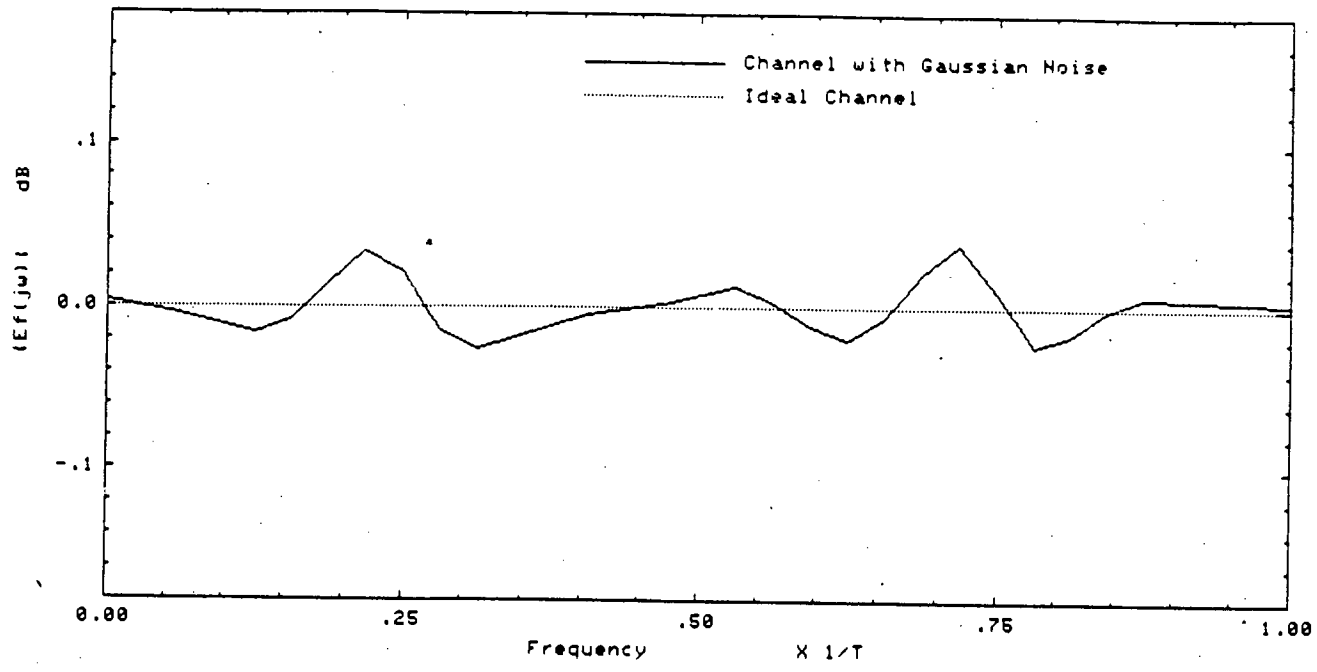

Fig 5.3b $|E_f(jw)|$ with added Gaussian Noise

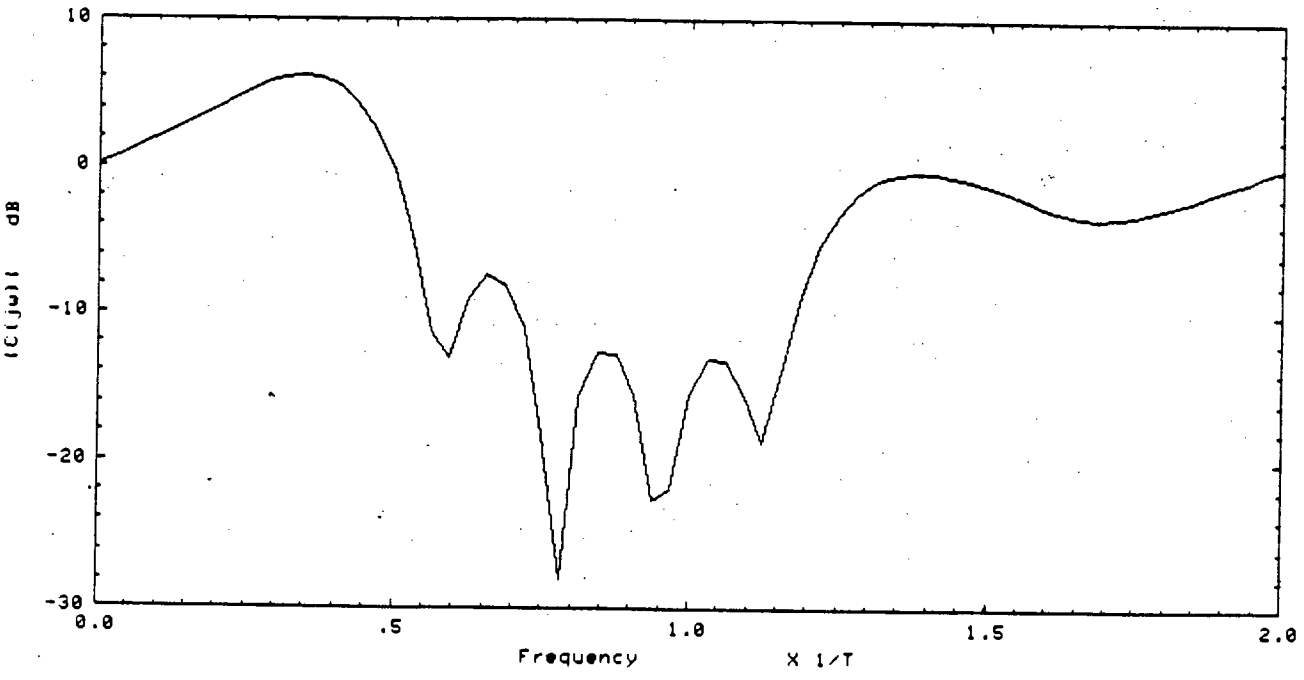

Fig 5.3c $|C(jw)|$ with added Gaussian Noise

In order to simulate a practical system and reduce the effect of truncation or rounding error in the computation, a ~60dB C/N is always added for the latter $\underline{C}_{opt}$ and $\mathcal{E}_{min}$ calculation unless otherwise specified.

5.1.2 The Effect of Finite Step Size

Unlike the T-spaced equalizer, there exists a strong correlation in the matrix element R_{ij} ($i \neq j$). So the approximation taken in equation (4.18b) does not always hold well and should be modified as:

$$E\langle |e_1|^2 \left(\sum_{i=-N}^{N} Q_i Q_i^*\right)^2\rangle = (1+d)\, P_{total}^2 E\langle |e_1|^2\rangle \quad \ldots\ldots (5.1)$$

where d is the correction factor and

$$P_{total} = \sum_{\substack{i=-N \\ i \text{ is even} \\ \text{including zero}}}^{N} Q_i Q_i^* + \sum_{\substack{i=-N \\ i \text{ is odd}}}^{N} Q_i Q_i^* \quad \ldots\ldots\ldots\ldots\ldots (5.2a)$$

The first term in equation (5.2a) is equivalent to the summation of P_{av} in the T-spaced equalizer, and the second term represents the summation of the average power with T/2 offset to P_{av}. Thus equation (5.2a) can be re-expressed as:

$$P_{total} = (N+1)P_{av} + N\, P_{av}' \quad \text{if N is even}$$

$$\text{or} \quad P_{total} = N\, P_{av} + (N+1)\, P_{av}' \quad \text{if N is odd} \quad \ldots\ldots\ldots (5.2b)$$

$$\text{where } P_{av}' = E\langle A_k A_k^* \rangle\, E\langle P^{\theta\theta}{}_{i-1/2} P^{\theta\theta}{}_{i-1/2}{}^* + c/r \rangle$$

$$\ldots\ldots\ldots\ldots\ldots\ldots\ldots\ldots (5.2c)$$

The correction factor d in equation (5.1) depends on the radio systems and the channel characteristics. A value of over 20% is quite common if the number of tap weights is less than 11. Equations (4.21b) and (4.21c) may still be applied but with a larger range of β value, e.g. 0.1 to 0.6. Hence it is hard to determine the β value. An alternative way is to estimate the d value from the received samples. With the same approach in section 4.2.2, the degradation due to the finite step size can be achieved as follows:

$$E\langle|e_{final}|^2\rangle \sim \frac{\xi_{min}}{1 - u(1+d')P_{total}/2} \quad \ldots\ldots\ldots\ldots\ldots\ldots \quad (5.3)$$

with

$$d' = \frac{0.21(1.15+a)(2N+1)\cdot^3 E\langle A_k A_k^*\rangle}{P_{total}} \quad \ldots\ldots\ldots\ldots\ldots\ldots \quad (5.4)$$

where a is the excess bandwidth

Here the estimator d' consists of d and the approximation holds in equation (4.20a). The d' estimator in equation (5.4) is reasonably accurate when $a \geq 0.3$, $\xi_{min}/E\langle A_k A_k^*\rangle$ is between -20dB to -50dB and the number of taps larger than 7. This finds support from Table 5.3 for various fading and excess bandwidth paramters. All the theoretical $E\langle|e_{final}|^2\rangle$ values are reasonably close to that of the simulated values if the step size is less than u'. For a larger step size, the estimation of d' value basing on the received sample power may not be accurate.

b=.9 (20dB fade notch)

	no of taps	a	T_d ns	f_0 MHz	step size	simulated $E\langle\lvert e_{final}\rvert^2\rangle$ dB	theoretical $E\langle\lvert e_{final}\rvert^2\rangle$ dB
A	9	.5	8	0	u'/5	-20.1	-20.2
					u'/2	-21.1	-21.0
					u'	-18.0	-18.4
					5u'/4	-15.9	-17.2
B	9	.3	8	0	u'/5	-17.3	-17.3
					u'/2	-18.2	-18.1
					u'	-15.2	-15.6
					5u'/4	-13.7	-14.3
C	9	.3	8	6	u'/5	-21.0	-21.0
					u'/2	-21.8	-21.8
					u'	-19.0	-19.3
					5u'/4	-17.8	-18.0
D	11	.4	9	2	u'/5	-21.1	-21.3
					u'/2	-22.0	-22.1
					u'	-18.6	-19.5
					5u'/4	-16.3	-18.3

Table 5.3 Comparison of the Simulated Result with the Theoretical Calculation for different Parameters

5.1.3 Convergence Properties of MSE

The strong correlation existing in the matrix element R_{ij} ($i \neq j$) does not only affect the degradation due to the finite step size, but also imposes influence on the MSE convergence property. Following the approach used in section 4.2.1 and Appendix 5, the u_{max} and u' can be obtained as follows:

$$u_{max} = \frac{2}{(1+d')P_{total}} \quad \ldots\ldots\ldots\ldots\ldots\ldots\ldots\ldots\ldots\ldots \quad (5.5)$$

$$u' = \frac{1}{(1+d')P_{total}} \quad \ldots\ldots\ldots\ldots\ldots\ldots\ldots\ldots\ldots\ldots \quad (5.6)$$

Here d' estimator is applied instead of d so that the actual u_{max} and u' are normally slightly higher than the values calculated from equations (5.5, 5.6). Compared with the T-spaced equalizer, the T/2-spaced equalizer exhibits extraordinary characteristics. Fig 5.4 shows, for the same multipath channel and radio system as in Fig 4.4, the performance of a 7 tap equalizer with step size of 0.548u'. The MSE convergence curve of a 7 tap T-spaced equalizer with same step size in terms of u' is also plotted for comparison. The same sampling phase which is optimized for the T-spaced equalizer is used for both curves. The T/2 spaced equalizer converges very fast initially, just like the T-spaced equalizer. After ~20 iterations, it starts to slow down slightly and then considerably after the MSE reaches -27dB.

This is because the ill-conditioning behaviour in $\underline{R}'$ causes instability in $\underline{C}$. A small change in MSE may correspond to

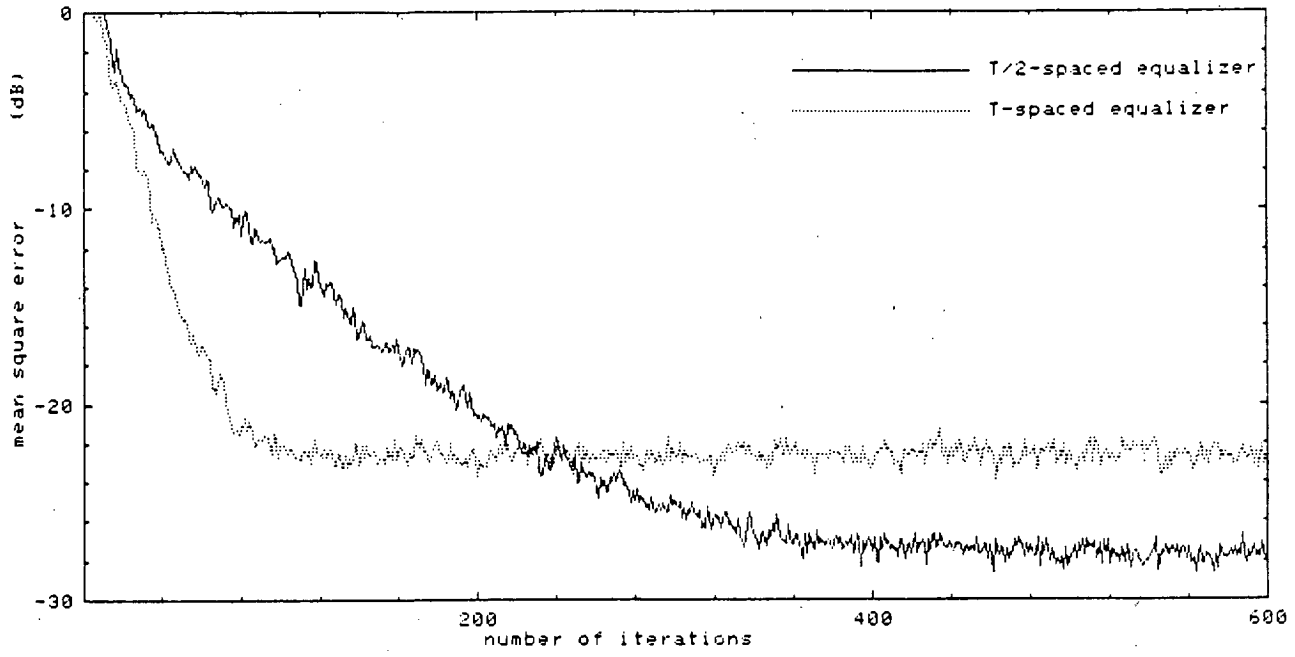

Fig 5.4 Convergence behaviour of T/2-spaced Equalizer

large changes in $\underline{C}$ and consequently it will slow down the convergence rate. The changes in the center 3 tap elements and $\mathcal{E}_{min}$ of the simulation are shown in Table 5.4 with iteration number. The result is obtained by ensemble average of 20 runs. The $\mathcal{E}_{min}$ is averaged from n-20 to n, where n is the stated iteration number. The change of C_{-1} and C_1 with $\mathcal{E}_{min}$ demonstrates this effect thoroughly.

Gitlin et al. [106] also report that the instability of tap weights may cause them to drift into high value regions and introduce overflow in the arithmetic. This instability may be due to the bias in the non-ideal hardware, time drift of the sampling phase, change of the channel parameters, or a long sequence of highly correlated data. This problem can be overcome by employing the tap leakage algorithm [106]:

$$\underline{C}_{j+1} = \underline{C}_j - u\,(\,e_j\underline{Q}_j^* + f\,\underline{C}_j\,) \quad \ldots\ldots\ldots\ldots\ldots\ldots \quad (5.7)$$

By adding a term opposed to the tap drift direction, the tap weight will be forced to converge into a low value region for a proper choice of f. However there are three major drawbacks:

(1) the MSE convergence rate may be slowed down

(2) more calculation steps are needed for each iteration

(3) an excess error is introduced

iterations n	ξ_{min} (dB)	C_{-1}		C_0		C_1	
		real	img	real	img	real	img
20	1.5	0.363	-0.020	1.638	-0.003	0.358	0.047
50	-6.2	0.412	-0.117	1.825	-0.017	0.414	0.138
100	-10.7	0.415	-0.164	1.941	-0.023	0.414	0.187
200	-19.0	0.400	-0.195	2.024	-0.025	0.399	0.217
300	-25.4	0.394	-0.203	2.026	-0.024	0.394	0.224
500	-27.4	0.390	-0.209	2.078	-0.021	0.389	0.230
1000	-27.5	0.390	-0.216	2.084	-0.021	0.387	0.237
3000	-27.8	0.383	-0.239	2.092	-0.024	0.379	0.263
18000	-28.9	0.332	-0.361	2.179	-0.037	0.323	0.411
50000	-30.8	0.193	-0.471	2.361	-0.063	0.189	0.562
100000	-34.1	-0.002	-0.527	2.593	-0.092	0.008	0.666
**	-41.1	-0.511	-0.615	3.195	-0.168	-0.457	0.877

** Theoretical value

Table 5.4 Covergence Characteristics of the Center three taps

Furthermore the background theory behind this algorithm is not well established and high resolution arithmetic is probably required to implement it. Thus this algorithm will not be considered further in this thesis.

5.2 The Effect of Quantization Noise in the ADC and Finite Precision Arithmetic

The equations regarding degradation due to quantization in the ADC and finite precision arithmetic (4.24 to 4.28, 4.30a to 4.32b) of the T-spaced equalizers are also valid for the T/2-spaced equalizers. So the overall degradation due to finite step size, quantization in the ADC and finite precision arithmetic is as follows:

$$E\langle|\check{e}_{final}|^2\rangle = \frac{\mathcal{E}_{min} + \Delta_q \underline{c}_{opt}^h \underline{c}_{opt} + \Delta_c \bar{P}_{total}}{1 - u(1+d')\bar{P}_{total}/2} \quad \ldots\ldots\ldots\ldots\ldots\ldots \quad (5.8)$$

Let us consider the same fading channel and radio system as in Table 4.3. With the same n_1, n_2 and N value as for the T-spaced equalizer, the simulated and theoretical estimates for the T/2-spaced equalizer are shown in Table 5.5.

The theoretical $E\langle|e_{final}|^2\rangle$ and $\mathcal{E}_{min}$ are found using equations (5.8) and (4.8) respectively. Since the S value is much higher than that in the T-spaced equalizer, the degradation due to quantization noise of the ADC is higher in the T/2-spaced equalizer. Although P_{total} is about half of that in the T-spaced equalizer, a large range of arithmetic is

required for the T/2-spaced equalizer and results in the same order of degradation of N_c. Thus even the ξ_{min} is much lower for the T/2-spaced equalizer, the T-spaced equalizer gives a better $E<|\check{e}_{final}|^2>$, as shown in Tables 4.3 and 5.5. The simulation result of case C is unexpectedly lower than case D. There might be a possibility that the two errors due to the ADC and finite precision arithmetic respectively cancel each other.

N = 7, P_{total} = 13.2

u = 0.049 (0.91u'), ξ_{min} = -43.0dB

	ADC bits (n_1)	arithmetic bits (n_2)	S	Theoretical MMSE (dB)	Simulation MMSE (dB)
A	5	7	10.9	-9.0	-10.0
B	5	8	10.9	-9.2	-10.0
C	6	7	11.1	-14.0	-15.9
D	6	8	11.1	-15.0	-15.4

Table 5.5 Comparison between the Theoretical and Simulation MMSE with finite ADC and Arithmetic Resolution

The equations regarding the early termination effect (4.37a to 4.38b) are also valid for the T/2-spaced equalizer, but $\bar{P}_{av}$ should be replaced by $Max(\bar{P}_{av},\bar{P}_{av}')$,** as shown in the following:

$$E<|e_{early}|^2> \sim \frac{1}{40\ Max(\bar{P}_{av},\bar{P}_{av}')} \left(\frac{1}{n_3}\right)^2 \quad \text{..... (5.9)}$$

**Max(A,B)=A if A>=B; Max(A,B)=B if B>A

Considering the same radio system and fading condition as in Table 4.5, the early termination effect for the T/2-spaced equalizer is shown in Table 5.6. With the same sampling phase as that in the T-spaced equalizer, the theoretical $E<|e_{early}|^2>$ and $E<|\check{e}_{final}|^2>$ are calculated by using equations (5.9) and (5.8) respectively.

u = 1 LSB $E<|e_{early}|^2>$ = -18.9dB

	A	B	C	D
number of taps	9	9	13	13
arithmetic bits	10	12	10	12
Simulation MMSE (dB)	-19.4	-19.3	-20.1	-20.0
$\mathcal{E}_{min}$ A (dB)	-53.3		-60.0	
$\mathcal{E}_{min}$ B (dB)	-53.4		-58.5	
$E<|e_{final}|^2>$(dB)	-33.9	-34.1	-34.0	-34.2

$\mathcal{E}_{min}$ A is calculated by equation (4.7) with C/N = 100dB before multipath fading

$\mathcal{E}_{min}$ B is obtained by adding offset to $\mathcal{E}_{min}$ A, as described in section 4.2.2

The summation of tap weight square (S) = 4.1 in all cases

Table 5.6 The effect of early termination on MMSE

The simulation result is achieved by averaging over the last 1000 iterations with an ensemble average of 20 runs. 150,000 iterations were used in cases A and C, while 400,000 iterations were required in cases B and D as the MSE convergence rate is slower. The results on Table 5.6 also demonstrate the loose dependency of $E<|e_{early}|^2>$ on N and n_2, as with the T-spaced equalizer.

5.3 Equalizer Length Considerations

With the same approach as section 4.5, the following can be established for an infinite tap T/2-spaced equalizer:

$$(|H(jw)|^2 + n) C(jw) = H(jw)^* \quad \ldots\ldots\ldots\ldots\ldots\ldots \quad (5.10a)$$

or

$$C(jw) = \frac{H(jw)^*}{|H(jw)|^2 + n} \quad \ldots\ldots\ldots\ldots\ldots\ldots\ldots\ldots\ldots \quad (5.10b)$$

if $H(jw)$ is not zero

Instead of equalizing the folded frequency response, $H_f(jw)$, like the T-spaced equalizer, it directly equalizes $H(jw)$. Thus the extra distortion due to the sampling phase (spectral null and group delay) does not exist and the equalizer can work more effectively on $H(jw)$. Just like the T-spaced equalizer, $\mathcal{E}_{min}$ decreases as N increases. However, the log-normal behaviour of $\mathcal{E}_{min}$ against N does not hold very well.

As mentioned in section 5.1.1, the ill-conditioning behaviour in $\underline{R}'$ may result in a very high value tap weight set. This becomes more serious if the number of taps increases. Therefore the degradation due to N_q and N_c are not well defined under such a condition.

Unlike the T-spaced equalizer, the matrix characteristic for 2N+1 tap and 2N+3 tap is entirely different** . So the MSE convergence characteristic for 2N+1 tap and 2N+3 tap T/2-spaced equalizers is completely different. As shown in

**with the same sampling phase

Fig 5.5, the MSE convergence curves of a 7 tap and 9 tap equalizer are plotted with the same radio system and fading channel as in Fig 4.4. The optimum sampling phase for the 7 tap equalizer is also used for the 9 tap equalizer.

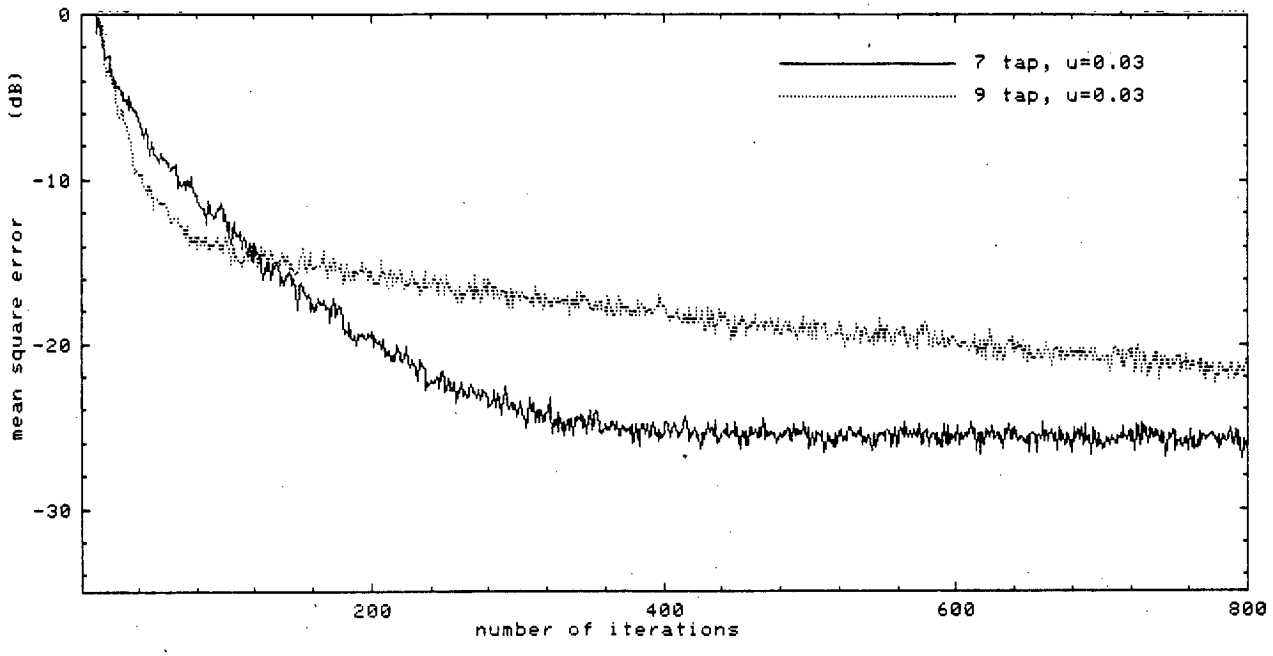

Fig 5.5 Convergence Property with different Number of Taps

5.4 The Effect of Demodulation and Sampling Phase

The response under demodulation phase is basically the same as for the T-spaced equalizer and will not cause any major degradation. Equations (4.40) to (4.42) are also valid. With the same number of taps, the T/2-spaced equalizer performance is superior to the T-spaced equalizer when fade notch is near bandedges as there is no overlapped spectral response in the T/2-spaced equalizer. Fig 5.6a shows $\mathcal{E}_{min}$ against sampling

phase, with the same radio system, multipath channel and number of equalizer taps as employed in Fig 4.10. Over the range of -170° to 180°, the change in MSE is less than 4dB for a=0.1 to 0.7. The result also reflects that when comparing with the T-spaced equalizer with a=0.3, $\mathcal{E}_{min}$ exhibits over 15dB improvement. Moreover, $\mathcal{E}_{min}$ is loosely dependent on the "a" value under such fading conditions.

But if the fade notch moves towards band-center, the performance of the T/2-spaced equalizer starts to degrade, in a sense that the $\mathcal{E}_{min}$ gradually lags behind that of the T-spaced equalizer, and the sensitivity to the sampling phase starts to increase. For a 7 tap T/2-spaced equalizer, over 10dB difference in $\mathcal{E}_{min}$ is quite common within 360° sampling phase range, as shown in Fig 5.6b with different excess bandwidth. The fading notch is 10dB at band-center with 8ns delay time in the 3-ray model and 22.6MHz 16QAM radio system. The response of the T-spaced equalizer with the same number of taps is also plotted for comparison.

Fig 5.7a,b show the $\mathcal{E}_{min}$ against sampling phase with the same radio system, multipath channels and number of equalizer taps as employed in Fig 4.11a,b respectively. The performance of the T-spaced equalizer is plotted for comparison as well. From the figures, the relative insensitivity to sampling phase is demonstrated for the T/2-spaced equalizer but with a higher optimum $\mathcal{E}_{min}$ value. Again, similar to the T-spaced equalizer, the optimum sampling phase is a few samples away

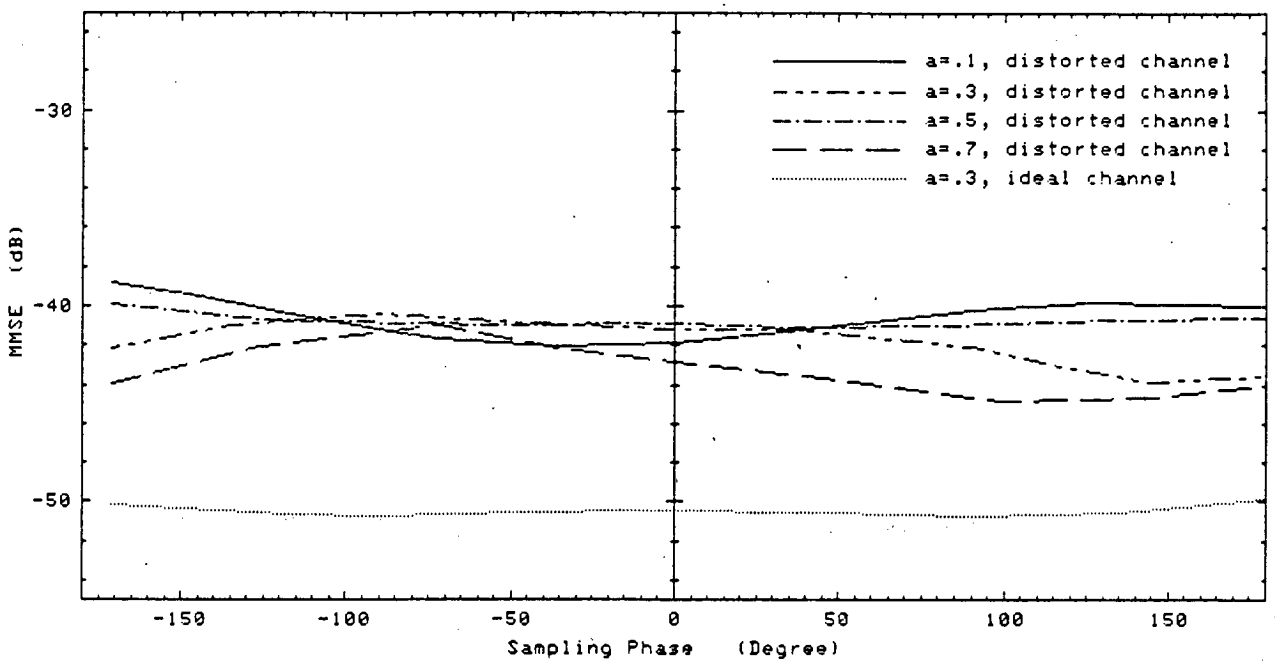

Fig 5.6a $\mathcal{E}_{min}$ Values for different Sampling Phase with Fade Notch at Band-edge

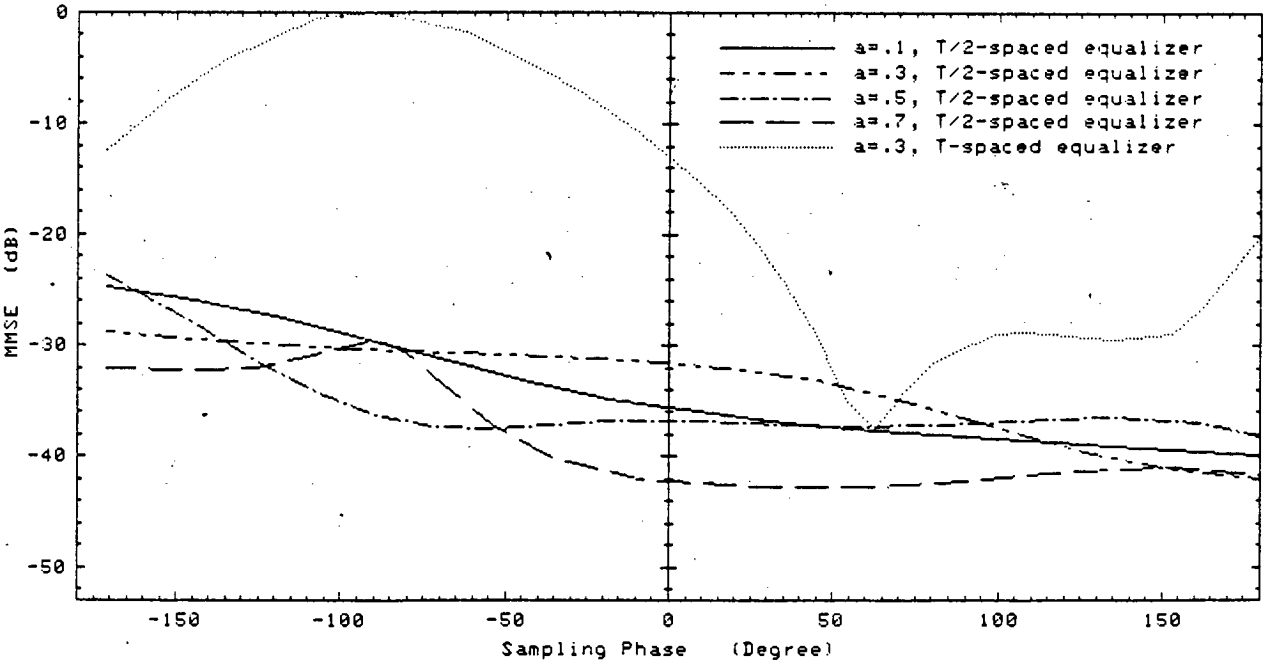

Fig 5.6b $\mathcal{E}_{min}$ Values for different Sampling Phase with Fade Notch at Band-center

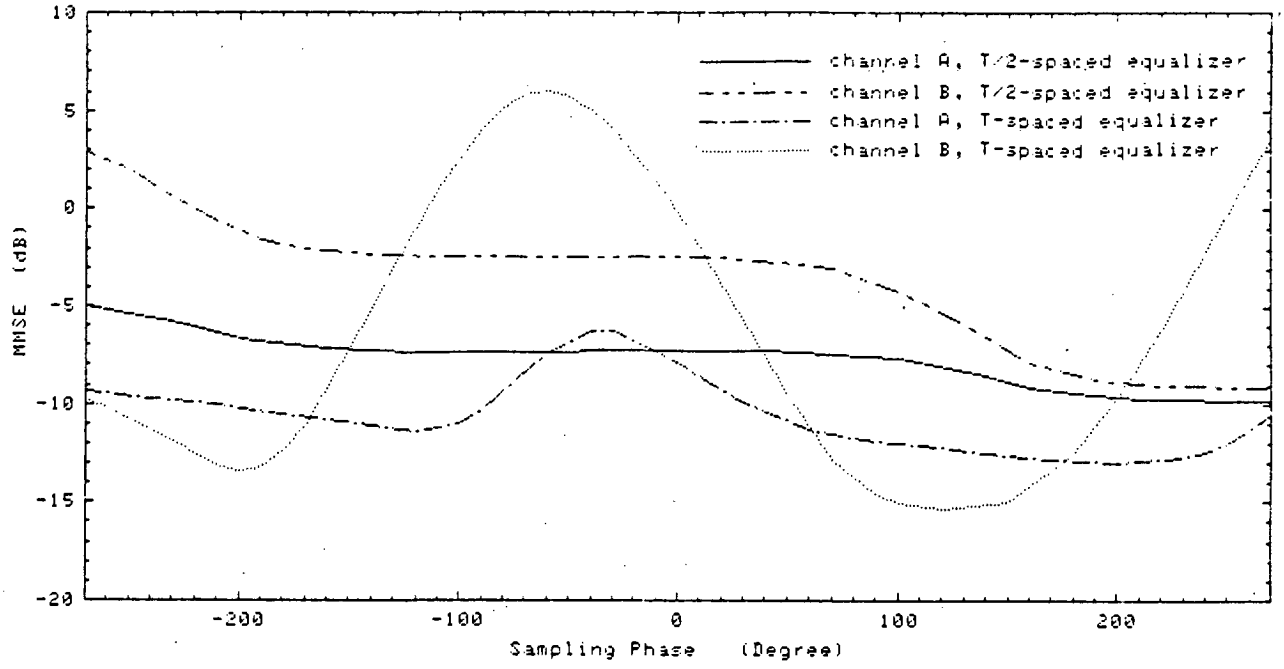

Fig 5.7a Effect of Sampling Phase on $\mathcal{E}_{min}$ for QPSK and 64QAM

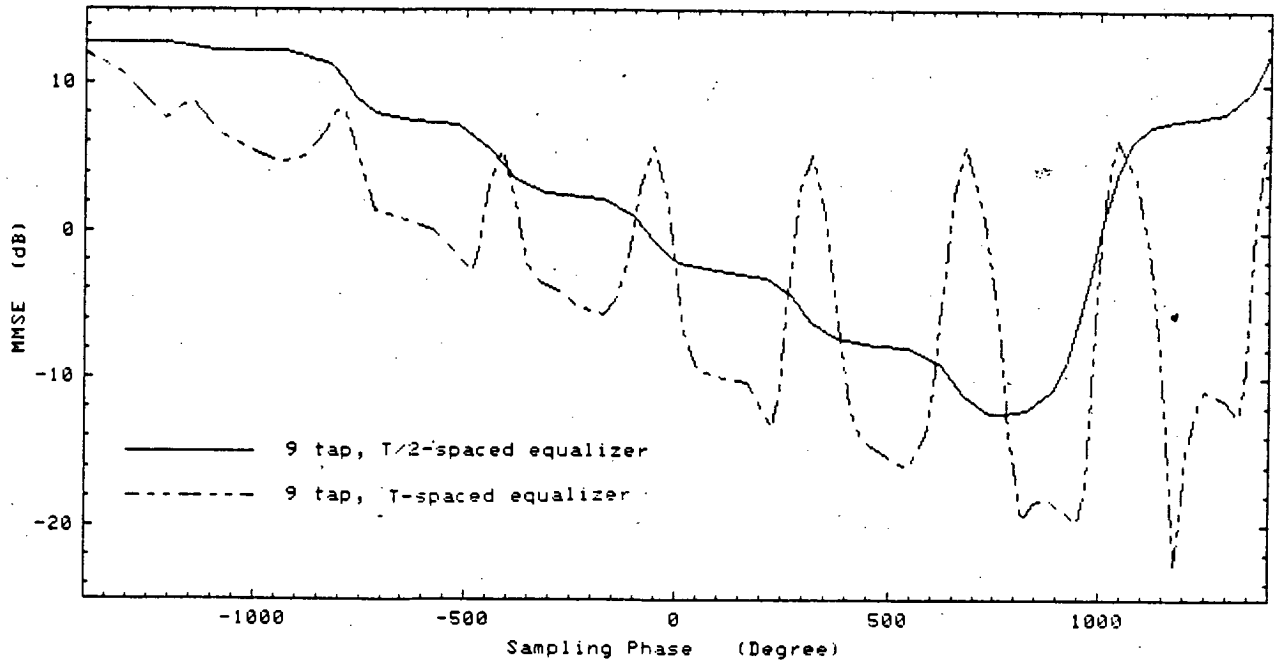

Fig 5.7b Effect of Sampling Phase on $\mathcal{E}_{min}$ under severe Fading

from the original time slot and is hard to achieve in a practical environment.

5.5 Complexity Considerations

As expressed in section 5.1, the ill-conditioning behaviour of $\underline{R}'$ may result a very high value tap weight set. Consequently, an enormous degradation due to N_q and N_c may be obtained. Although the quantization noise of the ADC in some sense can lessen the tap weight value, in general it is hard to estimate a reasonable N_q and N_c degradation.

Curves in Fig 5.8a,b,c,d,e plot the signatures of QPSK, 16QAM, 64QAM, 256QAM, 1024QAM respectively. All are 22.6MHz bandwidth with 30% excess bandwidth and 40dB flat fade margin. The signatures are progressively improved as the number of tap increases. Apart from QPSK, for every 2 tap increase in complexity, the improvement is small. The choice for the number of taps will thus depend on the cost, expected fading activity on the radio channel and the performance objective.

When compared with the corresponding signatures of T-spaced equalizers (Fig 4.15a,b,c,d), Fig 5.8b,c,d,e reflects the superior performance of the T/2-spaced equalizer when the fade notch is near band-edges, but inferior performance when the fade notch is near to band-center. Under ideal conditions, the comparison of these two structures is determined by the radio systems, delay time of the fading channel, and

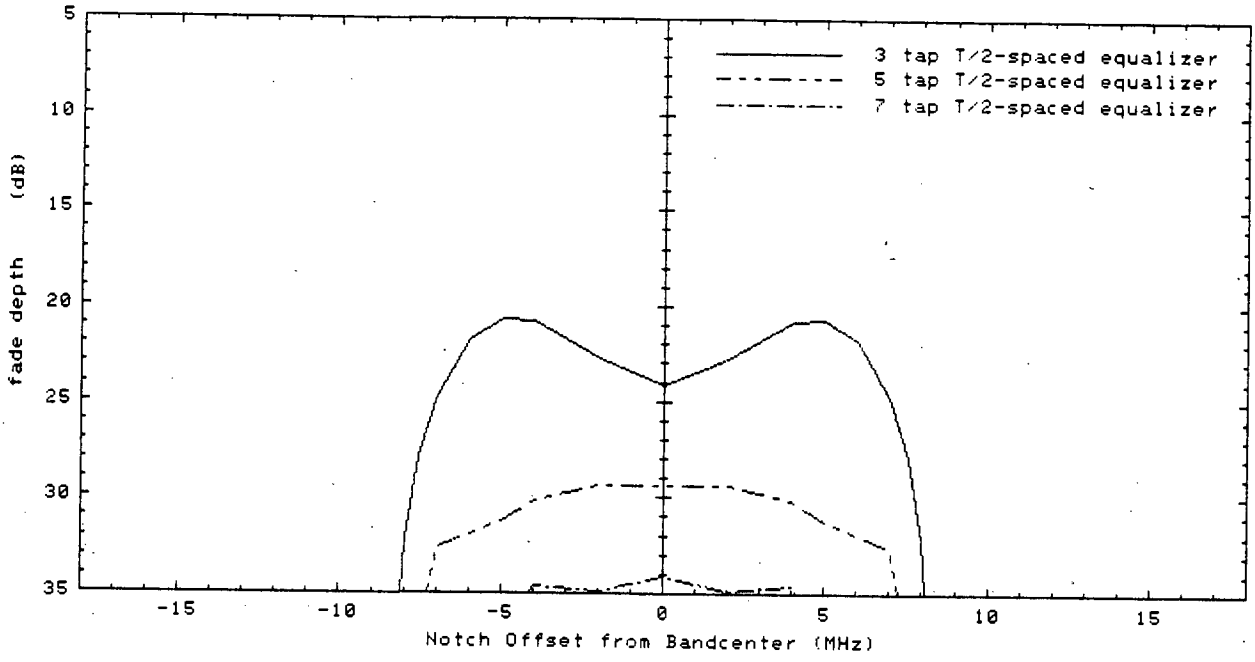

Fig 5.8a Signature Plots for a QPSK Radio System with different Numbers of Taps

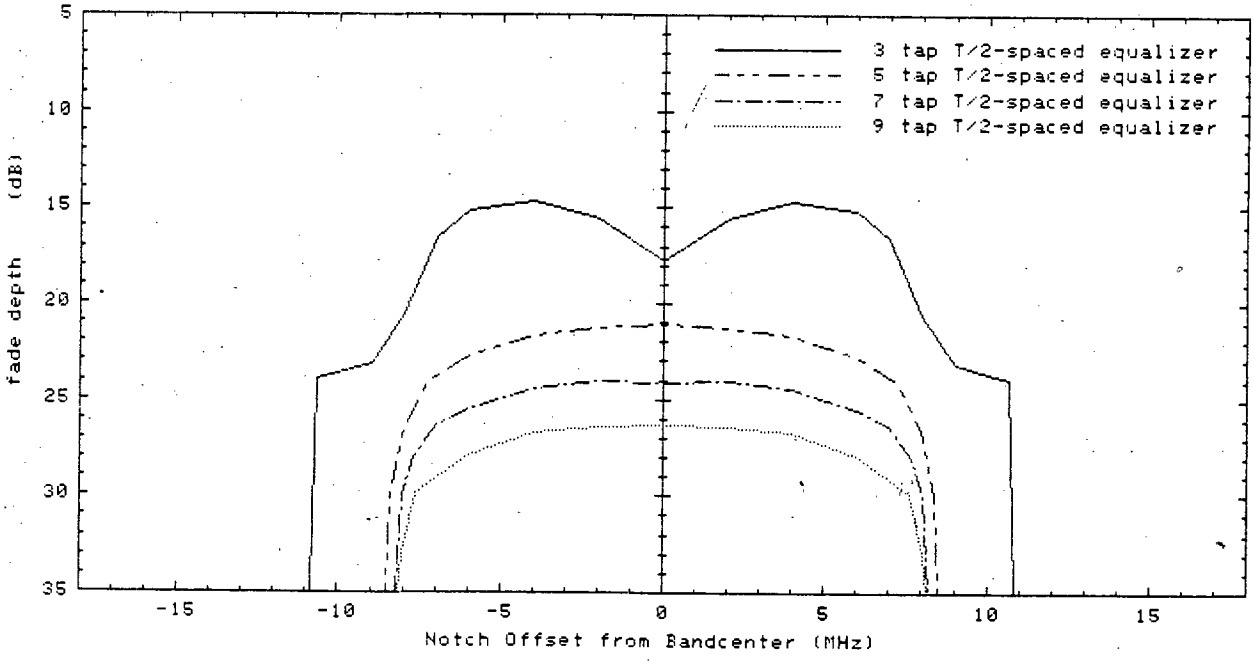

Fig 5.8b Signature Plots for a 16QAM Radio System with different Numbers of Taps

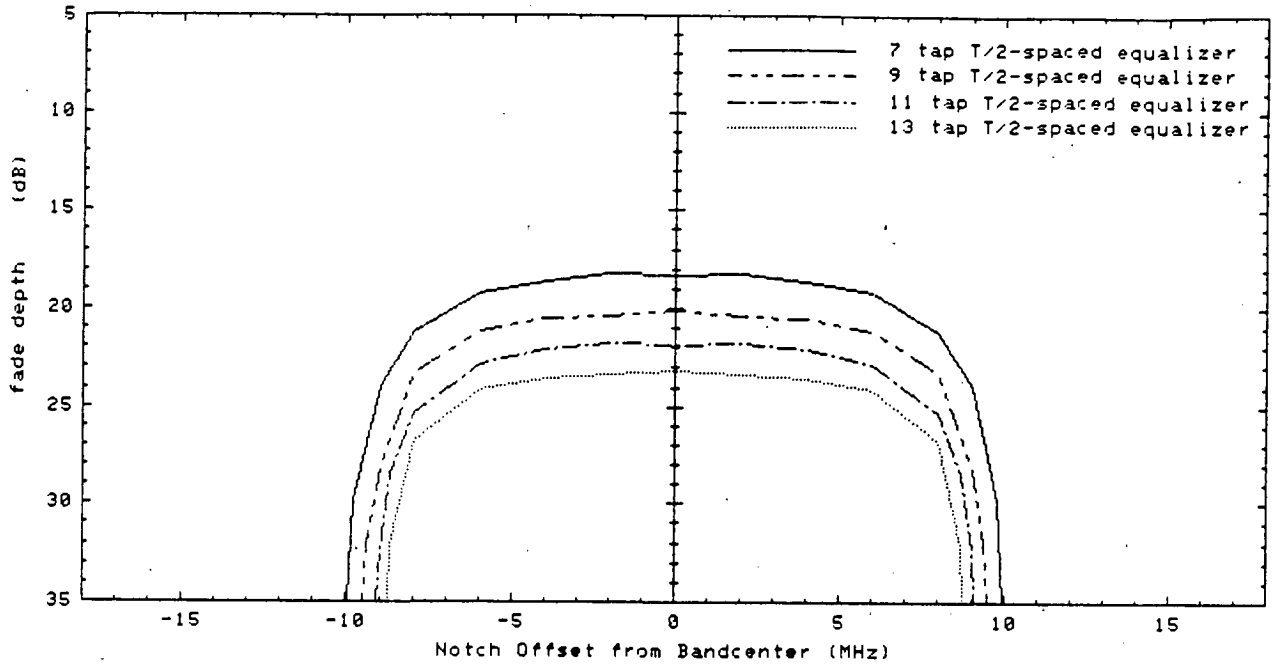

Fig 5.8c Signature Plots for a 64QAM Radio System with different Numbers of Taps

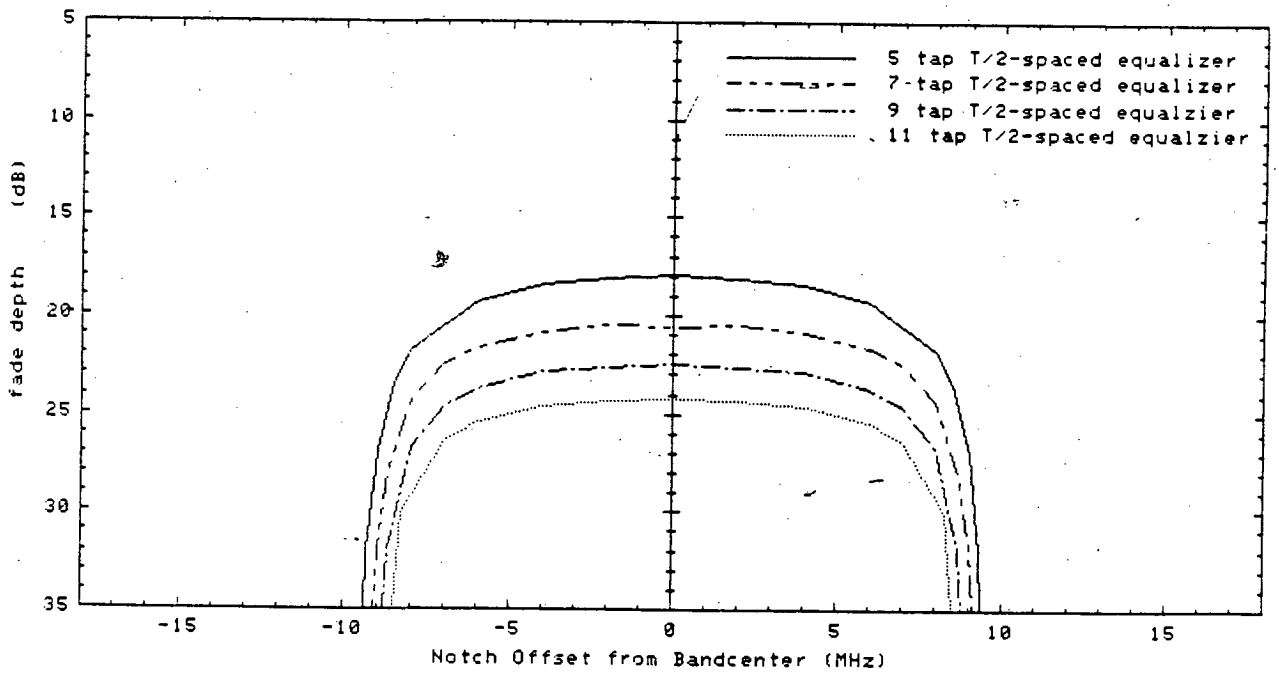

Fig 5.8d Signature Plots for a 256QAM Radio System with different Numbers of Taps

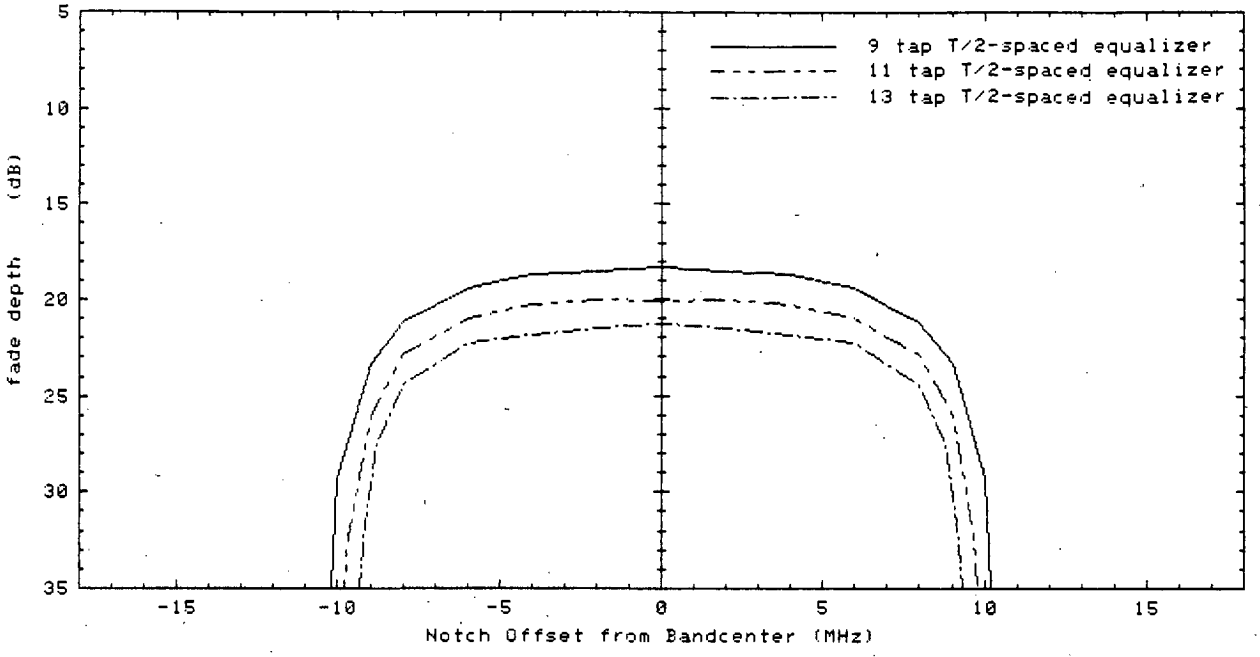

Fig 5.8e Signature Plots for a 1024QAM Radio System with different Numbers of Taps

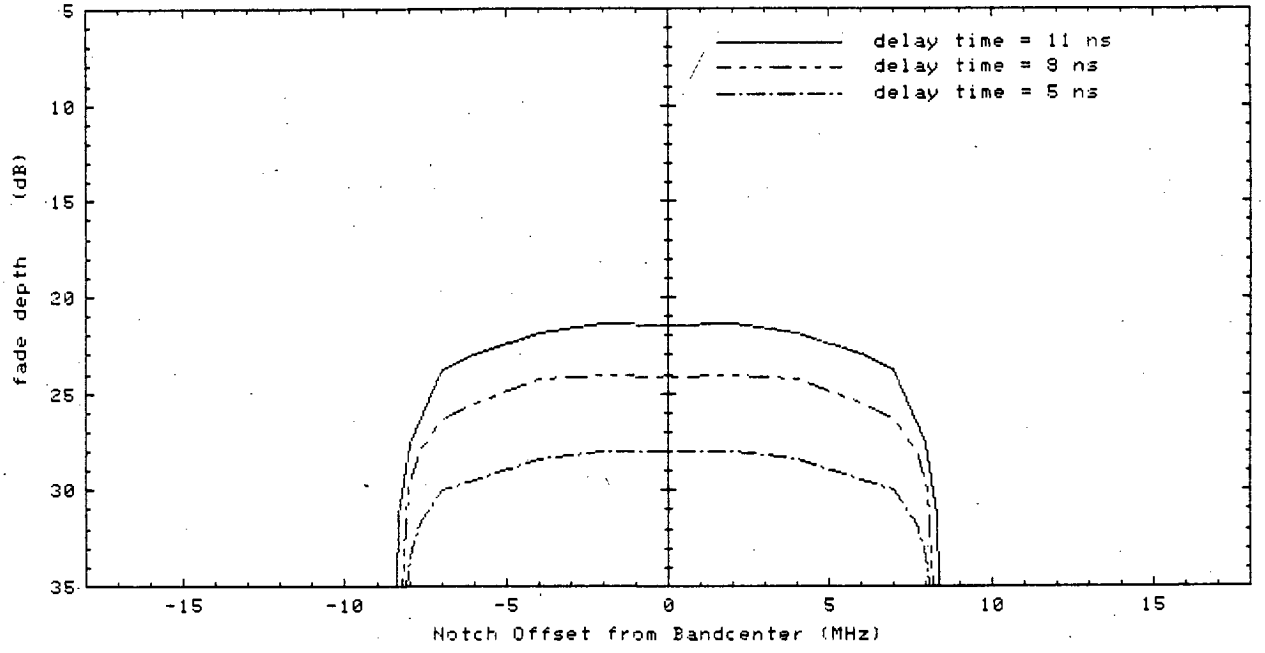

Fig 5.9 Signature Plots of 16QAM with different Multipath Delay parameters

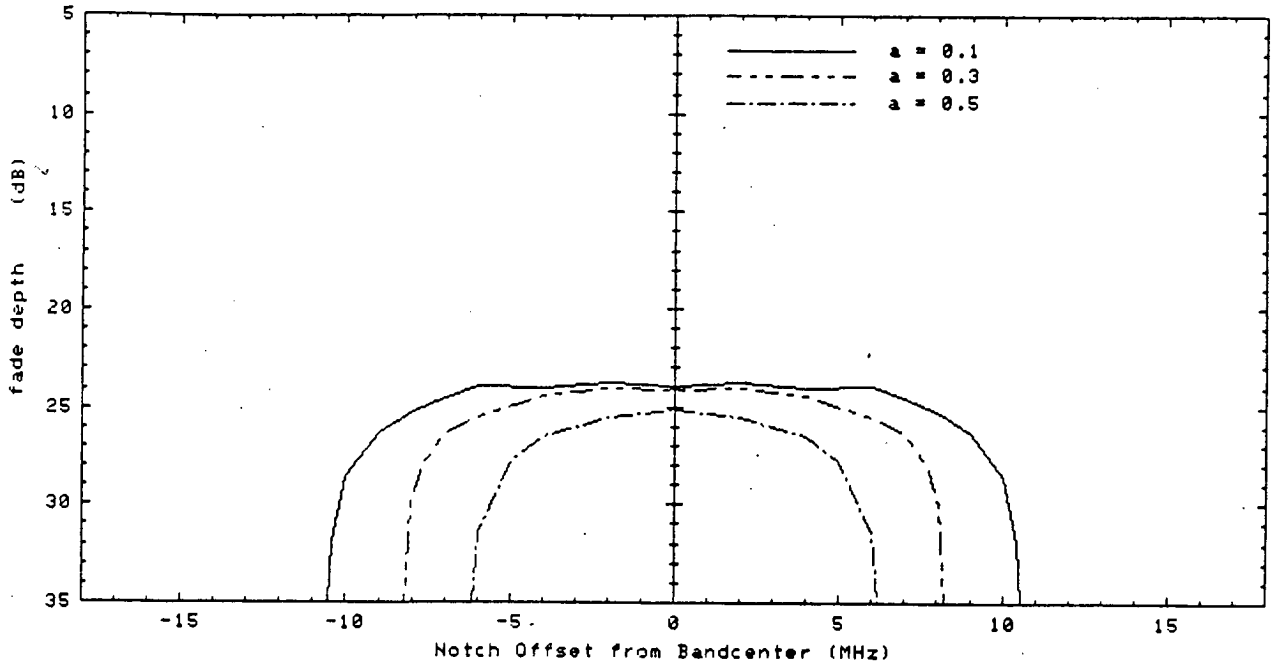

Fig 5.10 Signature Plots of 16QAM with different Raised Cosine Filter shapes

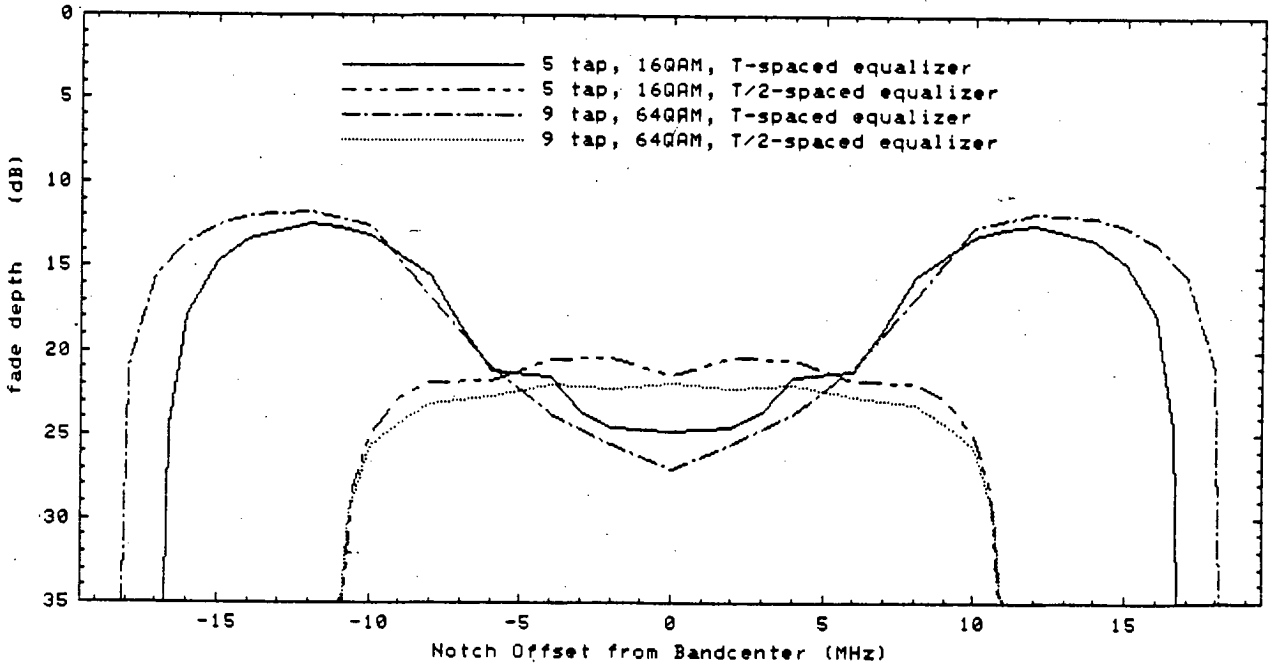

Fig 5.11 Signature Plots of 16QAM and 64QAM with 10% Excess Bandwidth

the number of taps. See for examples in Fig 4.15a and Fig 5.8b, for 16QAM radio with 30% excess bandwidth, the T/2-spaced structure shows better performance for a 3 tap equalizer, on the other hand, the T-spaced is better for a 7 tap equalizer design. However, neither of them shows overwhelming performance advantages for either a T-spaced or T/2-spaced design.

5.6 Various Delay Time and Raised Cosine Filters

With different delay time in the 3-ray model or excess bandwidth in raised cosine filter, a similar performance to the T-spaced equalizer can be achieved. A better signature will be obtained for a shorter delay time in the 3-ray model, as shown in Fig 5.9, with the same radio system and number of taps as in Fig 4.17. Again, the effect of different delay time will move the signature up or down but with the width basically unchanged, at ~1dB/ns for a 7 tap T/2-spaced equalizer design.

Fig 5.10 showed the signatures with various excess bandwidths on the same radio system and number of taps as in Fig 4.18. The T/2-spaced signatures exhibit less sensitivity to the excess bandwidth when the notch is near band-center, and the sensitivity increases progressively as the notch moves away from band-center. When the excess bandwidth is 10%, i.e. a=.1, the signature is far superior than the T-spaced equalizer, as shown in Fig 5.10 and Fig 4.18. Fig 5.11 also

demonstrates the above fact but with different number of tap weights and radio system. It is expected that the importance of the T/2-spaced equalizer will draw more attention to such narrow band transmission.

5.7 Summary

The performance of the T/2-spaced equalizer with LMS algorithm under stationary fading condition has been examined. Most of the equations regarding degradations due to the practical contraints studied in Chapter 4 have been extended to the T/2-spaced structure, with the exception of the finite step size effects. A new correction factor was proposed to take account of the strong correlations in matrix elements R_{ij} $(i \neq j)$.

The most significant problem in the T/2-spaced equalizer is the ill-conditioning behaviour in $\underline{R}'$. A large value tap weight set may be obtained which results in noise enhancement and requires high precision arithmetic. This is the major constraint that hinders the widespead usage of T/2-spaced equalizer designs in LOS digital radio application at present and it requires further investigation.

Compared with the T-spaced equalizer designs, the T/2-spaced equalizer is relatively insensitive to sampling phase. On the other hand if the fade notch is near band-center, over 10dB difference in MSE is possible within 360^{o} sampling phase.

Again the optimum sampling phase is also a few samples away from the original time slot. In order to gain full benefit of the T/2-spaced equalizer, an algorithm is required to calculate the optimum sampling phase. This will present a new potential research area if the high performance of the T/2-spaced equalizer is to be further investigated.

Under ideal conditions, the performance of these two structures depends on radio systems, fading parameters and the number of equalizer taps. However as the excess bandwidth becomes narrow, e.g. a=0.1, the performance of the T/2-spaced equalizer is usually superior to the T-spaced design, thus the former merits further investigation.

CHAPTER 6 NON-STATIONARY SIGNAL CONDITIONS

Unlike the cable or twisted wire transmission medium, where the channel distortion is almost constant, in LOS microwave transmission the multipath distortion is basically unpredictable. The equalizer performance under non-stationary conditions is thus quite important and worthy of investigation. This thesis only provides a preliminary investigation of performance under non-stationary signal conditions as this topic is the primary subject of an on going thesis in the Electrical Engineering Department of the University of Edinburgh.

6.1 Decision Directed Equalization

Fortunately the LOS path is close to an ideal Nyquist channel for the majority of the time. A training sequence for the equalizer is thus not necessary and the equalizer can always be operated in the adaptive mode or the so-called decision directed mode where the desired response is replaced by the estimated data from the equalizer output.

Let $\hat{}$ be the notation of the estimated value for the decision directed operation, then

$\hat{A}_k$ = bit slice of $(\sum_{i=-N}^{N} \hat{C}_i Q_i)$ to the nearest constellation point which can be expressed as:

$$\hat{A}_k = 2\ \text{Int}\ \{[(\sum_{i=-N}^{N} \hat{C}_i Q_i) + LL]/2\} - LL \quad \ldots\ldots\ldots\ldots \quad (6.1)$$

where LL = Complex value (2L-1, 2L-1), is the maximum magnitude of the constellation point and Int{d} is the integer format of d.** The error and tap weight updating at time k are:

$$\hat{e}_k = \sum_{i=-N}^{N} \hat{C}_i Q_i - \hat{A}_k \quad \ldots\ldots\ldots\ldots\ldots\ldots\ldots\ldots\ldots\ldots \quad (6.2)$$

$$\underline{\hat{C}}_{k+1} = \underline{\hat{C}}_k - u\ \hat{e}_k \underline{Q}_k^* \quad \ldots\ldots\ldots\ldots\ldots\ldots\ldots\ldots\ldots\ldots \quad (6.3)$$

The equalizer response will be identical to that using a training signal if no decision error has been made for the estimated data. However during the non-stationary condition when multipath fading is changing rapidly or under severe multipath fading, the equalizer may not track the channel properly and incorrect estimation of the data will occur. This will directly affect the equalizer performance.

Although decision directed operation has been widely used for many years, very little work has been published on its behaviour particularly on the tracking characteristics during non-stationary conditions.

6.1.1 The Effect on Minimum Mean Square Error

Let us separate the entire region into correct and wrong subregions. With a finite probability of incorrect estimates, the MSE can be evaluated as follows:

**Int{d} = P if and only if $P-.5 \leq d < P+.5$

Let $ERR = A_k - \hat{A}_k$ ..... (6.4)

$$E\langle|\hat{e}_k|^2\rangle = E\langle|\sum_{i=-N}^{N}\hat{C}_iQ_i - \hat{A}_k|^2\rangle_c + E\langle|\sum_{i=-N}^{N}\hat{C}_iQ_i - \hat{A}_k|^2\rangle_w \quad \text{..... (6.5a)}$$

where c: correct; w: wrong

$$= E\langle|e_k|^2\rangle + E\langle|ERR|^2\rangle + 2\text{Real } E\langle(\sum_{i=-N}^{N}\hat{C}_iQ_i - A_k)ERR^*\rangle \quad \text{.....(6.5b)}$$

or $$= E\langle|e_k|^2\rangle - E\langle|ERR|^2\rangle + 2\text{Real } E\langle(\sum_{i=-N}^{N}\hat{C}_iQ_i - \hat{A}_k)ERR^*\rangle \quad \text{.....(6.5c)}$$

Since $\{\text{Real } E\langle(\sum_{i=-N}^{N}\hat{C}_iQ_i - \hat{A}_k)ERR^*\rangle\} \leq |ERR|^2/2$ for decision directed detection,

$$E\langle|\hat{e}_k|^2\rangle \leq E\langle|e_k|^2\rangle \quad \text{..... (6.5d)}$$

Equation (6.5d) implies that the expectation of the MSE for the decision directed operation is always less than the actual value with the same tap values. This is reasonable because the maximum magnitude of the error in each channel is restricted to 1.

6.1.2 The Existence of Local Minima

The existence of local minima has already been pointed out by Mazo [115]. In this thesis, a more analytic explanation is given. With the same algorithm as in section (4.1), the optimum tap weight can be obtained by differentiating the MSE with respect to $\underline{C}$ to achieve the expression:

$$\hat{\underline{C}}_{opt} = \underline{R}^{-1}(\underline{D} - E\langle ERR\ \underline{Q}^{*}\rangle) \quad \ldots\ldots\ldots\ldots\ldots\ldots\ldots\ldots \quad (6.6)$$

With different PDFs of ERR, there may exist local minima. In the case of QPSK, the ERR is limited to ± 2, but for higher level modulations, the ERR constitutes with more combinations, e.g. ± 4, ± 6 or even ± 8, thereby resulting in more local minima. So high level QAM suffers more from the local minima problem. Furthermore, as the number of taps increases, the equalizer will also suffer more from this problem.

Consider the similar example as in [115], for an ideal Nyquist channel with a 3 tap T-spaced equalizer and QPSK radio system. With the center data always positive for I and Q channels, the set of data $\{(-1,X),(1,X),(-1,X)\}$ and $\{(X,-1),(X,1),(X,-1)\}$** will cause wrong decisions on I and Q channels respectively, but no problems will be encountered for the rest of the data Q_i. This represents an error ratio of 0.25 on the I or Q channel. Then from equation (6.6),

$$\hat{\underline{C}}_{opt} = \{(1/2,0),(1/2,0),(1/2,0)\}$$

The conditions for the different center data value will be similar. It is this behaviour that causes most of the trouble in decision directed operation. The equalizer may latch into a high error region. Although Mazo[115] shows that it is possible to escape from local minima, this may not be true in a practical system where a small step size is

---

**X is the don't care state

normally used and a long sequence of high correlation data may not occur.

In some conditions, this effect may be eliminated by monitoring the received sample power. If the received sample power is high enough (which implies a low distortion channel) but the tap weights and equalizer error output are unreasonable, then all the tap weights should be reset to zero with the exception of the center tap weight which is preset to (1,0).

Equation (6.6) also shows an interesting result. With 100% wrong decisions, one of the solutions for E<ERR $\underline{Q}^*$> is $2\underline{D}$. This implies $-\underline{C}_{opt}$ is also an optimum tap weight set in the decision directed mode of operation. With the same approach, for every local or global minimum, there will exist a mirror image which corresponds to negative tap weights set (180° phase offset) or with $\pm 90^\circ$ rotations. However these error images may not be a problem because differential encoding is normally employed in the modulation/demodulation process, thus the effects of the constant phase offsets can be eliminated.

6.1.3 Equalizer Gain

Fig 6.1 shows the typical PDFs of the constellation points in the I channel. The individual PDF is close to a Gaussian distribution. Here, let us introduce the equalizer gain concept. The equalizer gain equals 1 if the mean value of the PDF passes through its corresponding constellation point. It

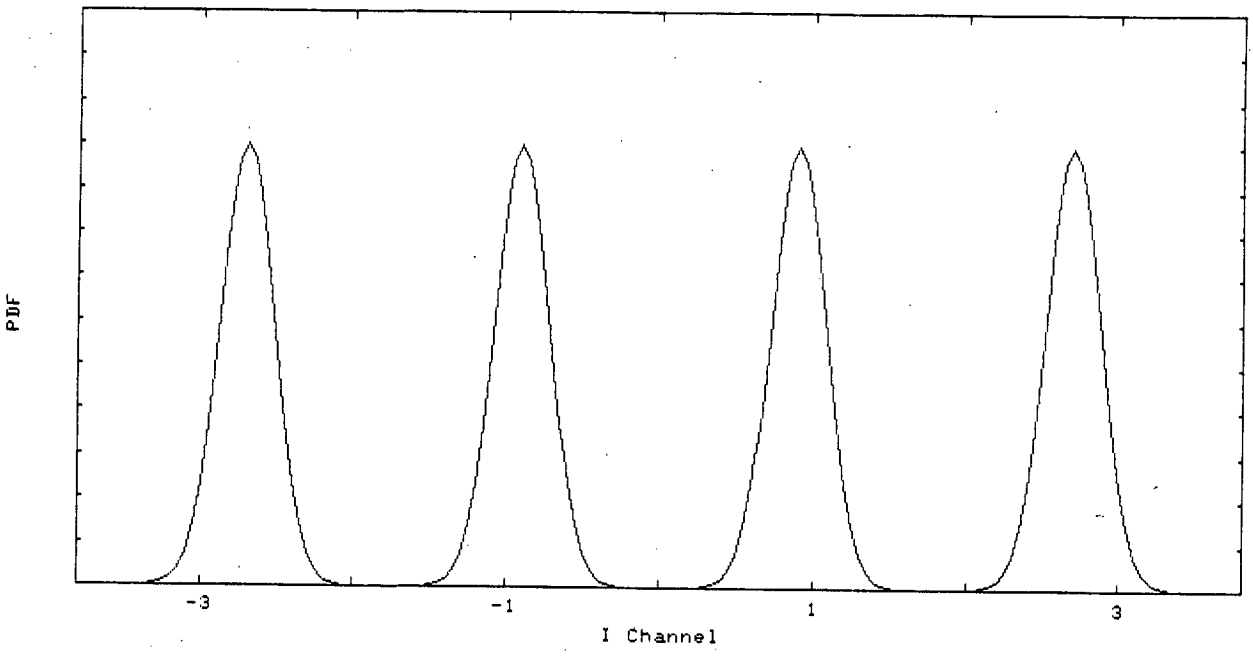

Fig 6.1 Typical PDF of I Channel Constellation Points

is less than 1 or greater than 1 respectively if the PDF mean value is less or greater than its constellation point. For example, the equalizer gain is less than 1 in Fig 6.1.

This idea is important when high level QAM is used. Consider an ideal Nyquist channel with a 1 tap equalizer. For an initial tap weight of (0,0), all the estimated data from the equalizer output will be within the set $\{(\pm 1, \pm 1)\}$ even for a 64QAM radio system. This corresponds to an error ratio of 0.75 on I or Q channel.** From equation (6.6) there exists a local minima with $\hat{\underline{C}}_{opt}=(4/21,0)$, corresponding to an equalizer gain of 4/21.

**Assume differential encoding is used.

From the simulation results, it is discovered that all such local minima correspond to low values of the tap weights, i.e. low equalizer gain. This can be explained based on the equalizer gain concept.

In order to simplify the mathematical notation, only the I channel is considered here. The Q-channel will be similar. In the following, let us consider the MSE provided the desired response A_k is given:

$$E\langle|e_I|^2\rangle = \sum_{j=-L+1}^{L} \int_{-\infty}^{\infty} [gy_j-(2j-1)]^2 P_j dy_j \quad \text{..... (6.7)}$$

where y_j = Real $\left(\sum_{i=-N}^{N} \hat{C}_i Q_i\right)$ for each constellation point j

P_j is the PDF of y_j

For a linear system with random data input, P_j can be approximated as follows:

$$P_j = A \exp\left\{-\frac{1}{2}\left[\frac{y_j-(2j-1)}{v}\right]^2\right\} \quad \text{..... (6.8)}$$

where A and v are respectively the normalization constants and MSE of I channel at g=1.

The minimum MSE corresponding to g, g', can be found by differentiating equation (6.7) with respect to g and setting it equal to zero. The following can be obtained from Appendix 7:

$$g' = \frac{1}{1 + 3v^2/[(2L)^2-1]} \quad \text{..... (6.9)}$$

i.e. $g' \leq 1$

Consider an example of a QPSK radio system and ideal Nyquist channel with 5 tap T-spaced equalizer. If the carrier to noise ratio equals 10dB, which is equivalent to a v^2 value of 0.1, the equalizer gain of 0.91 can be evaluated from equation (6.9). This corresponds to an equalizer with center tap of (0.91,0) and all the rest equal to zero. The same solution can be obtained by solving the matrix equation (4.6c). Thus when the equalizer converges to its MMSE, the equalizer gain is less than 1. The typical PDF distribution of y_j is shown in Fig 6.1.

The case for the decision directed operation will be similar but more tedious since the MSE is very dependent on the PDF of ERR. The actual derivation of $\hat{g}'$ is outwith the scope of this thesis. However it is expected that $\hat{g}'$ will be less than g' as v^2 will be much higher for the decision directed operation.

This is perhaps the main reason why the decision directed equalizer traps into a low level constellation point instead of a high level, which corresponds to $g>1$. In the case where the equalizer is trapped into the low level constellation point, one of the possible solutions is to increase all the tap weight values to pull the equalizer operation into the $g>1$ region.

6.2 Dynamic Tracking Characteristics

Widrow et al.[97] suggest a large step size, u, for better tracking capability during non-stationary operation. However this may create side effects when decision directed operation is employed -- convergence into local minima. The optimum step size will not only depend on the channel characteristics but also on the initial set up of the tap weight elements. Basically there are two characteristics that needed to be considered --- the abrupt change and slow variation of fading parameters.

6.2.1 Abrupt Change in Fading Parameters

Although most fading activities have slowly varying parameters, an abrupt change of parameters is also possible. Equation (6.3) can be re-expressed as:

$$E\langle \delta C_{k+1} \rangle = u \{ E\langle \hat{e}_k \underline{Q}_k^* \rangle_c + E\langle \hat{e}_k \underline{Q}_k^* \rangle_w \}$$

$$= u \{ E\langle e_k \underline{Q}_k^* \rangle + E\langle ERR\ \underline{Q}_k^* \rangle \} \quad \ldots\ldots\ldots\ldots \quad (6.10)$$

If there is no local minimum near by, then the decision error will only affect the convergence rate if

$$\text{sign} \{ E\langle e_k \underline{Q}_k^* \rangle + E\langle ERR\ \underline{Q}_k^* \rangle \} = \text{sign} \{ E\langle e_k \underline{Q}_k^* \rangle \}$$

$$\ldots\ldots\ldots\ldots\ldots\ldots\ldots\ldots \quad (6.11)$$

The importance of equation (6.11) is its independency of step size, u.

The condition is much more complicated if only some of the tap weight elements have the same sign. However, if most of the tap weight elements have the same sign, then the equalizer will still converge into the MMSE. The exact evaluation of equation (6.11) depends on the initial tap weight values and the channel characteristics. However most of the simulation results show that for an initial error ratio of .15 or less and with the initial equalizer gain greater than 0.9, the equalizer will have a high probability of converging but at a slower rate.

Radio System : 22.6MHz 16QAM with 0.3 raised cosine filter
Fading Channel: b=.8, T_d=8ns, f_0=28MHz (3-ray)
Equalizer : 5 tap T-spaced with all tap weights preset to zero with the exception of center tap weight which is set to (1,0). This corresponds to an equalizer gain of 0.75.
Initial error rate : ~0.08

Curve	Step Size	Operation Mode
A	0.004	Decision Directed
B	0.004	Training Signal
C	0.014	Decision Directed
D	0.014	Training Signal

Table 6.1 Equalizer, Radio System and Fading Parameters for Fig 6.2a

For a large step size with low equalizer gain, the equalizer will be more easily trapped into a local minimum. This is

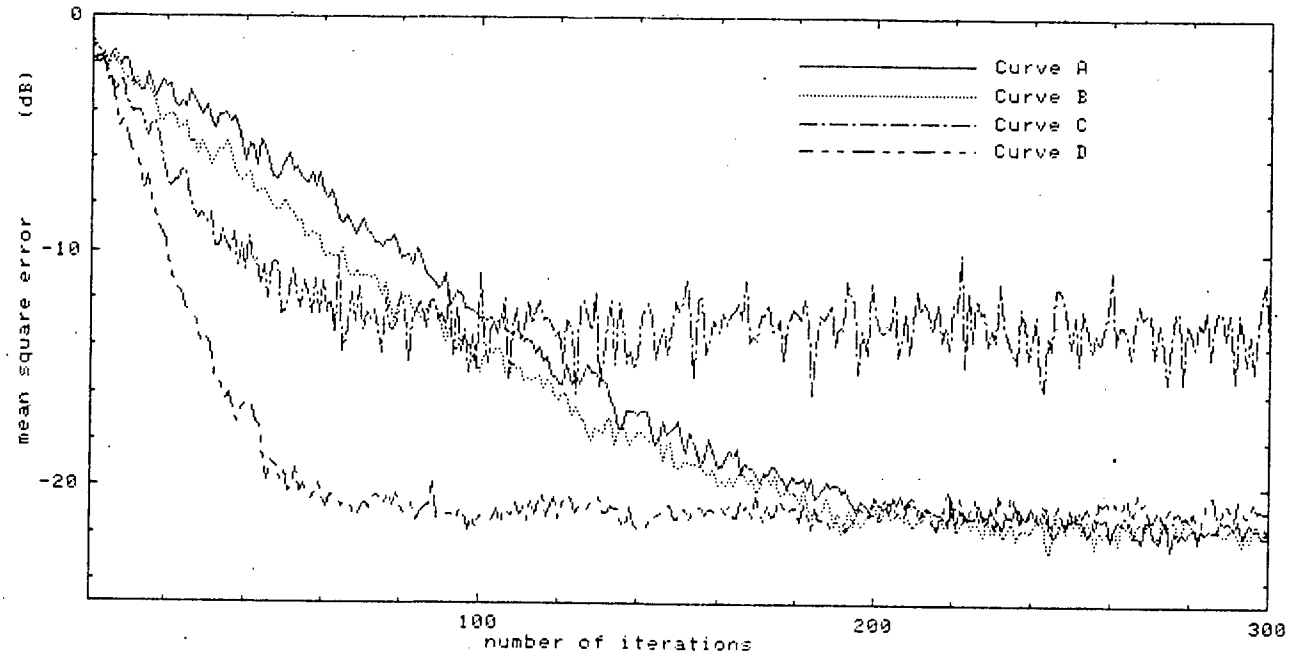

Fig 6.2a Convergence Plots with different Step Size and Initial Equalizer Gain of 0.75

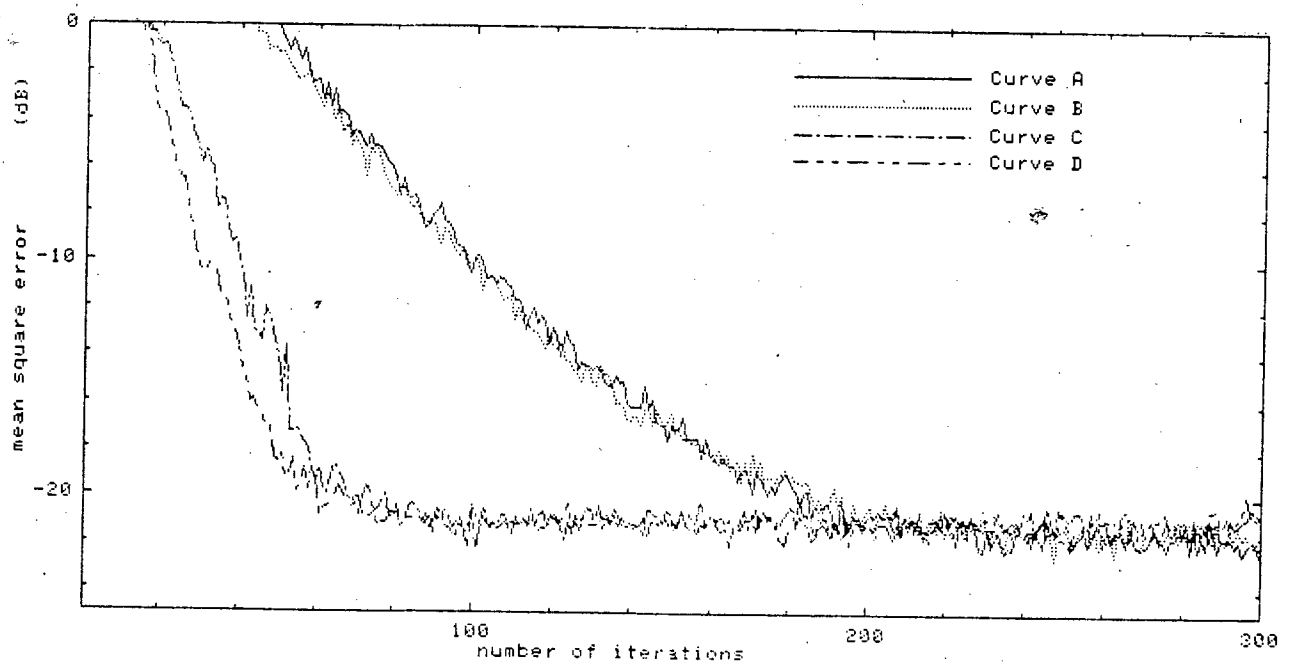

Fig 6.2b Convergence Plots with different Step Size and Initial Equalizer Gain of 1.80

because a small sequence of correlated data will move the equalizer into the local minimum. On the other hand if a small step size is used, a rather long sequence of correlated data is required. This results in less probability of being trapped in the local minimum. Consider the example shown in Fig 6.2a and with the parameters as in Table 6.1.

The MSE convergence rate of decision directed operation is less than that of obtained with training signals initially. For a small step size, i.e. u=0.12u' for curves A and B in Fig 6.2a, both curves reach the same final MMSE. This implies curve A reaches the same optimum tap weight for every ensemble average. With a large step size, i.e. u=0.40u' in the curves C and D of Fig 6.2a, the final MMSE of curve C is much higher than that of curve D. This indicates some of the ensemble average data is trapped into a local minimum.

The problems in curve C can be eliminated if high equalizer gain is used during the start up condition. Using the same fading channel, radio system and equalizer parameters but with the equalizer center tap weight set to (2.4,0) instead of (1,0). This corresponds to an equalizer gain of 1.80 with an initial error rate of 0.17 (double that in Table 6.1). The four MSE convergence plots in Fig 6.2b showed that the final MMSE of decision directed operation is basically identical to the one using a training signal. This implies that none of the ensemble data was trapped into local minima during decision directed operation.

6.2.2 Slow Variation in Fading Parameters

Let us consider a 16QAM 22.6MHz radio under a dynamic fading condition. A constant notch of 16dB at -100MHz is moving linearily to +100MHz. The total time taken is 16000 iterations,** and then all the fading parameters remain the same for another 16000 iterations. The delay time of the 3-ray model is fixed at 6ns. Two curves have been plotted in Fig 6.3a,b, which correspond to the step size of 0.008 and 0.020 respectively. The theoretical MMSE for the static condition with the same sampling phase is also plotted for reference in Fig 6.3c.

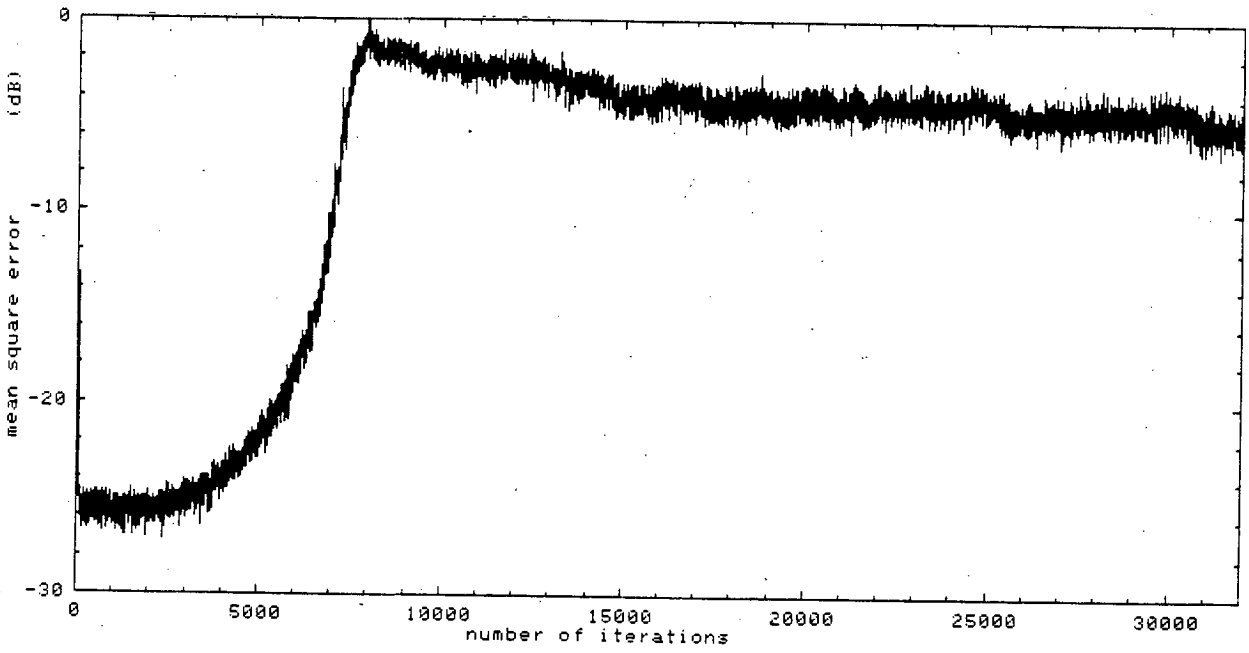

Fig 6.3a Tracking Characteristics for a 5 Tap T-spaced Equalizer with Step Size of 0.008

**Iteration cycle is used instead of the real time because the adaptive process may not be in the real time.

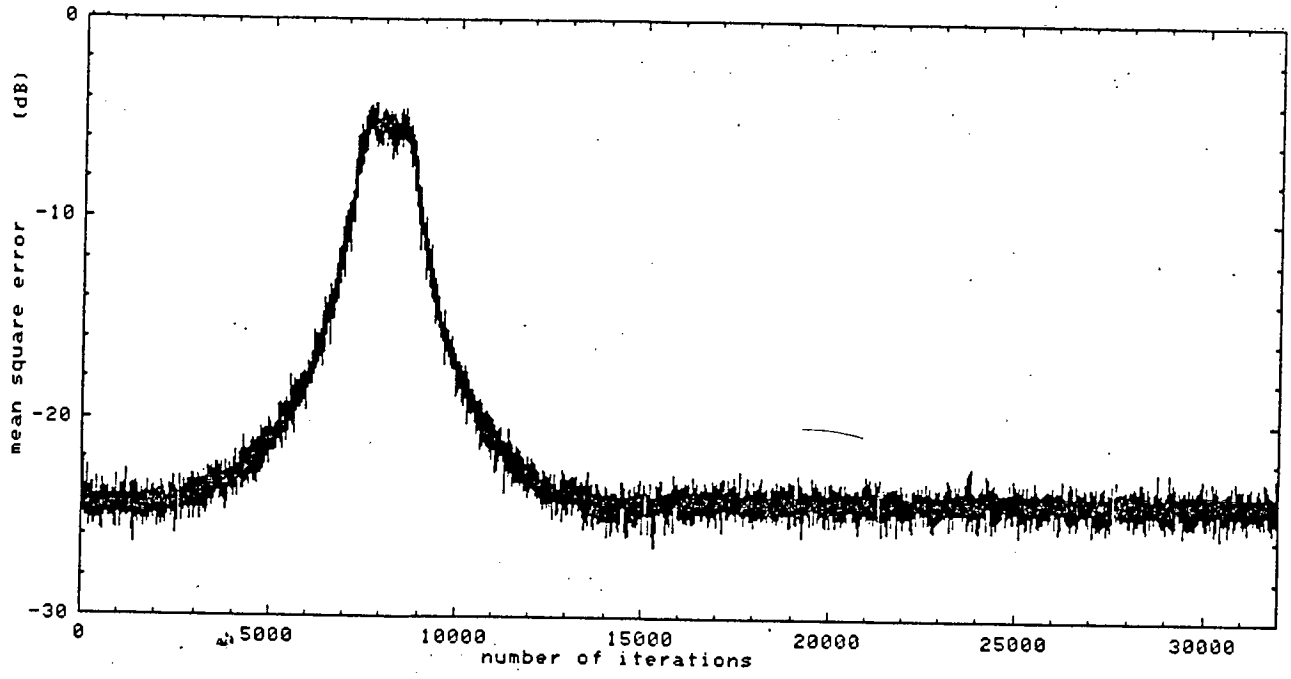

Fig 6.3b Tracking Characteristics for a 5 Tap T-spaced Equalizer with Step Size of 0.020

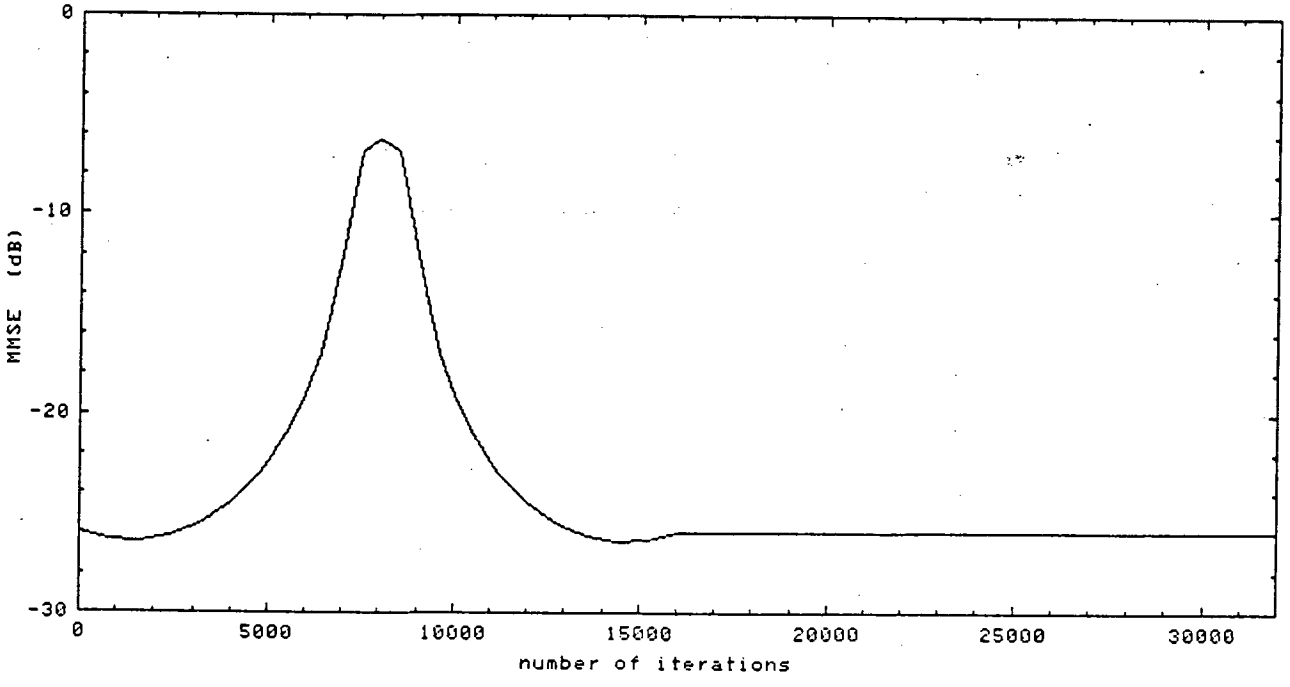

Fig 6.3c Ideal Performance of the 5 Tap T-spaced Equalizer

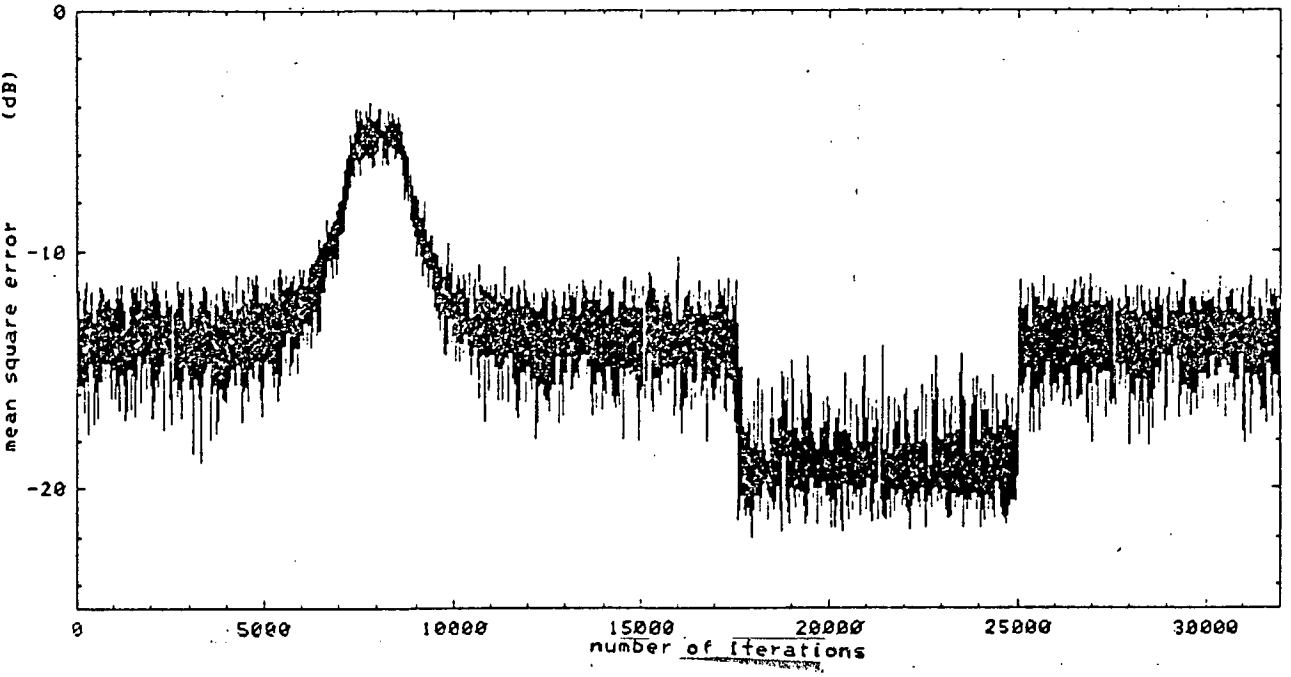

Fig 6.4a Tracking Characteristics for a 5 Tap T-spaced Equalizer with Step Size of 0.040

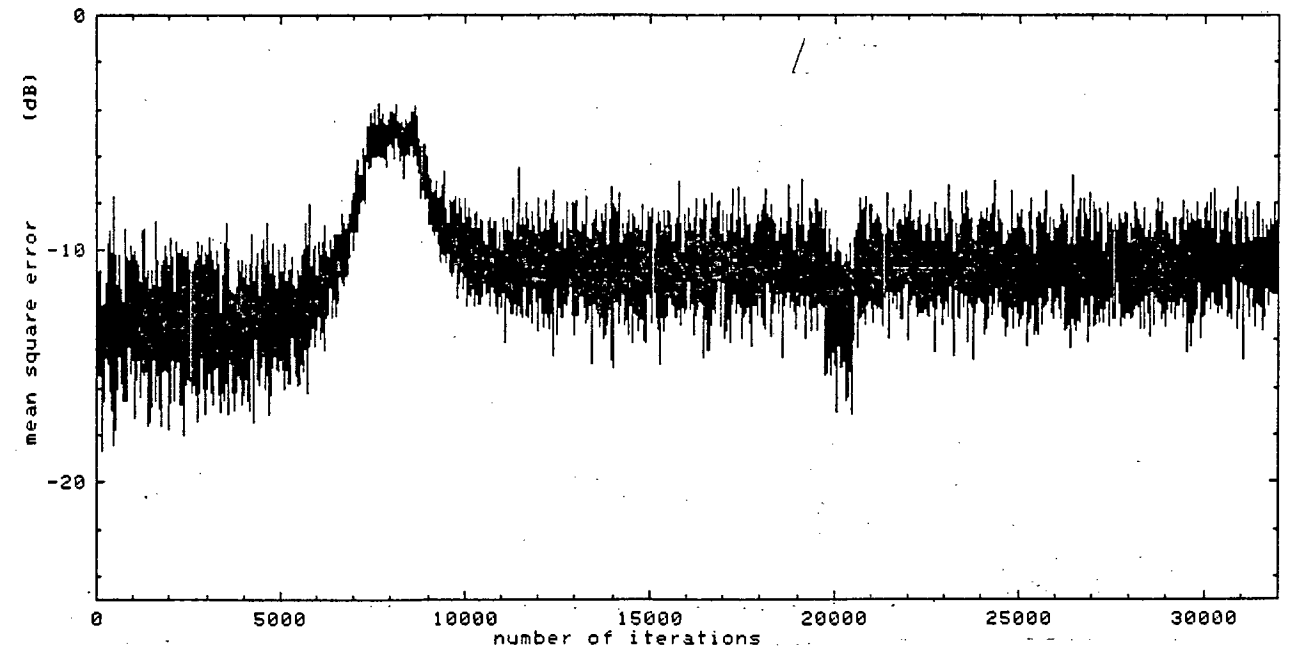

Fig 6.4b Tracking Characteristics for a 5 Tap T-spaced Equalizer with Step Size of 0.040 and different Transmitted Data

It is shown that the curve with small step size cannot track the fast changing channel. However, if the step size is further increased to 0.04,** strange behaviour occurs, as shown in Fig 6.4a,b. Two curves have been plotted with different random number data sequences which are generated by computer, both of them experience a "well" structure but with different positions. This is because some of the twenty ensemble averages have been trapped into a local minimum. The transition instant depends on the sequence of the random data, so the two curves may not be identical.

6.3 Phase Transitions

One of the major problems caused by multipath fading is the phase transition from minimum phase to non-minimum phase as the largest signal changes from the direct to refracted ray or vice versa. Unfortunately this is also a problem for the transversal equalizer. Although the equalizer can track both individual minimum or non-minimum phase conditions very well, it cannot handle the phase transition properly. This is because the phase transition is normally occurs during deep fading. The normal process is as follows:

-- deep fading -- phase transition -- deep fading -- ..

**less than the worst case $0.71u_{max}$ and with the final value of $0.65u_{max}$

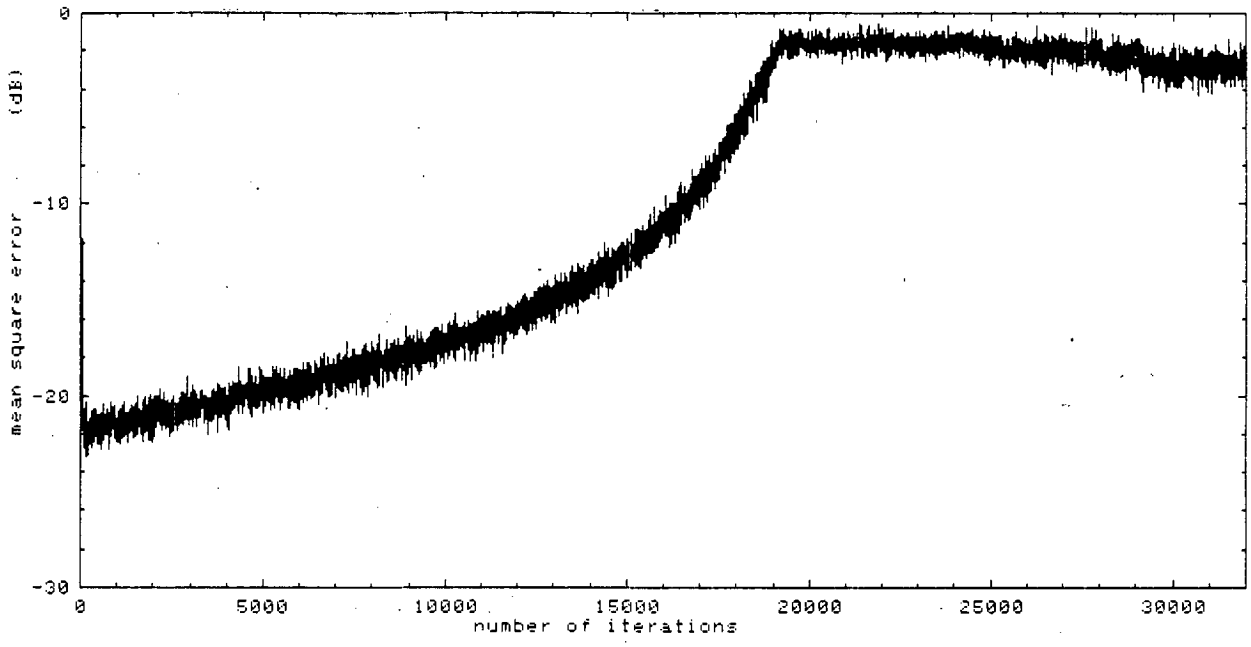

Fig 6.5 Equalizer performace during phase transition

During deep fading or phase transition the equalizer will probably lose track of the channel and converge to a local minimum. Thus even after the fading disappears, the equalizer may not recover. The recovered equalizer may also introduce a constant time or phase offset. The following table is a typical tap weight set for a 5 tap equalizer (T or T/2-spaced) after deep fading or phase transitions:

C-2	C-1	C0	C1	C2
(0,0)	(0,-1)	(0,0)	(0,0)	(0,0)

Table 6.2 One of the Typical Tap Weight Set after deep Fading

Fig 6.5 shows a typical tracking characteristic for a 22.6MHz 16QAM radio system with 5 tap equalizer. The fading channel starts with b=3,** for a delay time of 6ns, fading notch at 60MHz, and changes linearily to b=0, with a delay time of 8ns and fading notch at -20MHz over 30000 iterations. Thus the phase transition occurs at 22500 iterations, with a delay time of 7ns and the notch frequency at 0 MHz. Although the equalizer is still in the decision directed adaptive mode for another 2000 iterations after the fading disappears, it is trapped in a local minimum.

One of the possible methods to overcome this problem is to employ two equalizers. While the first one is tracking for a particular phase condition, the other will operate with the mirror conjugate tap weight, i.e. C_n of the second equalizer equals to C_{-n}^* of the first equalizer. During the phase transition, the first equalizer will be replaced by the second equalizer.

As shown in Appendix 8, $\underline{C}_{opt}$ for the minimum and non- minimum phase channel will be a mirror conjugate pair if

(1) all the other fading parameters except the phase are identical.

(2) the pulse response under no fading condition is symmetric, and there is no cross talk between the I and Q channels.

**b>1 is used to demonstrate the non-minimum phase here

Even the above conditions cannot be fully satisfied in most of the conditions. This approach can provide a better chance of tracking capability during phase transition because the mirror conjugate tap weight will be close to the required tap weight if the above conditions (1) and (2) can be closely met. The major constraint for the hardware implementation is obtaining the correct sampling phase corresponding to the optimum tap weight set.

However, before phase transition, the tap weight of the first equalizer needs to be frozen when the MSE reaches a certain value, this prevents it from trapping into a local minimum. The second equalizer will only start to operate when its error is less than a certain value or when phase transition has been detected by some other mechanism. Additional circuitry will be required to implement these functions.

6.4 Summary

The idea of equalizer gain is proposed to explain the most problematic factor in the decision directed operation -- the existence of local minima. It is found that all such local minima correspond to having an equalizer gain $\leq g' \leq 1$. Thus one of the possible solutions is to use high equalizer gain during the start up conditions or when the equalizer traps into a local minimum. This problem is more serious when high level modulation is employed or the number of equalizer taps increases, as more local minima will be created under such

conditions. Furthermore, it is probably necessary to employ the differential encoding scheme to correct the constant phase offsets which may be introduced in the decision directed operation.

During non-stationary conditions, the choice of the step size is quite crucial. It is shown that with a small step size, the equalizer may lose track of the fading channel. On the other hand if a large step size is used, the equalizer will have a higher chance of being trapped in a local minimum. Since most fading activities are slow varying, e.g. the rate of the fade notch position movement is normally less than 400MHz/s, a small step size can be used if the adaptive rate of the equalizer is fast enough. The optimum approach is to use the average received sample power to adjust the step size such that it is always within a certain range of u'.

Finally, the possibility of using two equalizers to compensate the effect of phase transitions during multipath fading is preliminary investigated and needs to be further examined. This is the progress in the form of a separate PhD programme at the University of Edinburgh.

CHAPTER 7 CONCLUSIONS AND DISCUSSIONS

7.1 Conclusions

The need to use the transversal equalizer to combat multipath fading in LOS digital radio was discussed in chapters 2 and 3. These equalizers are attractive as they can compensate for both minimum and non-minimum phase multipath fades. Appendixes 1 and 8, which use an ideal raised cosine filter, have demonstrated the symmetric characteristics of the signature plot for a 3-ray fade model and the identical behavior of minimum and non-minimum signature plots.

In the chapters that followed, the equalizer response during stationary conditions was first assessed. Various degradations due to finite step size, limited number of quantization levels in the ADC and rounding errors in the arithmetic have all been evaluated. The MMSE degradations resulting from the early termination effect were also investigated. It is found that these degradations are broadly equivalent for both the T-spaced and T/2-spaced equalizers for the same number of taps. Furthermore, the use of an equalizer ensures that there will be no rotation of the constellation.

Based on the above evaluations, it has been shown that the equalizer complexity (i.e. number of taps, arithmetic accuracy .. etc) increases as the number of QAM levels increases. Various signatures have been plotted with

different equalizer lengths, fading parameters and excess bandwidth of raised cosine filters. The required number of quantization levels in the ADC and finite precision arithmetic has been proposed for 4QAM up to 1024QAM T-spaced equalizers. In the T/2-spaced equalizer, the ill-conditioning problem precludes one obtaining a reasonable estimate for the quantization level in the ADC and finite arithmetic. This hinders the widespread usage of the T/2-spaced equalizer in LOS digital radio application.

From the study, it was shown that under ideal conditions with the same number of taps, neither T-spaced nor T/2-spaced structure gives overwhelming performance. The T-spaced structure normally provides superior performance when the notch is near the band-center, but the T/2-spaced structure is better if the notch is near the band-edges. However the overall performance of T/2-spaced structure was usually superior as the excess bandwidth becomes narrow.

According to theoretical study and computer simulations, the effect of demodulation phase was shown to be of minor significance. However, it is the sampling phase that causes most of the problems particularly for the T-spaced equalizer. The maximum power criteria for the sampling phase is proposed for the T-spaced equalizer. The main merit is its independence of the equalizer tap weight values.

Although the T/2-spaced equalizer is inherently less sensitive to sampling phase, it still shows a strong dependence on this parameter, e.g. over 10dB difference in converged MSE is

possible within a 7 tap equalizer design. Furthermore, from the simulations and calculations, it was found that the optimum sampling phase for both equalizer structures may be a few samples away from the original time slot. It has also been shown that there may be up to 10dB difference in MSE between the local minimum with sampling phase near 0^{o} and the global minimum. In the practical environment, this global minimum is difficult to obtain.

Finally, a preliminary investigation was conducted on non-stationary signal conditions. It was found that although a large step size may give better equalizer tracking characteristics [97], it may cause the equalizer to become trapped in a local minimum. One of the possible solutions is to increase the equalizer gain under such conditions. The most problematic behaviour during non-stationary conditions is the phase transition of the fading activities where the equalizer may lose its tracking capabilities. The use of two equalizers seems a possible solution in a theoretical sense. The actual practical implementation needs to be further investigated.

7.2 Validation of Static Signature Plot

Although the number of tap weights, quantization accuracy and the arithmetic precision required for calculations were all based on the static signature plot, this still provides

adequate indication of the likely radio performance under dynamic conditions.

The exact evaluation of the outage improvement factor not only requires a knowledge of the PDF of the fading parameters, but also its dynamic characteristics as well as knowledge of the out-of-synchronism and tracking characteristics of the equalizer. This will involve considerable testing and calculation, but the result may still not be accurate because of the uncertainties involved in atmospheric conditions. Thus an evaluation based on the static signature plot is expected to be of sufficient accuracy for evaluating the relative performance of different equalizer designs.

7.3 Validation of Simulation Assumptions

Apart from the minor error due to computer resolution, the two basic assumptions used in the calculations -- ideal raised cosine filter and a Gaussian type distribution of MMSE, may affect the accuracies of the simulation result when compared with a practical system.

(1) Practical Raised Cosine Filter

All the simulations are based on pulse response of the channel, which is obtained by performing an inverse Fourier transform on H(jw). For an ideal theoretical raised cosine filter, the pulse response is symmetric about its main lobe.

However a practical raised cosine filter has finite group delay and the pre-echo energy is normally less than the post-echo energy. Thus there may be an over estimation of the effects of the pre-echoes. The amount depends on the filter characteristics and channel parameters. For less than 30dB fades, 1 or 2 dB error on the upper portion of the signature plot is quite common when the pre-echo distortion dominates.

(2) Bounded Mean Square Error

The signature plot is based on a MMSE of -6.6dB and -6.3dB for 16QAM and 64QAM respectively, which corresponds to a BER of 10^{-3}. However, this is based on a Gaussian distribution. The MMSE of the equalizer output is bounded and its PDF is not exactly equal to a Gaussian type distribution. Nevertheless, the error in the signature plot will decrease as the number of QAM level increases. The error magnitude may be up to 1dB for 16QAM and is normally less than 1dB as the number of modulation levels increases beyond 16.

7.4 Adaptive Algorithm Implementation

After careful examination of the gradient estimate adaptive algorithm, one can deduce that there is neither a restriction to update all the tap weights in a single iteration nor to update at every symbol period. In other words, unlike the equalizer output, the tap weight updating algorithm need not necessarily be performed in real time. Thus the tap weight

updating can be performed on a single tap or block mode (or a combination of both).

In the former case, the tap weight updating is performed cyclically over all the equalizer tap weights. For the latter case, instead of updating at the symbol rate, updates can be calculated on a block of data samples, and loaded into the taps after the adaptive algorithm has completed the calculation of new weight values.

These techniques may ease the hardware/software design requirements for the high frequency equalizer application, at the expense of convergence rate. However, this is considered to be acceptable since the typical fading rate is less than 400dB/sec or 400MHz/sec, which is slow compared to the symbol rate.

7.5 The Application of the Cross Polarization Canceller

With the increase in modulation complexity, the effect of cross polar distortion becomes significant when dual polarization techniques are used to further increase the bandwidth efficiency or bits/s/Hz of the radio. This appears to be one of the major degradation factors after multipath fading. Cross polar distortion becomes more serious if:

(1) one of the polarization channels suffers severe multipath fading

(2) a high frequency band, e.g. 18GHz, is used where the cross polar distortion due to hydrometeors starts to be significant. Due to congestion in the low frequency bands, the use of high frequency bands is expected to become increasingly popular in the future.

The transversal equalizer structure can also be used as an interference canceller for such application. It is anticipated that this type of canceller will become essential equipment for high capacity radio links in the next decade.

7.6 Future Research

Apart from the ill-conditioning problem in the T/2-spaced equalizer, there are two major areas of possible future reserch -- sampling phase and non-stationary conditions, which are worthy of further investigation.

(1) Sampling Phase

(A) Sampling Phase Criteria for the T/2-spaced Equalizer

Although the T/2-spaced equalizer is inherently less sensitive to sampling phase, it has been shown in chapter 5 that some criterion to determine the receiver sampling phase is required if high performance has to be achieved. However care should be taken when it is linked to with the tap weight

updating algorithm, because of the possibility of creating dead zone, instabilities .. etc. This subject is now the subject of a separate PhD thesis programme in the Department.

(B) Global Minimum

It has been shown in chapters 4 and 5 that the global minimum may be a few samples away from the original time slot and there may exist local minima which are ~360° apart. This global minimum is difficult to obtain particularly when the fading is non-stationary. One of the possible solutions is to use two equalizers with the second one operating at ~360° or ~-360° away from the main one. The switch over between the two equalizers will occur if the performance of the second equalizer is superior.

(2) Non-stationary Conditions

(A) The Choice of the Step Size

As shown in chapter 6, the tracking of a fading channel not only depends on the step size but also on the equalizer gain. Although most of the fading is slow varying and a small step size can be used, the relationship between the optimum step size and the equalizer gain is still worthy of investigation if fast tracking is desirable.

(B) Phase Transitions during Multipath Fading

As described in chapter 6, one of the possible method to

combat the phase transitions problem during multipath fading is to employ two equalizers. The optimum instant to freeze the tap weight value and switch over between the two equalizers thus requires to be investigated. Furthermore, the method of providing the correct sampling phase after the phase transition also needs to be resolved before the design is implemented.

An alternative solution is to use some techniques which combines of the two diversity signals, e.g. maximum power. Since only one of the diversity signals experiences deep fading or phase transitions during most of the multipath activities, the abrupt change of group delay distortion pattern during phase transitions is avoided at the combiner output and the equalizer will give a better tracking characteristic. The equalizer response with different combining techniques also needs to be further examined.

References

[1] K. Kobayashi, " The Past, Present, and Furure of Telecommunications in Japan," IEEE Comm. Magazine, Vol 22, No 5, pp 96-103, May 1984.

[2] Y. Saito, S. Komaki, M. Murotani, " Feasibility considerations of High-Level QAM Multi-Carrier System," IEEE Int. on Comm. 84, 22.8, pp 665-671.

[3] T. Noguchi et al. " 6 GHz 135MBPS Digital Radio System with 64 QAM Modulation," IEEE Int. Conf. on Comm. 83, F2.4, pp 1431-1435.

[4] " CCIR News -- Interim meeting of Study Group 9, " Telecommunication Journal, Vol 51, pp 491-493, Sept 84.

[5] Federal Communications Commission, " Rules and Regulations, Part 21 -- Domestic Public Fixed Radio Services," Sept 1982.

[6] W.H. Bellchambers et al., " The International Telecommunication Union and Development of Worldwide Telecommunications," IEEE Comm. Magazine, Vol 22, No 5, pp 72-83, May 1984.

[7] M.B. Williams, " International standards for telecommunications," Telecommunications in the 1980s and after, The Royal Society of London, pp 185-205, 1977.

[8] F. Molina Negro, J.M. Novillo-Fertrell, Y. Paredes, " The International Telecommunication Convention from Madrid (1932) to Nairobi (1982): half a century in the life of the Union," Telecommunication Journal, Vol 49, pp 814-818, Dec 1982.

[9] CCIR Rec. 283-4, " Radio-frequency channel arrangement for analogue radio-relay systems with a capacity of 60, 120, 300 and up to 960 telephone channels or low and medium capacity digital systems of equivalent RF bandwidth operating in the 2 GHz band "

[10] CCIR Rec. 382-3, " Radio-frequency channel arrangements for radio-relay systems for television and telephony for 600 and 1800 telephone channels, or the equivalent, operating in the 2 and 4 GHz bands or for medium-capacity digital radio-relay systems operating in the 4 GHz band "

[11] CCIR Rec. 384-3, " Radio-frequency channel arrangements for analogue radio-relay systems with a capacity of 2700 telephone channels or up to 1260 telephone channels, or the equivalent, and digital radio-relay systems with a capacity of the order of 140 Mb/s, operating in the 6 GHz band "

[12] CCIR Rec. 387-3, " Radio-frequency channel arrangements for analogue television and teleophony radio-relay systems with a capacity of 600 to 1800 telephone channels, or the equivalent, or low and medium-capacity digital systems of equivalent bandwidth, operating in the 11 GHz band "

[13] CCIR Rec. 497-2, " Radio-frequency channel arrangements for analogue radio-relay systems for television and FDM telephony with a capacity of 960 telephone channels or the equivalent and for medium capacity digital systems operating in the 13 GHz band "

[14] CCIR Rec. 595, " Radio-frequency channel arrangements for digital radio-relay systems in the 17.7 to 19.7 GHz frequency band "

[15] CCIR Rec. 594, " Allowable bit error ratio at the output of the hypothethical reference digital path for radio-relay systems for telephony "

[16] CCIR Report 930, " Performance objectives for digital radio-relay systems "

[17] Bell Pub 43501, " 6 GHz Digital Radio Requirements and Objectives," Dec 1980.

[18] Bell Pub 43502, " 11 GHz Digital Radio Requirements and Objectives," Dec 1982.

[19] P. Cochrane, " Future trends in telecommunications transmission -- a personal view," Proc. IEE, Vol 131, Pt. F, No 7, pp 669-683, Dec 1984.

[20] C.W. Broderick, R.W. Gutshall, " A 20 Mb/s Digital Terminal for TD2 Radio," IEEE Int. Conf. on Comm. 69, pp27.21-26.

[21] S. Pasupathy, " Minimum Shift Keying; A spectrally efficient Modulation," IEEE Comm. Magazine, Vol 17, No 4, pp 12-22, Jul 1979.

[22] CCITT yellow book, Rec. V.23, " 600/1200-baud modem standardized for use in the general switched telephone network "

[23] S.Tackenaka et al., " A New 4 GHz 90 Mbps Digital Radio system using 64-QAM Modulation," IEEE Int. on Comm. 84, 22.3, pp 642-645.

[24] T. Shimamura, S. Kitazume, S. Seki, " 400mb repeater using a modified Costa carrier tracking loops for millimetric waveguide transmission system," IEE Int. Conf. on Millimetric Waveguide Systems, Nov 1976.

[25] S.A. Rhodes, " Effect of Noisy Phase Reference on Coherent Detection of Offset-QPSK Signals," IEEE Trans. on Comm., Vol COM-22, No 8, pp 1046-1055, Aug 1974.

[26] D.H. Morais, A. Sewerinson, K. Feher, " The Effects of the Amplitude and Delay Slope Components of Frequency Selective Fading on QPSK, Offset QPSK and 8 PSK Systems," IEEE Trans. on Comm., Vol COM-27, No 12, pp 1849-1853, Dec 1979.

[27] L. Greenstein, B.A. Czekaj, " Performance Comparison Among Digital Radio Techniques Subjected to Multipath Fading," IEEE Int. Conf. on Comm. 81, 12.1.1-6.

[28] W.J. Weber et al. " A Bandwidth Compressive Modulation System Using Multi-Amplitude Minimum Shift Keying (MAMSK)," IEEE Trans. on Comm., Vol COM-26, No 5, pp 543-551, May 1978.

[29] M.J. O'Mahony, " Combined Frequency and Phase-Shift Keying," Electronics Letters, Vol 12, No 21, pp 550-551, 14 Oct 76.

[30] H. Ishio et al. " A New Multilevel Modulation and Demodulation System for Carrier Digital Transmission," IEEE Int. on Comm. 76, pp29.7-12.

[31] D.P. Taylor, K.S. Yeung, " Conceptual Design of a Four Bits/Hz Radio System," IEEE Int. Conf. on Comm. 79, 5.8.1-5.

[32] P. Hervieux, " RD-3: an 8 GHz digital radio system for Canada," Telesis, Vol 4, pp 53-59, Summer 1975.

[33] J.K. Chamberlain, F.M. Clayton, P.V. Collin, " Reduced Bandwidth Quaternary Phase-Shift-Keying (RBQPSK) -- An Evolutionary Approach to Bandwidth Efficient Digital Microwave Transmission," 1980 Int. Zurich Seminar on Digital Communications, paper A.3.1-6.

[34] N.T. Dudek, J.M. Robinson, " A Decision Feedback Equaliser and Novel Carrier Recovery Circuit for Digital Radio Relay Systems Operating at up to 5 bit/Hz," IEEE Int. on Comm. 80, 41.5.1-6.

[35] CCIR Report 934, " Radio-frequency channel arrangements for high and medium-high capacity digital radio-relay systems operating in the frequency bands below about 10 GHz "

[36] CCIR Rec. 383-2, " Radio-frequency channel arrangements, for systems having a capacity of 1800 telephone channels, or the equivalent, operating in the 6 GHz band "

[37] " MSN Microwave Radio System Matrix," Microwave Systems News, Vol 10, No 6, pp 91-108, Jun 1980.

[38] V.K. Prabhu, J. Salz, " On the Performance of Phase-Shift-Keying Systems," Bell System Tech. J., Vol 60, No 10, pp 2307-2343, Dec 1981.

[39] I. Godier, " DRS Digital Radio for Long-Haul Transmission," IEEE Int. Conf. on Comm. 77, pp5.4.102-105.

[40] C.W. Anderson and S.G. Barber, " Modulation Considerations for a 91 Mbit/s Digital Radio," IEEE Trans. on Comm., Vol COM-26, No 5, pp 523-528, May 1978.

[41] CCITT yellow book, Rec. V.29, " 9600 bits per second modem standardized for used on point-to-point 4-wire leased telephone-type circuits "

[42] G.J. Foschini, R.D. Gitlin, S.B. Weinstein, " Optimization of Two-Dimensional Signal Constellations in the Presence of Gaussian Noise," IEEE Trans. on Comm., Vol COM-22, No 1, pp 28-38, Jan 1974.

[43] CCIR Rec. 338-4, " Propagation Data Required for Line-of-Sight Radio-Relay Systems "

[44] T.P. Murphy et al., " Practical Techniques for Improving Signal Robustness," National Telecomm. Conf. 81, C3.3.1-7.

[45] P.F. Panter, " Communication system Design, Line-of-sight and Tropo-scatter Systems," McGraw-Hill Book Company, 1972.

[46] CCIR Rec. 453, " The formula for the radio refractive index"

[47] A.B. Crawford, W.C. Jakes, " Selective Fading of Microwaves " Bell System Tech. J., Vol 31, No 1, pp 68-90, Jan 1952.

[48] O.E. DeLange, " Propagation Studies at Microwave Frequencies by Means of Very Short Pulses," Bell System Tech. J., Vol 31, No 1, pp 91-103, Jan 1952.

[49] C.L. Ruthroff, " Multiple-Path Fading on Line-of-Sight Microwave Radio Systems as a Function of Path Length and Frequency," Bell System Tech. J., Vol 50, No 7, pp 2375-2398, Sept 1971.

[50] A.J. Giger, W.T. Barnett, " Effects of Multipath Propagation on Digital Radio," 1980 Int. Zurich Seminar on Digital Communications, paper D.2.1-5.

[51] G. Hart et al., " Practical results from the performance evaluation of an 11 GHz 140 Mbit/s digital radio relay system," The Radio and Electronic Engineer, Vol 53, No 5, pp 181-189, May 1983.

[52] C.W. Anderson, S.G. Barber, R.N. Patel, " The Effect of Selective Fading on Digital Radio," IEEE Trans. on Comm., Vol COM-27, No 12, pp 1870-1876, Dec 1979.

[53] CCIR Rec. 338-4, " Propagation data required for line-of sight radio-relay systems "

[54] S.H. Lin, " Impact of Microwave Depolarization During Multipath Fading on Digital Radio Performance," Bell System Tech. J., Vol 56, No 5, pp 645-674, May 1977.

[55] CCIR Rec. 722-1, " Cross-polarization due to the atmosphere"

[56] W.D. Rummler, " A Multipath Channel Model for Line-of-Sight Digital Radio Systems," IEEE Int. Conf. on Comm. 78, 47.5.1-4.

[57] W.D. Rummler, " A New Selective Fading Model: Application to Propagation Data," Bell System Tech. J., Vol 58, No 5, pp 1037-1071, May-Jun 1979.

[58] S. Komaki et al., " Characteristics of a High Capacity 16 QAM Digital Radio System in Multipath Fading," IEEE Trans. on Comm., Vol COM-27, No 12, pp 1854-1861, Dec 1979.

[59] L.J. Greenstein, " A Multipath Fading Channel Model for Terrestrial Digital Radio Systems," IEEE Trans. on Comm., Vol COM-26, No 8, pp 1247-1250, Aug 1978.

[60] CCIR Report 721-1, " Attentuation by hydrometeors, in particular precipitation, and other atmospheric particles "

[61] S.H. Lin, " Nationwide Long-Term Rain Rate Statistics and Empirical Calculation of 11-GHZ Microwave Attentuation, " Bell System Tech. J., Vol 56, No 9, pp 1581-1604, Nov 1977.

[62] J.A. Garcia-Lopez, J. Peiro, " Simple Rain-Attentuation- Prediction Technique for Terrestrial Radio Links," Electronics Letters, Vol 19, No 21, pp 879-880, 13 Oct 1983.

[63] R.L.O. Tattersall, " Snow Fading on 1 March 1974 on microwave Links in the Mendlesham propagation experiment," Electronics Letters, Vol 11, No 24, pp 603-605, 27 Nov 1975.

[64] W.D. Rummler, " A comparison of calculated and observed performance of digital radio in the presence of interference," IEEE Int. Conf. on Comm. 81, 68.1.1-5.

[65] K. Nakamura, " A Class of Error Correcting Codes for DPSK Channels," IEEE Int. Conf. on Comm. 79, 45.3.1-5.

[66] Y. Nakamura, Y. Saito, S. Aikawa, " 256QAM Modem for Multicarrier 400 Mb/s digital Radio," IEEE J. on Selected Area in Comm., Vol SAC-5, No 3, pp 329-335, Apr 1987.

[67] Y. Aono, " Cross Polarization Interference Canceler for High Capacity Digital Radio System," IEEE Int. Conf. on Comm. 85, 39.5, pp 1254-1258.

[68] P.L. Dirner, S.H. Lin, " Measured Frequency Diversity Improvement for Digital Radio," IEEE Trans. on Comm., Vol COM-33, No 1, pp 106-109, Jan 1985.

[69] A. Vigants, M.V. Pursley, " Transmission Unavailability of Frequency-Diversity Protected Microwave FM Radio Systems caused by Multipath Fading," Bell System Tech. J., Vol 58, No 8, pp 1779-1796, Oct 1979.

[70] J.M. Robinson, A.J. Pate, J.K. Chamberlain, " An electronic diversity combining system for use in terrestrial radio relay systems," IEE Conf. Pub. No 193, pp 233-237, 1981.

[71] L. Lewin, " Diversity Reception and Automatic Phase Correction," Proc. IEE, Vol 109, Pt. B, No 46, Jul 1962.

[72] H. Matsue, H. Ohtsuka, T. Murase, " Digitized Cross-Pol Canceller for Microwave Radio Systems," IEEE J. on Selected Area in Comm., Vol SAC-5, No 3, pp 493-501, Apr 1987.

[73] S. Komaki, Y. Okamato, K. Tajima, " Performance of 16-QAM Digital Radio using new Space Diversity," IEEE Int. on Comm. 80, 52.2.1-6.

[74] K. Feher, " Digital Communication, microwave application," Prentice-Hall Inc., 1981.

[75] P. Hartmann, E.W. Allen, " An Adaptive Equalize for correction of Multipath Distortion in a 90MB/s 8PSK system," IEEE Int. Conf. on Comm. 79, 5.6.1-4.

[76] T.P. Murphy, J.W. Thielen, " Adaptive Equalizer Finds Application In Digital Microwave Transmission," MSN, pp 48-54, Jan 1984.

[77] Y.Y Wang, " Space Diversity Combining for 6GHz Digital Radio," IEEE Int. Conf. on Comm. 79, 48.2.1-6.

[78] T.S. Giuffrida, " Measurements of the Effects of Propagation on Digital Radio Systems Equipped with Space Diversity and Adaptive Equalization," IEEE Int. Conf. on Comm. 79, 48.1.1-6.

[79] " Adaptive Equalization," GTE Lenkurt Demodulator, Vol 30, No 5, pp 2-11, Sep/Oct 1981.

[80] R.D. Gitlin, S.B. Weinstein, " Fractionally-spaced-equalisation, an improved digital transversal equaliser," Bell System Tech. J., Vol 60, No 2, pp 275-296, Feb 1981.

[81] R.D. Gitlin, H.C. Meadors, S.B. Weinstein, " The tap-leakage algorithm for the stable operation of a digitally implemented fractionally spaced, adaptive equaliser," Bell System Tech. J., Vol 58, No 2, pp 301-321, Feb 1979.

[82] K. Aoki et al., " The Adaptive Transversal Equalizer for 90Mbps 64-QAM Radio Relay System," IEEE Int. on Comm. 84, 32.7, pp 1003-1006.

[83] M.F. Gardina, S.H. Lin, " Measured Performance of Horizontal Space Diversity on a Microwave Radio Path," Globecom 85, 36.6, pp 1104-1107.

[84] S. Komaki et al., " A Minimum Dispersion Combiner for High Capacity Digital Microwave Radio," IEEE Trans. on Comm. COM 32, No 4, pp 419-428, Apr 1984.

[85] C.A. Belfiore, J.H. Park, " Decision Feedback Equalization," IEEE Proc. Vol 67, No 8, pp 1143-1156, Aug 1979.

[86] M. Kavehrad, J. Salz, " Cross-Polarization Cancellation and Equalization in Digital Transmission Over Dually Polarized Multipath Fading Channels," Bell System Tech. J., Vol 64, No 10, pp 2211-2245, Dec 1985.

[87] W.K. Wong, " A Preliminary Study in Line of Sight Digital Radio," an essay to Edinburgh Univ, Oct 1982.

[88] H. Sari, L. Desperben, S. Moridi, " Minimum Mean-Square Error Timing Recovery Scheme for Digital Equalizer," IEEE Trans. on Comm., Vol COMM-34, No 7, pp 694-702, July 1986.

[89] G. Ungerboeck, " Fractional Tap-Spacing Equalizer and Consequences for Clock Recovery in Data Modem," IEEE Trans. on Comm., Vol COMM-24, No 8, pp 856-864, Aug 76.

[90] H.E. Kallmann, " Transversal Filters," Proc. IRE, Vol 28, pp 302-310, Jul 1940.

[91] R.W. Lucky, " Automatic Equalization for Digital Communication," Bell System Tech. J., Vol 44, No 4, pp 547-588, Apr 1965.

[92] H. Kobayashi, " Simultaneous adaptive estimation and decision algorithm for carrier modulated data transmission system," IEEE Trans. on Comm., Vol COMM-19, pp 268-280, June 1971.

[93] R.W. Lucky, J. Salz, E.J. Weldon,Jr., " Principle of Data Communication," McGraw Hill, 1968.

[94] G.L. Fenderson et al., " Adaptive Transversal Equalizer for 90Mb/s 16QAM Systems in the Presence of Multipath Propagation," IEEE Int. Conf. on Comm. 83, C8.7, pp 876-881.

[95] C.P. Bates and M.A. Skinner, " Impact of Technology on High Capacity Digital Radio Systems," IEEE Int. on Comm. 83, F2.3, pp 1478-1483.

[96] B. Widrow and M.E. Hoff, " Adaptive switching circuit," 1960 WESCON Conv. Rec., pt 4.

[97] B. Widrow et al., " Stationary and Nonstationary Learning Characteristics of the LMS Adaptive Filter," Proc. IEEE Vol 64, No 4, pp 1151-1162, Aug 1976.

[98] R.D. Gitlin and Weinstein, " On the Request Tap-Weight Precision for Digitally Implemented, Adaptive Mean-Squared Equalizers," Bell System Tech. J., Vol 58, No 2, pp 301-321, Feb 1979.

[99] J.E. Mazo, " On the Independence Theory of Equalizer Convergence," Bell System Tech. J., Vol 58, No 5, pp 963-993, May-Jun 1979.

[100] B. Widrow et al., " Adaptive Noise Cancelling: Principles and Applications," Proc. IEEE, Vol 63, No 12, pp 1692-1716, Dec 1975.

[101] M. Schwartz, L. Shaw, " Signal Processing: Discrete Spectral Analysis Detection and Estimation," McGraw-Hill, 1981.

[102] J.E. Mazo, " Optimum Timing Phase for an infinite Equalizer," Bell System Tech. J., Vol 54, No 1, pp 189-201, Jan 1975.

[103] S.U.H. Qureshi, G.D. Forney,Jr., " Performance and Properties of T/2 Equalizer," National Telecomm. Conf. 77, paper 11.1-1 to 11.1-9.

[104] W.K. Wong et al., " Adaptive transversal filters for multipath compensation," IEEE Int. Conf. on Comm. 84, 32.4, pp 989-992.

[105] R.D. Gitlin, S.B. Weinstein, " Fractional Spaced Equalization: An improved Digital Transversal Equalizer," Bell System Tech. J., Vol 60, No 2, pp 275-296, Feb 81.

[106] R.D. Gitlin, H.C. Meadors, S.B. Weinstein, " The Tap-Leakage Algorithm: An Algorithm for the Stable Operation of a Digitally Implemented, Fractionally Spaced, Adaptive Equalizer," Bell System Tech. J., Vol 61, No 8, pp 1817-1839, Oct 82.

[107] K.H. Mueller, M. Muller, " Timing Recovery in Data Receivers," IEEE Trans. on Comm., Vol COMM-24, No 5, pp 516-531, May 1976.

Appendix 1 The Proof of the Symmetric Characteristics of the Signature Plot for a 3-ray Model

Let us consider the minimum phase fade only, the non-minimum phase fade will be identical. The pulse response of the overall channel with sampling phase Ø and fading parameters a, b and w_o is:**

$$P^{\emptyset}_{(a,b,w_o)}(t) = \mathcal{F}^{-1}\{T(jw)R(jw)a[1-b\exp(-jwT_d+jw_oT_d)]\exp(-jw\tau)\}$$

where $\mathcal{F}^{-1}$ is the inverse Fourier transform, T(jw) and R(jw) are the equivalent baseband pulse response of transmitter and receiver respectively, and τ is the sampling phase in terms of symbol period, i.e. $\tau = T\emptyset/360$.

$$= -ab[\exp(jw_oT_d)]\mathcal{F}^{-1}\{T(jw)R(jw)\exp[-jw(T_d+\tau)]\} + a\mathcal{F}^{-1}[T(jw)R(jw)\exp(-jw\tau)]$$

$$= -ab[\exp(jw_oT_d)P^{0}_{(0,0,0)}(t-T_d-\tau)] + a[P^{0}_{(0,0,0)}(t-\tau)] \quad \ldots\ldots\ldots\ldots\ldots\ldots\ldots \text{(A1.1)}$$

where $P^{0}_{(0,0,0)}(t)$ is the pulse response of the overall channel with fading parameters a=0, b=0 and w_o=0, i.e. without multipath fading. Similarly, the pulse response with fading parameters a, b and $-w_o$ will be:

$$P^{\emptyset}_{(a,b,-w_o)}(t) = -ab[\exp(-jw_oT_d)P^{0}_{(0,0,0)}(t-T_d-\tau)] + a[P^{0}_{(0,0,0)}(t-\tau)] \quad \ldots\ldots\ldots\ldots\ldots \text{(A1.2)}$$

**the effect of demodulation phase is not considered here because of its insignificant effect.

For a random data input, the overall degradation due to ISI in each of these two cases will be equivalent, if the following expressions are satisfied:

$$|\text{Real } P^{\emptyset}_{(a,b,w_o)}(t)| = |\text{Real } P^{\emptyset}_{(a,b,-w_o)}(t)| \quad \ldots \quad (A1.3)$$

and $$|\text{Img } P^{\emptyset}_{(a,b,w_o)}(t)| = |\text{Img } P^{\emptyset}_{(a,b,-w_o)}(t)| \quad \ldots\ldots \quad (A1.4)$$

Equations (A1.3) and (A1.4) will be true if and only if :

$$|\text{Img } P^{0}_{(0,0,0)}(t-T_d-\tau)| = 0 \quad \ldots\ldots\ldots\ldots\ldots\ldots \quad (A1.5)$$

or $$|\text{Real } P^{0}_{(0,0,0)}(t-T_d-\tau)| = 0 \quad \ldots\ldots\ldots\ldots\ldots\ldots \quad (A1.6)$$

Basically, equations (A1.5) and (A1.6) are equivalent since there is only a 90^{o} phase shift between them. Thus, the signature plot for a 3-ray model will be symmetric about its center frequency if $|\text{Img } P^{0}_{(0,0,0)}(t-T_d-\tau)| = 0$.

Appendix 2 The Program for Calculating the BER from C/N

```
 100 REM This program will calculate the BER for QAM radio
 110 REM    with C/N input
 120 REM For X<2.75, the exponential function is expanded
 130 REM and 30 terms are taken to give good estimated
 140 REM longreal is used for the accuracies proposes
 150 REM For X>2.5, then integral is done by parts for five times
 160 REM
 170 REM Gray code is used and one symbol
 180 REM error will cause only one bit error is assumed
 190 REM So the result may not very accuracy for BER<10**-2
 200 REM
 210 REM          REV:00            16 DEC 84
 220 REM
 300 LONG Q,R,S,T
 310 INTEGER I,J
 320 DIM P$[10]
1000 PRINT "Type 1 for QPSK, 2 for 16QAM, 3 for 64QAM, 4 for 256QAM";
1010 PRINT "     otherwise 1024QAM will be used";
1020 INPUT P$
1030 A1=682,A2=31/32,A3=10
1040 IF P$="1" THEN A1=2,A2=1/2,A3=2
1050 IF P$="2" THEN A1=10,A2=3/4,A3=4
1060 IF P$="3" THEN A1=42,A2=7/8,A3=6
1070 IF P$="4" THEN A1=170,A2=15/16,A3=8
1080 PRINT "C/N =";
1090 INPUT X
1100 X=10**((X-10*LOG(A1)/LOG(10))/20)
1110 S=X
1120 IF X>=2.5 THEN 1330
1130 REM Do the expanded series here
1140 N=30
1150 IF X<.2 THEN N=15
1160 IF X<.1 THEN N=5
1170 IF X<.01 THEN N=1
1180 IF X<.000001 THEN X=0
1190 FOR I=1 TO N
1200   T=(-1)**I/(2*I+1)
1210   REM direct evaluate x**(2*i+1) is not accurate
1220   FOR J=1 TO 2*I+1
1230     T=T*X
1240   NEXT J
1250   Q=1
1260   FOR J=1 TO I
1270     Q=Q*J
1280   NEXT J
1290   S=S+T/Q
1300 NEXT I
1310 R=1-2*S/SQR(PIX(1))
1320 GOTO 1400
1330 REM Use different algorithm for x>2.75
1340 T=(1/2-1/(4*X*X)+3/(8*X*X*X*X)-15/(16*X**6)+105/(32*X**8))/X
1350 T=T*2*EXP(-X*X)/SQR(PIX(1))
1360 R=T
1370 IF R>1E-18 THEN 1400
1380 P=R
1390 GOTO 1410
1400 P=1-(1-R*A2)**2
1410 PRINT "BER =";P/A3
9999 END
```

Appendix 3 The Derivation of Equation (4.13)

Substituting equation (4.11) into (4.12), the MSE at iteration l+1 will be:

$$\xi_{min} + E\langle \sum_{i=-N}^{N} (C_i - C_i')^* Q_i^* \sum_{j=-N}^{N} Q_j (C_j - C_j') \rangle$$

$$+ u^2 E\langle \sum_{i=-N}^{N} e_l^* Q_i Q_i^* \sum_{j=-N}^{N} Q_j Q_j^* e_l \rangle$$

$$- u E\langle \sum_{i=-N}^{N} e_l^* Q_i Q_i^* \sum_{j=-N}^{N} Q_j (C_j - C_j') \rangle$$

$$- u E\langle \sum_{i=-N}^{N} (C_i - C_i')^* Q_i^* \sum_{i=-N}^{N} Q_j Q_j^* e_l \rangle$$

The sum of the first two terms is equal to $|e_l|^2$. The fourth and fifth terms can be represented as:

$$- u E\langle e_l^* (e_l - e_{min}) \sum_{i=-N}^{N} Q_i Q_i^* \rangle$$

$$= - u E\langle |e_l|^2 \sum_{i=-N}^{N} Q_i Q_i^* \rangle + u E\langle e_l^* e_{min} \sum_{i=-N}^{N} Q_i Q_i^* \rangle$$

and

$$- u E\langle e_l (e_l^* - e_{min}^*) \sum_{j=-N}^{N} Q_j Q_j^* \rangle$$

$$= - u E\langle |e_l|^2 \sum_{j=-N}^{N} Q_j Q_j^* \rangle + u E\langle e_l e_{min}^* \sum_{j=-N}^{N} Q_j Q_j^* \rangle$$

So the MSE at iteration l+1 is:

$$E\langle |e_{l+1}|^2 \rangle = E\langle |e_l|^2 [1 - u(\sum_{i=-N}^{N} Q_i Q_i^*)]^2 \rangle +$$

$$E\langle u(\sum_{i=-N}^{N} Q_i Q_i^*)(e_{min} e_l^* + e_l e_{min}^*) \rangle$$

Appendix 4 The Accuracies of all the Calculations and Simulations

HP3000 computer is used with BASIC language. There are two main programs -- "MMSECALC" and "EQUALIZE", written for the thesis. The "MMSECALC" is used for all the theoretical MMSE evaluations. There are three levels of accuracies as follows:

accuracy	no of points in Fast Fouier Transform for pulse evaluation	no of pre-echoes and post-echoes used
low	64	both 7
medium	128	both 10
high	256	both 14

and 2 points/symbol is used for all the cases.

The "EQUALIZE" is used for the MSE convergence and MMSE simulation. There are also three levels of accuracies as follows:

accuracy	no of points in Fast Fouier Transform for pulse evaluation	no of pre-echoes and post-echoes used
low	32	both 6
medium	64	both 9
high	128	both 12

and 2 points/symbol is used for all the cases.

The following definitions are used throughout the thesis:

(1) Sampling Phase

All the sampling phase is optimized for minimizing the MSE unless otherwise specified.

(2) Demodulation Phase

All the demodulation phase is chosen such that there is no cross talk at time slot zero.

(3) MMSE and B value Calculations

"MMSE" with high resolution is used.

(4) MMSE and $E\langle|e_{final}|^2\rangle$ Simulations

"EQUALIZE" with high accuracy is used. The result is otained by averaging the last 50 iterations after the MSE converge to its final value and with an ensemble average of 100 runs

(5) $E\langle|e_{early}|^2\rangle$ Simulation

"EQUALIZE" with medium accuracy is used. The result is obtained by averaging of the last 1000 iterations after the MSE converge to its final value and with an ensemble average of 20 runs.

(6) MSE Convergence Plot

(A) Stationary or Abrupt change of the Channel

Medium accuracy is used in "EQUALIZE" and with an ensemble average of 100 runs.

(B) Slow Varying Channel

Low accuracy is used in "EQUALIZE" and with an ensemble average of 20 runs.

Appendix 5 The Derivation of the Step Size Corresponding to Maximum Convergence Rate of MSE

During start up conditions, $|e_l| >> |e_{min}|$, so the following can be obtained from equation (4.13):

$$E\langle|e_{l+1}|^2\rangle \sim E\langle|e_l|^2[1-u(\sum_{i=-N}^{N} Q_iQ_i^*)^2\rangle \quad \text{..... (A5.1)}$$

The MSE convergence rate will be maximum if:

$$\frac{\partial E\langle|e_{l+1}|^2\rangle}{\partial u} = \frac{\partial E\langle|e_l|^2\rangle}{\partial u} = 0 \quad \text{..... (A5.2)}$$

let $E\langle|e_l|^2[1-u(\sum_{i=-N}^{N} Q_iQ_i^*)]^2\rangle$

$$= \gamma_l E\langle|e_l|^2\rangle E\langle[1-u(\sum_{i=-N}^{N} Q_iQ_i^*)]^2\rangle \quad \text{..... (A5.3)}$$

where $\gamma_l \sim 1$, is the correlation factor which depends on the number of taps and tap weights. The dependency of γ_l to u is small and can be negligible, i.e. $\partial\gamma_l / \partial u = 0$. After differentiating equation (A5.1) with respect to step size u, the following can be obtained:

$$-2\gamma_l E\langle|e_l|^2\rangle E\langle[\sum_{i=-N}^{N} Q_iQ_i^* - u(\sum_{i=-N}^{N} Q_iQ_i^*)^2]\rangle = 0 \quad \text{..... (A5.4)}$$

$E\langle(\sum_{i=-N}^{N} Q_iQ_i^*)^2\rangle \sim [E\langle(\sum_{i=-N}^{N} Q_iQ_i^*)\rangle]^2$ if $(2N+1) > 5$ and

$\mathcal{E}_{min}/E\langle A_kA_k\rangle$ less than -20dB,

$$\text{i.e. } u \sim \frac{1}{\sum_{i=-N}^{N} Q_iQ_i^*}$$

Appendix 6 The Derivation of the Quantization Noise due to ADC

Since the real and imaginary part of x_j are uncorrelated, i.e.

$$E\langle x_j x_j^* \rangle = E\langle |\text{real } x_j|^2 \rangle + E\langle |\text{img } x_j|^2 \rangle \quad \ldots\ldots\ldots\ldots \text{(A6.1)}$$

Let us consider $E\langle |\text{real } x_j|^2 \rangle$ first. From assumption (2) in page 94, the signal is evenly distributed for each quantization level, so the PDF of x_j is $1/z$, where $z=2(2L-1)/2^{n1}$. The following can be obtained:

$$E\langle |\text{real } x_j|^2 \rangle = \frac{1}{z} \int_{-1/(2z)}^{+1/(2z)} |\text{real } x_j|^2 \, d(\text{real } x_j) \quad \ldots\ldots \text{(A6.2)}$$

$$= \frac{1}{12\, z^2} \quad \ldots\ldots\ldots\ldots\ldots\ldots\ldots\ldots\ldots\ldots \text{(A6.3)}$$

An identical result can be obtained for $E\langle |\text{img } x_j|^2 \rangle$, so:

$$E\langle x_j x_j^* \rangle = \frac{(2L-1)^2}{6\,[2^{2(n_1-1)}]}$$

Appendix 7 The Derivation of Equation (6.9)

With the co-ordinate transformation as follows:

$$x_j = y_j - (2j-1) \quad \ldots\ldots\ldots\ldots\ldots\ldots\ldots\ldots\ldots\ldots \quad (A7.1)$$

The equations (6.7, 6.8) can be re-expressed as:

$$E\langle|e_I|^2\rangle = \sum_{j=-L+1}^{L} \int_{-\infty}^{\infty} g^2 \{[x_j^2 + (2j-1)^2 + 2(2j-1)x_j] - 2g(2j-1)[x_j+(2j-1)] + (2j-1)^2\} Q(x_j)\, dx_j$$

$$\ldots\ldots\ldots\ldots\ldots\ldots\ldots\ldots\ldots\ldots \quad (A7.2)$$

where $Q(x_j) = A \exp\left[-\frac{1}{2}\left(\frac{x_j}{v}\right)^2\right]$

Since $Q(x_j)$ is an even function and x_j is an odd function, therefore:

$$\int_{-\infty}^{\infty} x_j Q(x_j)\, dx_j = 0 \quad \ldots\ldots\ldots\ldots\ldots\ldots\ldots\ldots\ldots\ldots \quad (A7.3)$$

The minimum $E\langle|e_I|^2\rangle$ can be found by differentiating equation (A7.2) with respect to g. The following can be obtained:

$$g' = \frac{\sum_{j=-L+1}^{L} \int_{-\infty}^{\infty} (2j-1)^2 Q(x_j)\, dx_j}{\sum_{j=-L+1}^{L} \int_{-\infty}^{\infty} [(2j-1)^2 + x_j^2] Q(x_j)\, dx_j} \quad \ldots\ldots\ldots\ldots\ldots\ldots \quad (A7.4)$$

$$= \frac{1}{1 + 3v^2/[(2L)^2-1}$$

Appendix 8 The Proof of the Identical Signature Plot for both Minimum and Non-Minimum Phase Fades

Wih the same approach as in Appendix 1, under non-minimum phase fades, the pulse response of the overall channel with sampling phase Ø' and fading parameters a, b and w_o is:

$$P'^{\emptyset'}_{(a,b,w_o)}(t) = \mathcal{F}^{-1}\{T(jw)R(jw)a[1-b\exp(+jwT_d-jw_oT_d)]\exp(-jw\tau')\}$$

where τ' is the sampling phase in terms of symbol period, i.e. $\tau'=T\emptyset'/360$

$$= -ab[\exp(-jw_oT_d)]\mathcal{F}^{-1}\{T(jw)R(jw)\exp[jw(T_d-\tau')]\} + a\mathcal{F}^{-1}[T(jw)R(jw)\exp(-jw\tau')]$$

$$= -ab[\exp(-jw_oT_d)P^0_{(0,0,0)}(t+T_d-\tau')] + a[P^0_{(0,0,0)}(t-\tau')]$$

..... (A8.1)

If the pulse response $P^0_{(0,0,0)}(t)$ is symmetric against t=0, i.e.

$$P^0_{(0,0,0)}(t) = P^0_{(0,0,0)}(-t) \quad \text{..... (A8.2a)}$$

and

$$\emptyset=-\emptyset' \quad \text{..... (A8.2b)}$$

$$|\text{Img } P^0_{(0,0,0)}(t+T_d-\tau')| = 0 \quad \text{..... (A8.2c)}$$

then the following can be achieved:

$$\text{Real } P'^{\emptyset'}_{(a,b,w_o)}(t) = \text{Real } P^{\emptyset}_{(a,b,w_o)}(-t) \quad \ldots\ldots \quad (A8.3)$$

$$\text{and Img } P'^{\emptyset'}_{(a,b,w_o)}(t) = -\text{Img } P^{\emptyset}_{(a,b,w_o)}(-t) \quad \ldots\ldots\ldots \quad (A8.4)$$

Thus the optimum tap weight values for the minimum phase fades and the non-minimum phase fades will be a conjugated pairs.

Appendix 9 The "MMSECALC" Program for Theoretical MMSE Calculation

General Description

This program will calculate the MMSE for a given radio system, fading channel and equalizer structure. BASIC language is used because of the speed advantage compared with PASCAL in HP3000. The user is requested to supply the following data:

a) radio system : bandwidth and the excess bandwidth of the raised cosine filter

b) fading channel : the notch depth and notch position of the 3-ray model

c) equalizer : select of T-spaced or T/2-spaced equalizer, number of tap weights, sampling phase and carrier to noise ratio

The theoretical tap weight can be stored in a file "TAPS1" for other program access, e.g. "EQUALIZE" in Appendix 10. There are two aspects of the program:

a) Calculate the $\xi_{min}/E\langle A_k A_k^* \rangle$ and tap weights value for a particular parameters as specified above.

b) Calculate the $\xi_{min}/E\langle A_k A_k^* \rangle$ which is lower than a specified value for a given sampling phase range and fade depth step. The program will scan the whole sampling phase range and

decrease the fade depth until the required MMSE/$E\langle A_k A_k \rangle$ is reached. It is useful for signature plot.

Apart from these, there are also some intermediate steps for debug proposes, e.g. subroutine 7000-7700 is the auto plot routine for HP2648A graphic terminal.

The number of points used in Fast Fourier Transform is defined in Appendix 4 and the variable declaration can be found in the beginning of the program. The main algorithm is to evaluate the following:

$$\underline{C}_{opt} = \underline{R}'^{-1}\underline{D}'$$

$$\xi_{min}/E\langle A_k A_k^* \rangle = 1 - \underline{D}'\underline{C}_{opt}$$

of equation (4.6a) and (4.7) respectively. Since the matrix inversion in HP3000 can only handle real number, the following procedures are used:

M_{ij} = Real R_{ij} for $i \leq N1$ and $j \leq N1$, where $N1=2N+1$

M_{ij} = Img $R_{i'j}$ for $i > N1$ and $j \leq N$, where $i'=i-N1$

M_{ij} = - Img $R_{ij'}$ for $i \leq N1$ and $j > N1$, where $j'=j-N1$

M_{ij} = Real R_{ij} for $i > N1$ and $j > N1$

U_i = Real D_i, W_i = Real C'_i for $i \leq N1$

U_i = Img $D_{i'}$, W_i = Img $C'_{i'}$ for $i > N1$

Flow Diagram of MMSECALC

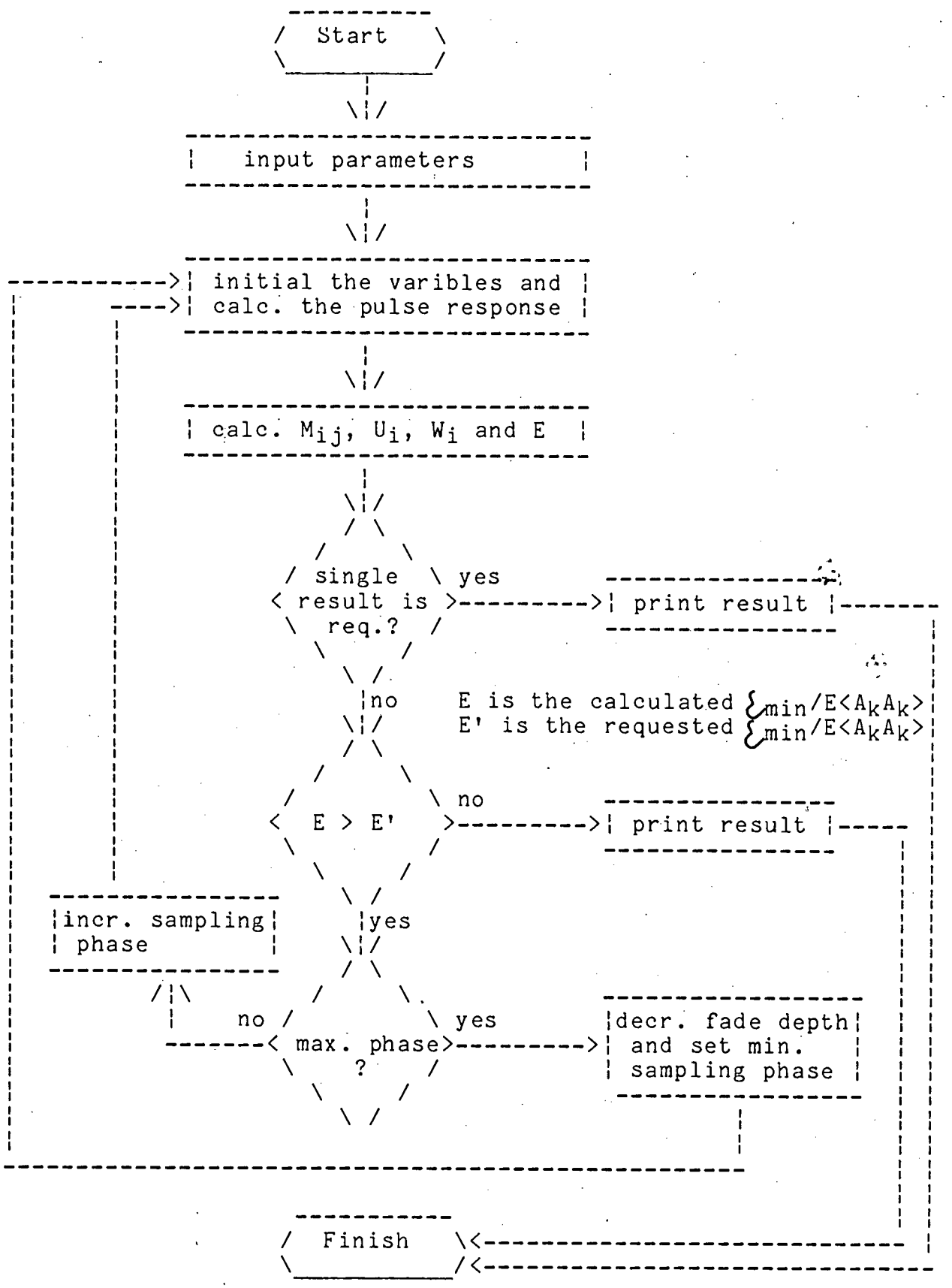

```
650 REAL B,F0
660 REM S3 is the sample phase
670 INTEGER S3
680 REM C,W1,W2,W3,W4 is the filter const
690 REAL C,W1,W2,W3,W4
700 REM T,B1,S1,F2 are delay time, notch shape, phase and notch positi
710 REAL T,B1,S1,F2
720 REM f3,f4 are the starting and stopping freq
730 REAL F3,F4
740 REM N4 is the gaussian noise
750 REAL N4
760 REM A1 to A4 is temporary storage
770 REAL A1,A2,A3,A4
780 REM o1,o2 is for plotting
790 INTEGER O1,O2
800 REM R$ is the flag for resulotion
810 REM P$ indicate the phase of fading
820 REM T$ indicates T or T/2 spacing
830 REM S$ is the flag for plotting
835 REM U$ is temporary string
840 REM Z$ is the string for T or T/2 equalizer
850 DIM Z$[100]
860 REM rem D$ is dynamic range in plotting
870 REM V$ is the string for different filters
880 DIM V$[20]
890 REM y$ is the single phase calculation
892 REM Y8 is the maximum phase offset
900 REM W$ is tap weight plotting
910 REM M$ is the the flag for finding MMSE
920 REM M8 is the required MMSE
930 REM m9 is the step in B
940 REAL M8,M9
950 REM M7 is the summation of the tap square
960 REAL M7
970 REM H2 is the mainlobe
980 COMPLEX H2
1000 U$="N"
1010 M$="N"
1020 V$="phase angle(degree)="
1030 P5=1
1040 PRINT "No perturbation terms and with the correct img Tap Weight"
1050 PRINT
1060 PRINT &
     "This program will do a theoretical calculation on the minimum"
1070 PRINT &
     "mean square error of a transversal equalizer under multipath fadi&
ng"
1080 PRINT "Bandwidth (doublesided Nyquist, MHz) =";
1090 REM print '27"*daG"
1100 PRINT " 22.6MHz"
1110 B=22.6
1120 IF 0>=B THEN 1080
1130 PRINT "IF ( MHz ) =";
1140 F0=70
1150 PRINT " 70MHz"
1160 IF B/2>=F0 THEN 1130
1170 PRINT "Type R,H for rough or high resolution, otherwise median"
1180 PRINT "resolution will be assumed";
1190 INPUT R$
1200 IF R$="r" THEN R$="R"
1210 IF R$="h" THEN R$="H"
1220 IF R$="R" OR R$="H" THEN 1280
1230 R$="M"
1240 M1=7,P1=2
1250 P2=50
1260 N2=10,N3=10
```

```
1270 GOTO 1360
1280 IF R$="R" THEN 1330
1290 M1=8,P1=2
1300 P2=100
1310 N2=14,N3=14
1320 GOTO 1360
1330 M1=6,P1=2
1340 P2=25
1350 N2=7,N3=7
1360 PRINT "The raised cosine filter a (0-1]=";
1370 INPUT C
1380 IF 0>=C OR C>1 THEN 1360
1390 PRINT &
    "Type Y if you only want to get the result at a particular fading"
1400 PRINT &
    "otherwise the result will be plotted against diff notch freq";
1410 PRINT " y"
1420 S$="y"
1430 IF S$="y" THEN S$="Y"
1440 PRINT "The shape of the notch (dB) =";
1450 INPUT B1
1460 B1=1-10**(-B1/20)
1470 IF 0>B1 OR B1>=1 THEN 1440
1480 IF M$="Y" THEN 2100
1490 PRINT &
    "Type Y for non-minimum phase fading, otherwise minimum phase";
1500 PRINT "fading will be assumed";
1510 PRINT " n"
1520 P$="n"
1530 S1=1
1540 IF P$="y" OR P$="Y" THEN S1=-1
1550 PRINT "The delay time (ns) =";
1560 INPUT T
1570 IF S$<>"Y" THEN 1630
1580 PRINT "The fading notch frequency offset from center (MHz) =";
1590 INPUT F2
1600 F2=F0+F2
1610 IF 0>F2 THEN 1580
1620 GOTO 1730
1630 PRINT "Type in the freq range of interest, f min  (MHz) =";
1640 INPUT F3
1650 IF 0>F3 THEN 1630
1660 PRINT "                                                f max  (MHz) =";
1670 INPUT F4
1680 IF F3>=F4 THEN 1660
1690 PRINT &
    "Type Y if 35dB dynamic range is used in plotting, otherwise"
1700 PRINT "60 dB dynamic range will be used";
1710 INPUT D$
1720 IF D$="y" THEN D$="Y"
1730 PRINT "Number of taps (3-21) =";
1740 INPUT N1
1750 IF N1<3 OR N1>21 THEN 1730
1760 PRINT "Type Y if T/2 spacing transversal equalizer is used";
1770 INPUT T$
1780 P3=1
1790 IF T$="y" THEN T$="Y"
1800 IF T$="Y" THEN P3=2
1810 PRINT "Sampling phase (degree) =";
1820 INPUT S3
1830 PRINT "Demodulation phase";
1840 PRINT " compensate"
1850 D4=0
1860 IF U$="Y" THEN 2140
1870 PRINT "Type Y if you want to plot tap weight";
1880 INPUT W$
```

```
1890 IF W$="y" THEN W$="Y"
1900 PRINT "C/N (dB) before fading =";
1910 INPUT N5
1920 N4=10**(-N5/10)
1930 PRINT "Type Y if only 1 sample phase is required";
1940 INPUT Y$
1950 IF Y$="y" THEN Y$="Y"
1960 D7=7,Y8=0
1970 IF Y$="Y" THEN 2090
1980 PRINT "Required MMSE (dB) =";
1990 INPUT M8
2000 PRINT "Input step in B (>.01dB)";
2010 INPUT M9
2020 IF M9<.01 THEN 2000
2030 M$="Y"
2040 PRINT "Input sampling phase range";
2050 INPUT Y8
2060 PRINT "Input phase step (degree)";
2070 INPUT D7
2080 IF D7<=0 THEN 2060
2090 PRINT "Phase MMSE       BX1000 B'X1000 Error(%)  N         S"
2100 REM set up initial condition
2110 FOR D6=S3 TO S3+Y8 STEP D7
2120   P4=0
2130   P5=1
2140   N=2**M1
2150   FOR I=1 TO P2+1
2160     E[I]=0
2170   NEXT I
2180   A=P1*PIX(2)/N
2190   REM set up filter characteristics
2200   W1=PIX(1)*(1-C)
2210   W2=PIX(1)*(1+C)
2220   W3=A/(4*C)
2230   W4=PIX(1)*(1-C)/(4*C)
2240   D1[1]=(1,0)
2250   FOR I=2 TO N/2+1
2260     A1=(I-1)*A
2270     IF A1>=W1 THEN 2300
2280     D1[N-I+2]=D1[I]=CPX(1,0)
2290     GOTO 2350
2300     IF A1>=W2 THEN 2340
2310     A1=COS(W3*(I-1)-W4)
2320     D1[N-I+2]=D1[I]=CPX(A1*A1,0)
2330     GOTO 2350
2340     D1[N-I+2]=D1[I]=(0,0)
2350   NEXT I
2360   FOR I=1 TO N
2370     D[I]=D1[I]
2380   NEXT I
2390   F=1
2400   GOSUB 9000
2410   A1=REA(D[1])
2420   REM cancel the perturbation terms here
2430   D[1]=CPX(REA(D[1]),0)
2440   FOR J=2 TO N
2450     D[J]=CPX(0,0)
2460   NEXT J
2470   FOR J=1 TO N3*P3+1
2480     U3[P3*N3+J]=REA(D[1+(J-1)*P1/P3])/A1
2490     U4[P3*N3+J]=IMG(D[1+(J-1)*P1/P3])/A1
2500   NEXT J
2510   FOR J=1 TO P3*N2
2520     U3[P3*N3+1-J]=REA(D[N-J*P1/P3+1])/A1
2530     U4[P3*N3+1-J]=IMG(D[N-J*P1/P3+1])/A1
2540   NEXT J
```

```
2550    J1=(B/2)/(N/(2*P1))
2560    IF S$<>"Y" THEN 2590
2570    P2=0,I1=1
2580    GOTO 2630
2590    REM display the heading
2600    GOSUB 7000
2610    I1=(F4-F3)/P2
2620    F2=F3
2630    REM add the multipath fading
2640    Z$="n"
2650    D4=0
2660    FOR I=1 TO P2+1
2670      A1=-J1*PIX(2)*.001*T*S1
2680      A2=(F0-F2-(I-1)*I1)*PIX(2)*.001*T*S1
2690      FOR J=1 TO N/2+1
2700        A3=(J-1)*A1-A2
2710        H1=CPX(1-B1*COS(A3),-B1*SIN(A3))
2720        D[J]=D1[J]*H1
2730      NEXT J
2740      FOR J=N TO N/2 STEP -1
2750        A3=(J-N-1)*A1-A2
2760        H1=CPX(1-B1*COS(A3),-B1*SIN(A3))
2770        D[J]=D1[J]*H1
2780      NEXT J
2790      REM Add demodulation phase and sampling phase
2800      A1=D6*PIX(2*P1)/(N*360)
2810      FOR J=1 TO N/2
2820        A2=(J-1)*A1+D4
2830        H1=CPX(COS(A2),-SIN(A2))
2840        D[J]=D[J]*H1
2850      NEXT J
2860      FOR J=N TO N/2 STEP -1
2870        A2=(J-N-1)*A1+D4
2880        H1=CPX(COS(A2),-SIN(A2))
2890        D[J]=D[J]*H1
2900      NEXT J
2910      F=1
2920      GOSUB 9000
2930      IF Z$="y" THEN 3060
2940      Z$="y"
2950      D4=ATN(D[1])
3050      GOTO 2670
3060      REM get the pulse response
3070      A1=ABS(D6/180)
3080      IF A1>N/2-3 THEN A1=N/2-3
3090      IF D6<=-90 THEN 3120
3100      H2=D[1+A1]
3110      GOTO 3130
3120      H2=D[N-A1+.999]
3130      GOTO 3160
3140      PRINT "mainlobe =";H2
3150      PRINT "demodulation phase =";D4*360/PIX(2)
3160      A3=0
3170      FOR J=1 TO N-1 STEP 2
3180        A3=A3+ABS(REA(D[J]))+ABS(IMG(D[J]))
3190      NEXT J
3200      GOTO 3220
```

```
3210 PRINT "total ISI =";A3-ABS(REA(D[1]))
3220 IF P3<1.5 THEN 3280
3230 A2=0
3240 FOR J=2 TO N STEP 2
3250   A2=A2+ABS(REA(D[J]))+ABS(IMG(D[J]))
3260 NEXT J
3270 IF A2>A3 THEN A3=A2
3280 REM normalize the amplitude to be summation hi=1
3290 H2=CPX(A3,0)
3300 A1=REA(H2)
3310 A4=1
3320 IF P4>=0 THEN 3360
3330 U1[P3*N3+1]=REA(D[N+1+P4])/A1
3340 U2[P3*N3+1]=IMG(D[N+1+P4])/A1
3350 A4=2
3360 FOR J=A4 TO N3*P3+1
3370   U1[P3*N3+2-J]=REA(D[1+(J-1)*P1/P3+P4])/A1
3380   U2[P3*N3+2-J]=IMG(D[1+(J-1)*P1/P3+P4])/A1
3390 NEXT J
3400 FOR J=1 TO P3*N2
3410   U1[P3*N3+1+J]=REA(D[N-J*P1/P3+P4+1])/A1
3420   U2[P3*N3+1+J]=IMG(D[N-J*P1/P3+P4+1])/A1
3430 NEXT J
3440 REM do a T/2 shift for 3,7,11,15,19 tap T/2 equalizer
3450 IF P3<1.5 THEN 3540
3460 P=(N1+1.0001)/4
3470 A1=ABS(P-(N1+1)/4)
3480 IF A1>.1 THEN 3540
3490 FOR J=1 TO 2*P3*N2
3500   U1[J]=U1[J+1]
3510   U2[J]=U2[J+1]
3520 NEXT J
3530 U1[2*P3*N2+1]=U2[2*P3*N2+1]=0
3540 REM initialization
3550 REDIM U[2*N1],M[2*N1,2*N1],V[2*N1,2*N1]
3560 FOR J=1 TO 2*N1
3570   U[J]=0
3580 NEXT J
3590 FOR J=1 TO 2*N1
3600   FOR K=1 TO 2*N1
3610     M[J,K]=0
3620   NEXT K
3630 NEXT J
3640 FOR K1=1 TO P3
3650   FOR K2=1 TO K1
3660     A2=P3+K2-K1+1
3670     A3=P3+1-K2
3680     A4=K2
3690     FOR K=A2 TO N1 STEP A3
3700       A1=K-K2
3710       FOR L=A4 TO (N2+N3)*P3+1 STEP P3
3720         IF L+A1>(N2+N3)*P3+1 THEN 3740
3730         M[K2,K]=M[K2,K]+U1[L]*U1[L+A1]+U2[L]*U2[L+A1]
3740       NEXT L
3750       M[K2+N1,K+N1]=M[K+N1,K2+N1]=M[K,K2]=M[K2,K]
3760     NEXT K
3770     IF K1=2 AND K2=1 THEN 3820
3780     FOR L=K2 TO (N2+N3)*P3+1 STEP P3
3790       M[K2,K2]=M[K2,K2]+U1[L]*U1[L]+U2[L]*U2[L]
3800     NEXT L
3810     M[K2+N1,K2+N1]=M[K2,K2]
3820   NEXT K2
3830 NEXT K1
3840 FOR J=P3+1 TO N1
3850   FOR K=J TO N1
3860     M[J+N1,K+N1]=M[J,K]=M[J-P3,K-P3]
```

```
3870    NEXT K
3880    FOR K=P3+1 TO J
3890      M[J+N1,K+N1]=M[J,K]=M[K,J]
3900    NEXT K
3910  NEXT J
3920  FOR K1=1 TO P3
3930    FOR K2=1 TO K1
3940      A2=P3+K2-K1+1
3950      A3=P3+1-K2
3960      A4=K2
3970      FOR K=A2+N1 TO 2*N1 STEP A3
3980        A1=K-K2-N1
3990        FOR L=A4 TO (N2+N3)*P3+1 STEP P3
4000          IF L+A1>(N2+N3)*P3+1 THEN 4020
4010          M[K2,K]=M[K2,K]+U1[L]*U2[L+A1]-U2[L]*U1[L+A1]
4020        NEXT L
4030        M[K,K2]=M[K2,K]
4040        M[K-N1,K2+N1]=M[K2+N1,K-N1]=-M[K2,K]
4050      NEXT K
4060    NEXT K2
4070  NEXT K1
4080  FOR J=P3+1 TO N1
4090    FOR K=J+N1 TO 2*N1
4100      M[K,J]=M[J,K]=M[J-P3,K-P3]
4110    NEXT K
4120    FOR K=P3+1+N1 TO J+N1
4130      M[K,J]=M[J,K]=-M[K-N1,J+N1]
4140    NEXT K
4150  NEXT J
4160  REM shift back the T/2 for 3,7,11,15,19 tap T/2 equalizer
4170  P=(N1+1)/4
4180  A1=ABS(P-(N1+1)/4)
4190  IF P3<1.5 OR A1>.1 THEN 4250
4200  FOR J=2*N3*P3 TO 1 STEP -1
4210    U1[J+1]=U1[J]
4220    U2[J+1]=U2[J]
4230  NEXT J
4240  U1[1]=U2[1]=0
4250  IF N1/2<=N3*P3 THEN 4410
4260  FOR J=1 TO P3*(N2+N3)+1
4270    U[N1/2-N3*P3+J-1]=U1[J]
4280  NEXT J
4290  FOR J=1 TO P3*(N2+N3)+1 STEP P3
4300    IF J=P3*(N2+N3)/2+1 THEN 4320
4310    U[N1/2-N3*P3+J-1]=U[N1/2-N3*P3+J-1]+U3[J]
4320  NEXT J
4330  FOR J=1 TO P3*(N2+N3)+1
4340    U[3*N1/2-N3*P3+J-1]=U2[J]
4350  NEXT J
4360  FOR J=1 TO P3*(N2+N3)+1 STEP P3
4370    IF J=P3*(N2+N3)/2+1 THEN 4390
4380    U[3*N1/2-N3*P3+J-1]=U[3*N1/2-N3*P3+J-1]+U4[J]
4390  NEXT J
4400  GOTO 4580
4410  FOR J=1 TO N1
4420    U[J]=U1[P3*N3+J-N1/2]
4430  NEXT J
4440  FOR J=1 TO N1 STEP P3
4450    IF J=(N1+1)/2 THEN 4470
4460    U[J]=U[J]+U3[P3*N3+J-N1/2]
4470  NEXT J
4480  FOR J=1 TO N1
4490    U[N1+J]=U2[P3*N3+J-N1/2]
4500  NEXT J
4510  FOR J=1 TO N1 STEP P3
4520    IF J=(N1+1)/2 THEN 4540
```

```
4530    U[N1+J]=U[N1+J]+U4[P3*N3+J-N1/2]
4540 NEXT J
4550 FOR J=1 TO 2*N1
4560    M[J,J]=M[J,J]+N4/(2*REA(H2))**2
4570 NEXT J
4580 REDIM M[2*N1,2*N1],V[2*N1,2*N1],U[2*N1],W[2*N1]
4590 MAT V=INV(M)
4600 MAT W=V*U
4610 FOR J=1 TO 2*N1
4620    E[I]=U[J]*W[J]+E[I]
4630 NEXT J
4640 A1=0
4650 FOR J=1 TO P3*(N2+N3)+1 STEP P3
4660    A1=A1+U3[J]*U3[J]+U4[J]*U4[J]
4670 NEXT J
4680 E[I]=ABS(A1-E[I])
4690 IF E[I]<1E-8 THEN E[I]=1E-8
4700 E[I]=10*LOG(E[I])/LOG(10)
4710 IF S$<>"Y" THEN 5290
4720 INTEGER Q4,Q5,Q6,Q7,Q8,Q9
4730 A2=A3=0
4740 FOR J=1 TO 2*N1
4750    FOR K=1 TO 2*N1
4760       A2=A2+M[J,K]*M[J,K]
4770    NEXT K
4780    A2=A2-M[J,J]*M[J,J]
4790    A3=A3+M[J,J]
4800 NEXT J
4810 A3=A3/2
4820 A1=A2/A3/A3
4830 Q5=100*A1
4840 Q8=1000*M[1,1]
4850 Q9=1000*M[2,2]
4860 Q7=100*E[I]
4870 M7=0
4880 FOR J=1 TO N1
4890    M7=M7+W[J]*W[J]+W[J+N1]*W[J+N1]
4900 NEXT J
4910 IF M7>3200 THEN M7=3200
4920 Q6=10*M7/(2*REA(H2))**2
4930 Q4=M7*10
4940 GOTO 4960
4950 PRINT "S  =";M7,"S' =";M7/(2*REA(H2))**2
4960 PRINT D6;Q7/100;Q8;Q9;Q5;Q6/10;Q4/10
4970 IF W$<>"Y" THEN 5010
4980 FOR J=1 TO N1
4990    PRINT "W (  ";J;") =";W[J],-W[J+N1]
5000 NEXT J
5010 IF Y$<>"Y" THEN 5310
5020 FILES *,*
5030 ASSIGN "TAPS1",1,A1,NR
5040 ASSIGN "RAYMP",2,A2,NR
5050 PRINT "Type Y if you want to store the tap weigth in file TAPS1";
5060 INPUT V$
5070 IF V$="y" THEN V$="Y"
5080 IF V$<>"Y" THEN 5150
5090 PRINT #1;"Tap weigth from TRESPON5"
5100 PRINT #1;N1,1/P3
5110 FOR J=1 TO N1
5120    W0[J]=CPX(W[J],-W[J+N1])
5130 NEXT J
5140 PRINT #1;(FOR J=1 TO N1,W0[J]),END
5150 PRINT &
     "Type Y if you want to store the pulse response in file RAYMP";
5160 INPUT V$
5170 IF V$="y" THEN V$="Y"
```

```
5180 IF V$<>"Y" THEN 5490
5190 PRINT #2;"pulse response from TRESPON5"
5200 PRINT #2;FO,B,M1,P1,C,-1,B1,F2,T,S1,N2,N3
5210 A1=REA(D[1])
5220 FOR J=1 TO N
5230   D[J]=D[J]/A1
5240 NEXT J
5250 PRINT #2;(FOR J=1 TO N2*P1,D[N-N2*P1+J])
5260 PRINT #2;(FOR J=1 TO N3*P1+1,D[J])
5270 PRINT #2;END
5280 GOTO 5490
5290 PRINT (I-1)*25/P2+6.25,E[I]
5300 GOTO 5490
5310 IF E[I]>M8 THEN 5600
5320 M$="N"
5330 PRINT
5340 PRINT
5350 PRINT
5360 PRINT "notch offset =";F2-FO,
5370 PRINT "notch depth =";-20*LOG(1-B1)/LOG(10)
5380 PRINT "sample phase =";D6,"Gaussian Noise =";N5;"dB"
5390 A1=M7/(2*REA(H2))**2
5400 PRINT "Degradation in C/N =";10*LOG(A1)/LOG(10)
5410 PRINT "MMSE =";E[I]
5420 PRINT "Excessive bandwidth in raised cosine filter =";C
5430 PRINT "Number of Taps =";N1;
5440 IF P3<1.5 THEN PRINT "(T-spaced)"
5450 IF P3>=1.5 THEN PRINT "(T/2-spaced)"
5460 PRINT "Delay time in fading channel =";T
5470 PRINT "steps in B =";M9
5480 D6=D6+Y8+D7
5490 A2=A3=0
5500 FOR J=1 TO 2*N1
5510   FOR K=1 TO 2*N1
5520     A2=A2+M[J,K]*M[J,K]
5530   NEXT K
5540   A2=A2-M[J,J]*M[J,J]
5550   A3=A3+M[J,J]
5560 NEXT J
5570 A3=A3/2
5580 PRINT "Total Power =";A3
5590 PRINT "Error =";A2/A3/A3
5600 NEXT I
5610 NEXT D6
5620 IF M$="N" THEN 5700
5630 PRINT
5640 PRINT
5650 B1=-20*LOG(1-B1)/LOG(10)
5660 B1=B1-M9
5670 PRINT B1
5680 IF B1>5 THEN 1460
5690 PRINT "B is less than 5dB"
5700 IF P2=0 THEN 5970
5710 PRINT '27"*abG"
5720 PRINT '27"*aaA"
5730 A1=1
5740 IF D$<>"Y" THEN A1=2
5750 FOR I=22 TO 26
5760   PRINT I,-P5*1.5*A1
5770 NEXT I
5780 PRINT '27"*abG";
5790 PRINT '27"*dcskG";
5800 FOR I=1 TO N1
5810   PRINT W[J],W[J+N1]
5820 NEXT I
5830 PRINT '27"*ds10,-4pG";
```

```
5840 PRINT V$;
5850 PRINT S3
5860 PRINT '27"*dtlG"
5870 PRINT '7'17
5880 PRINT '27"*deG"
5890 PRINT '27"*ddG"
5900 P5=P5+1
5910 IF P5>5.5 THEN 5970
5920 PRINT "Type Y if you want to plot another curve";
5930 INPUT U$
5940 IF U$="y" THEN U$="Y"
5950 IF U$<>"Y" THEN 5970
5960 GOTO 1810
5970 END
7000 REM this routine display the heading
7010 IF P5>1.5 THEN 7580
7020 PRINT '27"*ddG"
7030 PRINT '27"*m1m1npQ"
7040 PRINT '27"*ds40,20okG"
7050 PRINT '27"*ds40,20okG"
7060 Z$="complex T spacing equalizer under multipath fading (3-ray)"
7070 IF T$="Y" THEN Z$=&
    "complex T/2 spacing equalizer under multipath fading (3-ray)"
7080 PRINT "Mean square error of a";
7090 PRINT N1;
7100 PRINT '27"*ds-18,0pG";
7110 PRINT "taps";
7120 PRINT '27"*ds253,20okG"
7130 PRINT Z$
7140 PRINT '27"*ds40,10okG"
7150 PRINT "Delay time (ns)=";
7160 PRINT T;
7170 PRINT '27"*ds180,10okG"
7180 PRINT ", a=1, b=";
7190 PRINT '27"*ds240,10okG"
7200 PRINT B1
7210 PRINT '27"*ds270,10okG"
7220 PRINT "("
7230 O1=ABS(20*LOG(1-B1))/LOG(10)
7240 PRINT '27"*ds275,10okG"
7250 PRINT O1
7260 PRINT '27"*ds300,10okG"
7270 PRINT "dB ),"
7280 PRINT '27"*ds340,10ok"
7290 PRINT B
7300 PRINT '27"*ds370,10okG"
7310 PRINT "MHz QPSK with IF=";
7320 PRINT FO
7330 PRINT '27"*ds525,10okG"
7340 PRINT "MHz,";
7342 IF C<>1 THEN 7347
7344 PRINT " 1.0 raised cos filter"
7346 GOTO 7350
7347 PRINT C;
7348 PRINT '27"*ds587,10okG"
7349 PRINT "raised cos filter"
7350 PRINT '27"*ds143,40okG"
7360 PRINT F3
7370 PRINT '27"*ds200,30okG"
7380 PRINT "( notch frequency )"
7390 PRINT '27"*ds360,40okG"
7400 PRINT (F4+F3)/2
7410 PRINT '27"*ds450,30okG"
7420 PRINT " ( MHz )"
7430 PRINT '27"*ds579,40okG"
7440 PRINT F4
```

```
7450 PRINT '27"*ds70,350okG";
7500 PRINT "White Gaussian Noise(rms)=";
7510 PRINT SQR(N4)
7520 IF P5>1.5 THEN 7550
7530 PRINT '27"*ds495,360oksG"
7540 PRINT DAT$(1,27)
7550 PRINT '27"*m1m2nQ"
7560 PRINT '27"*ds30,125okG"
7570 PRINT "mean square error       ( dB )"
7580 PRINT '27"*dtIF"
7590 PRINT '27"*ad2h1i2j"
7600 IF P5=1 THEN PRINT "1k"
7610 IF P5=2 THEN PRINT "8k"
7620 IF P5=3 THEN PRINT "3k"
7630 IF P5=4 THEN PRINT "2k"
7640 IF P5=5 THEN PRINT "6k"
7650 IF D$="Y" THEN 7680
7660 PRINT "1.25136.25m-63n7o50p1.25q20r5s0v0wcA"
7670 GOTO 7690
7680 PRINT "1.25136.25m-37n3o50p1.25q10r2s0v0wcA"
7690 PRINT '27"*dcG"
7700 RETURN
9000 REM THIS SUBROUTINE PERFORM COOLEY-TUKEY FFT
9010 REM F=1 FOR BACKWARD TRANSFORM AND F=-1 FOR FORWARD TRANSFORM
9020 REM THE FFT WILL BE PERFORM ON D(I) AND THE RESULT WILL BE RETURNE
9030 REM IN D(I)
9040 L2=1
9050 FOR L1=1 TO N
9060   IF L1>=L2 THEN 9100
9070   H=D[L2]
9080   D[L2]=D[L1]
9090   D[L1]=H
9100   REM IMPLEMENT J=J+1, BIT-REVERSED COUNT
9110   M=N/2
9120   IF L2<=M THEN 9160
9130   L2=L2-M
9140   M=M/2
9150   GOTO 9120
9160   L2=L2+M
9170 NEXT L1
9180 L3=1
9190 IF L3>=N THEN 9330
9200 L4=2*L3
9210 FOR L1=1 TO L3
9220   A1=PIX(1)*(F*(L1-1))/L3
9230   H=CPX(COS(A1),SIN(A1))
9240   FOR L5=L1 TO N STEP L4
9250     P=L5+L3
9260     H1=H*D[P]
9270     D[P]=D[L5]-H1
9280     D[L5]=D[L5]+H1
9290   NEXT L5
9300 NEXT L1
9310 L3=L4
9320 GOTO 9190
9330 IF F=-1 THEN 9370
9340 FOR L1=1 TO N
9350   D[L1]=D[L1]/N
9360 NEXT L1
9370 RETURN
>
```

Appendix 10 The "EQUALIZE" Program for MSE Convergence and MMSE Simulation

General Description

This program will simulate the equalizer response for a given radio system, fading channel and equalizer structure. Again, BASIC language is used because of the speed advantage. The simulation is performed by feeding a random data sequence which is generated by the computer to the fading channel.

The program is separated into a main program and 14 sub-programs. There are 9 common areas to share with the common variables. The following is a brief description of the programs:

EQUALIZE : the main program

INPUT : request the user to supply the following data --

a) radio system -- select of QPSK to 256QAM, the excess bandwidth of the raised cosine filter

b) fading channel -- fading model and its parameters

c) equalizer -- T-spaced or T/2-spaced, number of taps, intial setup of the tap weights, mode select, algorithm select, convergence factor, demodulation and sampling phase, quantization levels in ADC and arithmetic

SETFILR : set up radio channel without multipath fading

SETCHAN : calculate the pulse response with multipath fading, various demodulation and sampling phase

SETPULSE : normalize the pulse response

SETEQUAL : initialize the equalizer

SHIFTT : shift the random data by 1 symbol period

SHIFTG : shift the received data by 1 symbol period

RANDOM : generate a random data

ARITHM : quantize the arithmetic calculation

QUANTIZE : quantize the receive data

UPDATE : update the equalizer tap weight

PLOT : plot the MMSE convergence by using HP2648 graphic terminal

SPECTRUM : print the spectrum data of the channel, equalizer plus channel and the group delay distortion of equalizer plus channel

CONSYEL : plot the constellation of the radio with and without equalizer

Flow Diagram of EQUALIZE

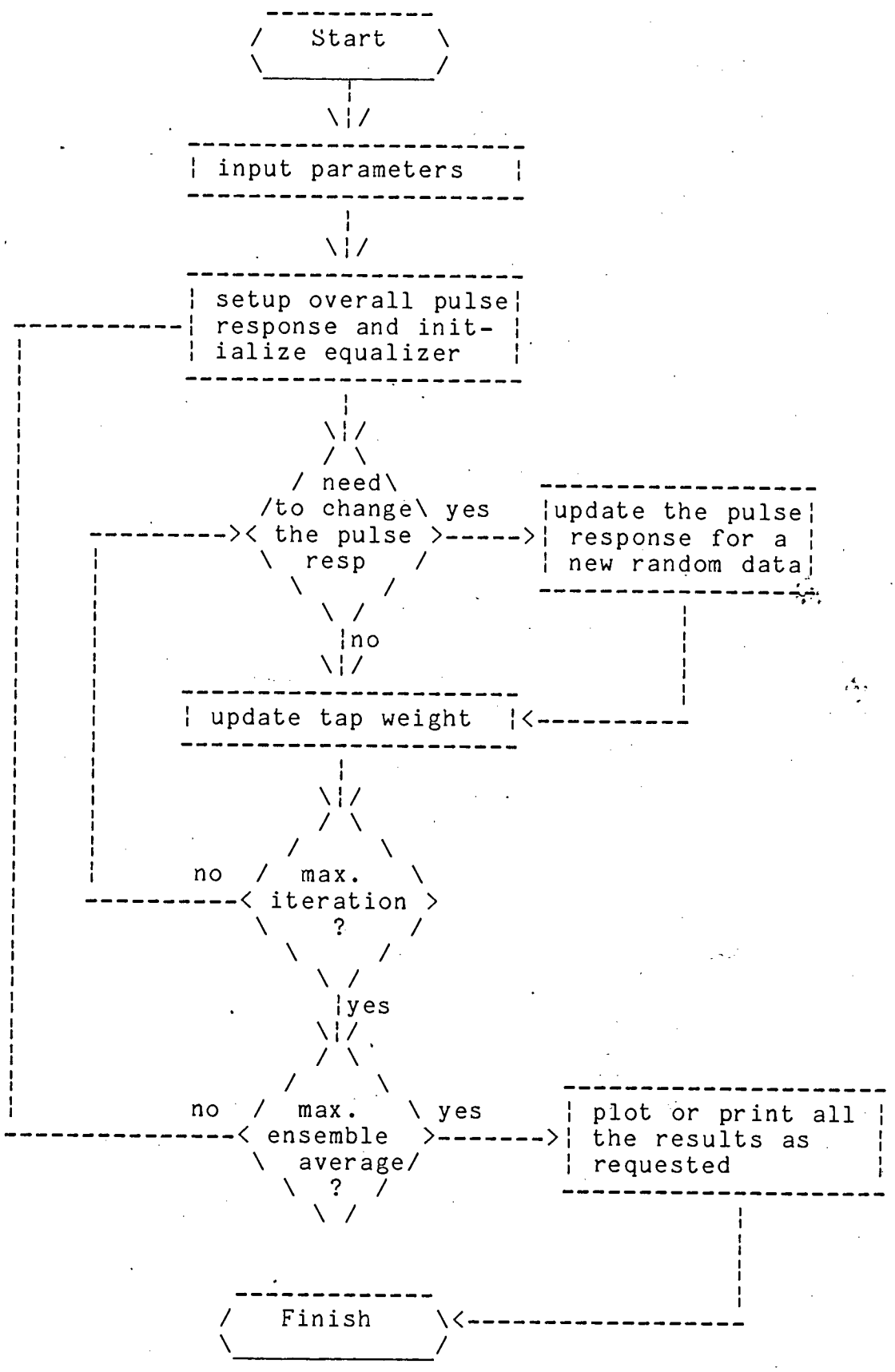

Program Listing

```
EQUALIZE
   10 REM This program will perform the equalizer response with
   20 REM a seperated training or decision directed method
   30 REM
   40 REM The equalizer structure is Transversal type with T or T/2
   50 REM spacing.
   60 REM
   70 REM The overall transmit & receive filter is raised cosine
   80 REM type with 1/sinc(x) correction factor.
   90 REM
  100 REM The channel is either a Rummler's 3-ray model
  110 REM or just a simplified 2-ray model.
  120 REM
  130 REM The overall pulse response is done by 32-128 pts FFT.
  140 REM Each symbol occupied 2 points in time domain.
  150 REM
  160 REM Gradient Search or Zero Forcing Algorithm is used.
  170 REM The channel is dynamically changed for each iteration.
  180 REM
  190 REM Four Radio System  -- (1) 70Mb/s (70MHz) QPSK
  200 REM                          (2)  90Mb/s (22.6MHz) 16QAM
  210 REM                          (3)  135Mb/s (22.6MHz) 64QAM
  220 REM                          (4)  180Mb/s (22.6MHz) 256QAM
  230 REM    can be chosen.
  240 REM
  250 REM The user needed to defined the number of iterations, the
  260 REM initial & final conditions of the channel.
  270 REM
  280 REM      REV:02              18 Oct 86
  290 REM
  300 REM M1,M2,M3 are changed, a small offsets have been added
  310 REM (1/2 LSB)
  320 REM display B value and the summation of tap weights
  330 REM
 1000 REM Comm area 0 is for tap arithmetics
 1010 COM COMPLEX E,REAL M1,M2,M3,M4,M5
 1020 REM M1-5 are the parameters for calculations
 1030 REM E is the entry variables for bit slice
 1040 REM Common area(1) is the channel & filter parameters
 1050 COM(1) R$,C,M$,T1,T2,B1,B2,F1,F2
 1060 REM Common area(2) is the equalizer parameters
 1070 COM(2) INTEGER N,REAL S,COMPLEX W0[32],W[32],L$,A$,U,INTEGER M,M0&
      ,K,G$
 1080 REM Common area(3) is the phase & arithmetics parameters
 1090 COM(3) D$,REAL D1,S$,INTEGER S1,N1,N2,REAL N3
 1100 REM R$ is the radio system
 1110 REM C is the raised cosine filter paramter
 1120 REM M$ is the multipath fading model
 1130 REM T1 & T2 are the initial & final condition of the multipath
 1140 REM delay time
 1150 REM B1 & B2 are the initial & final condition of the amplitude of
 1160 REM the multipath
 1170 REM F1 & F2 are the initial & final condition of the notch offset
 1180 REM frequencies
 1190 REM N$ is the title of the File
 1200 REM N and S are the number of taps & tap spacing
```

```
1210 REM W0(32) and W(32) are the initial & adaptive tap weigths
1220 REM L$ is the equalizer adaptive mode
1230 REM A$ is the equalization algorithm
1240 REM U is the convergence factor
1250 REM M is the number of iteration
1260 REM K is the number of ensemble average
1270 REM G$ is the auto-gain flag
1280 REM O$ is constant phase cancelling
1290 REM O1 is the initial demodulation angle
1300 REM S$ is the sampling phase adjustment
1310 REM S1 is the initial sampling angle
1320 REM N1 & N2 are the number of bits in ADC & Tap Weight
1330 REM N3 is the range of the arithmetics
1340 REM Common area (4) is the data for the raised cosine filter & FFT
1345 REM D2(128) is the freq response of the overall channel
1350 REM D1(128) is the data for performing FFT
1360 REM D(128) is the frequency data for raised cosine filter
1370 REM P1 is the number of points/symbol in time domain
1380 REM P2 is the total number of points for FFT
1390 COM(4) COMPLEX D[128],COMPLEX D1[128],COMPLEX D2[128],INTEGER P1,&
    INTEGER P2
1400 REM Common area(5) is the channel parameters for FFT
1410 COM(5) F5,S5,D$,D5,P5,T0,B0,F0
1420 REM F5 is the frequncy step
1430 REM S5 is the multipath model
1440 REM T0, B0, F0 are the multipath parameters
1450 REM D$ is the flag for constant demodulation cancelling
1460 REM D5 is the demodulation phase in terms of rad
1470 REM P5 is the sampling phase in terms of delay time
1480 REM Com(6) is the pulse response paramters
1490 COM(6) COMPLEX H[65],INTEGER N6,REAL M6,REAL R6
1500 REM H(65) is the pulse array
1510 REM N6 is the number of pre-echoes & post echoes to be considered
1520 REM M6 is the maximum sampling data
1530 REM R6 is the amplitude of the main lobe
1540 REM Common area (7) is transmit & receive data
1550 COM(7) COMPLEX G[165],COMPLEX T[100],COMPLEX R7,INTEGER I7
1560 REM G(165) is the receive data after sampler
1570 REM T(100) is the transmit data
1580 REM R7 is the random data generator
1590 REM I7 is maximum level value of radio, e.g. 15 for 256QAM
1600 REM Common area (8) is for equalizer response parameters
1610 COM(8) COMPLEX E8,INTEGER W8,O8
1620 REM E8 is the error at equalizer output
1630 REM W8 is the number of wrong decisions in decision direct mode
1640 REM O8 is the number of overflow in tap arithmetics
1650 REM Common area (9) is the avarage error & tap weight for plotting
1660 COM(9) E2[8000],COMPLEX W2[32]
1670 REM E2(*) is the avarage error array
1680 REM W2(*) is the average tap weigth
1800 REM H$ is the overall accuracies
1810 REM I,J,L are counters
1820 INTEGER I,J,L
1838 INTEGER G1,G2,G3
1840 REM A1-9 are temporary variables
1850 REAL A1,A2,A3,A4
1860 COMPLEX A6,A7,A8,A9
1870 REM X$ is the flag for spectrum plotting
2000 REM Get the input parameter
2010 INVOKE "INPUT"
2020 PRINT &
    "Type 1 for low resolution, 2 for high resolution, otherwise"
2030 PRINT "medium resolution will be used";
2040 INPUT H$
2050 P1=2,P2=64
2060 IF H$="1" THEN P2=32
```

```
2070 IF H$="2" THEN P2=128
2080 REM Set up the raised cosine filter paramter
2090 INVOKE "SETFILR"
2100 REM Set up channel & phase angle
2110 REM Set up frequency steps
2120 F5=22.6*P1/P2,P5=S1*1000/(22.6*360)
2130 IF R$<>"1" THEN 2150
2140 F5=70*P1/P2,P5=S1*1000/(70*360)
2150 D5=01*PIX(2)/360
2160 REM Set up multipath parameters
2170 T0=T1,B0=B1,F0=F1
2180 S5=-1
2190 IF M$="2" THEN S5=1
2200 D$=0$
2210 INVOKE "SETCHAN"
2220 REM Set up the pulse response in time domain propertly
2230 REM Set up tap spacing, number of pre-echoes $ post-echoes
2240 N6=9
2250 IF H$="1" THEN N6=6
2260 IF H$="2" THEN N6=12
2270 INVOKE "SETPULSE"
2280 REM Set up maximum level value for radio
2290 I7=15
2300 IF R$="1" THEN I7=1
2310 IF R$="2" THEN I7=3
2320 IF R$="3" THEN I7=7
2330 REM Set up M1-3
2340 M1=2**(N1-1)/(I7*M6)
2350 M2=I7*M6-.5/M1
2360 M3=M2*M1
2370 REM Re-Set U with finit arithmetics
2380 IF N2<3 OR N2>16 THEN 2540
2390 REM Set up range
2400 IF N3<>0 THEN 2460
2410 N3=2
2420 R0=ABS(1-B1)
2430 IF R0>ABS(1-B2) THEN R0=ABS(1-B2)
2440 IF R0<.2 THEN N3=2.5
2450 IF R0<.1 THEN N3=3
2460 REM Set up M4,M5
2470 M5=2**(N2-1)/N3
2480 M4=N3*(1-1/(2**(N2-1)))
2490 REM Set zero errors
2500 W8=08=0
2510 E=CPX(U,0)
2520 INVOKE "ARITHM"
2530 U=REA(E)
2540 REM Set up average error array & tap weigth
2550 IF M>8000 THEN 2600
2560 FOR I=1 TO M
2570   E2[I]=0
2580 NEXT I
2590 GOTO 2630
2600 FOR I=1 TO M/4
2610   E2[I]=0
2620 NEXT I
2630 FOR I=1 TO N
2640   W2[I]=CPX(0,0)
2650 NEXT I
2660 FOR I=1 TO K
2670   REM Set up equalizer initially
2680   INVOKE "SETEQUAL"
2690   REM Set up initial tap weigths
2700   FOR J=1 TO N
2710     IF N2<3 OR N2>16 THEN 2760
2720     E=W0[J]
```

```
2730      INVOKE "ARITHM"
2740      W[J]=E
2750      GOTO 2770
2760      W[J]=WO[J]
2770    NEXT J
2780    REM Set up final fading parameters
2790    A1=1/MO
2800    FOR J=1 TO M
2810      IF J>1/A1 THEN 2850
2820      T3=(T2-T1)*J*A1+T1
2830      B3=(B2-B1)*J*A1+B1
2840      F3=(F2-F1)*J*A1+F1
2850      IF S$="y" THEN 2870
2860      IF (T3=TO) AND (B3=BO) AND (F3=FO) THEN 2920
2870      TO=T3,BO=B3,FO=F3
2880      REM Set up the channel again
2890      INVOKE "SETCHAN"
2900      REM Set up the pulse response again
2910      INVOKE "SETPULSE"
2920      REM Update the equalize & get the error response
2930      INVOKE "UPDATE"
2940      IF M>8000 THEN 2970
2950      E2[J]=(REA(E8)*REA(E8)+IMG(E8)*IMG(E8))+E2[J]
2960      GOTO 2990
2970      REM Since we haven't got enough memory, we used averaging for
2980      E2[1/4+J/4]=(REA(E8)*REA(E8)+IMG(E8)*IMG(E8))+E2[1/4+J/4]
2990    NEXT J
3000    REM Update average Tap weight
3010 FOR J=1 TO N
3020    W2[J]=W[J]+W2[J]
3030 NEXT J
3040 REM Monitor the status
3050 PRINT I,DAT$(1,27)
3060 NEXT I
3070 REM Get the average data
3080 FOR I=1 TO N
3090    W2[I]=W2[I]/K
3100    IF N2<3 OR N2>16 THEN 3140
3110    E=W2[I]
3120    INVOKE "ARITHM"
3130    W2[I]=E
3140 NEXT I
3150 A1=K
3160 IF M>8000 THEN 3210
3170 FOR I=1 TO M
3180    E2[I]=E2[I]/K
3190 NEXT I
3200 GOTO 3240
3210 FOR I=1 TO M/4
3220    E2[I]=E2[I]/(4*K)
3230 NEXT I
3240 INVOKE "PLOT"
3250 A1=A2=0
3260 REM Get average power
3270 FOR I=1 TO 2*N6/S+1 STEP 1/S
3280    A1=A1+H[I]*CNJ(H[I])
3290 NEXT I
3300 IF S>.6 THEN 3340
3310 FOR I=2 TO 4*N6 STEP 2
3320    A2=A2+H[I]*CNJ(H[I])
3330 NEXT I
3340 PRINT
3350 PRINT " demodulation phase =";D5*360/PIX(2)
3360 PRINT " B =";A1," B1 =";A2
3370 PRINT " main lobe (h0) =";H[N6/S+1]
3380 PRINT " h1 =";H[(N6+1)/S+1]
```

```
 3390 PRINT " h-1  =";H[(N6-1)/S+1]
 3400 IF S>.6 THEN 3430
 3410 PRINT ".h1/2  =";H[2*N6+2]
 3420 PRINT " h-1/2  =";H[2*N6]
 3430 REM Get summation of W(i)W(i)*
 3440 A1=0
 3450 FOR I=1 TO N
 3460    A1=A1+W2[I]*CNJ(W2[I])
 3470 NEXT I
 3480 PRINT "Summation of tap weight square is =";A1
 3490 REM Get the average MSE for the last 50 interations
 3500 A1=M-49,A2=M
 3510 IF M>8000 THEN A1=M/4-249,A2=M/4
 3520 IF M<50 THEN A1=1
 3530 A3=0
 3540 FOR I=A1 TO A2
 3550    A3=E2[I]+A3
 3560 NEXT I
 3570 IF A3<1E-8 THEN A3=1E-8
 3580 A4=A2-A1+1
 3590 A1=10*(LOG(A3/A4)/LOG(10))
 3600 IF M<=8000 THEN 3630
 3610 PRINT "Average MSE for the last 1000 iterations os :";A1
 3620 GOTO 3640
 3630 PRINT "Average MSE for the last 50 iterations is :";A1
 3640 PRINT "Type y if you want to plot the spectrum of equalizer";
 3650 INPUT X$
 3660 IF X$="Y" THEN X$="y"
 3670 IF X$<>"y" THEN 3700
 3680 REM Plot Equalizer Spectrum
 3690 INVOKE "SPECTRUM"
 3700 FILES TAPS1
 3710 PRINT &
      "Type Y if you want to store this set of tap weigth in File TAPS1"&
      ;
 3720 INPUT T$
 3730 IF T$<>"y" AND T$<>"Y" THEN 3770
 3740 PRINT #1;"Tap weigths"
 3750 PRINT #1;N,S
 3760 PRINT #1;(FOR I=1 TO N,W2[I])
 3770 PRINT &
      "Type Y if you want to plot the constellation of the equalizer out&
put";
 3780 INPUT P$
 3790 IF P$<>"y" AND P$<>"Y" THEN 3810
 3800 INVOKE "CONSTEL"
 3810 END
>
```

```
INPUT
   100 REM This module will set up all the input parameters
   110 REM for the main program EQUALIZE
   120 REM
   200 REM Common area (1) is the channel & filter parameters
   210 COM(1) R$,C,M$,T1,T2,B1,B2,F1,F2
   220 REM Common area (2) is the equalizer parameters
   230 COM(2) INTEGER N,REAL S,COMPLEX WO[*],W[*],L$,A$,U,INTEGER M,MO,K&
      ,G$
   240 REM Common area (3) is the phase angles & bit arithmetics paramete
   250 COM(3) O$,REAL O1,S$,INTEGER S1,N1,N2,REAL N3
   260 REM R$ is the radio system
   270 REM C is the raised cosine filter parameter
   280 REM M$ is the multipath fading model
   290 REM T1 & T2 are the initial & final condition of the multipath
   300 REM delay time
   310 REM B1 & B2 are the initial & final condition of the amplitude of
   320 REM the multipath
   330 REM F1 & F2 are the initial & final condition of the notch offset
   340 REM frequencies
   350 REM N$ is the title of the File
   360 REM N, S is the number of taps & tap spacing
   370 REM WO(*) & W(*) are the initial tap weigth & adaptive tap weigth
   380 REM L$ is the equalizer adaptive mode
   390 REM A$ is the equalization algorithm
   400 REM U is the convergence factor
   410 REM M is the number of iteration
   415 REM MO is the number of iteration for the final fading parameters
   420 REM K is the number of ensemble average
   430 REM G$ is the flag for auto-gain control at receiver i/p
   440 REM O$ is constant phase cancelling
   450 REM O1 is the initial demodulation phase offset
   460 REM S$ is the sampling phase adjustment
   470 REM S1 is the initial sampling angle
   480 REM N1 & N2 are the number of bits in ADC & Tap Weight
   485 REM N3 is the range of tap weigth arithmetics
   490 FILES TAPS1
   800 INTEGER I
  1000 PRINT "Type 1 for 70Mb/s (70MHz) QPSK"
  1010 PRINT "      2 for 90Mb/s (22.6MHz) 16QAM"
  1020 PRINT "      3 for 135Mb/s (22.6MHz) 64QAM"
  1030 PRINT " otherwise 180Mb/s (22.6MHz) 256QAM will be used.";
  1040 INPUT R$
  1050 IF R$<>"1" AND R$<>"2" AND R$<>"3" THEN R$="4"
  1060 PRINT "The overall raised cosine filter a [0-1]";
  1070 INPUT C
  1080 IF C<0 OR C>1 THEN 1060
  1090 PRINT &
      "Type 2 for the 2-ray model, otherwise 3-ray model will be used.";
  1100 INPUT M$
  1110 T1=T2=0,B1=B2=0,F1=F2=0
  1120 PRINT &
      "Type Y if you want to set up the initial condition of the channel&
,"
  1130 PRINT &
      "otherwise the channel transfer function is assumed to be 1 + j0";
  1140 INPUT I$
  1150 IF I$="Y" THEN I$="y"
  1160 IF I$<>"y" THEN 1190
  1170 PRINT "The initial delay time of the multipath ray (ns)";
  1180 INPUT T1
  1190 PRINT "The final delay time of the multipath ray (ns)";
  1200 INPUT T2
  1210 IF I$<>"y" THEN 1240
  1220 PRINT "The initial amplitude of the multipath ray ( b )";
  1230 INPUT B1
```

```
1240 PRINT "The final amplitude of the multipath ray ( b )";
1250 INPUT B2
1260 IF M$="2" THEN 1310
1270 PRINT "The initial offsets of the notch frequency (MHz)";
1280 INPUT F1
1290 PRINT "The final offsets of the notch frequency (MHz)";
1300 INPUT F2
1310 PRINT &
    "Type Y if you want to use the tap value stores in File 'TAPS1'";
1320 INPUT T$
1330 IF T$="Y" THEN T$="y"
1340 IF T$<>"y" THEN 1390
1350 READ #1;N$
1360 READ #1;N,S
1370 READ #1;(FOR I=1 TO N,WO[I])
1380 GOTO 1620
1390 PRINT "Input number of Taps [1-32]";
1400 INPUT N
1410 IF N<1 OR N>32 THEN 1390
1420 PRINT "Type Y if T/2 tap spacing is used";
1430 INPUT P$
1440 S=1
1450 IF P$="Y" OR P$="y" THEN S=.5
1460 FOR I=1 TO N
1470   WO[I]=(0,0)
1480 NEXT I
1490 PRINT &
    "Type Y if you want to preset the tap weigth, otherwise all zero"
1500 PRINT "will be used initially";
1510 INPUT P$
1520 IF P$<>"Y" AND P$<>"y" THEN 1620
1530 PRINT "Type Y if you only want to preset (1,0) at the center tap"&
    ;
1540 INPUT P$
1550 IF P$<>"Y" AND P$<>"y" THEN 1580
1560 WO[N/2]=(1,0)
1570 GOTO 1620
1580 FOR I=1 TO N
1590   PRINT "W (   ";I;")=";
1595   INPUT A1,A2
1600   WO[I]=CPX(A1,A2)
1610 NEXT I
1620 PRINT &
    "Type Y if decision direct method is used, otherwise a separated"
1630 PRINT "training signal will be used";
1640 INPUT L$
1650 IF L$="Y" THEN L$="y"
1660 PRINT &
    "Type Y if Zero Forcing Algorithm is used, otherwise normal LMS"
1670 PRINT "Gradient Algorithm will be used";
1680 INPUT A$
1690 IF A$="Y" THEN A$="y"
1700 PRINT "Input Convergence factor [0-1]";
1710 INPUT U
1720 IF U<0 THEN U=0
1730 IF U>1 THEN U=1
1740 PRINT "Input number of iteration [1-32000]";
1750 INPUT M
1760 IF M<1 OR M>32000 THEN 1740
1770 PRINT &
    "Input the number of iteration for which final fading occurred";
1780 INPUT MO
1790 IF MO<1 OR MO>M THEN 1770
1800 PRINT "Input number of ensemble average";
1810 INPUT K
1820 IF K<1 THEN K=1
```

```
1830 PRINT &
    "Type Y if you want to insert auto-gain control at receiver input"&
    ;
1840 INPUT G$
1850 IF G$="Y" THEN G$="y"
1860 PRINT &
    "Type Y if you want to eliminate the constant phase offset,"
1870 PRINT "otherwise no attempt will be made to cancel it";
1880 INPUT O$
1890 IF O$="Y" THEN O$="y"
1900 O1=0
1910 IF O$="y" THEN 1940
1920 PRINT "Demodulation phase angle (degree)";
1930 INPUT O1
1940 PRINT "Type 1 if sample phase is adjusted by algorithm 1,"
1950 PRINT "otherwise no adjustment will be made";
1960 INPUT S$
1970 IF S$="Y" THEN S$="y"
1980 PRINT "Initial sampling angle (degree)";
1990 INPUT S1
2000 PRINT &
    "Input number of bits in sampler from 3 to 12, otherwise computer"
2010 PRINT "resolution will be used";
2020 INPUT N1
2030 PRINT &
    "Input number of bits in tap weight from 3 to 16, otherwise"
2040 PRINT "computer resolution will be used";
2050 INPUT N2
2060 N3=2
2070 IF N2<3 OR N2>16 THEN 2110
2080 PRINT &
    "Input the max range of the arithmetics, type 0 if automatic";
2090 PRINT &
    "(if autu-gain used, used 2 to 3 for low & deep fading resp.)";
2100 INPUT N3
2110 END
```

```
SETFILR
  100 REM This module will set up the raised cosine filter in D(128)
  120 REM
  200 REM Common area (1) is the channel & filter parameters
  210 COM(1) R$,C,M$,T1,T2,B1,B2,F1,F2
  220 REM R$ is the radio system
  230 REM C is the raised cosine filter parameter
  240 REM M$ is the multipath fading model
  250 REM T1 & T2 are the initial & final condition of the multipath
  260 REM delay time
  270 REM B1 & B2 are the initial & final condition of the amplitude of
  280 REM the multipath
  290 REM F1 & F2 are the initial & final condition of the notch offset
  300 REM frequencies
  310 REM Common area (4) is the data for the raised cosine filter & FFT
  315 REM D2(128) is the freq response for the overall channel
  320 REM D1(128) is the data for performing FFT
  330 REM D(128) is the frequency data for raised cosine filter
  340 REM P1 is number of points/symbol in time domain
  350 REM P2 is total number of points in FFT
  360 COM(4) COMPLEX D[*],COMPLEX D1[*],COMPLEX D2[*],INTEGER P1,&
      INTEGER P2
  370 REM A1,A2,A3,A4,A5,A6 are temporary variables
  380 REM I is used as a counter
  390 INTEGER I
 1000 A1=PIX(1)*(1-C)
 1010 A2=PIX(1)*(1+C)
 1020 A3=PIX(2*P1)/P2
 1030 A4=A5=0
 1040 IF C=0 THEN 1070
 1050 A4=A3/(4*C)
 1060 A5=PIX(1)*(1-C)/(4*C)
 1070 D[1]=CPX(1,0)
 1080 D[P2/2+1]=(0,0)
 1090 FOR I=2 TO P2/2
 1100    A6=(I-1)*A3
 1110    IF A6>=A1 THEN 1140
 1120    D[P2-I+2]=D[I]=CPX(1,0)
 1130    GOTO 1190
 1140    IF A6>=A2 THEN 1180
 1150    A6=COS(A4*(I-1)-A5)
 1160    D[P2-I+2]=D[I]=CPX(A6*A6,0)
 1170    GOTO 1190
 1180    D[P2-I+2]=D[I]=CPX(0,0)
 1190 NEXT I
 1200 END
```

```
SETCHAN
  100 REM This module will first set up the channel parameter and then
  110 REM perform a FFT to get the impulse response in D1(128)
  120 REM
  200 REM Common area (4) is the data for the raised cosine filter & FFT
  210 REM D2(128) is the overall channel freq response
  220 REM D1(128) is the data for performing FFT
  230 REM D(128) is the frequency data for raised cosine filter
  240 REM P1 is the number of points/symbol in time domain
  250 REM P2 is the total number of points for FFT
  260 COM(4) COMPLEX D[*],COMPLEX D1[*],COMPLEX D2[*],INTEGER P1,&
      INTEGER P2
  270 REM Common area(5) is the channel parameters for FFT
  280 COM(5) F5,S5,D$,D5,P5,T0,B0,F0
  290 REM F5 is the frequncy step
  300 REM S5 is the multipath model
  310 REM D$ is the constant demodulation angle cancelling flag
  320 REM D5 is the constant demodution angle in term of rad/s
  330 REM P5 is the sampling phase in terms of delay time
  340 REM T0, B0, F0 are the multipath parameters
  350 REM I,J are used as counter
  360 REM k,l,m,p are temporary variables
  370 INTEGER I,J,K,L,M,P
  380 REM J1,J2 are looping constant
  390 INTEGER J1,J2
  400 REM T & W are complex variables for FFT
  410 COMPLEX T,W
  420 REM A1, A2 are temporary variables
 1000 REM Add the channel response
 1010 J2=1,D=D5
 1020 IF D$="y" THEN J2=2,D=0
 1030 FOR J1=1 TO J2
 1040   F=-F5*PIX(2)*.001*T0
 1050   B=S5*B0
 1060   D=-F0*PIX(2)*.001*T0
 1070   FOR I=1 TO P2/2
 1080     A1=(I-1)*F-D
 1090     T=CPX(1+B*COS(A1),B*SIN(A1))
 1100     D1[I]=D[I]*T
 1110   NEXT I
 1120   FOR I=P2 TO P2/2-1 STEP -1
 1130     A1=(I-P2-1)*F-D
 1140     T=CPX(1+B*COS(A1),B*SIN(A1))
 1150     D1[I]=D[I]*T
 1160   NEXT I
 1170   REM Add the demodulation phase & sampling phase
 1180   F=F5*PIX(2)*.001*P5
 1190   FOR I=1 TO P2/2
 1200     A1=(I-1)*F+D
 1210     T=CPX(COS(A1),-SIN(A1))
 1220     D1[I]=D1[I]*T
 1230   NEXT I
 1240   FOR I=P2 TO P2/2-1 STEP -1
 1250     A1=(I-P2-1)*F+D
 1260     T=CPX(COS(A1),-SIN(A1))
 1270     D1[I]=D1[I]*T
 1280   NEXT I
 1290   FOR I=1 TO P2
 1300     D2[I]=D1[I]
 1310   NEXT I
 1320   GOSUB 4000
 1330   IF J2<1.5 OR J1>1.5 THEN 1450
 1340   D5=ATN(D1[1])
```

```
1440    D=D5
1450  NEXT J1
1990  END
4000  REM Perform FFT here
4010  REM The pulse response will be restored in D1(128)
4020  J=1
4030  FOR I=1 TO P2
4040    IF I>=J THEN 4080
4050    T=D1[J]
4060    D1[J]=D1[I]
4070    D1[I]=T
4080    REM implement j=j+1, bit reversed count
4090    M=P2/2
4100    IF J<=M THEN 4140
4110    J=J-M
4120    M=M/2
4130    GOTO 4100
4140    J=J+M
4150  NEXT I
4160  L=1
4170  IF L>=P2 THEN 4310
4180  K=2*L
4190  FOR I=1 TO L
4200    A1=PIX(1)*(I-1)/L
4210    W=CPX(COS(A1),SIN(A1))
4220    FOR J=I TO P2 STEP K
4230      P=J+L
4240      T=W*D1[P]
4250      D1[P]=D1[J]-T
4260      D1[J]=D1[J]+T
4270    NEXT J
4280  NEXT I
4290  L=K
4300  GOTO 4170
4310  A1=P1*1/P2
4320  FOR I=1 TO P2
4330    D1[I]=D1[I]*A1
4340  NEXT I
4350  RETURN
```

```
SETPULSE
  100 REM This module will output a proper pulse response in H(65)
  110 REM with the first data corresponds to last post-echoe.
  120 REM The spacing in H(65) follows the equalizer spacing
  130 REM
  140 REM REV:01                23 Feb 86
  150 REM
  160 REM Add small offset at M6 for the ease of quantization definition
  170 REM
  200 REM Common area (2) is the equalize parameters
  210 COM(2) INTEGER N,REAL S,COMPLEX WO[*],W[*],L$,A$,U,INTEGER M,MO,K&
      ,G$
  220 REM only S & G$ are used in this module, S dihines the tap
  230 REM spacing & G$ defines the auto-gain control
  240 REM Common area (4) is the data for the raised cosine filter & FFT
  245 REM D2(*) is the freq response of the overall channel
  250 REM D1(128) is the data for performing FFT
  260 REM D(128) is the frequency data for raised cosine filter
  270 REM P1 is the number of points/symbol in time domain
  280 REM P2 is the total number of points for FFT
  290 COM(4) COMPLEX D[*],COMPLEX D1[*],COMPLEX D2[*],INTEGER P1,&
     INTEGER P2
  300 REM Common area (6) is the pulse response
  310 COM(6) COMPLEX H[*],INTEGER N6,REAL M6,REAL R6
  320 REM H(65) is the array for pulse response
  330 REM N6 is the number of pre-echoes & post-echoes to be considered
  340 REM M6 is the maximum sampling data
  350 REM R6 is the amplitude of the main lobe
  800 INTEGER I
 1000 REM This module tries to optmize the speed instead of program size
 1010 IF S<.6 THEN 1100
 1020 REM Perform T space pulse response
 1030 FOR I=1 TO N6+1
 1040    H[I]=D1[(N6-I)*2+3]
 1050 NEXT I
 1060 FOR I=2 TO N6+1
 1070    H[N6+I]=D1[P2-2*I+3]
 1080 NEXT I
 1090 GOTO 1170
 1100 REM Perform T/2 pulse response
 1110 FOR I=1 TO 2*N6+1
 1120    H[I]=D1[2*N6-I+2]
 1130 NEXT I
 1140 FOR I=2 TO 2*N6+1
 1150    H[2*N6+I]=D1[P2-I+2]
 1160 NEXT I
 1170 REM Get the maximum sampling data & the main lobe data
 1180 M6=0,R6=0
 1190 IF S<.6 THEN 1260
 1200 REM Perform T equalizer
 1210 FOR I=1 TO 2*N6+1
 1220    M6=ABS(REA(H[I]))+ABS(IMG(H[I]))+M6
 1230 NEXT I
 1240 R6=H[N6+1]
 1250 GOTO 1370
 1260 REM Perform T/2 equalizer
 1270 A1=A2=0
 1280 FOR I=1 TO 4*N6+1 STEP 2
 1290    A1=ABS(REA(H[I]))+ABS(IMG(H[I]))+A1
 1300 NEXT I
 1310 FOR I=2 TO 4*N6 STEP 2
 1320    A2=ABS(REA(H[I]))+ABS(IMG(H[I]))+A2
 1330 NEXT I
 1340 M6=A1
 1350 IF A2>M6 THEN M6=A2
 1360 R6=H[2*N6+1]
```

```
1370 REM Set up auto-gain for the pulse response if necessary
1380 REM Add small offsets for the ease of quantization definition
1390 REM Refer to file QUANTIZE
1400 REM Old Program -- IF G$<>"Y" THEN 1490
1410 A1=2*N6+1
1420 IF S<.6 THEN A1=4*N6+1
1430 A2=1/M6
1435 IF G$<>"y" THEN A2=1/REA(H[A1/2])
1440 FOR I=1 TO A1
1450   H[I]=H[I]*A2
1460 NEXT I
1470 R6=R6*A2
1480 M6=1
1490 END
```

```
SETEQUAL
  100 REM This module will set up the sample data array for the
  110 REM receiver in G(165). The transmit random data in stored in
  120 REM T(100). The lower index implies a newer data in time domain.
  130 REM
  200 REM Comm area 0 is for tap arithmetics
  210 COM COMPLEX E,REAL M1,M2,M3,M4,M5
  220 REM M1-5 are the parameters for calculations
  230 REM E is the entry variables for bit slice
  240 REM Common area (2) is the equalize parameters
  250 COM(2) INTEGER N,REAL S,COMPLEX W0[*],W[*],L$,A$,U,INTEGER M,M0,K&
     ,G$
  260 REM N is the number of taps
  270 REM S is the spacing parameters
  280 REM The rest variables of common area 2 are not used
  290 REM Common area (4) is the data for the raised cosine filter & FFT
  295 REM D2(*) is the freq response of the overall channel
  300 REM D1(128) is the data for performing FFT
  310 REM D(128) is the frequency data for raised cosine filter
  320 REM P1 is the number of points/symbol in time domain
  330 REM P2 is the total number of points for FFT
  340 REM Common area (3) is the phase & arithmetics parameters
  350 COM(3) D$,REAL D1,S$,INTEGER S1,N1,N2,REAL N3
  360 REM N1 is the quantization levels
  370 REM the rest variables are not used
  380 COM(4) COMPLEX D[*],COMPLEX D1[*],COMPLEX D2[*],INTEGER P1,&
     INTEGER P2
  390 REM Common area (6) is the pulse response
  400 COM(6) COMPLEX H[*],INTEGER N6,REAL M6,REAL R6
  410 REM H(65) is the array for pulse response
  420 REM N6 is the number of pre-echoes & post-echoes to be considered
  430 REM M6 is the maximum sampling data
  440 REM R6 is the amplitude of the main lobe
  450 REM Common area (7) is for transmit & receive data
  460 COM(7) COMPLEX G[*],COMPLEX T[*],COMPLEX R7,INTEGER I7
  470 REM G(*) is the receive data after the sampler
  480 REM T(*) is the transmit data at transmitter
  490 REM R7 is the random data
  500 REM I7 is the maximum level value of equalizer
  800 REM A1,A2,A3 are temporary variables
  810 REM I,J,L are temporary variables
  820 INTEGER I,J,L
 1000 REM Initialize G(*) first
 1010 FOR I=1 TO 4*N6/S+N
 1020    G[I]=CPX(0,0)
 1030 NEXT I
 1040 FOR I=N+N6*2 TO 1 STEP -1
 1050    INVOKE "RANDOM"
 1060    T[I]=R7
 1070    FOR J=1 TO 2*N6/S+1
 1080       G[J]=H[J]*T[I]+G[J]
 1090    NEXT J
 1100    REM Shift G(*) data by 1 symbol
 1110    INVOKE "SHIFTG"
 1120 NEXT I
 1130 IF N1<3 OR N1>12 THEN 1230
 1140 REM Perform the quantization here
 1180 FOR I=2*N6/S+2 TO (2*N6/S+N)
 1190    E=G[I]
 1200    INVOKE "QUANTIZE"
 1210    G[I]=E
 1220 NEXT I
 1230 REM Shift the Transmit data by 1 symbol
 1240 INVOKE "SHIFTT"
 1250 END
```

```
SHIFTT
  100 REM This module will shift the T(*) data by 1 symbol
  110 REM
  200 REM Common area (2) is the equalize parameters
  210 COM(2) INTEGER N,REAL S,COMPLEX WO[*],W[*],L$,A$,U,INTEGER M,MO,K&
     ,G$
  220 REM N is the number of taps
  230 REM S is the spacing parameters
  240 REM All the rest vraiables in common area (2) are not used
  320 COM(6) COMPLEX H[*],INTEGER N6,REAL M6,REAL R6
  330 REM H(65) is the array for pulse response
  340 REM N6 is the number of pre-echoes & post-echoes to be considered
  350 REM M6 is the maximum sampling data
  360 REM R6 is the amplitude of the main lobe
  370 REM Common area (7) is for transmit & receive data
  380 COM(7) COMPLEX G[*],COMPLEX T[*],COMPLEX R7,INTEGER I7
  390 REM G(*) is the receive data after the sampler
  400 REM T(*) is the transmit data at transmitter
  410 REM R7 is the random data
  420 REM I7 is the maximum level value of equalizer
 1000 REM Shift the transmit data by one symbol
 1010 FOR I=N+N6*2 TO 2 STEP -1
 1020   T[I]=T[I-1]
 1030 NEXT I
 1040 END
```

```
SHIFTG :
  100 REM This module will shift the G(*) data by 1 symbol
  110 REM
  200 REM Common area (2) is the equalize parameters
  210 COM(2) INTEGER N,REAL S,COMPLEX WO[*],W[*],L$,A$,U,INTEGER M,MO,K&
     ,G$
  220 REM N is the number of taps
  230 REM S is the spacing parameters
  240 REM The rest parameters are not used
  320 COM(6) COMPLEX H[*],INTEGER N6,REAL M6,REAL R6
  330 REM H(65) is the array for pulse response
  340 REM N6 is the number of pre-echoes & post-echoes to be considered
  350 REM M6 is the maximum sampling data
  360 REM R6 is the amplitude of the main lobe
  370 REM Common area (7) is for transmit & receive data
  380 COM(7) COMPLEX G[*],COMPLEX T[*],COMPLEX R7,INTEGER I7
  390 REM G(*) is the receive data after the sampler
  400 REM T(*) is the transmit data at transmitter
  410 REM R7 is the random data
  420 REM I7 is the maximum level value of equalizer
 1000 REM Shift the sampling data G(*) by one symbol
 1010 IF S<.6 THEN 1080
 1020 REM Here is the T space equalizer
 1030 FOR I=N+4*N6 TO 2 STEP -1
 1040   G[I]=G[I-1]
 1050 NEXT I
 1060 G[1]=CPX(0,0)
 1070 GOTO 1130
 1080 REM Here is the T/2 equalizer
 1090 FOR I=N+8*N6 TO 3 STEP -1
 1100   G[I]=G[I-2]
 1110 NEXT I
 1120 G[1]=G[2]=CPX(0,0)
 1130 END
```

```
RANDOM
  100 REM This module will output a random data, the number of
  120 REM levels depend on the radio system
  130 REM
  200 REM Common area (0) is for arithmetics
  210 COM COMPLEX E,REAL M1,M2,M3,M4,M5
  220 REM M1-5 are the parameters for calculations
  230 REM E is the entry varible for bit slice
  240 REM Common area 3 is the phase and arithmetics parameters
  250 COM(3) O$,REAL O1,S$,INTEGER S1,N1,N2,REAL N3
  260 REM N2 is the number of quantization level in arithmetics
  270 REM The rest of parameters is not used in this program
  280 REM Common area (7) is for transmit & receive data
  290 COM(7) COMPLEX G[*],COMPLEX T[*],COMPLEX R7,INTEGER I7
  300 REM G(*) is the receive data after the sampler
  310 REM T(*) is the transmit data at transmitter
  320 REM R7 is the random data
  330 REM I7 is the maximum level value of radio
  800 REM A1,X1,Y1 are temporary variables
  810 INTEGER X1,Y1
 1000 X1=(I7+1)*(RND(1)-.999999/(2+I7+I7))
 1010 Y1=(I7+1)*(RND(1)-.999999/(2+I7+I7))
 1020 X1=2*(X1-I7/2)
 1030 Y1=2*(Y1-I7/2)
 1040 R7=CPX(X1,Y1)
 1050 IF N2<3 OR N2>16 THEN 1100
 1060 IF N2>10.5 THEN 1100
 1070 X1=REA(R7)*M5
 1080 Y1=IMG(R7)*M5
 1090 R7=CPX(X1,Y1)/M5
 1100 R7=R7
 1110 END
```

```
ARITHM
  100 REM This module is used for tap weigth arithmetics
  110 REM
  200 REM Comm area 0 is for tap arithmetics
  210 COM COMPLEX E,REAL M1,M2,M3,M4,M5
  220 REM M1-5 are the parameters for calculations
  230 REM E is the entry variables for bit slice
  240 REM Common area(3) is the phase & arithmetics parameters
  250 COM(3) O$,REAL O1,S$,INTEGER S1,N1,N2,REAL N3
  260 REM O$ is constant phase cancelling
  270 REM O1 is the initial demodulation angle
  280 REM S$ is the sampling phase adjustment
  290 REM S1 is the initial sampling angle
  300 REM N1 & N2 are the number of bits in ADC & Tap Weight
  310 REM N3 is the range of the arithmetics
  320 REM Common area (8) is for error & error count
  330 COM(8) COMPLEX E8,INTEGER W8,O8
  340 REM O8 is the overflow count
  350 REM E8 & W8 are not used in this module
  800 REM I,J are temparory variables
  810 INTEGER I,J
 1000 I=REA(E)*M5
 1010 J=IMG(E)*M5
 1020 E=CPX(I,J)/M5
 1030 REM Use +-N3 as overflow detect (it may not be appropriated)
 1040 IF ABS(REA(E))<N3 THEN 1070
 1050 IF O8<32000 THEN O8=O8+1
 1060 IF REA(E)<-N3 THEN E=CPX(-N3,IMG(E))
 1070 IF ABS(IMG(E))<N3 THEN 1100
 1080 IF O8<32000 THEN O8=O8+1
 1090 IF IMG(E)<-N3 THEN E=CPX(REA(E),-N3)
 1100 IF REA(E)>=N3 THEN E=CPX(REA(M4),IMG(E))
 1110 IF IMG(E)>=N3 THEN E=CPX(REA(E),IMG(M4))
 1120 END
```

```
QUANTIZE
  100 REM This module is used for quantization
  110 REM
  200 REM Comm area 0 is for tap arithmetics
  210 COM COMPLEX E,REAL M1,M2,M3,M4,M5
  220 REM M1-5 are the parameters for calculations
  230 REM E is the entry variables for bit slice
  800 REM I,J are temparory variables
  810 INTEGER I,J
 1000 I=(REA(E)+M2)*M1
 1010 J=(IMG(E)+M2)*M1
 1020 E=(CPX(I,J)-CPX(M3,M3))/M1
 1030 END
```

```
UPDATE
  100 REM This module is for equalizer updating
  110 REM
  200 REM Comm area 0 is for tap arithmetics
  210 COM COMPLEX E,REAL M1,M2,M3,M4,M5
  220 REM M1-5 are the parameters for calculations
  230 REM E is the entry variables for bit slice
  240 REM Common area(2) is the equalizer parameters
  250 COM(2) INTEGER N,REAL S,COMPLEX WO[*],W[*],L$,A$,U,INTEGER M,MO,K&
      ,G$
  260 REM N & S are the number of taps & tap spacing
  270 REM WO(*) & W(*) are the initial tap weigth & adaptive tap weigth
  280 REM L$ is the equalizer adaptive mode
  290 REM A$ is the equalization algorithm
  300 REM U is the convergence factor
  310 REM M is the number of iteration
  320 REM K is the number of ensemble average
  330 REM G$ is the auto-gain control at the receiver i/p
  340 REM P5 is the sampling phase in terms of delay time
  350 REM Com(6) is the pulse response paramters
  360 REM Common area (3) is the phase & arithmetics parametics
  370 COM(3) O$,REAL O1,S$,INTEGER S1,N1,N2,REAL N3
  380 REM N1 is the number of quantization levels
  390 REM the rest variables are not used
  400 COM(6) COMPLEX H[65],INTEGER N6,REAL M6,REAL R6
  410 REM N6 is the number of pre-echoes & post echoes to be considered
  420 REM Common area (7) is transmit & receive data
  430 REM M6 is the maximum sampling data
  440 REM R6 is the amptilude of the main lobe
  450 COM(7) COMPLEX G[*],COMPLEX T[*],COMPLEX R7,INTEGER I7
  460 REM G(165) is the receive data after sampler
  470 REM T(100) is the transmit data
  480 REM R7 is the random data generator
  490 REM I7 is the maximum level value of the radio
  500 REM Common area (8) is for equalizer response parameters
  510 COM(8) COMPLEX E8,INTEGER W8,O8
  520 REM E8 is the error of this iteration
  530 REM W8 is the number of desicion errors in decision direct mode
  540 REM O8 is the number of overflow
  800 REM A1, A1 are temporary variables
  810 REM I1,I2,X1,X2 are variables for decision direct
  820 INTEGER I1,I2,X1,X2
  830 REM SO is the equalize output
  840 COMPLEX SO
  850 REM I,J are integer variables
  860 INTEGER I,J
  870 REM PO is the position of the expected data
  880 INTEGER PO
 1000 REM Get the position of expected data
 1010 PO=N/2+N6
 1020 IF S<.6 THEN PO=(N+1)/4+N6
 1030 REM Get the random transmit data
 1040 INVOKE "RANDOM"
 1050 T[1]=R7
 1060 REM Transfer it into receive data through the channel
 1070 FOR I=1 TO 2*N6/S+1
 1080    G[I]=H[I]*T[1]+G[I]
 1090 NEXT I
 1100 REM Perform the quantization here
 1110 IF N1<3 OR N1>12 THEN 1200
 1120 E=G[2*N6/S+1]
 1130 INVOKE "QUANTIZE"
 1140 G[2*N6/S+1]=E
 1150 IF S>.6 THEN 1200
 1160 REM Perform one more quantization for T/2 equalizer
 1170 E=G[2*N6/S]
```

```
1180 INVOKE "QUANTIZE"
1190 G[2*N6/S]=E
1200 REM Get the equalizer response
1210 S0=0
1220 N8=2*N6
1230 IF S>.6 THEN 1290
1240 N8=4*N6
1250 I=N/2
1260 A=I/2
1270 I=I/2
1280 IF ABS(A-I)<.001 THEN N8=N8-1
1290 FOR I=1 TO N
1300    S0=S0+W[I]*G[N8+I]
1310 NEXT I
1320 IF L$<>"y" THEN 1440
1330 REM Here is the decision direct mode
1340 A1=REA(S0)
1350 GOSUB 4000
1360 X1=I2
1370 A1=IMG(S0)
1380 GOSUB 4000
1390 Y1=I2
1400 E8=S0-CPX(X1,Y1)
1410 IF (X1-REA(T[P0]))<>0 AND W8<32000 THEN W8=W8+1
1420 IF (Y1-IMG(T[P0]))<>0 AND W8<32000 THEN W8=W8+1
1430 GOTO 1460
1440 REM Here is the training mode
1450 E8=S0-T[P0]
1460 REM Set upper limit for the error
1470 IF ABS(REA(E8))>2 THEN E8=E8-CPX(REA(E8),0)+2*CPX(SGN(REA(E8)),0)
1480 IF ABS(IMG(E8))>2 THEN E8=E8-CPX(0,IMG(E8))+2*CPX(0,SGN(IMG(E8)))
1482 IF N2<3 OR N2>16 THEN 1490
1484 E=E8
1486 INVOKE "ARITHM"
1487 E8=E
1490 IF A$="y" THEN 1550
1500 REM Here is the normal LMS Gradient Algorithm
1510 FOR I=1 TO N
1520    W[I]=W[I]-U*CNJ(G[N8+I])*E8
1530 NEXT I
1540 GOTO 1610
1550 REM Here is the Zero Forcing Algorithm
1560 FOR I=1 TO N
1570    A1=SGN(REA(E8))*SGN(REA(G[N8+I]))+SGN(IMG(E8))*SGN(IMG(G[N8+I]))&
     )
1580    A2=SGN(REA(G[N8+I]))*SGN(IMG(E8))-SGN(IMG(G[N8+I]))*SGN(REA(E8))&
     )
1590    W[I]=W[I]-U*CPX(A1,A2)
1600 NEXT I
1610 REM Add tap arithmetics if necessary
1620 IF N2<3 OR N2>16 THEN 1680
1630 FOR I=1 TO N
1640    E=W[I]
1650    INVOKE "ARITHM"
1660    W[I]=E
1670 NEXT I
1680 REM Shift G(*) & T(*) by 1 symbol
1690 INVOKE "SHIFTG"
1700 INVOKE "SHIFTT"
1710 END
4000 REM Perform bit slice for decision direct mode
4010 IF A1=0 THEN A1=-1E-77
4020 IF ABS(A1)<17 THEN 4050
4030 I2=17
4040 GOTO 4080
4050 I1=(ABS(A1)-1)/2
```

```
4060 I2=2*I1+1
4070 IF I2>I7 THEN I2=I7
4080 I2=I2*SGN(A1)
4090 RETURN
```

```
PLOT
   100 REM This module will set up the autoplot facilities of 2648A graph
   110 REM terminal.
   120 REM
   200 REM Common area(1) is the channel & filter parameters
   210 COM(1) R$,C,M$,T1,T2,B1,B2,F1,F2
   220 REM Common area(2) is the equalizer parameters
   230 COM(2) INTEGER N,REAL S,COMPLEX WO[*],W[*],L$,A$,U,INTEGER M,MO,K&
      ,G$
   240 REM Common area(3) is the phase & arithmetics parameters
   250 COM(3) O$,REAL O1,S$,INTEGER S1,N1,N2,REAL N3
   260 REM R$ is the radio system
   270 REM C is the raised cosine filter paramter
   280 REM M$ is the multipath fading model
   290 REM T1 & T2 are the initial & final condition of the multipath
   300 REM delay time
   310 REM B1 & B2 are the initial & final condition of the amplitude of
   320 REM the multipath
   330 REM F1 & F2 are the initial & final condition of the notch offset
   340 REM frequencies
   350 REM N$ is the title of the File
   360 REM N and S are the number of taps & tap spacing
   370 REM WO(32) and W(32) are the initial & adaptive tap weigths
   380 REM L$ is the equalizer adaptive mode
   390 REM A$ is the equalization algorithm
   400 REM U is the convergence factor
   410 REM M is the number of iteration
   420 REM K is the number of ensemble average
   430 REM G$ is the auto-gain control at the receiver input
   440 REM O$ is constant phase cancelling
   450 REM O1 is the initial demodulation angle
   460 REM S$ is the sampling phase adjustment
   470 REM S1 is the initial sampling angle
   480 REM N1 & N2 are the number of bits in ADC & Tap Weight
   490 REM N3 is the range of the arithmetics
   500 COM(8) COMPLEX E8,INTEGER W8,O8
   510 REM E8 is the error at equalizer output
   520 REM W8 is the number of wrong decisions in decision direct mode
   530 REM o8 is the number of overflow in tap weigth iteration
   540 REM Common area (9) is the avarage error & tap weight for plotting
   550 COM(9) E2[*],COMPLEX W2[*]
   560 REM E2(*) is the avarage error array
   570 REM W2(*) is the average tap weigth
   800 REM P1, P2 & P3 strings are radio, filter & channel model resp.
   810 DIM P1$[50],P2$[25],P3$[25]
   820 REM A1$ & A2$ are for the equalizer mode & algorithm
   830 DIM A1$[50],A2$[50]
   840 REM P4$ string is for equalizer
   850 DIM P4$[75]
   860 REM A1 & A2 are plotting variables
   870 INTEGER A1,A2
   875 REM X0-4, Y0-4 are the co-odinates of writing text
   880 INTEGER X0,X1,X2,X3,X4,Y0,Y1,Y2,Y3,Y4
   890 REM Z1-8 are for auto-plot
   900 INTEGER Z1,Z2,Z3,Z4
   905 REM C$ is the clear graphic flag
   910 REM Z$ is input string flag
   920 REM H$ is the input string
   930 DIM H$[50]
   940 REM C9 is the curve number
   950 INTEGER C9
  1000 REM Set up radio string -- P1$
  1010 P1$="180Mb/s 256QAM radio with"
  1020 IF R$="1" THEN P1$="70Mb/s QPSK radio with"
  1030 IF R$="2" THEN P1$="90Mb/s 16QAM radio with"
  1040 IF R$="3" THEN P1$="135Mb/s 64QAM radio with"
```

```
1050 REM Set up filter string -- P2$
1060 P2$="raised cosine filter"
1070 REM Set up channel model string -- P3$
1080 P3$="(3-ray)"
1090 IF M$="2" THEN P3$="(2-ray)"
1100 PRINT '27"*m1m1npQ"
1102 PRINT "Type y if you want to clear the existing graphic display";
1104 INPUT C$
1105 IF C$="y" OR C$="Y" THEN 1110
1107 PRINT '27"*dc70,360oksG"
1108 GOTO 1120
1110 PRINT '27"*da70,360oksG"
1120 PRINT P1$;
1130 IF C<>1 AND C<>0 THEN 1170
1140 IF C=1 THEN PRINT " 1.0 ";
1150 IF C=0 THEN PRINT " 0.0 ";
1160 GOTO 1200
1170 REM plot filter other than 0.0 or 1.0
1180 PRINT C;
1190 PRINT '27"*dc-50,0pkG";
1200 PRINT P2$;
1210 PRINT '27"*dc495,360okG"
1220 PRINT DAT$(1,27)
1230 PRINT '27"*dc70,20okG"
1240 PRINT "Performance of";
1250 PRINT N;
1260 PRINT '27"*dc-14,10pG";
1270 P4$=&
    "Tap (T complex) Transversal Equalizer under multipath fading "
1280 IF S>.6 THEN 1300
1290 P4$=&
    "Tap (T/2 complex) Transversal Equalizer under multipath fading "
1300 PRINT P4$;P3$
1310 PRINT '27"*dc70,10okG"
1320 IF D$<>"y" THEN 1350
1330 PRINT "demodulation phase : compensated";
1340 GOTO 1360
1350 PRINT "demodulation phase (degree) =";D1;
1360 PRINT '27"*dc310,10okG"
1370 IF S$<>"y" THEN 1400
1380 PRINT "; sampling phase : compensated"
1390 GOTO 1410
1400 PRINT "; sampling phase (degree) =";S1;
1402 REM readjust the pos. of the string, prev is 110,30
1410 PRINT '27"*dc270,30okG"
1420 PRINT " number of iterations"
1423 REM skip 1430-1470 temporary for thesis
1425 GOTO 1490
1430 PRINT '27"*dc300,30okG"
1433 REM skip 1440-1470 temporary
1440 A1$="decision direct with"
1450 IF L$<>"y" THEN A1$="separated training signal with"
1460 A2$="Zero Forcing Algorithm"
1470 IF A$<>"y" THEN A2$="LMS Gradient Algorithm"
1480 PRINT A1$;" ";A2$
1490 C9=1
1495 PRINT '27"*ddltG"
1500 PRINT &
    "Type y if you want to input a string for the curve, otherwise"
1510 PRINT "fading parameters will be plotted.";
1520 INPUT Z$
1530 IF Z$="y" OR Z$="Y" THEN Z$="Y"
1540 IF Z$<>"Y" THEN 1582
1550 PRINT "Input curve number";
1560 INPUT C9
1570 PRINT "Input Curve String";
```

```
1580 INPUT H$
1582 PRINT '27"*dskG"
1585 IF Z$="Y" THEN 2530
2000 X0=465,Y0=335
2010 PRINT '27"*dc";X0;Y0;"okG"
2020 A1=N1
2030 IF A1<3 OR A1>12 THEN A1=24
2040 PRINT A1;"bit ADC"
2050 PRINT '27"*dc";X0;Y0-10;"okG"
2060 A2=N2
2070 IF A2<3 OR A2>16 THEN A2=24
2080 PRINT A2;"bit arithmetics"
2090 X1=X0,Y1=Y0-30
2100 PRINT '27"*dc";X1;Y1;"okG"
2110 PRINT "      initial   final (";
2120 PRINT M0;
2130 A1=X1+182
2140 IF M0>999 THEN A1=A1+7
2150 PRINT '27"*dc";A1;Y1;"okG"
2160 PRINT ")"
2170 A1=100*B1,A2=100*B2
2180 PRINT '27"*dc";X1;Y1-10;"okG"
2190 PRINT " b : ";A1/100;
2200 PRINT '27"*dc";X1+112;Y1-10;"okG"
2210 PRINT A2/100
2220 A1=100*T1,A2=100*T2
2230 PRINT '27"*dc";X1;Y1-20;"okG"
2240 PRINT " t : ";A1/100;
2250 PRINT '27"*dc";X1+112;Y1-20;"okG"
2260 PRINT A2/100
2270 IF M$="2" THEN 2350
2280 PRINT '27"*dc";X1;Y1-30;"okG"
2290 A1=100*F1,A2=100*F2
2300 PRINT " f0: ";A1/100
2310 PRINT '27"*dc";X1+112;Y1-30;"okG"
2320 PRINT A2/100
2330 X2=X1,Y2=Y1-50
2340 GOTO 2360
2350 X2=X1,Y2=Y1-40
2360 PRINT '27"*dc";X2;Y2;"okG"
2370 IF U<.3 THEN 2410
2380 A1=10000*U
2390 PRINT " Convergence Factor    :";A1/10000
2400 GOTO 2430
2410 A1=100000*U
2420 PRINT " Convergence Factor    :";A1/100000
2430 PRINT " No of ensemble av.    :";K
2440 IF G$<>"y" THEN 2460
2450 PRINT " auto-gain at receiver"
2460 X3=X2,Y3=Y2-30
2470 IF G$<>"y" THEN Y3=Y2-20
2480 PRINT '27"*dc";X3;Y3;"okG"
2490 IF L$<>"y" THEN 2510
2500 PRINT " No of wrong decision :";W8
2510 IF N2<3 OR N2>16 THEN 2530
2520 PRINT " No of overflow        :";O8
2530 PRINT '27"*m1m2nQ"
2540 PRINT '27"*dc30,125okG"
2550 PRINT "mean square error        (dB)"
2560 PRINT '27"*m1m1npQ"
2570 PRINT '27"*dcG"
2580 PRINT '27"*dtIG"
2590 REM Start Auto-plot here
2600 PRINT '27"*ddG"
2610 PRINT &
    "Input Yaxis(min) in terms of dB [-10 to -80] in 5dB steps, or typ&
```

```
e";
 2620 PRINT "0 if auto-scaling is required";
 2630 INPUT A2
 2640 Z4=0
 2650 IF A2=0 THEN 2740
 2660 A1=A2/5
 2670 PRINT &
      "Input Yaxis(max) in terms of dB [-40dB to 40dB] in 5dB steps"
 2680 PRINT &
      "( if it is >0, then better used 5dB if Yaxis(min) is -35dB, or"
 2690 PRINT "  10dB if Yaxis(min) is -25dB";
 2700 INPUT Z4
 2710 Z4=Z4/5
 2720 Z4=5*Z4
 2730 GOTO 2850
 2740 REM Find the minimum mean square error
 2750 M9=.1
 2760 REM Ignore the first 40 points for m>50
 2770 A1=1,A2=M
 2780 IF M>50 AND M<=8000 THEN A1=2*M/3
 2790 IF M>8000 THEN A1=M/6,A2=M/4
 2800 FOR I=A1 TO A2
 2810   IF E2[I]<M9 THEN M9=E2[I]
 2820 NEXT I
 2830 IF M9<1E-8 THEN M9=1E-8
 2840 A1=LOG(M9)*2/LOG(10)-.5
 2850 PRINT '27"*ad2h1i2j"
 2860 IF C9=1 THEN PRINT "1k"
 2861 IF C9=2 THEN PRINT "5k"
 2862 IF C9=3 THEN PRINT "6k"
 2863 IF C9=4 THEN PRINT "8k"
 2864 IF C9=5 THEN PRINT "3k"
 2865 IF C9=6 THEN PRINT "2k"
 2870 REM Get Xmin & Xmax
 2880 REM Trunc Xmax to the nearest 100
 2890 Z1=1
 2900 Z2=M/100+.499
 2910 Z2=Z2*100
 2920 REM Get Ymin to the nearest 5dB steps
 2930 Z3=5*A1
 2940 REM Get Ymax
 2950 Z4=Z4
 2960 REM Get Xlabel
 2970 Z5=25
 2980 IF Z2>=200 AND Z2<300 THEN Z5=50
 2990 IF Z2>=300 AND Z2<600 THEN Z5=100
 3000 IF Z2>=600 AND Z2<1500 THEN Z5=200
 3010 IF Z2>=1600 AND Z2<3500 THEN Z5=500
 3020 IF Z2>=3500 AND Z2<10000 THEN Z5=1000
 3030 IF Z2>=10000 AND Z2<20000 THEN Z5=2000
 3040 IF Z2>=20000 THEN Z5=5000
 3050 REM Get Xtic
 3060 Z6=Z5/5
 3070 REM Get Ylabel
 3080 Z7=5
 3090 IF (Z4-Z3)>=25 AND (Z4-Z3)<60 THEN Z7=10
 3100 IF (Z4-Z3)>=60 THEN Z7=20
 3110 REM Get Ytic
 3120 Z8=Z7/5
 3130 PRINT Z1;"l";Z2;"m";
 3140 PRINT Z3;"n";Z4;"o";
 3150 PRINT Z5;"p";Z6;"q";
 3160 PRINT Z7;"r";Z8;"s";
 3170 PRINT "OvOwcA"
 3180 IF M>8000 THEN 3270
 3190 FOR I=1 TO M
```

```
3200    IF E2[I]>1E-8 THEN 3230
3210    PRINT I,"-80"
3220    GOTO 3250
3230    A1=100*LOG(E2[I])/LOG(10)
3240    PRINT I,A1/10
3250 NEXT I
3260 GOTO 3340
3270 FOR I=1 TO M/4
3280    IF E2[I]>1E-8 THEN 3310
3290    PRINT 4*I-2,"-80"
3300    GOTO 3330
3310    A1=100*LOG(E2[I])/LOG(10)
3320    PRINT 4*I-2,A1/10
3330 NEXT I
3340 PRINT '27"*abG"
3350 PRINT '27"*aaA"
3360 REM skip the following 8 lines
3370 GOTO 3440
3380 FOR I=Z2/4 TO 2*Z2/5
3390    PRINT I,(Z4-Z3)/10
3400 NEXT I
3410 PRINT '27"*abG"
3420 PRINT '27"*dscG"
3430 PRINT "assdddf"
3440 REM Turn off auto-plot
3450 IF Z$<>"Y" THEN 3560
3460 A8=2,A9=3
3470 IF Z3<-28 THEN 3490
3480 A8=1.2,A9=2
3482 IF Z3<-18 THEN 3490
3485 A8=1,A9=1.5
3490 FOR I=.6*Z2 TO 3*Z2/4
3500    PRINT I,Z4-A9-(C9-1)*A8
3510 NEXT I
3520 PRINT '27"*abG"
3530 PRINT '27"*dcskG"
3540 PRINT '27"*ds10,16pG"
3550 PRINT H$
3560 PRINT '27"*abG"
3570 PRINT '27"*ddtG"
3580 PRINT '7'17
3590 PRINT " After ";M;"iterations and ";K;"ensemble average"
3600 FOR I=1 TO N
3610    PRINT "W (     ";I;")=";WO[I];W2[I]
3620 NEXT I
3630 REM PRINT '27"&p5uOC"
3640 END
```

```
SPECTRUM
  100 REM This program will calculate the spectrum of the equalizer
  110 REM The plotting routine is not available for the time being
  120 REM
  130 REM      REV: 00                        Date: 6/10/86
  140 REM
 1000 REM Common area(1) is the channel & filter parameters
 1010 COM(1) R$,C,M$,T1,T2,B1,B2,F1,F2
 1020 REM Common area(2) is the equalizer parameters
 1030 COM(2) INTEGER N,REAL S,COMPLEX W0[32],W[32],L$,A$,U,INTEGER M,M0&
     ,K,G$
 1040 REM Common area(3) is the phase & arithmetics parameters
 1050 COM(3) D$,REAL D1,S$,INTEGER S1,N1,N2,REAL N3
 1060 REM R$ is the radio system
 1070 REM C is the raised cosine filter paramter
 1080 REM M$ is the multipath fading model
 1090 REM T1 & T2 are the initial & final condition of the multipath
 1100 REM delay time
 1110 REM B1 & B2 are the initial & final condition of the amplitude of
 1120 REM the multipath
 1130 REM F1 & F2 are the initial & final condition of the notch offset
 1140 REM frequencies
 1150 REM N$ is the title of the File
 1160 REM N and S are the number of taps & tap spacing
 1170 REM W0(32) and W(32) are the initial & adaptive tap weigths
 1180 REM L$ is the equalizer adaptive mode
 1190 REM A$ is the equalization algorithm
 1200 REM U is the convergence factor
 1210 REM M is the number of iteration
 1220 REM K is the number of ensemble average
 1230 REM G$ is the auto-gain flag
 1240 REM D$ is constant phase cancelling
 1250 REM D1 is the initial demodulation angle
 1260 REM S$ is the sampling phase adjustment
 1270 REM S1 is the initial sampling angle
 1280 REM N1 & N2 are the number of bits in ADC & Tap Weight
 1290 REM N3 is the range of the arithmetics
 1300 REM Common area (4) is the data for the raised cosine filter & FFT
 1305 REM D2(*) is the freq response for the overall channel
 1310 REM D1(128) is the data for performing FFT
 1320 REM D(128) is the frequency data for raised cosine filter
 1330 REM P1 is the number of points/symbol in time domain
 1340 REM P2 is the total number of points for FFT
 1350 COM(4) COMPLEX D[*],COMPLEX D1[*],COMPLEX D2[*],INTEGER P1,&
    INTEGER P2
 1360 REM Common area(5) is the channel parameters for FFT
 1370 COM(5) F5,S5,D$,D5,P5,T0,B0,F0
 1380 REM F5 is the frequncy step
 1390 REM S5 is the multipath model
 1400 REM T0, B0, F0 are the multipath parameters
 1410 REM D$ is the flag for constant demodulation cancelling
 1420 REM D5 is the demodulation phase in terms of rad
 1430 REM P5 is the sampling phase in terms of delay time
 1440 REM Common area (9) is the avarage error & tap weight for plotting
 1450 COM(9) E2[8000],COMPLEX W2[32]
 1460 REM E2(*) is the avarage error array
 1470 REM W2(*) is the average tap weigth
 1480 REM H$ is the overall accuracies
 1490 REM I,J,L are counters
 1500 INTEGER I,J,L
 1510 INTEGER G1,G2,G3
 1525 REM A1-A9 are temporary variables
 1530 COMPLEX A1
 1535 REAL A2,A3,A4
 1550 REM D3(i) is the data for equalzier spectrum
 1560 REM D4(i) is the data for the overall channel spectrum
```

```
1570 REM d5(i) is the combined spectrum for equalizer and channel
1580 COMPLEX D3[128]
1590 COMPLEX D4[128]
1600 COMPLEX D5[128]
2000 REM Initialize the variables
2010 FOR I=1 TO P2
2020   D3=D4=D5=CPX(0,0)
2030 NEXT I
2040 REM Get the overall folded spectrum
2050 IF S<.6 THEN 2100
2060 FOR I=1 TO P2/2
2070   D4[I]=D2[I]+D2[I+P2/2]
2080 NEXT I
2090 GOTO 2130
2100 FOR I=1 TO P2
2110   D4[I]=D2[I]
2120 NEXT I
2130 REM Get the equalizer freq response
2140 FOR I=1 TO P2/(2*S)
2150   A1=CPX(0,0)
2160   FOR J=1 TO N
2170     A2=(J-(N+1)/2)*(I-1)*2*S*PIX(2)/P2
2180     A1=A1+W2[J]*CPX(COS(A2),-SIN(A2))
2190   NEXT J
2200   D3[I]=A1
2210 NEXT I
2220 REM Get the freq resp of equalizer and channel
2230 FOR I=1 TO P2/(2*S)
2240   D5[I]=D3[I]*D4[I]
2250 NEXT I
2260 PRINT
2270 PRINT &
    "  Channel          Equalizer          Combined            Group Delay"
2280 PRINT "                          SPECTRUM"
2290 PRINT
2300 A2=D3[1]*CNJ(D3[1])
2310 A3=D4[1]*CNJ(D4[1])
2320 A4=D5[1]*CNJ(D5[1])
2330 A5=ATN(IMG(D5[1])/REA(D5[1]))
2340 PRINT A3,A2,A4
2350 FOR I=2 TO P2/(2*S)
2360   A2=D3[I]*CNJ(D3[I])
2370   A3=D4[I]*CNJ(D4[I])
2380   A4=D5[I]*CNJ(D5[I])
2390   A6=A5
2400   A5=ATN(IMG(D5[I])/REA(D5[I]))
2410   PRINT A3,A2,A4,A6-A5
2420 NEXT I
2430 IF S>.6 THEN 2540
2440 REM Print folded spectrum of T/2 equalizer + channel
2450 PRINT
2460 PRINT
2470 PRINT "Fold spectrum of T/2 due to 1/T sampling rate"
2480 PRINT
2490 FOR I=1 TO P2/2
2500   D3[I]=D5[I]+D5[I+P2/2]
2510   A5=D3[I]*CNJ(D3[I])
2520   PRINT A5
2530 NEXT I
2540 END
```

```
CONSTEL
  100 REM This module plot the consellation of the equalizer output
  110 REM
  200 REM Comm area 0 is for tap arithmetics
  210 COM COMPLEX E,REAL M1,M2,M3,M4,M5
  220 REM M1-5 are the parameters for calculations
  230 REM E is the entry variables for bit slice
  240 REM Common area(1) is the channel & filter parameters
  250 COM(1) R$,C,M$,T1,T2,B1,B2,F1,F2
  260 REM Common area(2) is the equalizer parameters
  270 COM(2) INTEGER N,REAL S,COMPLEX WO[32],W[32],L$,A$,U,INTEGER M,MO&
      ,K,G$
  280 REM Common area(3) is the phase & arithmetics parameters
  290 COM(3) O$,REAL O1,S$,INTEGER S1,N1,N2,REAL N3
  300 REM R$ is the radio system
  310 REM C is the raised cosine filter paramter
  320 REM M$ is the multipath fading model
  330 REM T1 & T2 are the initial & final condition of the multipath
  340 REM delay time
  350 REM B1 & B2 are the initial & final condition of the amplitude of
  360 REM the multipath
  370 REM F1 & F2 are the initial & final condition of the notch offset
  380 REM frequencies
  390 REM N$ is the title of the File
  400 REM N and S are the number of taps & tap spacing
  410 REM WO(32) and W(32) are the initial & adaptive tap weigths
  420 REM L$ is the equalizer adaptive mode
  430 REM A$ is the equalization algorithm
  440 REM U is the convergence factor
  450 REM M is the number of iteration
  460 REM K is the number of ensemble average
  470 REM G$ is the auto-gain flag
  480 REM O$ is constant phase cancelling
  490 REM O1 is the initial demodulation angle
  500 REM S$ is the sampling phase adjustment
  510 REM S1 is the initial sampling angle
  520 REM N1 & N2 are the number of bits in ADC & Tap Weight
  530 REM N3 is the range of the arithmetics
  540 REM Common area (7) is transmit & receive data
  550 REM Common araa (6) is the pulse resposne parameters
  560 COM(6) COMPLEX H[65],INTEGER N6,REAL M6,REAL R6
  570 REM h(*) is the array response array
  580 REM n6 in the number of echoes considered
  590 REM M6 is the maximum sampling data
  600 REM R6 is the amplitude of the main lobe
  610 COM(7) COMPLEX G[165],COMPLEX T[100],COMPLEX R7,INTEGER I7
  620 REM G(165) is the receive data after sampler
  630 REM T(100) is the transmit data
  640 REM R7 is the random data generator
  650 REM I7 is maximum level value of radio, e.g. 15 for 256QAM
  660 REM Common area (9) is the avarage error & tap weight for plotting
  670 COM(9) E2[8000],COMPLEX W2[32]
  680 REM E2(*) is the avarage error array
  690 REM W2(*) is the average tap weigth
  750 REM P1, P2 & P3 strings are radio, filter & channel model resp.
  760 DIM P1$[50],P2$[25],P3$[25]
  770 REM A1$ & A2$ are for the equalizer mode & algorithm
  780 DIM A1$[50],A2$[50]
  790 REM P4$ string is for equalizer
  800 DIM P4$[75]
  810 REM A1 & A2 are plotting variables
  820 INTEGER A1,A2
  830 REM X0-4, Y0-4 are the co-odinates of writing text
  840 INTEGER X0,X1,X2,X3,X4,Y0,Y1,Y2,Y3,Y4
  850 REM Z1-8 are for auto-plot
  860 REM S0 is the equalizer output
```

```
 870 COMPLEX SO
 880 REM PO is the position of the expected data
 890 INTEGER PO
 900 REM I1-4 is the integer for bit slice
 910 INTEGER I1,I2,I3,I4
 920 REM E8 & EO are bit slice variables
 930 COMPLEX E8,EO
 940 REM W8,W9 are the error count for equalizer & without equalizer
 950 INTEGER W8,W9
 960 REM C8,C9 are the random data counter
 970 INTEGER C8,C9
 980 INTEGER I,J
1000 REM Set up error count
1010 W9=W8=0
1020 REM Set up radio string -- P1$
1030 P1$="180Mb/s 256QAM radio with"
1040 IF R$="1" THEN P1$="70Mb/s QPSK radio with"
1050 IF R$="2" THEN P1$="90Mb/s 16QAM radio with"
1060 IF R$="3" THEN P1$="135Mb/s 64QAM radio with"
1070 REM Set up filter string -- P2$
1080 P2$="raised cosine filter"
1090 REM Set up channel model string -- P3$
1100 P3$="(3-ray)"
1110 IF M$="2" THEN P3$="(2-ray)"
1120 PRINT '27"*m1m1npQ"
1130 PRINT '27"*da70,360oksG"
1140 PRINT P1$;
1150 IF C<>1 AND C<>0 THEN 1190
1160 IF C=1 THEN PRINT " 1.0 ";
1170 IF C=0 THEN PRINT " 0.0 ";
1180 GOTO 1220
1190 REM plot filter other than 0.0 or 1.0
1200 PRINT C;
1210 PRINT '27"*dc-50,0pkG";
1220 PRINT P2$;
1230 PRINT '27"*dc495,360okG"
1240 PRINT DAT$(1,27)
1250 PRINT '27"*dc70,20okG"
1260 PRINT "Performance of";
1270 PRINT N;
1280 PRINT '27"*dc-14,10pG";
1290 P4$=&
    "Tap (T complex) Transversal Equalizer under multipath fading "
1300 IF S>.6 THEN 1320
1310 P4$=&
    "Tap (T/2 complex) Transversal Equalizer under multipath fading "
1320 PRINT P4$;P3$
1330 PRINT '27"*dc70,10okG"
1340 IF O$<>"y" THEN 1370
1350 PRINT "demodulation phase : compensated";
1360 GOTO 1380
1370 PRINT "demodulation phase (degree) =";O1;
1380 PRINT '27"*dc310,10okG"
1390 IF S$<>"y" THEN 1420
1400 PRINT "; sampling phase : compensated"
1410 GOTO 1430
1420 PRINT "; sampling phase (degree) =";S1;
1430 PRINT '27"*dc200,30okG"
1440 A1$="decision direct with"
1450 IF L$<>"y" THEN A1$="separated training signal with"
1460 A2$="Zero Forcing Algorithm"
1470 IF A$<>"y" THEN A2$="LMS Gradient Algorithm"
1480 PRINT A1$;" ";A2$
1490 XO=465,YO=335
1500 PRINT '27"*dc";XO;YO;"okG"
1510 A1=N1
```

```
1520 IF A1<3 OR A1>12 THEN A1=24
1530 PRINT A1;"bit ADC"
1540 PRINT '27"*dc";X0;Y0-10;"okG"
1550 A2=N2
1560 IF A2<3 OR A2>16 THEN A2=24
1570 PRINT A2;"bit arithmetics"
1580 X1=90,Y1=55
1590 PRINT '27"*m2mQ"
1600 PRINT '27"*dc";X1;Y1;"okG"
1610 PRINT "with equalizer"
1620 X2=440,Y2=Y1
1630 PRINT '27"*dc";X2;Y2;"okG"
1640 PRINT "without equalizer"
1650 PRINT '27"*m1mQ"
1660 PRINT '27"*dcG"
1670 PRINT '27"*dtIG"
1680 PRINT '27"*ddG"
1690 REM Start Auto-plot here
1700 PRINT '27"*ad2h1i2j"
1710 PRINT "9k"
1720 REM Get Xmin & Xmax
1730 REM Set X=-1.4 to 1.4 for equalized constellation
1740 REM Set X=2.5 to 4.5 for un-equalized constellation
1750 Z1=-1.4
1760 Z2=4.5
1770 REM Set up Ymin & Ymax
1780 Z3=-1.4
1790 Z4=1.8
1800 REM Get Xlabel
1810 Z5=(Z2-Z1)/5
1820 REM Get Xtic
1830 Z6=Z5/5
1840 REM Get Ylabel
1850 Z7=(Z3-Z4)/4
1860 REM Get Ytic
1870 Z8=Z7/5
1880 PRINT Z1;"l";Z2;"m";
1890 PRINT Z3;"n";Z4;"o";
1900 PRINT Z5;"p";Z6;"q";
1910 PRINT Z7;"r";Z8;"s";
1920 PRINT "OvOwA"
1930 REM Turn off auto-plot
1940 PRINT '27"*ddG"
1950 PRINT '27"*abG"
1960 REM Reset the random data counter
1970 C9=0
1980 PRINT "Type in number of random data"
1990 INPUT C8
2000 REM Get the position of expected data
2010 PO=N/2+N6
2020 IF S<.6 THEN PO=(N+1)/4+N6
2030 REM Turn on auto-plot
2040 PRINT '27"*aaA"
2050 FOR J=1 TO C8
2060   REM Get the random transmit data
2070   INVOKE "RANDOM"
2080   T[1]=R7
2090   REM Transfer it into receive data through the channel
2100   FOR I=1 TO 2*N6/S+1
2110     G[I]=H[I]*T[1]+G[I]
2120   NEXT I
2130   REM Perform the quantization here
2140   IF N1<3 OR N1>12 THEN 2230
2150   E=G[2*N6/S+1]
2160   INVOKE "QUANTIZE"
2170   G[2*N6/S+1]=E
```

```
2180    IF S>.6 THEN 2230
2190    REM Perform one more quantization for T/2 equalizer
2200    E=G[2*N6/S]
2210    INVOKE "QUANTIZE"
2220    G[2*N6/S]=E
2230    REM Get the equalizer response
2240    S0=0
2250    N8=2*N6
2260    IF S>.6 THEN 2320
2270    N8=4*N6
2280    I=N/2
2290    A=I/2
2300    I=I/2
2310    IF ABS(A-I)<.001 THEN N8=N8-1
2320    FOR I=1 TO N
2330      S0=S0+W2[I]*G[N8+I]
2340    NEXT I
2350    REM Perform a bit slice process
2360    E0=S0
2370    GOSUB 6000
2380    E8=E0-T[P0]
2390    IF ABS(REA(E8))>.001 THEN W8=W8+1
2400    IF ABS(IMG(E8))>.001 THEN W8=W8+1
2410    E0=G[N8+N/2]
2420    GOSUB 6000
2430    E8=E0-T[P0]
2440    IF ABS(REA(E8))>.001 THEN W9=W9+1
2450    IF ABS(IMG(E8))>.001 THEN W9=W9+1
2460    REM Plot the constellation
2470    A1=100*REA(S0)/(17*M6),A2=100*IMG(S0)/(17*M6)
2480    PRINT A1/100,A2/100
2490    A1=100*REA(G[N8+N/2])/(17*M6)+350
2500    A2=100*IMG(G[N8+N/2])/(17*M6)
2510    PRINT A1/100,A2/100
2520    REM Shift G(*) & T(*) by 1 symbol
2530    INVOKE "SHIFTG"
2540    INVOKE "SHIFTT"
2550  NEXT J
2560  PRINT '27"*ddG"
2570  PRINT '27"*abG"
2580  PRINT '7'17
2590  C9=C9+C8
2600  PRINT "Type 0 for abort & any number if you want to continue";
2610  INPUT C8
2620  IF C8<>0 THEN 2030
2630  X3=100,Y3=335
2640  PRINT '27"*dsckG"
2650  PRINT '27"*dc";X3;Y3;"okG"
2660  PRINT "total number of wrong decisions"
2670  PRINT "with equalizer     :";W8
2680  PRINT "without equalizer :";W9
2690  X4=X0,Y4=Y0-20
2700  PRINT '27"*ds";X4;Y4;"okG"
2710  PRINT " number of random data :";2*C9
2720  PRINT '27"*ddG"
2730  PRINT '27"*dtIG"
2740  PRINT '27"*abG"
2750  PRINT '7'17
2760  END
```

APPENDIX 11 The Paper present in IEEE International Conference of Communications, May 1984.

LINKS FOR THE FUTURE
Science, Systems & Services for Communications
P. Dewilde and C.A. May (editors)
IEEE/Elsevier Science Publishers B.V. (North-Holland), 1984

ADAPTIVE TRANSVERSAL FILTERS FOR MULTIPATH COMPENSATION IN MICROWAVE DIGITAL RADIO

W.K. WONG+, B. WILLIAMSON+, P.M. GRANT* and C.F.N. COWAN*

+ Hewlett Packard, Queensferry Telecomms Division, South Queensferry, West Lothian, Scotland.

* Department of Electrical Engineering, University of Edinburgh, The King's Buildings, Mayfield Road, Edinburgh, Scotland.

This paper describes the implementation of adaptive transversal filters and their application in wideband microwave line of sight digital radio systems. These filters are attractive for use in multipath reduction as they can compensate for both minimum and non-minimum phase multipath fades. The relative performance of symbol (T) spaced and T/2 spaced linear transversal equalisers are assessed by computer simulations which compare the error reduction obtained with different numbers of equaliser taps and various levels of input signal quantisation and arithmetic accuracy in these decision directed equalisers.

1. INTRODUCTION

The early studies on equalisers for multipath fade [1] compensation were based on frequency domain techniques. Amplitude slope equalisation [2] provides a good first order correction when combined with an IF in phase combiner. If there are notches within the signal bandwidth then multiple bump equalisers [3] are satisfactory provided the equaliser bump corresponds to the notch frequency and that the fade type, minimum or non-minimum, has been correctly preset in advance. Moveable bumps based on variable resonators have also been reported.

This paper is concerned with linear adaptive transversal filters [4] which can handle both of these fade types in one filter structure. These filters can be implemented either at IF or baseband. When implemented at IF the delayed samples must feed complex weighting networks. Alternatively, after conversion to baseband, four separate real filter structures are required.

The most widely used adaptive filter in communications is the non-linear decision feedback equaliser [5]. This design requires a high carrier to noise ratio to avoid incorrect decisions perturbing the weight convergence. On transition between minimum and non-minimum phase fades the filter must calculate a new set of weight values. This introduces a severe step discontinuity in long delay multipath. It is for this reason that we have elected to study the linear transversal, Figure 1, adaptive filter [4] with decision directed feedback as this only has to time reverse the weight values in the filter to accommodate a change in fade type.

2. FUNDAMENTALS OF TRANSVERSAL EQUALISERS

The IF and baseband equaliser implementations are mathematically equivalent once carrier phase coherence has been established in the receiver. Therefore all the computer simulation is done at baseband to ease the computing effort.

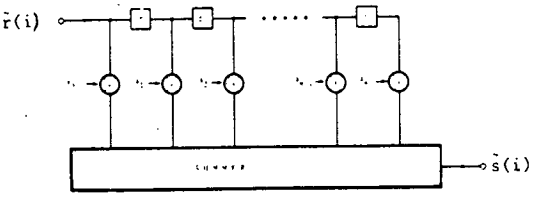

Figure 1 - Finite impulse response transversal filter.

With the notation as used in Figure 1, the output sequence is $\tilde{s}(i)$ where $\tilde{}$ implies the complex representation

$$\tilde{s}(i) = \sum_{k=0}^{m} \tilde{a}_k . \tilde{r}(i-k)$$

assuming symbol spaced taps. If $\tilde{d}(i)$ is the desired response and $\tilde{e}(i)$ is the error between the actual output and desired responses, the the mean square error ε or the expectation of $|e(i)|^2$ is given by:

$$\varepsilon = E[|e(i)|^2] = E[\sum_{k=0}^{m} (\tilde{a}_k . \tilde{r}(i-k) - \tilde{d}(i-m/2))^2]$$

where m is even.
We will use ε as a measure of equaliser performance when investigating aspects of the design. In order to minimise the variation of the mean square error against tap weight

$$\frac{\partial \varepsilon}{\partial a_k} = 0$$

for all real and imaginary a_k.

This results in a set of 2(m+1) linear equations. The solution of these gives the well known Weiner-Hopf least mean square result.

Since these equalisers will be operated on signals with 10's of MHz bandwidth it is impractical in todays technology to fabricate structures with greater than eleven taps (ten discrete time delays in Figure 1). Although the IF equaliser has lower complexity it is difficult to implement digitally. Thus an equaliser of 5-9 taps appears to be a realistic practical design. Unfortunately, the performance of an equaliser of this length has not been adequately defined for a deep fade occurring near the band centre.

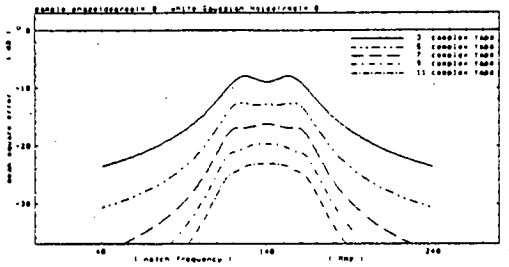

Figure 2 - T spaced equaliser performance in multipath fade where two almost equal amplitude rays provide a 20 dB deep notch. Graphs show variation in mean square error with notch position for 3 to 11 tap complex equaliser designs.

Figure 2 shows a set of comparative results for perfectly synchronised 3 to 11 tap T (symbol) spaced equalisers. The curves show the theoretical mean square error under 3 ray fades [1]. These comprised large primary and secondary rays of 2 ns delay with relative amplitude 0.9 resulting in a single 20 dB deep notch at the various positions with regard to the 140 MHz band centre as defined on the horizontal axis. These curves, which model a 70 MHz (140 Mb/sec) QPSK system, clearly show the progressive performance improvement which is obtained by using the longer equalisers. In all simulations it was assumed that the signals were bandlimited by a 0.3 raised cosine filter shape. The effect of altering the multipath delay time is shown in Figure 3. All further simulations are set at 2 ns delay.

3. PERFORMANCE OF T AND T/2 SPACED EQUALISERS

A number of investigations have been performed to assess the optimum equaliser tap spacing [6]. Symbol spacing (T) or half symbol spacing (T/2) seem to be most applicable due to the ease of clock extraction. Although a T spaced equaliser

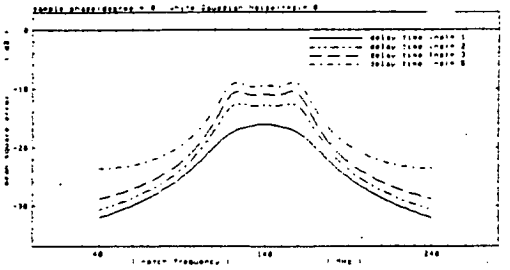

Figure 3 - Shows how the performance of 5 tap complex equaliser in Figure 2 varies with multipath delay times of 1 to 5 ns.

requires about half the number of taps to span a given channel dispersion, it is sensitive to the timing phase or delay in the channel. Figure 4 shows results for the T spaced 5 tap equaliser (Figure 2) when timing inaccuracy up to $\pm$ T/4 ($\pm$ 90°) is included in the receiver symbol timing. This sensitivity arises from the fact that, unlike the T/2 spaced equaliser, the spectrum of a T equaliser overlaps at Nyquist frequency.

In comparison with Figure 4 which relates to T spaced equalisers, Figure 5 shows similar results for T/2 spaced equalisers with 5 taps. The T/2 spaced equaliser performance is similar when the notch is near the bandcentre. However, when it is at the bandedges or in the adjacent band they offer considerable improvement over T spaced equalisers, showing evidence of their improved filtering, even though they cover half the time span of the T spaced equalisers.

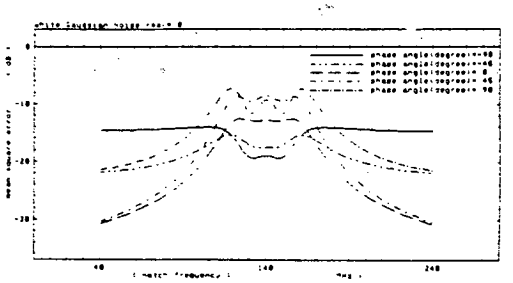

Figure 4 - 5 tap T spaced equaliser performance in multipath fade for comparison with Figure 2 where the receiver synchronisation or timing error varies between $\pm$ T/4.

From these results it has been concluded that these 5-9 tap equalisers will provide sufficient margin to give an error rate of better than 10^{-3} during most of a fading period. The T spaced equaliser shows much more dependence on accurate synchronisation than the T/2 equaliser, which is relatively insensitive.

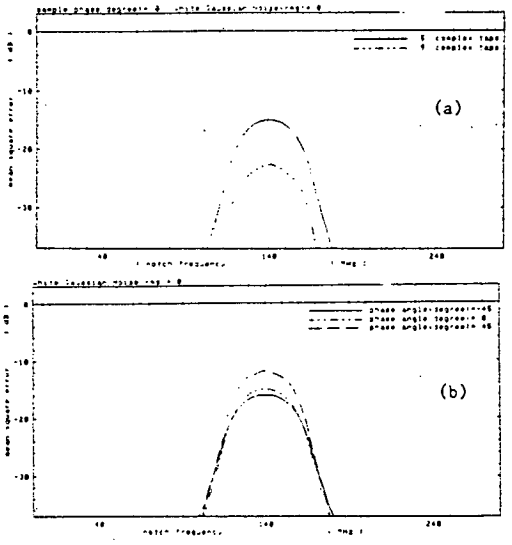

Figure 5 - (a) Effect of different equaliser lengths and (b) synchronisation error in a 5 tap T/2 spaced equaliser with ± T/8 timing error.

However, T/2 equalisers suffer from an ill-conditioning problem when the tap weights are evaluated using the least mean square (LMS) or stochastic descent algorithm. Problems can arise, especially in the adaptive mode when the tap weight is calculated with finite length arithmetic as they may converge to a local instead of the global minimum. Furthermore, they may drift to a high tap weight region and cause filter overflow if the normal steepest descent algorithm is used [7]. These problems may be overcome by employing the tap leakage algorithm.

4. SIMULATION RESULTS WHEN USING STEEPEST DESCENT ALGORITHM

The steepest descent gradient search algorithm provides a simple but effective approximate solution to the calculation of the optimum tap weight in real time. It does not require any division or matrix inversion. The tap weight adjustment at the (n+1)th iteration is

$$\tilde{a}_k(n+1) = \tilde{a}_k(n) - \alpha.\tilde{e}(n).\tilde{r}_k^*(n)$$

where * implies complex conjugate and α is the convergence factor. A large value of α will increase the convergence rate but result in more gradient noise.

In the computer simulations, the overall pulse response of the channel is calculated using 1024 point FFT's with up to 7 post-echoes and 7 pre-echoes being considered. The sampling phase is referred to the maximum eye opening position when there is no multipath fading. The amplitude of the I and Q data is set to be ± 1 to represent the QPSK signal. All the tap weights are preset to zero except the centre tap which is set initially to 1. The plotted mean square error is the error measured in one channel only. Figures 6 and 7 show the convergence properties of the equalizers under 20 dB fade depth with the notch 20 MHz above bandcentre. Although a separate training signal is not available in practice it is used in these simulations to provide a measure of the relative performance of the equalizers. The convergence rate depends on the initial and final tap weight values, the latter being determined by the fading conditions. However, an equalizer with fewer taps will generally converge faster.

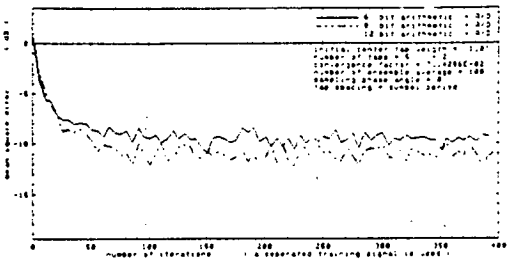

Figure 6 - Convergence plots for T spaced complex equalisers with a 20 dB deep notch located 20 MHz above band-centre. This shows the effect of introducing 12, 8 and 6 bit precision in both A/D and internal arithmetic.

The convergence plots for the 5 tap T spaced equalisers presented in Figure 6 show the effect of reducing the accuracy of the input quantisation and arithmetic from 12 bits to 8 bit to 6 bit precision. The results for 9 tap equalisers are similar for 6 bit precision but 8 and 12 bit precision gives a reduced ε of $\sim$ -15 dB. In comparison Figure 7 shows performance for a T/2 spaced equaliser where the input quantisation was fixed at 6 bits but the accuracy of the internal arithmetic was varied from 6 to 12 bit precision. A comparison of these figures and other simulations has shown that quite acceptable performance can be obtained with 6 bit quantisation provided 8 bit precision arithmetic is used, as the degradations from infinite precision are only minimal with this configuration. These results now need to be extended to investigate the effects of 4 bit input quantisation with 6 and 8 bit arithmetic. Initial results on a 5 tap T spaced equaliser indicate that 4 bit quantisation with 8 bit arithmetic is equivalent to 6 bit quantisation with 6 bit arithmetic, Figure 8.

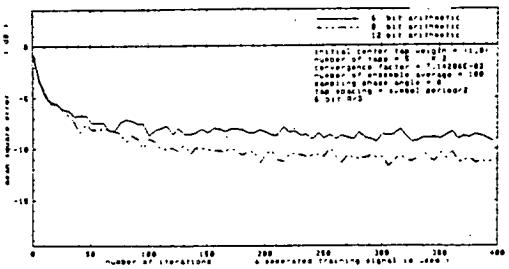

Figure 7 - Shows the effect of introducing reduced precision input quantisation into the 5 tap T/2 spaced equaliser. This uses 6 bit A/D with 12, 8 and 6 bit internal precision arithmetic.

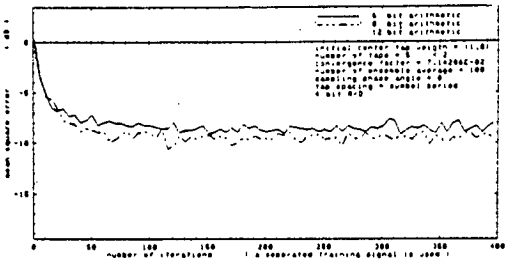

Figure 8 shows the effects of introducing 4 bit A/D with 6, 8 and 12 bit internal precision arithmetic in a T spaced 5 tap equaliser.

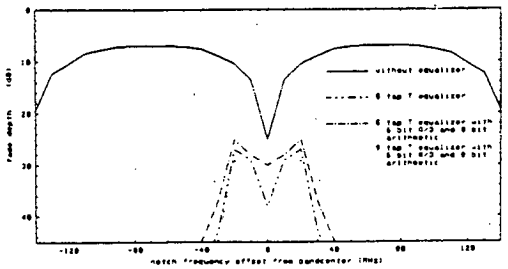

Figure 9 - Signatures for a QPSK receiver with and without equalisation for a bit error rate of 10^{-3}.

Figure 9 shows signature plots for a 140 Mb/sec QPSK system at a bit error rate of 10^{-3} with a flat fade margin of 43 dB. This clearly shows the improvement obtained by deploying 5 and 9 tap T spaced equalisers with and without quantisation and arithmetic inaccuracies.

5. CONCLUSIONS

The paper has addressed the design of adaptive transversal equalisers for multipath fade compensation in digital microwave radio systems. It has shown the likely theoretical performance of 5-9 tap equalisers. Further investigation of T and T/2 spaced equalisers has shown that the converged performance of equalisers with similar numbers of taps is broadly equivalent. However significant advantages can occur from the deployment of the T/2 spaced design which offers reduced timing sensitivity and superior filtering properties when the multipath notch is located at the edges of the signal bandwidth. Further studies on the effect of incorporating finite precision arithmetic into the digital delay lines and multipliers shows that 6 bit input quantisation with 8 bit precision arithmetic is likely to be required to implement these as digital equaliser structures. 5 tap complexity appears from our simulations to offer acceptable performance and represents the level of complexity we envisage in practical equaliser designs.

6. ACKNOWLEDGEMENT

One of the authors (WKW) wishes to thank Hewlett-Packard for their generous support of this work which is being conducted as part of his Ph.D. studies at the University of Edinburgh.

7. REFERENCES

1. W D RUMMLER: "A new selective fading model: Application to propagation data", Bell System Technical Journal, Vol.58, pp.1037-71, May-June 1979.

2. C W ANDERSON, S G BARBER and R N PATEL: "The effect of selective fading on digital radio", IEEE Trans COM-27, No.12, pp.1870-5, December 1979.

3. T P MURPHY, F M BAKER, C L GARNER and P J KRUZINSKI: "Practical techniques for improving signal robustness", National Telecommunication Conference Paper C3.3, November 1981.

4. G L FENDERSON, S R SHEPARD and M A SKINNER: "Adaptive Transversal Equaliser for 90-Mb/s 16 QAM Systems in the presence of Multipath Propagation", International Communications Conference Paper C8.7, June 1983.

5. C A BELFIORE and J H PARK Jr: "Decision feedback equalisation" Proc. IEEE, 67, No.8, pp.1143-1156, August 1979.

6. R D GITLIN, S B WEINSTEIN: "Fractionally-spaced-equalisation, an improved digital transversal equaliser", BSTJ Vol.60, No.2, pp.275-296, February 1981.

7. R D GITLIN, H C MEADORS, S B WEINSTEIN: "The tap-leakage algorithm: an algorithm for the stable operation of a digitally implemented fractionally spaced, adaptive equaliser", BSTJ, Vol.61, No.8, October 1982.